



Copyright Undertaking

This thesis is protected by copyright, with all rights reserved.

By reading and using the thesis, the reader understands and agrees to the following terms:

1. The reader will abide by the rules and legal ordinances governing copyright regarding the use of the thesis.
2. The reader will use the thesis for the purpose of research or private study only and not for distribution or further reproduction or any other purpose.
3. The reader agrees to indemnify and hold the University harmless from and against any loss, damage, cost, liability or expenses arising from copyright infringement or unauthorized usage.

IMPORTANT

If you have reasons to believe that any materials in this thesis are deemed not suitable to be distributed in this form, or a copyright owner having difficulty with the material being included in our database, please contact lbsys@polyu.edu.hk providing details. The Library will look into your claim and consider taking remedial action upon receipt of the written requests.

**SELF-ADAPTIVE VISION-BASED
VEHICLE REIDENTIFICATION SYSTEM FOR
DYNAMIC FREEWAY TRAVEL TIME ESTIMATION**

WANG JIANKAI

Ph.D

The Hong Kong Polytechnic University

2014



The Hong Kong Polytechnic University

Department of Civil and Environmental Engineering

**Self-Adaptive Vision-Based Vehicle Reidentification
System for Dynamic Freeway Travel Time Estimation**

WANG JIANKAI

A Thesis Submitted in Partial Fulfillment
of the Requirements for the Degree of
Doctor of Philosophy

February, 2014

Certificate of originality

I hereby declare that this thesis entitled "Self-Adaptive Vision-Based Vehicle Reidentification System for Dynamic Freeway Travel Time Estimation" is my own work and that, to the best of my knowledge and belief, it reproduces no material previously published or written, nor material that has been accepted for the award of any other degree or diploma, except where due acknowledgement has been made in the text.

Signature:

Name of student: WANG JIANKAI

Dedicated with love and gratitude to my family.

Abstracts

Due to its potential for anonymous vehicle tracking, vehicle reidentification (VRI) has emerged as an effective approach for directly estimating freeway travel time. As real-time video of traffic scenes contains a wealth of vehicle information that may not be available from conventional detectors (e.g. inductive loops), there is a growing interest in development of vision-based VRI system. To further improve the robustness of VRI system against the potential changes in traffic condition, a self-adaptive time window component is also required. To this end, the thesis aims to contribute to the development of a self-adaptive vision-based vehicle reidentification (VRI) system for dynamic freeway travel time estimation.

As a preliminary investigation, the thesis first considers developing a basic vision-based VRI system under static traffic conditions. Various vehicle feature data (e.g. color, length and type) are extracted from the video record, and a data fusion approach is then introduced to combine these features to generate a probabilistic measure for reidentification decision. The vehicle-matching problem is then formulated as a combinatorial problem and solved by a minimum-weight bipartite matching method.

The proposed basic vision-based VRI system is then extended and applied for automatic incident detection under free condition. The relatively high matching accuracy of basic VRI would allow for a prompt detection of the incident vehicle and, hence, reduce the incident detection time. An enhanced vehicle feature matching technique is adopted in the basic VRI component to explicitly calculate the matching probabilities for each pair of vehicles. Also, a screening method, which is based on the ratios of the matching probabilities, is introduced to reduce the false alarm rate.

The basic VRI is also extended to the static case where multiple video cameras exist. A hierarchical Bayesian matching model is then proposed to consider vehicle reidentification over multiple detectors as an integrated process such that the overall matching accuracy could be improved.

For the dynamic traffic conditions, the thesis introduces an additional self-adaptive time

window component into the basic VRI system to improve its performance in terms of dynamic travel time estimation. Specifically, an iterative VRI system with temporal adaptive time window constraint is proposed. To capture the traffic dynamics in real-time, the inter-period/temporal adjusting based on exponential smoothing technique is introduced to define an appropriate time window constraint for the basic VRI. To handle the non-predictable traffic congestions, the modified basic VRI is performed iteratively (i.e. iterative VRI) such that the improved VRI is capable of adjusting its parameters automatically.

Finally, the thesis focuses on developing an integrated self-adaptive VRI system for a freeway with multiple video cameras under dynamic traffic conditions. The spatial dependencies between the travel time over different freeway segments are utilized for the further adjustment of the time window constraint. An iterative VRI system with spatial-temporal adaptive time window constraint is then proposed to cope with the purpose of dynamic travel time estimation.

Publications arising from the thesis

Journal paper

Sumalee, A., Wang, J., Jedwanna, K., Suwansawat, S., 2012. [Probabilistic fusion of vehicle features for re-identification and travel time estimation using video image data](#). Transportation Research Record 2308, 73–82. (The content in Chapter 4 is mainly from this paper.)

Wang, J., Indra-Payoong, N., Sumalee, A., Panwai, S., 2014a. [Vehicle reidentification with self-adaptive time windows for real-time travel time estimation](#). IEEE Transactions on Intelligent Transportation Systems 15 (2), 540–552.

Wang, J., Sumalee, A., Ho, H.W., 2014b. A vehicle re-identification based automatic expressway incident detection system for free flow conditions. Paper revised for IEEE Transactions on Intelligent Transportation Systems.

Wang, J., Sumalee, A., 2014. Hierarchical Bayesian model for vehicle reidentification on freeway with multiple detectors. To be submitted. (The content in Chapter 6 is mainly from this paper.)

Conference papers

Wang, J., 2013. Vehicle re-identification with self-adaptive time windows for real-time freeway travel time estimation under traffic demand and supply uncertainty. In: Paper accepted for presentation in the 18th International Conference of Hong Kong Society for Transportation Studies. Hong Kong.

Wang, J., Sumalee, A., 2013a. Robust vehicle re-identification system for real-time travel time estimation. In: Proceedings of 18th National Convention on Civil Engineering. Vol. 2. Chiang Mai, Thailand (Best paper award in the field of transportation engineering).

PUBLICATIONS ARISING FROM THE THESIS

- Wang, J., Sumalee, A., 2013b. Vehicle re-identification with self-adaptive time windows for real-time travel time estimation. In: Proceedings of International Symposium on Recent Advances in Transport Modelling. Gold Coast, Australia.
- Wang, J., Sumalee, A., Ho, H.W., 2013. A vehicle re-identification based automatic expressway incident detection system for free flow conditions. In: Proceedings of Transportation Research Board 92nd Annual Meeting. Washington, D.C.
- Wang, J., Sumalee, A., Ho, H.W., 2012. A vehicle re-identification based automatic expressway incident detection system for free flow condition: A case study of Thai Expressway. In: Paper accepted for presentation in the 17th International Conference of Hong Kong Society for Transportation Studies. Hong Kong.
- Sumalee, A., Wang, J., 2011. Travel time estimation from video image data: Probabilistic fusion approach for vehicle re-identification. In: Paper accepted for presentation in the 16th International Conference of Hong Kong Society for Transportation Studies. Hong Kong.

Acknowledgements

First of all, I would like to express my sincere gratitude to my supervisors, i.e., Dr. Agachai Sumalee, and Prof. H.K. Lam for their kind guidance and supervision. I have gained a lot of knowledge from them that are applicable for my future career. I would like to thank the Hong Kong Polytechnic University for providing my PhD studentship.

I would also like to thank Prof. Hong Kam Lo and Dr Wei Hua Lin for serving in my thesis committee, and for their valuable suggestions and advices.

Many past and present members in transportation group of the Hong Kong Polytechnic University deserve my thanks for their friendship and technical expertise, including Dr. Julio Ho, Dr. Renxin Zhong, Tianlu Pan, Treerapot Siripirote, Ekalux Ua-areemitr, and Piyanit Wepulanon. Particularly, I would like to thank Dr. Julio Ho and Ekalux Ua-areemitr for the fruitful discussions over the past two years. I would also like to thank them for always being there to support me through the tough times as well as to share the great moments, for filling my last two years with so many unforgettable memories.

Finally, my love and thanks go to my parents. Mere words, in any of the languages that I know, are inadequate to express my gratitude for the unconditional love and support they have given to me.

Table of Contents

Certificate of originality	i
Dedication	ii
Abstracts	iii
Publications arising from the thesis	v
Acknowledgements	vii
Table of contents	viii
1 Introduction and overview	1
1.1 Research motivation	1
1.2 Research objectives	3
1.3 Organization of the thesis	5
1.4 Research contribution	8

Part I:

Foundations of the study

2 Problem statements and literature review	11
2.1 Travel time estimation problem	11
2.1.1 Problem description	12
2.1.2 Spot-speed-based method	13
2.1.3 Traffic-flow-based method	15
2.1.4 Probe-vehicle-based method	16
2.2 Overview of vehicle reidentification (VRI)	17
2.2.1 Vehicle signature extraction	17
2.2.2 Vehicle signature matching method	18

2.2.3	Discussion of the existing VRI systems	19
2.3	Framework of intelligent video surveillance	22
2.3.1	Video sensor networks	24
2.3.2	Low-level image processing	25
2.4	Traffic incident detection algorithms	27
2.4.1	Incident detection system	28
2.4.2	Incident detection algorithms for congested traffic condition	28
3	High-level intelligent video surveillance	32
3.1	Introduction	32
3.2	Single-camera analytics	34
3.2.1	Object detection	34
3.2.2	Feature extraction	35
3.3	Multi-camera analytics	39
3.3.1	Object reidentification (ORI)	39
3.3.2	People reidentification (PRI)	41
3.4	Vehicle reidentification: A variant of PRI	42
3.5	Conclusion remarks	44

Part II:

VRI system under static traffic conditions

4	Basic vision-based VRI system	48
4.1	Introduction	48
4.2	Overall framework of the travel time estimation system	51
4.3	Probabilistic fusion of vehicle features	54
4.3.1	Time window constraint	54
4.3.2	Probabilistic modeling of feature distance	55
4.3.3	Probability distribution estimation	57
4.3.4	Calculation of <i>posterior</i> probability	57
4.3.5	Data fusion rule	59
4.4	Bipartite matching method	62
4.4.1	Reduction to a weighted bipartite graph	62
4.4.2	Formulation as a minimum-weight bipartite matching problem	63
4.5	Test results	64
4.5.1	Travel time distribution	65
4.5.2	Performance of probabilistic feature fusion approach	66

4.5.3	Vehicle reidentification across multiple lanes	67
4.6	Conclusion remarks	68
Appendices		70
4.A	Freeway segment with entry/exit ramps	70
5	VRI based incident detection under free flow condition	73
5.1	Introduction	73
5.2	Dataset for algorithm development and evaluation	77
5.2.1	Dataset description	78
5.3	Overall framework of automatic incident detection system	79
5.3.1	Vehicle count approach	79
5.3.2	AID algorithm based on VRI system	81
5.4	Flexible time window estimation	83
5.5	Incident-detection-oriented VRI	84
5.5.1	Reidentification problem	84
5.5.2	Calculation of matching probability	85
5.5.3	Ratio method for final matching decision	87
5.6	Test results	89
5.6.1	Simulated tests	90
5.6.2	Real-world case study	92
5.7	Conclusion remarks	94
Appendices		96
5.A	Incident detection on freeway segment with entry/exit ramps	96
6	Hierarchical Bayesian model for VRI on freeway with multiple detectors	99
6.1	Introduction	99
6.2	Pair-wise VRI process	102
6.2.1	Basic VRI subsystem	103
6.2.2	A discussion on pair-wise VRI	105
6.3	Hierarchical matching model	107
6.3.1	Hierarchical structure for vehicle matching	107
6.3.2	Construction of vehicle tree structure: Preliminary clustering	108
6.3.3	Statistical framework for hierarchical matching	109
6.4	Hierarchical Bayesian modeling on feature distances	111
6.4.1	Hierarchical model of a sequence of feature distances	112
6.4.2	Probabilistic modeling of feature distances over space	115

6.5	Test results	117
6.5.1	Dataset for algorithm evaluation	118
6.5.2	Comparison between pair-wise VRI and the improved method	119
6.6	Conclusion remarks	121

Part III:

Self-adaptive VRI system under dynamic traffic conditions

7	Iterative VRI system with temporal adaptive time window	123
7.1	Introduction	123
7.2	Simplified version of basic VRI	127
7.2.1	Vehicle feature data	127
7.2.2	Vehicle signature matching method	128
7.3	Post-processing technique	134
7.3.1	Stratified sampling technique	134
7.3.2	Thresholding process	136
7.4	Self-adaptive time window constraint	137
7.4.1	Inter-period adjusting: Temporal adaptive time window	138
7.4.2	Intra-period adjusting: Iterative VRI	139
7.5	Experimental results	141
7.5.1	Simulation model configuration and calibration	141
7.5.2	Preliminary comparison between basic VRI and improved VRI	142
7.5.3	Performance evaluation under recurrent traffic congestion	144
7.5.4	Performance evaluation under bottleneck effect	145
7.5.5	Performance evaluation under non-recurrent traffic congestion	148
7.6	Conclusion remarks	150
8	Iterative VRI system with spatial-temporal adaptive time window	152
8.1	Introduction	152
8.2	Basic temporal adaptive time window	155
8.3	Spatial-temporal adaptive time window	157
8.3.1	Spatial and temporal correlation in travel time	157
8.3.2	Shrinkage-thresholding method	159
8.4	Preliminary Results	161
8.4.1	Simulation model configuration and calibration	161
8.4.2	Performance evaluation under serious non-recurrent traffic congestion	162

TABLE OF CONTENTS

8.5	Conclusion remarks	165
-----	------------------------------	-----

Part IV:

Conclusions and future works

9	Summary of the thesis and future research topics	168
9.1	Summary of the thesis	168
9.2	Future works	171
9.2.1	Extension of the VRI system to a network case	171
9.2.2	Network-wide travel time estimation using partial VRI data	172
	References	183

List of Figures

1.1	A freeway system equipped with intelligent video surveillance system . . .	4
1.2	Overall framework of the thesis	6
2.1	Demonstration of the trajectory-based method (source: (Ni and Wang, 2008))	14
2.2	Demonstration of the time window constraints in VRI system	18
2.3	General framework of IVS	23
2.4	Digital image representation	25
2.5	Illustrative example of image deblurring caused by motion blur	27
2.6	The basic California algorithms (source: (Payne and Tignor, 1978))	29
2.7	Image processing method	31
3.1	(a) Background estimation; (b) Effect of object detection	35
3.2	Another example of vehicle color recognition	36
3.3	Example of vehicle color recognition	37
3.4	An illustration of vehicle shape extraction	38
3.5	Similarity score for each template	38
3.6	Similar vehicle feature	43
3.7	Thesis architecture demonstrating the mutual dependencies and the logical connections between the three parts	45
4.1	Test site in Bangkok, Thailand.	52
4.2	Overall framework of travel time estimation system.	54
4.3	The pdfs p_1 and p_2 estimated by gaussian mixture model	58
4.4	Bipartite graph representation	62
4.5	Bipartite matching procedure	64
4.6	Travel time distribution: (a) the pdf of historical travel time distribution; (b) estimated and manual observed travel time distribution.	65
4.7	Vehicle matching across multiple lanes	67
4.8	Conceptual test site	70

4.9 (a) Topological structure; (b) Bipartite graph representation	71
5.1 Test site in Bangkok, Thailand	77
5.2 Illustrative example of vehicle count approach	80
5.3 Overall framework of AID system	82
5.4 Illustrative example of a false alarm	88
5.5 Mean detection time and false alarm rate	91
5.6 Comparison between the proposed AID algorithm and vehicle count approach	92
5.7 Real-world case study #1: (a) Incident vehicle passes the upstream detector; (b) Tow truck passes the upstream detector; (c) Incident vehicle and truck passes through the downstream detector	93
5.8 Real-world case study #2: (a) Incident vehicle passes the upstream detector; (b) Incident vehicle and truck passes through the downstream detector	93
5.9 Conceptual test site	96
5.10 Topological structure	97
6.1 Freeway segment with multiple detectors	101
6.2 Conceptual freeway corridor	103
6.3 A hierarchical structure of vehicle matching across multiple detectors	108
6.4 Illustrative example of the construction of vehicle tree	110
6.5 Multivariate histogram and the fitted normal distribution	117
6.6 Test site in Bangkok, Thailand	118
6.7 Illustrative matching example	120
7.1 Illustrative example of the basic VRI system for real-time implementation	133
7.2 Travel time for different vehicle types.	135
7.3 Detailed implementation of the improved VRI system.	140
7.4 Test site in Bangkok, Thailand.	141
7.5 Effectiveness of temporal-adaptive time window.	143
7.6 Effectiveness of post-processing technique under fixed time window.	144
7.7 Performance of the proposed method with exceeding traffic demand	146
7.8 Merge and Diverge along the freeway segment	147
7.9 Performance of the proposed method (on-ramp vehicle flow distribution: 25%)	147
7.10 Incident simulation	149
7.11 Performance of the proposed method (incident duration: 10 min; starts from 90 min)	149

7.12	Adjustment of time window constraint	150
8.1	Freeway with multiple detectors	154
8.2	Temporal adjustment of time window	156
8.3	Ground truth travel time on two consecutive segments with incident hap- pening on segment2 (incident duration: 10 minutes)	158
8.4	Overall framework of the proposed VRI system	161
8.5	Test site in Bangkok, Thailand	162
8.6	Performance of spatial-temporal adaptive time window (incident duration: 20 minutes; Segment 1)	164
8.7	Performance of spatial-temporal adaptive time window (incident duration: 10 minutes; Segment 1)	164
8.8	Performance of spatial-temporal adaptive time window (incident duration: 20 minutes; Segment 2)	165
9.1	Conceptual network	175
9.2	Two-detectors-with-common-links network	177
9.3	Vehicle platoon information	178

List of Tables

2.1	Summary of existing VRI systems	20
3.1	Extracted vehicle data based on IVS	39
4.1	Performance of Vehicle Re-Identification Algorithm Regarding Different Fusion Weights	66
6.1	Comparison between pair-wise VRI and the improved method	119
7.1	Descriptive statistics from simulation outputs	145
7.2	Performance of the proposed method with different vehicle flow distributions	148
7.3	Performance of the proposed method with different incident durations	150
9.1	Performance of random initialization technique	180
9.2	Asymptotic properties of the estimators	181
9.3	Performance of the link travel time estimation	181

Chapter 1

Introduction and overview

1.1 Research motivation

The rapid population growth and worldwide urbanization have substantially increased the travel demand and resulted in serious traffic congestion, which could produce a number of negative effects on the drivers, the environment and the economy. According to the 2012 Urban Mobility Report (Schrank et al., 2012), congestion caused urban Americans to travel 5.5 billion hours more and to purchase an extra 2.9 billion gallons of fuel for a congestion cost of \$121 billion in 2011. In addition to the high travel demand (i.e. traffic demand exceeding the roadway capacity), the non-recurring traffic accidents could also lead to traffic congestion and injuries (Guner et al., 2012). Statistics also suggest the high chance of a more severe secondary accident following the initial accident (Sheu et al., 2001). In this case, expanding or building new traffic infrastructures (i.e. increasing the traffic capacity) has been the natural and traditional response to the aforementioned congestion problems (Beckmann, 2013). However, it is becoming increasingly difficult to undertake in practice because of the funding constraints, as well as political and environmental issues arising from the construction. Also, the unpredictable traffic accidents pose series challenges to the maintenance and management of traffic networks.

Recently, Intelligent Transportation Systems (ITS) have received considerable attention due to their abilities to alleviate traffic congestion and improve the safety for traffic networks (Chowdhury and Sadek, 2003). Simply put, ITS are strategies that aim to integrate

modern communication and information technologies into transportation to make more efficient utilization of the existing transportation facilities. Recognized as one of the most widely used ITS applications, the Advanced Traveler Information Systems (ATIS) provide travelers with updated traffic information (e.g. travel time on a freeway segment) to help them make better route decisions and, hence, avoid the congested road segments (Toledo and Beinhaker, 2006). In the meantime, by analyzing the real-time traffic information (e.g. travel time, traffic flow), the Advanced Traffic Management Systems (ATMS) would allow the traffic operators to conduct efficient traffic incident management in the sense that the traffic incident can be detected promptly and removed quickly, which could eventually contribute to the alleviation of traffic congestion.

As illustrated above, one of the basic components of ITS applications (e.g. ATIS and ATMS) would be the dynamic travel time estimation¹. Unlike the traditional traffic parameters (e.g. vehicle speed, traffic flow, density), travel time cannot be directly measured through the pointer sensors (e.g. loop detector and magnetic sensor). In this case, vehicle reidentification (VRI)² has emerged as an alternative approach due to its potential for effective tracking of the individual vehicles. As opposed to analyzing the macroscopic/aggregated traffic parameters (e.g. traffic flow, density and average speeds), vehicle reidentification focuses on matching the vehicle signatures (e.g. vehicle length, color and waveform) derived from the detectors so that each individual vehicle could be tracked in traffic network. And accordingly the travel time could be easily obtained by calculating the difference of the vehicle arrival times at different locations.

Based on the above-mentioned principle, various VRI systems have been developed by using different kinds of sensing technologies (e.g. inductive signature systems, magnetic sensors, intelligent video surveillance system). Due to its ease of implementation and relatively low cost, the inductive loop is the most widely used sensing technology for the development of VRI systems (Holt et al., 2003; Parkany and Xie, 2005). Only a limited number of studies have been conducted to utilize the emerging sensing technologies (i.e. intelligent video surveillance). Compared with the inductive signature system, intelligent video surveillance (IVS)³ provides real-time and vivid image from which the human operators can gain better insight into the current traffic state. Moreover, IVS would also allow for an automatic interpretation (e.g. vehicle detection, feature extraction) of the scenes by

¹We will introduce the problem of dynamic travel time estimation in detail in Section 2.1.

²A more detailed introduction of VRI will be presented in Section 2.2.

³The overall framework of IVS can be found in Section 2.3, and a more detailed description of the image processing techniques in IVS is presented in Chapter 3.

using the advanced image processing techniques. In light of this, this study attempts to investigate the feasibility of developing a vision (i.e. intelligent video surveillance) based VRI system for freeway travel time estimation.

Regardless of the sensing technologies, the existing VRI systems still suffer from two inherent limitations. First, mismatches caused by the non-uniqueness of vehicle signatures are inevitable, which suggests that the following task of travel time calculation may not be straightforward. To overcome this problem, a great deal of effort has been devoted to improving the matching accuracy (i.e. reducing mismatches) by imposing stringent assumptions on vehicles' traveling behaviors (e.g. no overtaking and no lane-changing). Although these studies are theoretically enlightening and valuable, they are still not practically feasible for real-world application. Second, the stochastic and dynamic nature of traffic network (Watling and Cantarella, 2013) would eventually result in the dynamic travel time, which also implies that the traffic condition may substantially change from time to time (e.g. free flow to congested). However, most of the existing VRI systems are specifically designed for a short time period (e.g. pre-defined time window, fixed system initialization parameters) in which the traffic condition is relatively stable (i.e. static condition)¹. To sum up, most of the proposed VRI systems are concentrating on improving the vehicle matching accuracy and are subjected to adaptation at run-time due to the potential changes in traffic conditions.

To this end, this dissertation research presents a self-adaptive vision-based VRI system for dynamic freeway travel time estimation. From the viewpoint of travel time estimation, the vehicle matching accuracy would not be the major concern. Therefore, this study performs post-processing technique to filter out the erroneous travel time caused by the mismatches. The self-adaptivity of this proposed system also allows it to automatically adjust its initialization parameters (e.g. time window constraints and *prior* knowledge) in response to the substantial changes in traffic conditions.

1.2 Research objectives

As explained previously, the ultimate goal of this dissertation is to develop a self-adaptive vehicle reidentification system for freeway travel time estimation under dynamic traffic

¹This will be further illustrated in Chapter 4.

flow or congestion). In order to handle the dynamic traffic conditions, we would further develop an improved self-adaptive VRI system for dynamic travel time estimation, which serves as the essential part of this study. The detailed procedures can be described as follows:

- IV. Based on the basic VRI subsystem developed in I, an **iterative VRI subsystem with temporal adaptive time window** is proposed to improve its robustness against the potential changes in traffic conditions. An appropriate strategy (e.g. post-processing and adjustable time window) is devised to perform the basic VRI iteratively such that the new system is capable of adjusting its parameters automatically under traffic demand and supply uncertainties (e.g. recurrent congestion, and non-recurrent congestion).
- V. For a freeway system with **multiple** video cameras, we introduce a spatial-temporal adaptive time window component to further improve the performance of the system developed in IV, which eventually gives rise to the **iterative VRI system with spatial-temporal adaptive time window**.

1.3 Organization of the thesis

More specifically the overall framework of the thesis is described in Figure 1.2, in which the presentation is divided into three major parts. After the brief introduction to the research in Chapter 1, we proceed to consider the foundations for the development of vision-based VRI system. Chapter 2 describes the problem statements (e.g. travel time estimation problem, vehicle reidentification, and automatic incident detection) and reviews the relevant literatures on these problems. Since this study focuses on utilizing the emerging video surveillance system, a comprehensive introduction to this sensing technology is presented in Chapter 3. The associated image processing techniques that used for traffic data collection (e.g. vehicle detection, and vehicle feature extraction) are described, and some preliminary results are also presented in this chapter. Note that this study focuses on using the existing image processing techniques for further development of VRI system. Therefore, a complete introduction of the underlying theory of image processing is out the scope of this thesis.

Within the second part of this thesis, we would formally deal with the development of VRI

1.3 Organization of the thesis

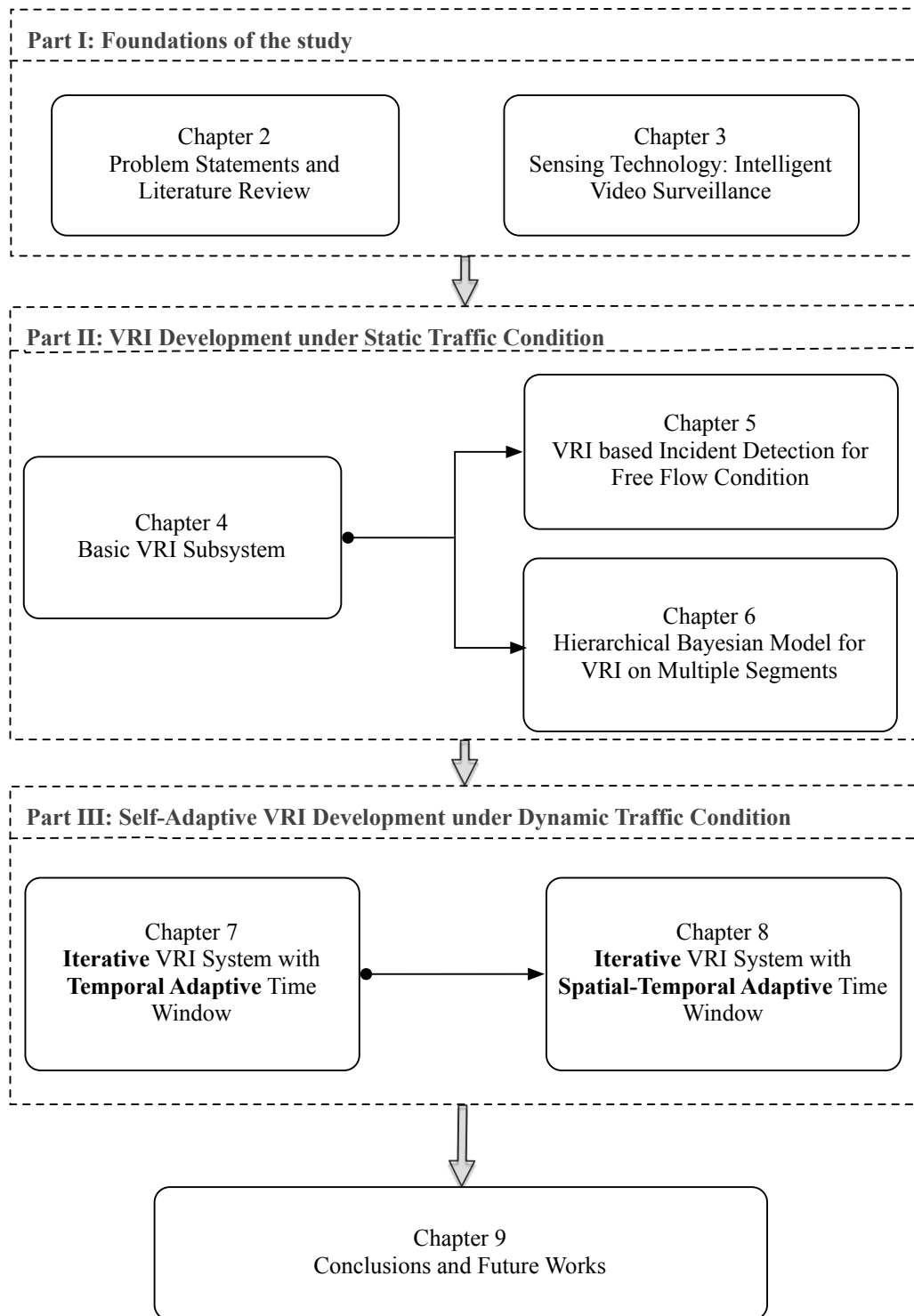


Figure 1.2: Overall framework of the thesis

system under static traffic condition. The central goal of this part is to devise vision-based VRI system with relatively high matching accuracy, through which a large percentage of

individual vehicles could be re-identified. The potential benefits of high matching accuracy are huge and obvious: reliable travel time estimates and efficient vehicle tracking. In light of this, a basic vision-based VRI subsystem is developed in Chapter 4. Various detailed vehicle features (e.g. vehicle color, length, and type) are extracted for the further development of vehicle matching method. Due to its capability of efficient vehicle tracking in the freeway system, the basic VRI subsystem is further designed and improved for incident detection under free flow condition (see Chapter 5). Chapter 6 further proposes a hierarchical Bayesian matching model for vehicle reidentification by taking full advantage of the vehicle feature data collected from multiple detectors.

For the dynamic traffic condition, a further improved self-adaptive VRI system is developed in the third part of this thesis. Chapter 7 presents a novel iterative VRI system with temporal adaptive time window constraints. To capture the traffic dynamics in real-time, the exponential smoothing technique (e.g. based on temporal traffic information) is utilized to adjust the time window constraint from time period to time period. The additional iterative process together with the post-processing technique is introduced to achieve reliable travel time estimates under non-predictable traffic condition (e.g. traffic incident). In Chapter 8, a further improved iterative VRI system with spatial-temporal adaptive time window is presented. This system is specifically designed for the freeway system with multiple detectors. By utilizing the traffic information (e.g. spatial information) from different pairs of detectors, we may obtain a more reliable time window constraint under traffic demand and supply uncertainties.

Finally, Chapter 9 summarizes remarks and conclusions of this research. Some topics of the future works are also highlighted in this chapter.

As a guide to the reader it should be remarked that the first part (see Figure 1.2) is the building block of this research. Based on the emerging sensing technology (i.e. intelligent video surveillance), we specifically design the self-adaptive VRI system to support the ITS applications (e.g. ATIS and ATMS) under dynamic traffic conditions. Therefore, the readers are firstly suggested to read Chapter 2 and Chapter 3 to get the major ideas of the this study. The mutual dependencies and the logical connections between the three parts will be further illustrated in Section 3.5 (also see Figure 3.7).

1.4 Research contribution

In order to clarify the research contributions of this thesis, a brief overview of the main methodologies and results presented in each of the different parts will be given.

Chapter 4

- A probabilistic fusion strategy is devised to integrate the various vehicle features (e.g. color, length and type) obtained from intelligent video surveillance technology. The logarithmic opinion pool (LOP) approach is utilized for generating an overall *posterior* probability for vehicle matching decision-making.
- The vehicle matching problem is formulated as a combinatorial optimization problem and solved by the minimum-weight bipartite matching method.
- The proposed basic VRI system is tested on a 3.6-kilometer segment of the freeway system in Bangkok, Thailand. The overall matching accuracy is about 54.75%. As the developed vehicle matching algorithm does not require lane sequence information, it allows vehicle reidentification across multiple lanes.

Chapter 5

- An enhanced vehicle feature matching technique is adopted in the VRI component for explicitly calculating the matching probability for each pair of vehicles.
- A screening method based on the matching probabilities is introduced for vehicle matching decision-making such that the incident vehicle could be identified in a timely and accurate manner.
- The proposed VRI based incident detection algorithm is tested on a 3.6-km segment of a closed freeway in Bangkok, Thailand. The associated incident detection time of the proposed method is substantially shorter than the traditional vehicle count approach.

Chapter 6

- A hierarchical matching model is proposed such that vehicle matching over multiple detectors is treated as an integrated process. A hierarchical tree structure is also incorporated for representing the matching result over multiple detectors.

- The associated hierarchical Bayesian model is introduced to describe the spatial dependencies between vehicle feature distances, which would yield a more reliable probabilistic measure for matching decision-making.
- The proposed method is tested on a 9.7-km freeway segment with three detectors. The results show that the hierarchical matching method outperforms the pair-wise VRI matching method.

Chapter 7

- The temporal adaptive time window component is introduced into the basic VRI system for improving its robustness against the potential changes in traffic conditions.
- A post-processing technique is performed on the raw results produced by basic VRI system to rule out the erroneous travel time and, hence, obtain a more reliable mean travel time estimator.
- An appropriate iterative process is developed to perform basic VRI iteratively (i.e. iterative VRI) such that the non-recurrent traffic congestions can be captured.
- Several representative tests are carried out to evaluate the performance of the iterative VRI system with temporal-adaptive time window. The results show that the proposed method can perform well under dynamic traffic conditions.

Chapter 8

- An improved spatial-temporal adaptive time window component based on shrinkage-thresholding method is proposed to consider the spatial and temporal correlations in travel time over multiple segments.
- The improved iterative VRI system with spatial-temporal adaptive time window is tested on a 9.7-km freeway with two consecutive segments. The results justify the potential advantages of the proposed method for capturing serious non-recurrent traffic congestions.

This thesis was typeset using L^AT_EX.

Part I

Foundations of the study

Chapter 2

Problem statements and literature review

This chapter presents a formal description of the travel time estimation problem and explores the literature on the associated estimation methods. As one of the alternative approaches, vehicle reidentification (VRI) has emerged due to its potential for effective tracking of the individual vehicles. Therefore, a general overview of the VRI system (e.g. the underlying principle of VRI and the detailed vehicle matching process) is provided in this chapter. Since this study focuses on developing the vision-based VRI system, a brief review of the sensing technology (i.e. intelligent video surveillance) is then conducted. Last but not least, this chapter provides a comprehensive review of the traffic automatic incident detection (AID) algorithms, which could be beneficial to the development of new AID algorithm under free flow condition (see Research Objective II).

2.1 Travel time estimation problem

Travel time, a period of time spent traveling between any two nodes of interest in the traffic network (Shao et al., 2013), is widely recognized as one of the best indicators of the quality of traffic facilities, since it is easy for both the transportation engineers and the travelers to understand. Traffic manager requires travel time to evaluate the performance of the road network, while the individual traveler desires such information to make a better

route decision for their journeys. Therefore, it is of great importance for us to estimate the travel time in an accurate and robust manner, which is also essential for the successful implementation of the advanced traveler information systems (ATIS) in the framework of intelligent transportation system (ITS) (Dharia and Adeli, 2003).

2.1.1 Problem description

Travel time estimation is still a challenging problem for several reasons. One of which is that travel time are by nature stochastic and dynamic (Quiroga and Bullock, 1998; Tam and Lam, 2008) due to the traffic network uncertainty (Clark and Watling, 2005). As noted in Luathep (2011), traffic networks are primarily exposed to two sources of uncertainty, i.e. uncertainty in traffic demand and supply. The demand uncertainty arising from the temporal variation (e.g. time of the day, day of the week) of travel demand can potentially cause recurrent traffic congestion and, hence, lead to travel time variability (Chen et al., 2011; Taylor, 2013). On the supply side, some unpredictable traffic scenarios (e.g. accidents, illegal parking and adverse weather) could disrupt the normal traffic flow and, consequently, affect the road capacity and lead to non-recurrent congestion (Chen et al., 2002; Lo et al., 2006). Therefore, travel time are heavily dependent on current traffic, physical, and environmental conditions that cause the travel time to exhibit stochastic and time-variant (i.e. dynamic) behavior. Mathematically speaking, travel time are random variables and the associated probability density distributions (PDF) vary with the time of day (e.g. the particular time period). More specifically, the travel time can be modeled as a discrete-/continuous-time stochastic process (Fu and Rilett, 1998). Let $\{TT(t), t \in N\}$ denote a discrete stochastic process, where $TT(t)$ is the travel time for vehicles arriving at the downstream station during time period t (e.g. a 5-minute-period). For a specified time period t , $TT(t)$ is a continuous random variable with its PDF denoted by $f(\cdot, t)$. In view of this, the dynamic travel time estimation problem would be to estimate the statistical parameters of the travel time, i.e. $\{\mu(t), t \in N\}$, where $\mu(t)$ is the mean value of vehicle travel time during time period t . Because of the dynamic nature of travel time, the mean value $\mu(t)$ may change substantially from time to time, which imposes a great challenge on the development of estimation methods for real-time application.

Another critical issue is that travel time cannot be directly measured from the traditional point sensors such as inductive loops and microwave sensors (Kwong et al., 2009). To overcome this difficulty, a large number of studies focused on utilizing the macroscopic

traffic parameters (e.g. traffic flow, density, and speed) to deduce the travel time between the discrete locations (which could be termed as **indirect methods**). These algorithms could be roughly divided into two groups: spot-speed-based method (see Section 2.1.2) and the flow-based method (see Section 2.1.3). Recently, considerable attention has been paid to using the emerging sensing technologies (e.g. Bluetooth, global positioning system, license plate recognition, and cellular phones) to directly track the individual probe vehicle for travel time estimation purpose, which eventually gives rise to the probe-vehicle-based method (see Section 2.1.4).

Before proceeding to discuss the detailed estimation methods, the following two comments should be taken into account.

- First, it is necessary for us to briefly explain the terms "travel time estimation" and "travel time prediction". Travel time estimation calculates travel time $\mu(t)$ based on collected traffic information up to the current time point (i.e. period t), whereas travel time prediction forecasts the travel time $\mu(t + \Delta t)$ up to a time point (i.e. $t + \Delta t$) in the future (Lint, 2004). In this study, we focus on travel time estimation on freeway system, i.e. we estimate how long it takes vehicles to travel along a freeway route when they arrive at the downstream station.
- Since this study attempts to estimate travel time along a freeway, the network-wide (i.e. link) travel time estimation is then out the scope of this research. As a matter of fact, link travel time estimation is a highly under-specified problem, where the number of traffic detectors is typically much less than the number of unknown parameters (i.e. mean travel time on each link) of interest. We will investigate this problem and present some preliminary results in the future work (see Section 9.2.2). Also, a detailed review regarding network-wide travel time estimation can be found in Chapter 9.

2.1.2 Spot-speed-based method

The rational behind this method is quite straightforward. Given the distance L between two consecutive detectors, the travel time is defined as

$$T = \frac{L}{v} \tag{2.1}$$

2.1 Travel time estimation problem

where v is the average speed between the two detectors. In such a case, the derivation of the average speed v would be the major concern. As one of the most widely used algorithm, the extrapolation method is then developed based on the assumption that spot-speeds are representatives of the average travel speeds on the roadway segments (Turner et al., 1998). However, in practice the vehicle speeds may not remain constant (especially on the urban road network). Thus, some improved methods were proposed such as half-distance approach and minimum speed approach (Lindveld et al., 2000; Cortés et al., 2002).

In a more complicated case (i.e. urban road network), stop-and-go situation usually occurs and, hence, the vehicle speed would change dramatically in traveling. In this case, the aforementioned extrapolation methods may not be applicable. To compensate for this, the trajectory-based methods were proposed (Lint and Zijpp, 2003; Ni and Wang, 2008; Sun et al., 2008). By utilizing some smoothing schemes (e.g. piecewise linear function, quadratic function), it is possible for these approaches to reconstruct the hypothetical vehicle speed trajectory as a function a space and time. The travel time of this vehicle can be easily calculated through the associated vehicle speed trajectory (see Figure 2.1). The per-

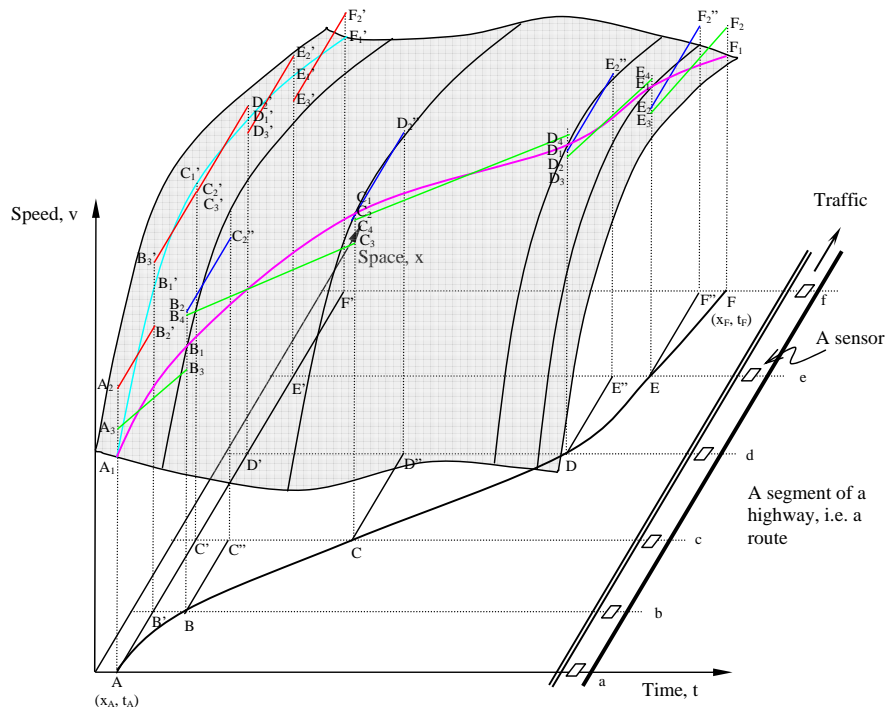


Figure 2.1: Demonstration of the trajectory-based method (source: (Ni and Wang, 2008))

formance of these methods is then heavily dependent on the accuracy of the collected spot

speed and the adopted smoothing techniques. According to some literatures concerning the vehicle speed estimation (Sun and Ritchie, 1999; Wang and Nihan, 2000), the accuracy of speed measurement from the inductive loops largely depends on the sampling rate of the sensor and the length of the vehicle. Simply put, the traditional sensor (i.e. inductive loops) may not be capable of measuring the speed of the "short" vehicles accurately. In addition, some studies also suggested that the use of these spot-speed based methods would result in large errors when it comes to a serious traffic congestion (Lindveld et al., 2000; Li et al., 2006).

In light of the above-mentioned problems, some researchers tried to investigate the feasibility of estimating travel time using other reliable macroscopic traffic parameters such as traffic flow and volume. In the following part, the detailed review of the traffic flow-based-method is presented.

2.1.3 Traffic-flow-based method

To handle the difficulties encountered by spot-speed-based methods, several studies were conducted to estimate travel time by using the other traffic data (e.g. traffic flow and density), which could also be readily extracted from the point sensors. An extensive literature review of these methods was conducted by Sisiopiku and Roupail (1994). Coifman (2002) utilized a linear approximation of the flow-density relationship to estimate travel time from dual loop detector data. In addition, a rich body of research utilized the macroscopic traffic flow model to represent the propagation of the traffic stream through the road network (Nam and Drew, 1996; Petty et al., 1998; Nam and Drew, 1999; Vanajakshi et al., 2009). By applying the principal of FIFO and flow conservation, the aggregated travel time information could be obtained. Although these approaches appear promising when traffic congestion is present, the successes of these methods are based on the stringent FIFO assumption. In practice overtaking between vehicles, however, may frequently exist and, accordingly, these methods may not work well under these scenarios.

Recently, considerable attention has been focused on utilizing the emerging sensing technologies (e.g. Bluetooth, global positioning system, license plate recognition, and cellular phones) to track the individual probe vehicle such that the associated travel time can be easily calculated (which can be referred to as probe-vehicle-based method). In what follows, a brief review regarding these methods is presented.

2.1.4 Probe-vehicle-based method

As discussed previously, most of the indirect travel time estimation methods focused on utilizing the traditional point sensors (e.g. inductive loops). In recent years, the rapid development of information and communication technologies has provided us a chance to measure the travel time of each probe vehicle directly. Various advanced sensing technologies, such as Bluetooth (Wasson et al., 2008; Haghani et al., 2010; Quayle et al., 2010), global positioning system (Hofleitner et al., 2012), license plate recognition technique (Chang et al., 2004), and cellular phones (Rose, 2006), have been incorporated to assign an unique identity (e.g. media access control address, plate number, and wifi address) to the probe vehicle. By the accurate matching of vehicle identities, the travel time of probe vehicles can be easily calculated. Moreover, many researchers have proposed various models to use this new source of data (i.e. probe-vehicle data) for other transport applications. Castillo et al. (2008) have included, in addition to link counts, the license plate matching data for path flow estimation which was then formulated as a least square problem. Zhou and Mahmassani (2006) extended the bi-level DTA approach for dynamic OD estimation by using the probe-vehicle data.

Despite their theoretical simplicity and ease of practical implementation, the probe-vehicle-based methods still suffer from two serious limitations. First, the low-level of market penetration of the probe vehicles would potentially lead to biased estimation of the mean travel time (Dion and Rakha, 2006). The vehicles without proper probe equipment (e.g. GPS receiver, Bluetooth and high-quality license plate image) cannot be tracked and, consequently, a large amount of travel time data cannot be collected. In addition, the continuous vehicle tracking based on the unique identity could also raise privacy concerns (Hoh et al., 2012; Ohkubo et al., 2005).

In this case, the vehicle reidentification (VRI) scheme, which neither intrudes driver's privacy, requires installation of on-board tag/equipment, nor needs permission to obtain the identification, provides an alternative way for travel time estimation. As opposed to using the unique vehicle identities, VRI focuses on utilizing the non-unique vehicle signatures (e.g. waveform, vehicle length, and vehicle color), which allows for anonymously tracking the vehicles. Also, the penetration rate would be 100% in principle, since no in-vehicle equipment is required (i.e. non-intrusive). As this study concentrates on developing a self-adaptive VRI system for dynamic travel time estimation, an overview of a typical VRI system is presented in Section 2.2.

2.2 Overview of vehicle reidentification (VRI)

Generally speaking, VRI is the process of matching vehicle signatures from one traffic detector to the next in the road network. Along with the identification of individual vehicles across several traffic detectors, the associated vehicle signatures can also be extracted. As opposites of the vehicle identities in the probe-vehicle-based method (Section 2.1.4), the vehicle signatures within the VRI framework are not unique. Therefore a robust and efficient vehicle signature matching algorithm is required for the practical implementation of VRI. To sum up, a typical VRI system usually consists of two parts: vehicle signature extraction and vehicle signature matching.

2.2.1 Vehicle signature extraction

It is quite obvious that the process of vehicle signature extraction is closely related to the traffic sensors. Different traffic surveillance systems may result in different vehicle signatures. Coifman and Cassidy (2002) and Coifman and Krishnamurthy (2007) utilized vehicle length measurement derived from inductive loops as the vehicle signature, while Sun et al. (1999) directly used the inductive waveform for signature matching. Since the length measurement as well as the waveforms from inductive loops is heavily dependent on the vehicle velocity and sampling rate of loop detectors, the additional signature normalization process is needed for eliminating the measurement errors¹. In view of this, Kwong et al. (2009) investigated the feasibility of utilizing the speed invariant data (i.e. peak value of magnetic signal) from magnetic wireless sensors for VRI. With the advancement in image processing, several studies also developed VRI system based on the vehicle color information (e.g. Kamiyo et al., 2005; Sun et al., 2004). Due to the poor quality of vehicle image and privacy concerns, some closely related research focused on utilizing the partial number plate information for VRI purpose (Watling and Maher, 1992; Watling, 1994). Also, some other emerging traffic sensors, such as microwave based detectors and axle sensors, have been utilized for vehicle matching (Cetin et al., 2011; Tawfik et al., 2002).

By using the sensing technologies mentioned above, the associated vehicle signature (e.g.

¹A more detailed review of the history and evolution of the inductive-loop-based VRI could be found in Jeng (2007).

length, color, axle space, and waveform) denoted as X , can be extracted. The following task of VRI is then to make matching decision based on these vehicle signatures (i.e. vehicle signature matching method).

2.2.2 Vehicle signature matching method

Consider a vehicle i arrives at downstream station, and its associated vehicle signature and arrival time are, respectively, denoted as X_i^D and t_i^D (see Figure 2.2). The vehicle

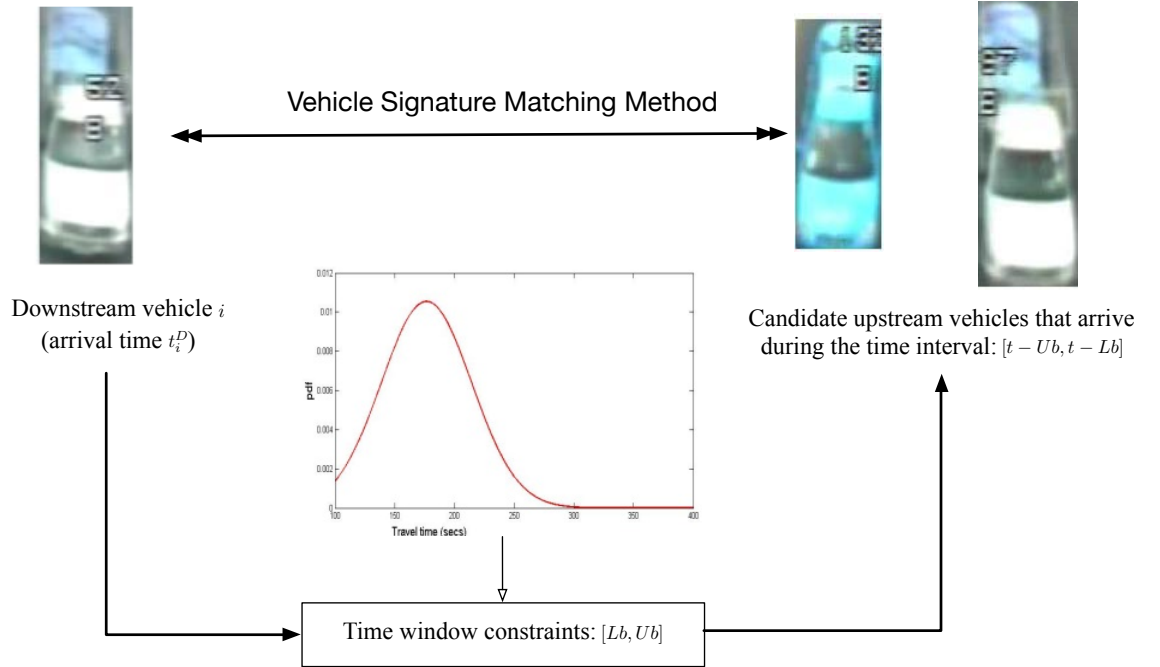


Figure 2.2: Demonstration of the time window constraints in VRI system

signature matching method is then devised to find the corresponding vehicle (i.e. vehicle with similar signature) at upstream station. For practical implementation, the time window constraints are then introduced to rule out the unlikely candidate upstream vehicles for improving the computational efficiency and matching accuracy. Based on the historical travel time data, a time window, i.e. $[Lb, Ub]$, is derived for setting the upper and lower bounds of the vehicle travel time. In such a case, the search space \mathcal{S}_i (i.e. the set of the candidate upstream vehicles) can be well defined as shown in Figure 2.2, and the signature matching process can be performed between X_i^U and its search space \mathcal{S}_i . As a matter of fact, the concept of time window (which is also referred to as search space reduction in [Jeng et al. \(2010\)](#)) has been commonly adopted in the existing VRI systems.

2.2 Overview of vehicle reidentification (VRI)

For the matching problem mentioned above, there already exists a broad field of well studied algorithms. Roughly speaking, vehicle signature matching algorithms can be divided into two groups, i.e. distance-based methods and probabilistic methods. For the distance-based methods, appropriate distance measures are incorporated to represent the similarity $d(i, j)$ between a pair of vehicle signatures $\{(X_i^U, X_j^D) | j \in \mathcal{S}_i\}$. The corresponding upstream vehicle for downstream vehicle i is then given by

$$\arg \min_{j \in \mathcal{S}_i} d(i, j) \quad (2.2)$$

In other words, the downstream vehicle is matched to the upstream one with the smallest signature distance (e.g. Coifman, 1998; Sun et al., 2004; Kamijo et al., 2005). Because of the non-uniqueness of the vehicle signatures, the distance-based methods, however, may not work well under some circumstances, especially when the feature data is corrupted by the potential noise. To account for the uncertainty involved in the vehicle signature, the probabilistic approaches (e.g. Huang and Russell, 1998; Kwong et al., 2009; Cetin et al., 2011) are developed, in which the signature data are treated as random variables and a probabilistic measure is incorporated for the reidentification decision. Mathematically speaking, the signature distance $d(i, j)$ is a random variable and the underlying statistical model is built up from the training dataset. By applying Bayesian statistics, a matching probability indicating the likelihood of each pair of signatures belonging to the same vehicle, i.e. $P(i \text{ matches } j | d(i, j))$, is then provided and the result is given by

$$\arg \max_{j \in \mathcal{S}_i} P(i \text{ matches } j | d(i, j)) \quad (2.3)$$

Simply put, within the framework of statistical matching approaches, the downstream vehicle is matched to the upstream one with the highest "chance" given the observed signature distance.

2.2.3 Discussion of the existing VRI systems

Table 2.1 compares different types of VRI systems in terms of the sensing technologies they relied on and the associated vehicle signature matching methods¹. A number of comments should be made with respect to the existing VRI systems.

¹The readers can refer to Section 4.1 for a more comprehensive review of the existing VRI systems.

Table 2.1: Summary of existing VRI^a systems

VRI system	Sensor technology	Signature data ^b	Matching method	Capability	
				Multiple-lane matching	Overtaking constraint
Coifman (1998)	Single loop detector	Vehicle length	Distance-based	× ^c	× ^d
Coifman and Cassidy (2002)	Dual loop detector	Vehicle length	Distance-based ^f	×	×
Coifman and Krishnamurthy (2007) ^e	Loop detector	Vehicle length	Distance-based	✓	✓
Sun et al. (1999); Sun et al. (2004)	Loop detector	Waveform	Distance-based	×	×
Lin and Tong (2011)	Loop detector	Vehicle length	Distance-based	×	×
Oh et al. (2007)	Blade sensor	Blade signatures	Distance-based	✓	✓
Cetin et al. (2011)	Axle sensor	Axle weight and spacings	Statistical method ^g	✓	✓
Kwong et al. (2009)	Magnetic sensor	Peak value of waveform	Statistical method	×	×
Kamijo et al. (2005)	Vision-based sensor	Vehicle feature ^h	Distance-based	✓	×

^a In general, vehicle reidentification (VRI) system consists of two parts: sensor technology and vehicle signature matching method.

^b Detailed vehicle signature derived from the traffic sensor.

^c The corresponding VRI system cannot re-identify/match the vehicle across multiple lanes.

^d Overtaking between vehicles is not allowed.

^e The corresponding VRI system only reidentifies those vehicles with distinct length measurements (i.e. the "long" vehicles).

^f Distance-based method tries to find the matched pairs of vehicles with minimum distance (i.e. most similar).

^g Statistical method tries to find the matched pairs of vehicles with minimum "statistical" error.

^h Vehicle color, length and type.

2.2 Overview of vehicle reidentification (VRI)

1. As explained in Section 2.2.2, the time window constraints are essential for the efficient implementation of VRI system. However, it is noticed that normally the time window is derived from historical travel time data (i.e. fixed time window), which cannot really reflect the current traffic condition. Under dynamic traffic condition, the recurrent and non-recurrent traffic congestion may occur, which may eventually lead to the substantial changes in travel time. Therefore, a self-adaptive time window component is required so that the VRI system can be applicable for dynamic travel time estimation purpose (see Chapter 7).
2. It is also observed that most of the existing VRI systems are focusing on improving the matching accuracy. Some research even imposed stringent assumptions on vehicle traveling behavior (e.g. no overtaking and no lane-changing) so that the matching accuracy can be improved. From the perspective of travel time estimation (i.e. mean travel time), the matching accuracy, however, may not be the major concern. The mean travel time can be obtained using a subset of vehicles that have "distinctive" signatures. An appropriate selection strategy (e.g. sampling and thresholding) may potentially contribute to the estimation accuracy.
3. Due to the worldwide deployment of inductive loop sensors, a large number of studies focused on utilizing the measurements derived from the inductive loops. However, it should be noted that the raw signature data obtained from loop detectors may be speed-dependent, which means that a vehicle traveling at different speeds may generate different loop signatures. This phenomenon may potentially undermine the performance of the VRI system.

To this end, this study aims to propose a VRI system based on the emerging intelligent video surveillance technology (IVS), in which overtaking between vehicles as well as the reidentification across multiple lanes are both allowed. With the development of the image processing techniques and the network bandwidth, the intelligent video surveillance technology plays a more and more important role in the transport applications for safety and security purpose (e.g. [Beymer et al., 1997](#); [Tseng et al., 2002](#); [Wang et al., 2007](#)). Compared with the traditional inductive loop sensors, IVS enjoys several advantages as follows ([Klein et al., 2006](#)).

- First, IVS technology is capable of monitoring multiple lanes and can function as zone detectors rather than point sensors (e.g. magnetic sensors and inductive loops).

- IVS can provide us the speed-independent vehicle signature. Various detailed and vivid vehicle features (e.g. vehicle color, length, and type), which are independent of the vehicle speed, can be extracted. However, it should also be noted that the above-mentioned vehicle features are not readily obtainable from the video camera. Various image processing techniques are then employed and performed on the video image data to extract the desired information.

Since IVS plays a fundamental role in our research and serves as the main building block for our VRI system, a brief review regarding the framework of intelligent video surveillance is presented in Section 2.3.

2.3 Framework of intelligent video surveillance

As the name suggests, intelligent video surveillance (IVS) aims to provide real-time and automatic interpretation of scenes (e.g. detecting, tracking and recognizing objects of interest) by analyzing the images acquired from the video cameras. Therefore, IVS can be viewed as a multidisciplinary field closely related to information and communication, signal/image processing, computer vision and pattern recognition (Dufour, 2013). The advances in information and communication technologies has led to the worldwide deployment of the camera networks which provide the possibility for remote manual monitoring and surveillance. Moreover, the rapid development of image processing techniques enables us to efficiently and automatically extract the useful information from huge amount of video records. The following high-level processing based on computer vision and pattern recognition technologies would allow for better understanding of the scenes (e.g. activity analysis) in the video record.

Figure 2.3 shows the overall framework of the intelligent video surveillance system. In general, a typical IVS consists of three critical components, i.e. video sensor networks, low-level processing and high-level understanding. Video sensor networks are responsible for real-time monitoring and collection of the raw video record, while low-level processing focuses on digitalizing the collected image in a form suitable for further computer processing, such as image enhancement, image denoising and image deblurring. The video stream after preprocessing would be fed into the component of video analytics (see Figure 2.3) for high-level understanding. Single camera analytics, also referred

2.3 Framework of intelligent video surveillance

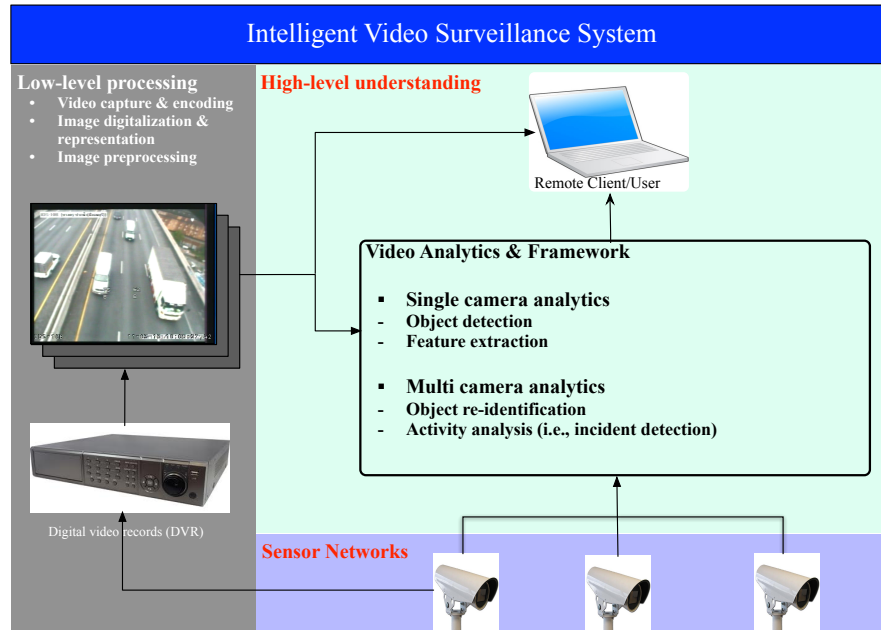


Figure 2.3: General framework of IVS

to as intra-camera analytics, deal with the video stream within the single camera view. Various image processing techniques are explored in an attempt to detect the object of interest and its associated features. Since the view of single camera surveillance is finite and limited, the multi camera analytics, which aim to monitor a wider area (e.g. tracking vehicle/pedestrian across the traffic network), are required. Therefore, one of the essential capabilities of the multi camera analytics is being able to re-identify the object across different cameras (i.e. object reidentification). The following activity analysis would enable us to gain a better understanding of the monitored area (e.g. travel time estimation, incident detection).

It is noted that the introduced high-level IVS is closely related to our research topic, i.e. vehicle reidentification based on video image data. As a matter of fact, the proposed VRI system can be viewed as an application and variant of the object reidentification (ORI). This section focuses on presenting a brief review of the first two components of IVS (i.e. video sensor networks, and low-level processing). A more detailed discussion on the high-level IVS (e.g. image processing techniques used for vehicle feature extraction) can be found in Chapter 3. Also, the readers can refer to two recent review papers, i.e. [Valera and Velastin \(2005\)](#) and [Wang \(2013\)](#) for a more comprehensive review of the history and evolution of IVS.

2.3.1 Video sensor networks

As the basic component of IVS, the video sensor networks are devised to capture all possible information (i.e. raw video) from the physical environment at the key locations (i.e. nodes) by utilizing the video cameras. In this sense, the video sensor networks are commonly comprised of a set of sensor nodes, and the communication infrastructures/devices that are responsible for the transmission of video data between the nodes (Cordeiro and Assuncao, 2012).

Generally speaking, a sensor node consists of a camera for video capturing and an associated video encoder to compress the video for transmission. Due to the advantages in capturing high-quality image, the digital charge-coupled device (CCD) has been used in the surveillance cameras (e.g. CCTV system (Dadashi et al., 2009) and Autoscope (Michalopoulos, 1991)). However, it is worthwhile to notice that the CCD based cameras are power consuming and relatively costly. Recently, the complementary metal-oxide semiconductor (CMOS) image sensors (Spivak et al., 2011) have received considerable attention because of the energy-savings opportunities and the economically feasibility they present for large-scale application.

With the advancement of information and communication technologies, the communication rates between the sensor nodes increase dramatically, which eventually gives rise to the development of the wireless video sensor network (e.g. Soro and Heinzelman, 2005; Aghdasi et al., 2008). Therefore, the specific dedicated communication infrastructure may not be absolutely necessary in the future. Nevertheless, it should be noted that a higher communication rates would lead to a higher energy cost. In this case, how to improve the energy efficiency would become the major concern for the video sensor networks.

To sum up, there are still two problems need to be tackled for the video sensor networks, namely (1) the need of improving the video quality, and (2) the need of improving the energy efficiency for large-scale application. Actually, these two problems are closely related to each other. The high video image quality would inevitably lead to the transmission of massive video data and, hence, increase the energy cost. Note that this study does not attempt to resolve these two problems since we aim to utilize the existing video sensor networks. The main contribution of this study is developing the generic VRI system, which would still be applicable when the video quality is poor.

2.3.2 Low-level image processing

Upon completion of the collection of the raw video record from the video sensor networks (Section 2.3.1), a further low-level processing is performed so that the collected image stream could be digitalized for computer processing (i.e. image digitalization) and improved in terms of the image quality (e.g. image denoising and deblurring).

According to Jähne (2005), an image would constitute a spatial distribution of the irradiance at the plane, which means that image digitalization is the process of measuring the irradiance across the image plane. However, it is worthwhile to notice that computers cannot deal with continuous images but only arrays of digital numbers, which eventually leads to the concept of digital image (Ghosh, 2013). As shown in Figure 2.4, a digital

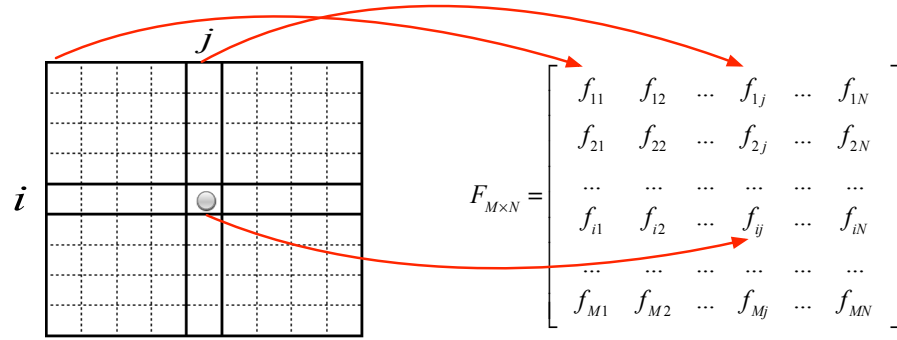


Figure 2.4: Digital image representation

image is usually represented by a two-dimensional matrix of intensity samples, each of which is represented by using a limited precision. A point on the two-dimensional (e.g. $M \times N$) grid (i.e. the left-hand-side of Figure 2.4) is called a pixel and the associated pixel value is denoted as f_{ij} . In such a case, the gray digital image is then represented by the intensity matrix $F_{M \times N}$ (i.e. the right-hand-side of Figure 2.4), where the element value f_{ij} is quantized into 256 gray values (i.e. $1 \leq f_{ij} \leq 255$). For a color digital image, The RGB color model (Ladson, 2005) where red, green, and blue light are added together to reproduce the colors, is utilized. Mathematically speaking, the color digital image is then jointly represented by three matrix, i.e. $\{F_{M \times N}^{(R)}, F_{M \times N}^{(G)}, F_{M \times N}^{(B)}\}$, where each of them respectively represents the red, green, and blue channel of the image.

Before proceeding to the high-level understanding of the video image, various preprocessing techniques (e.g. image contrast enhancement, image denoising and image deblurring) need to be performed on the digitalized image in the hope of improving the overall image

quality. Due to the reduced and perhaps nonlinear image amplitude range, the poor contrast between the foreground object (i.e. vehicle) and background often exists in the digital image. In such a case, the necessary image enhancement, such as histogram equalization (e.g. Saha et al., 2010; Acharya and Ray, 2005) would greatly contribute to the high-level processing (e.g. object detection and feature extraction) at the later stages. Also the digital image may tend to suffer from two inherent problems, namely (1) the occurrence of the potential noise in the image (e.g. electrical sensor noise and channel transmission errors), and (2) the presence of image blur (e.g. lens blur, Gaussian blur and motion blur caused by subject movement) during the recording of a digital image. Therefore, the reconstruction (i.e. image denoising and deblurring) of the original image $I_{M \times N}$ from the contaminated measurement $F_{M \times N}$ plays an important role in the low-level IVS.

For the image denoising problem, the underlying mathematical model can be described by

$$F = I + \epsilon \quad (2.4)$$

where $F \in \mathbb{R}^{MN}$ is the vectorized grayscale image and I is the original image, whereas ϵ is the white noise. Since noise added to an image generally has a higher-spatial frequency spectrum, the simple low-pass filtering technique (Abhari et al., 2012) is employed to remove the noise. Later on, the other filters (e.g. mean filter (Wang et al., 2012), winner filter (Zhang et al., 2012) and adaptive filter (Nasri et al., 2013)) have also been introduced for image denoising. With respect to the image deblurring problem, the underlying mathematical model can be described by

$$F = KI + \epsilon \quad (2.5)$$

where the $K \in \mathbb{R}^{MN \times MN}$ represents the blurring (i.e. convolution) operator. It is easily observed that this is an inverse problem, which is to recover as much information (i.e. I) as possible from the given data (i.e. F). As a matter of fact, this inverse problem has been widely studied and solved as the large-scale (e.g. with extremely large image size) optimization problem (e.g. Yuan et al., 2007; Dong et al., 2011). Figure 2.5 shows one illustrative example of the traffic image deblurring. Due to the motion blur, the collected traffic image may be of generally poor quality. The essential image preprocessing is then required for eliminating the potential noise and image blurry (Figure 2.5).

As illustrated above, it is expected that the richness of traffic data provided by IVS (i.e. vivid traffic image) could potentially contribute to the development of the vision-based



Original image

Blurry image

Restored image

Figure 2.5: Illustrative example of image deblurring caused by motion blur

VRI system (see Chapter 4). Also, the proposed VRI method together with the video surveillance technology enable us to handle the non-recurrent traffic incidents more efficiently in the sense that the incidents can be promptly detected and validated through the video image data (see Chapter 5). In what follows, we briefly review the traffic incident detection algorithms.

2.4 Traffic incident detection algorithms

One major problem associated with the rapid growth of large cities is the increase in traffic congestion and incidents. In these congested traffic networks, one minor incident could cause serious traffic delays and have far-reaching consequences for safety, congestion and pollution. In addition, statistics also suggested the high chance of a more severe secondary accident following the initial incident (particularly on a high-speed network, e.g. freeway). Therefore, in order to overcome the aforementioned difficulties, considerable effort has been devoted to the development of an efficient traffic incident management system (TIMS). The roles of TIMS are to efficiently detect the incident and then provide a series of traffic information to drivers to alleviate the impact/delay caused by the incident. In general, TIMS includes the following steps, i.e. i) incident detection, ii) incident response, and iii) incident clearance (Chang and Su, 1995; Ozbay and Kachroo, 1999). As the first step, incident detection plays a critical role in incident management. It affects consequent actions of the following steps and determines the efficiency of the whole system. To this end, this review focuses on the comparison and evaluation of available incident detection algorithms for both congested traffic conditions and light traffic conditions.

2.4.1 Incident detection system

An incident detection system primarily consists of two components: traffic data collection and data mining approach. Data collection is the process of measuring traffic parameters from the traffic surveillance technologies (e.g. loop detectors, magnetic sensor, GPS-based sensor, intelligent video surveillance). Data mining approaches refer to the algorithms that are utilized for detecting incidents through analyzing the traffic data collected from the traffic sensors. It is quite obvious that the success of incident detection system relies on the effectiveness of data collection and the robustness of the corresponding data mining approaches. Therefore, a combined consideration of the available sensing technologies and their corresponding data mining algorithms is necessary for the thorough evaluation of the incident detection systems. In the following parts, the incident detection algorithms regarding two specific traffic conditions (i.e. heavy and light traffic) will be discussed.

2.4.2 Incident detection algorithms for congested traffic condition

Most existing algorithms were developed specifically for detecting incidents under heavy traffic conditions (e.g. the California algorithm series). The assumption behind these algorithms is that the traffic parameters (e.g. travel time, traffic flow, and traffic delay) would change dramatically when incidents occur under congested traffic. Generally speaking, these algorithms can be broadly into five groups: 1) comparative algorithms; 2) statistical algorithms (e.g. Bayesian networks); 3) filtering algorithms; and 4) dynamic traffic modeling algorithm. Because of the worldwide deployment of inductive loop sensors, most studies focuses on detecting incidents using the data collected from the loop detectors. Nevertheless, some other algorithms (e.g. image processing method) also consider the emerging traffic surveillance technologies.

Owing to their computational and theoretical simplicity, California algorithms (Payne and Tignor, 1978; Payne and Thompson, 1997) are the most widely known comparative algorithms. The underlying assumption of these algorithms is that an incident would normally result in a substantial increase in upstream occupancy while simultaneously reducing downstream occupancy. Thus, a direct comparison between the upstream and downstream occupancy data obtained from the consecutive loop detectors would enable us to

2.4 Traffic incident detection algorithms

determine the occurrence of an incident. An incident alarm is issued if the difference between the occupancy exceeds a predefined threshold. In order to reduce the false alarm rate, the decision tree technologies were also introduced. Several occupancy differences were discussed and analyzed in a decision tree structure (see Figure 2.6). It is quite obvi-

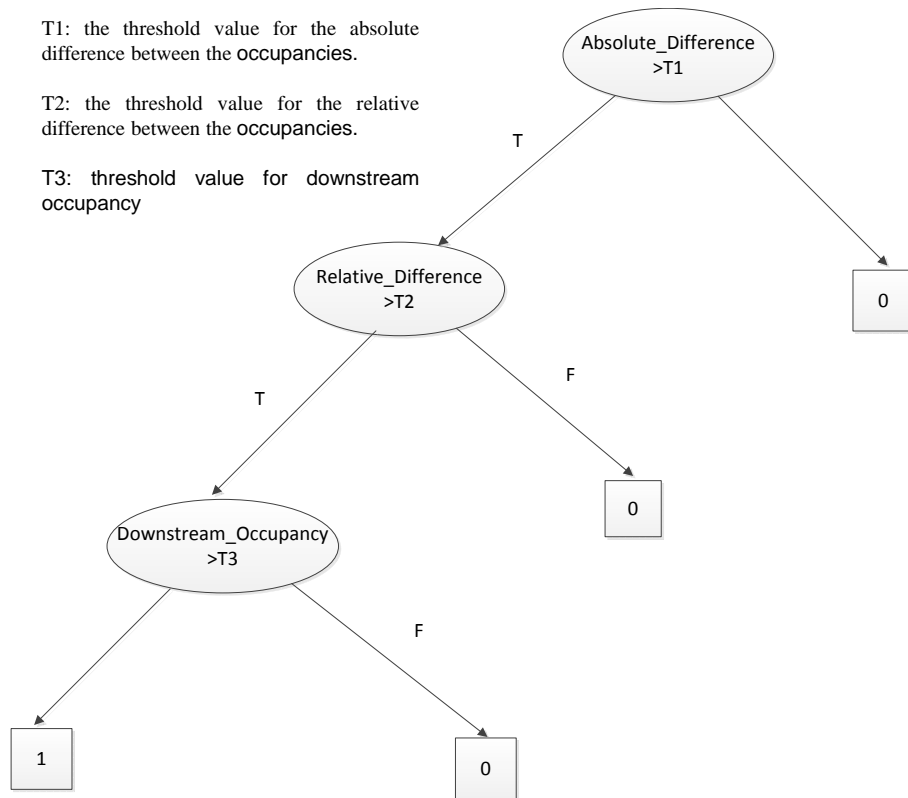


Figure 2.6: The basic California algorithms (source: (Payne and Tignor, 1978))

ous that the success of the comparative algorithms is heavily dependent on the accuracy of the traffic sensor technologies. However, it is unavoidable that the traffic data contains potential noise, especially under the congested conditions.

To compensate for this, the so-called statistical incident detection algorithms are proposed. These approaches adopt standard statistical technique to determine whether the collected traffic data (i.e. occupancy) differ "statistically" from the estimated traffic parameters. Levin and Krause (1978) utilized Bayesian statistics to compute the likelihood of an incident. Within the Bayesian framework, it is assumed that the collected traffic data is a random variable and follows a statistical distribution. Some prior knowledge (*prior* distribution) about the likelihood of an incident happening are also calibrated from the historical data. Based on the aforementioned statistical model, a *posterior* probability regarding the likelihood of an incident is then obtained.

The filtering algorithms (e.g. [Stephanedes and Chassiakos, 1993a](#); [Stephanedes and Chassiakos, 1993b](#)) are also designed to remove the noise from the collected traffic data. As opposed to introducing a statistical model to represent the uncertainties of the traffic data, these filtering algorithms use the typical filters (e.g. low-pass filter, Kalman filter) to eliminate noises directly from the data. After the filtering process, some comparative algorithms are utilized to determine the occurrence of incidents.

However, the accuracy of those algorithms stated above, relies on the availability and diversity of the incident data, which requires a dense deployment of the traffic sensors along the traffic network. Besides, those approaches also fail to consider the temporal evolution and temporal/spatial correlation of the collected traffic data. In order to overcome these difficulties, several researches focused on the development of dynamic traffic modeling algorithms for incident detection (e.g. [Willsky et al., 1980](#); [Lee and Taylor, 1999](#); [Balke et al., 2005](#)). These algorithms utilize the dynamic traffic flow models (e.g. queue model, cell transmission model (CTM)) to capture the dynamic nature of traffic and estimate the traffic parameters (e.g. travel time, speed, traffic flow). By comparing the real-time measurements and estimation of these traffic parameters, the abrupt changes may be identified in real time and, hence, the incident occurrence may be recognized.

2.4.2.1 Incident detection algorithms for light traffic conditions

Incident detection under light traffic condition is difficult as a drop in the traffic capacity due to an accident (e.g. one lane blocking) may not cause any delay for traffic passing through that location. Therefore, it is not feasible to detect an incident under light traffic condition based on measuring the abnormal delay or sudden change in traffic flow pattern.

To this end, some studies focused on utilizing the emerging traffic surveillance technologies (i.e. intelligent video surveillance) to detect a stationary or slow-moving vehicle (see [Figure 2.7](#)) in the traffic network so as to detect the incident (e.g. [Wu et al., 2008](#); [Shehata et al., 2008](#)). These image processing algorithms, however, require an extensive deployment of video cameras at all key locations.

On the other hand, for a closed highway system if one can trace all vehicles along designated points on the highway, a disappearance of a certain vehicle movement from one point to another can be detected and identified as a potential accident. Based on this prin-



Figure 2.7: Image processing method

principle, [Fambro and Ritch \(1979\)](#) designed an incident detection algorithm for low volume traffic condition using vehicle count data obtained from the loop detectors. When a vehicle passed the upstream detector, the corresponding speed and arrival time of the vehicle is recorded. Accordingly, the projected arrival time of this vehicle at downstream site was also calculated based on the assumption that the vehicle's speed remains constant over short segment of freeway. Under incident-free condition, we can expect the appearance of this vehicle during its arrival time interval at downstream site (i.e. the link counts would increase during this time period). Thus a disappearance of this vehicle would imply a potential accident. Owing to its computational efficiency and theoretical simplicity, this algorithm works well under some special circumstances. However, the performance of this approach is greatly dependent on the accuracy of the link count data and the estimation of the projected arrival time. In general case, the unreliability of the traffic data and the frequent overtaking between vehicles would seriously undermine the performance of this incident detection algorithm in terms of the incident detection time.

In light of this, this study attempts to investigate the feasibility of utilizing the VRI scheme (see Section 2.2) for tracking and identifying the "missing" vehicle such that the incident could be detected promptly. The detailed work is presented in Chapter 5.

Chapter 3

High-level intelligent video surveillance

In this chapter we introduce and explain the high-level intelligent video surveillance (IVS), which consists of two critical components, i.e. single-camera analytics (Section 3.2) and multi-camera analytics (Section 3.3). The detailed image processing techniques involved in each component will be presented in the context of transportation analysis (e.g. vehicle detection, tracking, and feature extraction). Section 3.4 further clarifies the relationship between high-level IVS and the associated vision-based VRI system. As the ultimate goal of this study is dynamic travel time estimation, Section 3.4 also explains the two possible research directions in the development of VRI, which eventually lead to the work presented in Part II and Part III of this thesis, respectively.

3.1 Introduction

High-level intelligent video surveillance not only provides real-time monitoring (e.g. traffic data collection) by analyzing images from single camera, but also performs activity analysis by utilizing continuous video sequences from adjacent/multiple cameras. In other words, the high-level processing of IVS is comprised of two parts, i.e. single-camera analytics and multi-camera analytics.

From the viewpoint of intelligent transportation system, the objects of interest in a video record would be the vehicles. Therefore, the first step of single-camera analytics is the

vehicle detection, which is also referred to as the foreground object detection in image processing. Then the continuous detection of the very same vehicle (i.e. tracking) in the single camera (Yilmaz et al., 2006) would allow for the further collection of the extrinsic vehicle data, such as vehicle speed, and its arrival time. Also, following the vehicle detection process, the intrinsic vehicle feature data (e.g. vehicle color, length, and type) can also be extracted by applying various image processing techniques.

With regard to multi-camera analytics, the major task would be object reidentification (ORI), which aims at re-identifying the same object appearing in adjacent cameras by only using its visual features extracted from the single-camera analytics (Javed et al., 2005). Following the concept of ORI, various studies have been conducted to match the individual pedestrians (i.e. people reidentification) in public places (e.g. airport and road network) relating to safety and security (e.g. Farenzena et al., 2010; Mazzon and Cavallaro, 2012). In such cases, the matching accuracy associated with the multi-camera analytics would be the major concern. The mismatches caused by the pose variations of objects and illumination changes in different cameras could seriously undermine the performance of multi-camera analytics in terms of safety and security.

Although vision based VRI and people reidentification (PRI) may share some common features (e.g. feature extraction process, underlying matching method), there are still several major differences between them. One of which is that the ultimate goal of VRI is to estimate dynamic travel time, whereas PRI only focuses on improving the matching accuracy. From the perspective of travel time estimation, the high matching accuracy of individual vehicles is sufficient but not necessary for obtaining reliable travel time estimates¹. This phenomenon provides us an alternative way to estimate travel time through the "proper" usage of the VRI system. In other words, the proposed self-adaptive vision-based VRI system, which can also be viewed as a variant of PRI, is specifically tailored for dynamic travel time estimation purpose.

In what follows, the detailed introduction and explanation regarding each component of high-level IVS will be presented. Section 3.2 introduces the various image processing techniques that used for vehicle detection and feature extraction within the single-camera environment. A further explanation of the tasks and the applications (PRI) of multi-camera analytics is presented in Section 3.3. In Section 3.4, a preliminary comparison between

¹Under some circumstances, a suitable post-processing on the individual travel time data can also enable us to accurately estimate the mean travel time.

PRI and VRI is conducted so that two possible research directions have been pointed out. Finally, we close this chapter with conclusion remarks.

3.2 Single-camera analytics

In general single-camera analytics is performed in two stages, namely (1) object detection, and (2) feature extraction. As the name suggests, object detection is responsible for identifying the object of interest from the video record (e.g. moving vehicle), whereas feature extraction is the process of collecting the associated object features for further analysis in multi-camera analytics.

3.2.1 Object detection

Object (e.g. vehicle) detection from video record plays a fundamental role in single-camera analytics. The success of object detection largely depends on the degree to which the moving object (e.g. vehicle) can be distinguished from its surroundings (i.e. background). Thus the first and foremost step is background estimation, which is completed by calculating the median of a sequence of video frames (Zhou et al., 2007). The foreground object (vehicle) can then be obtained by performing background subtraction and automatic image segmentation (Otsu, 1979). Figure 3.1(a) shows the gray image of the background of a freeway station, while Figure 3.1(b) demonstrates a video frame in which the detected vehicles are surrounded by bounding boxes. Once the individual vehicle crosses the red horizontal line (see Figure 3.1(b)), the vehicle image in the associated surrounding box will be clipped from the video record and stored for further feature extraction.

Also, an additional vehicle tracking process based on Kalman filter (Patel and Thakore, 2013) will be employed such that the detected vehicle can be continuously tracked in the single camera view. This tracking process would then allow for efficient collection of the extrinsic vehicle data, such as vehicle speed, and its arrival time.

To sum up, the preliminary object detection provides us the detailed vehicle image¹ I , its

¹which can be jointly represented by three matrix (i.e. matrix representation of digital image) as explained in Section 2.3.2.



Figure 3.1: (a) Background estimation; (b) Effect of object detection

associated arrival time t and the vehicle spot speed v . Moreover, the normalized height of vehicle image can be adopted for representing vehicle length L .

3.2.2 Feature extraction

Upon completion of object detection, various image processing techniques can be applied on the object image for feature extracting. It is noted that different objects of interest may lead to totally different features. As this study focuses on utilizing high-level IVS for transportation analysis, the vehicle feature extraction would be our major concern. Generally speaking, vehicle features can be divided into two groups, i.e. global feature and local feature. The global features characterize the overall appearance of the individual vehicle (e.g. vehicle color, length, and type), while the local features (which can also be referred to as interest point features) describe the appearance at distinctive locations (e.g. corners and T-junctions of front window of the car) in the vehicle image.

3.2.2.1 Vehicle color recognition

Vehicle color is one of the most essential features for characterizing vehicles. However, recognizing vehicle color from a given image is not a straightforward task because color may vary dramatically in response to illumination and weather changes. To overcome this difficulty, the hue saturation value (HSV) color space model, which is believed to be

illumination invariant (Baek et al., 2007), is then utilized to represent the vehicle image. In the HSV model, the hue and saturation values of a pixel remain almost constant under different illumination conditions, making HSV representations more reliable and less sensitive to lighting changes.

Vehicle color recognition is conducted in two steps. First, the general red-green-blue color images (see Section 2.3.2) are converted into HSV color model-based images (Oleari et al., 2013). Hue and saturation values are then exploited for color detection, and value information is separated out from the color space. Second, a two-dimensional color histogram is formed to represent the distribution (frequency) of different colors across the whole image. More specifically, the hue and saturation channels are divided into 36 and 10 bins, respectively. Thus, a color feature vector (C) with 360 elements is obtained (see e.g. Figure 3.2 and Figure 3.3).

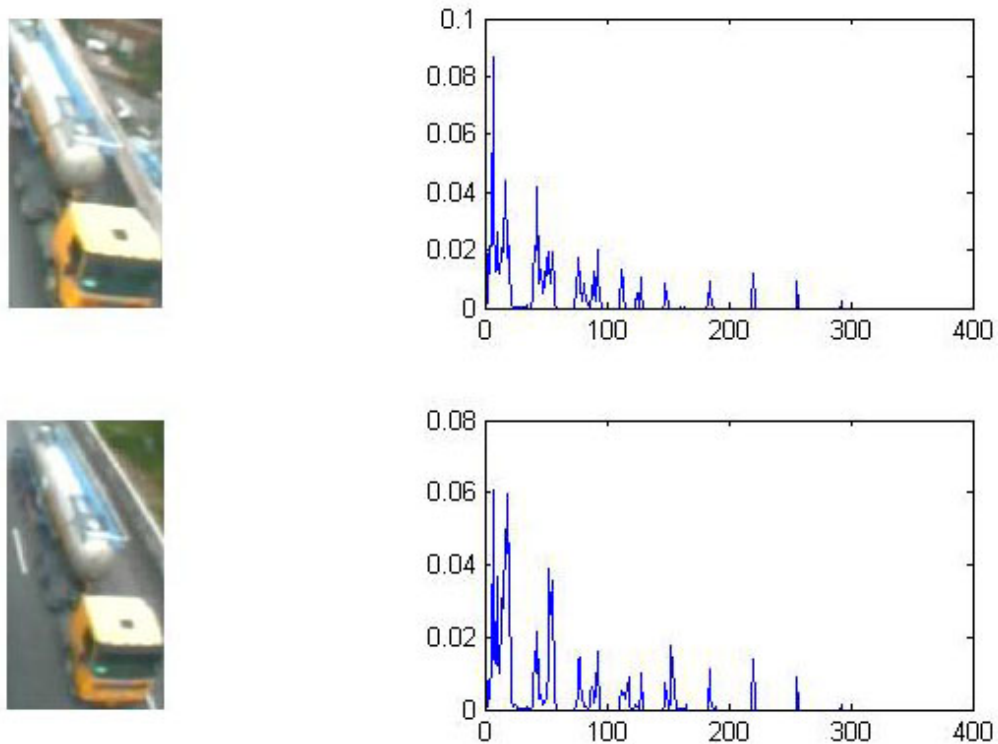


Figure 3.2: Another example of vehicle color recognition

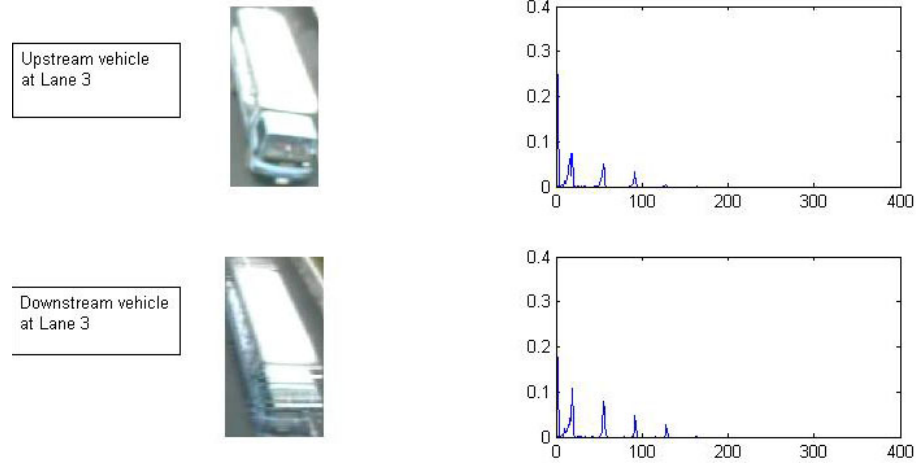


Figure 3.3: Example of vehicle color recognition

3.2.2.2 Vehicle type recognition

Vehicle type feature also provides important information to describe a vehicle. In this part, we adopt a template matching method (e.g. [Thiang and Lim, 2001](#)) to recognize vehicle type. This method uses L_2 distance metric to measure the similarity between vehicle image and template images. Specifically, vehicles are classified into six categories. And for each category, the corresponding template image is built for each lane.

In order to remove the useless color information while preserving the structural properties of a vehicle image, we first convert the image from RGB style to gray scale (I). Then the process of thresholding is fulfilled to subtract the background from the images (see [Figure 3.4](#)). Finally, the normalized similarity value for k th template image (T) is given by

$$S(k) = \frac{\sum_{m=1}^{\mathcal{M}} \sum_{n=1}^{\mathcal{N}} |I(m, n) - T(m, n)|^2}{\mathcal{G}\mathcal{M}\mathcal{N}} \quad (3.1)$$

where \mathcal{G} denotes the maximum gray level (255); \mathcal{M} and \mathcal{N} are dimensions of the template images. Thus vehicle type S is a 6-D vector that consists of the similarity score for each template (see [Figure 3.5](#)).

To sum up, a vehicle signature, i.e. $X = \{C, S, L\}$, is generated for each detected vehicle, where C and S are the normalized feature vector and type (shape) feature vector, respec-

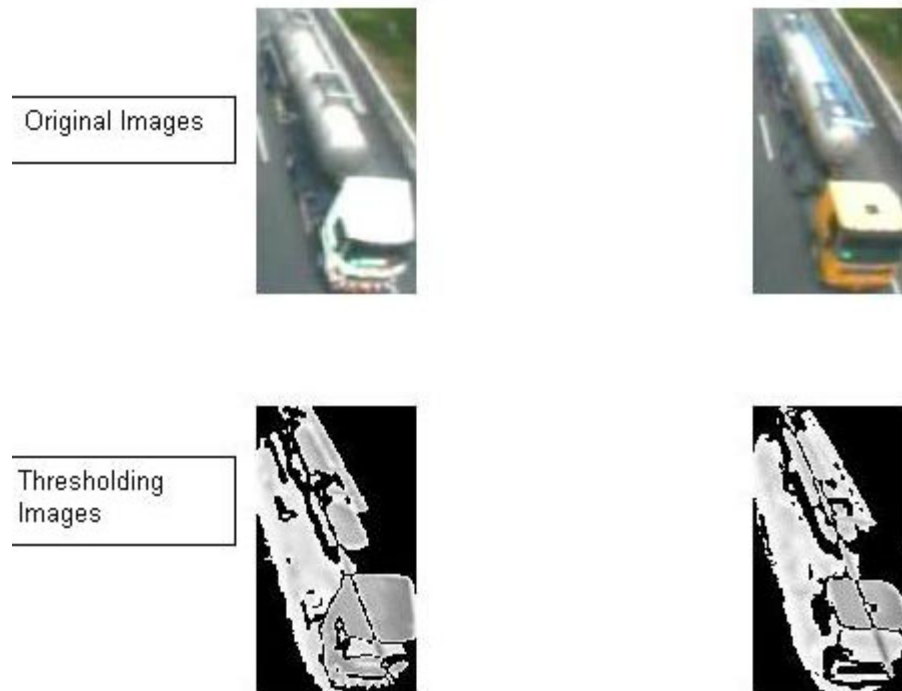


Figure 3.4: An illustration of vehicle shape extraction

Template images \ Test images					
	0.9153	0.8135	0.7956	0.7570	0.7531
	0.9164	0.7720	0.8138	0.7261	0.7464

Figure 3.5: Similarity score for each template

tively; L denotes the vehicle length. As mentioned previously, the associated arrival time t and spot speed v are also obtained during the detection process. Therefore, the individual vehicle record can then be represented as (t, v, X) . Table 3.1 summarizes the notations¹

¹which are used throughout the thesis unless otherwise specified.

and the associated descriptions of the extracted vehicle data through IVS technology.

Table 3.1: Extracted vehicle data based on IVS

Notation	Vehicle data description	
t	Arrival time of the vehicle	Extrinsic vehicle data
v	Spot speed of the detected vehicle	
L	Normalized vehicle length	Intrinsic global features
C	Color distribution in the vehicle image	
S	Type vector of the detected vehicle	

3.3 Multi-camera analytics

Since the video sensor networks in IVS could provide the real-time monitoring at discrete locations (see Section 2.3), a further integration and analysis (i.e. multi-camera analytics) of these single-camera-information would allow for a more efficient network-wide surveillance.

3.3.1 Object reidentification (ORI)

As one the most essential tasks in multi-camera analytics, object reidentification (ORI) has received considerable attention during recent years. The basic idea, which is quite straightforward, is to match objects of interest (e.g. pedestrians and vehicles) in different camera views by only using the visual information extracted by single-camera analytics (Wang, 2013). The underlying assumption of ORI is that the visual features (e.g. color, length and type) of the observed objects in different camera views may remain unchanged. By simply comparing these visual features (i.e. calculating the feature distances), the matching results can then be obtained. In this sense, the selection of an appropriate feature distance measure becomes critical for the development of ORI.

From the perspective of transportation analysis, the distance measure are specifically selected based on the vehicle features (i.e. color, length, and type). Let (X_i^U, X_j^D) denote a pair of vehicle signatures respectively observed at upstream and downstream stations,

where $X_i^U = \{C_i^U, S_i^U, L_i^U\}$ and $X_j^D = \{C_j^D, S_j^D, L_j^D\}$ are upstream and downstream vehicle feature data (see Table 3.1), respectively. For a pair of color feature vectors (C_i^U, C_j^D) ¹, the Bhattacharyya distance (Bhattacharyya, 1943), which has been widely used in research of feature extraction (Choi and Lee, 2003) and image processing (Goudail et al., 2004), is employed to calculate the degree of similarity between these two histograms², i.e.

$$d_{\text{color}}(i, j) = \left[1 - \sum_{k=1}^{360} \sqrt{C_i^U(k) \cdot C_j^D(k)} \right]^{1/2} \quad (3.2)$$

where k denotes the k th component of the color feature vector, and the value of $d_{\text{color}}(i, j)$ ranges from 0 to 1. The L_1 distance measure is introduced to represent the difference between the type feature vectors (S_i^U, S_j^D) , i.e.

$$d_{\text{type}}(i, j) = \sum_{k=1}^6 |S_i^U(k) - S_j^D(k)| \quad (3.3)$$

The length difference is given by

$$d_{\text{length}}(i, j) = |L_i^U - L_j^D| \quad (3.4)$$

Strictly speaking, the necessary camera calibration (normalization) should be performed before the comparison between vehicle features. Different camera parameters (e.g. focal length of camera, camera height and angle of camera view) may potentially lead to different properties of video record. In this thesis, however, the author would not explicitly explain the camera calibration process for several reasons:

- The freeway in Bangkok, Thailand is equipped with Autoscope system, of which the cameras follow the standard configuration (i.e. same intrinsic parameters, camera angles and heights). Therefore, we did not strictly follow the normal calibration procedures. Instead, we are more concerned with the normalization of vehicle features across different cameras.
- With respect to the detailed vehicle features (e.g. color, type and length), the necessary normalization is carried out in the study:

¹The vehicle feature C is a 360-D vector (see Section 3.2.2.1).

²Since color histogram is robust to change in camera viewing angle and to partial occlusion, the difference between vehicle colors can be quantified by directly comparing the histograms (Shapiro and Stockman, 2001).

- As color histogram is robust to change in camera viewing angle and to partial occlusion (Shapiro and Stockman, 2001), the color normalization is not necessary.
- To normalize the vehicle type vector, the template vehicle image is independently built up for each camera (see Section 3.2.2.2). Therefore, the camera angles and heights would not affect the type vectors (theoretically speaking).

Based on the aforementioned distance measures, one may make the final matching decision in an "optimal" way (e.g. minimum feature distance). As illustrated above, ORI attempts to match objects solely based on the visual features, which may not be practically applicable when the feature information change dramatically due to the pose variations and environmental changes (e.g. illumination changes). Also, the large candidate set to be matched could impose a heavy burden on the computational resources (e.g. massive computation of the distance measures). In this sense, the preliminary investigation of ORI based on the visual features should be further integrated with spatial and temporal reasoning (e.g. time window constraint, prior knowledge on the activity model) at the later stages to reduce the size of the candidate set and improve the overall computational efficiency. As a direct application of ORI, the problem of people reidentification (PRI¹) has been well-studied due to the increasing demand for video surveillance in public areas where pedestrians are the objects of interest. In what follows, a brief review on PRI is presented.

3.3.2 People reidentification (PRI)

As the name suggests, people reidentification (PRI) focuses on matching pedestrians across different cameras. Compared with the other objects of interest (e.g. vehicles), the pedestrians may have more "distinctive" features, such as clothes, shape, and facial features, which could potentially lead to a higher matching accuracy. Therefore, a large amount of studies (e.g. Javed et al., 2005; Farenzena et al., 2010; Nakajima et al., 2003; Gheisari et al., 2006; Bird et al., 2005) have been conducted to re-identify people by simply borrowing the idea from ORI (i.e. comparing the associated appearance-based features).

However, it is noted that the above-mentioned studies on PRI only utilized the visual

¹which can also be viewed as an improved version of ORI.

feature observed in the single-camera. In real-world application, the individual may walk randomly in public areas, which makes it difficult and challenging to predict where and when the same person will appear in the next camera. This phenomenon imposes a great challenge on the matching process that solely based on visual feature. In this case, the essential spatial (i.e. where) and temporal (i.e. when¹) reasoning is required such that the candidate set can be pruned and consequently the matching accuracy could be improved. [Mazzon and Cavallaro \(2012\)](#) utilized the social force model to simulate the desire of people traveling to specific interest point/camera station (which can be classified as spatial reasoning), while [Javed et al. \(2003\)](#) introduced kernel density estimators to estimate the probability of the objects arriving at the next camera station with a certain travel time (which could be classified as temporal reasoning). By employing the spatial and temporal constraints, the improved PRI is expected to outperform the ORI that solely based on the appearance comparison.

Since PRI is mainly designed for the safety and security in public areas, the matching accuracy of the system would be of utmost importance. As a variant of PRI, the vision based vehicle reidentification (VRI) was originally designed to match the vehicles across different cameras such that the associated travel time can be collected. Although vision based VRI and PRI may share some common features such as visual appearance comparison and time window constraints ([Matei et al., 2011](#)), there are still several major differences between them. In Section 3.4, a preliminary comparison between VRI and PRI is conducted, and two possible research directions of the development of VRI for dynamic travel time estimation are pointed out.

3.4 Vehicle reidentification: A variant of PRI

In this section, we will clarify the major differences between the classical PRI mentioned in Section 3.3.2 and the VRI system we intend to propose in this study. As explained previously, PRI systems are specifically designed for public safety and security and, consequently, the matching accuracy of the individual pedestrian would be the major concern. On the other hand, the ultimate goal of the development of VRI systems is to estimate the dynamic travel time on freeway.

¹Time window constraint

3.4 Vehicle reidentification: A variant of PRI

In principle, the high matching accuracy of the individual vehicle could eventually lead to a reliable travel time estimator. In light of this, improving the matching accuracy would still be a possible research direction of the development of VRI system. The methodologies utilized in PRI (e.g. feature comparison, spatial and temporal reasoning mentioned in Section 3.3.2) are also readily applicable to VRI. However, it is worthwhile to notice that the matching accuracy of RPI is usually higher than that of VRI system for several reasons.

- First, in comparison with vehicle features (e.g. color, length, type), the visual features of pedestrians (e.g. color, shape, and facial feature) are more "distinctive"¹, which allows for a better matching accuracy of PRI. With regard to VRI systems, the mismatches are inevitable due to the potential noise (e.g. image blurry caused by long-distance transmission) involved in data collection and the non-uniqueness of the vehicle features. As shown in Figure 3.6, a large number of vehicles may share similar features, which imposes a great challenge on the development of associated matching method.

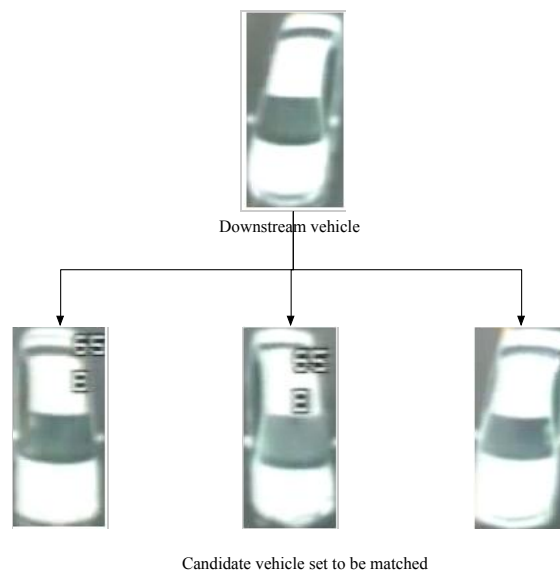


Figure 3.6: Similar vehicle feature

- Second, compared with pedestrians, vehicles tend to travel at a much higher speed, which could potentially result in larger variety of the travel time and, consequently, yield a larger candidate vehicle set to be matched. Based on our experiments, the

¹To some extent, the visual features can be viewed as unique (i.e. facial features).

size of the candidate vehicle set would increase dramatically when the traffic condition changes from free flow to congested (i.e. dynamic situation). And accordingly, the matching accuracy of VRI system is expected to decrease significantly regardless of the matching methodologies used (see Chapter 7). Therefore, additional data processing is required to improve the performance of VRI in terms of mean travel time estimation under dynamic traffic conditions.

From the viewpoint of travel time estimation, the high matching accuracy, however, is sufficient but not necessary for obtaining reliable travel time estimates. A suitable post-processing (e.g. thresholding and sampling) technique would allow us to select those vehicles with "distinctive" features, which can then be "accurately" reidentified. To handle the dynamic traffic conditions, the flexible time window constraints (i.e. temporal reasoning) are also required such that the VRI system can adapt well against the potential traffic changes. To sum up, the second research direction of the study would be to furnish the basic VRI¹ with additional post-processing component and self-adaptive time window constraint for travel time estimation purpose.

3.5 Conclusion remarks

Following the two research directions illustrated in Section 3.4, two separate but closely related tasks, namely the development of VRI under static and dynamic traffic conditions, have been performed in this study. Figure 3.7 shows the overall thesis architecture focusing on demonstrating the mutual dependencies and the logical connections between the three parts in the thesis.

As the building blocks of this study, intelligent video surveillance systems provide the real-time traffic data, which are essential for the further development of VRI systems. Single camera analytics allows for the efficient vehicle detection and feature extraction, whereas the multi camera analytics is responsible for the preliminary feature comparison (e.g. feature distance calculation).

The first pillar of this study follows the traditional method for developing VRI system,

¹which focuses on improving the vehicle matching accuracy, and is applicable under static traffic conditions

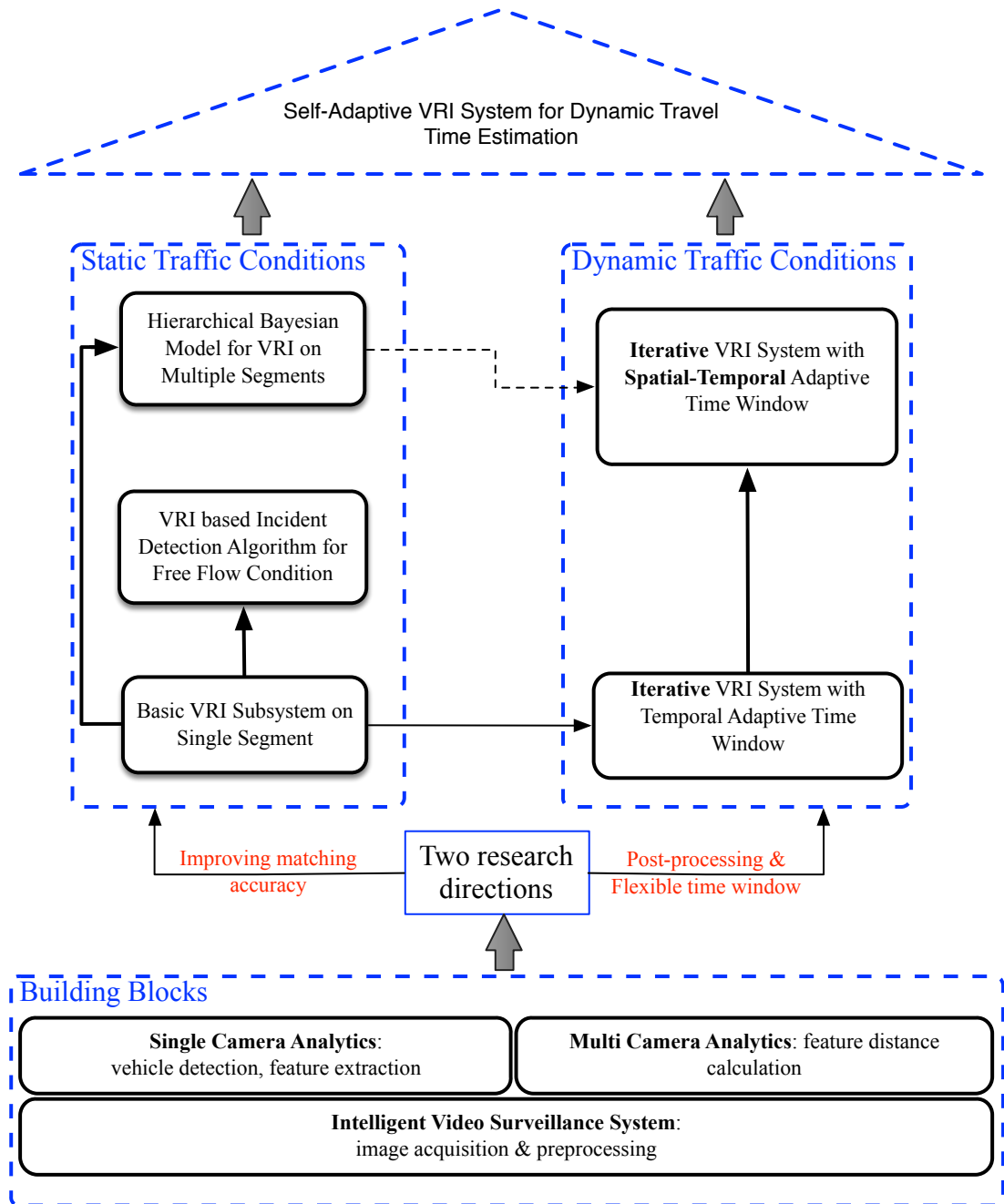


Figure 3.7: Thesis architecture demonstrating the mutual dependencies and the logical connections between the three parts

which focuses on improving the vehicle matching accuracy. Basic vision based VRI system has been developed by the statistical fusion of various vehicle features (Chapter 4). Due to the capability of efficient vehicle tracking in the freeway system, the basic VRI subsystem is then revised and improved for incident detection purpose (Chapter 5). In

this case, the high matching accuracy of basic VRI system is beneficial to the prompt and accurate detection of traffic incidents under free flow conditions. To further improve the matching accuracy when there are multiple detectors along the freeway, the hierarchical Bayesian model is proposed (Chapter 6). Note that the aforementioned VRI systems are designed under static traffic conditions, which suggests that they are only applicable during a short/stable time period.

The second pillar of this study concentrates on improving the self-adaptivity of the basic VRI in response to the dynamic traffic conditions. A novel iterative VRI system with temporal adaptive time window constraints is proposed to capture the traffic dynamics in real-time (Chapter 7). The additional iterative process together with the post-processing technique is introduced to achieve reliable travel time estimates under non-predictable traffic condition (e.g. traffic incident). A further improved iterative VRI system with spatial-temporal adaptive time window is specifically designed for the freeway system with multiple detectors (Chapter 8). By utilizing the traffic information (e.g. spatial information) from different pairs of detectors, we may obtain a more reliable time window constraint under traffic demand and supply uncertainties.

Resting on these two pillars, the so-called self-adaptive VRI system could be developed for dynamic freeway travel time estimation.

Part II

VRI system under static traffic conditions

Chapter 4

Basic vision-based VRI system

This chapter aims to propose a probabilistic vehicle reidentification algorithm for estimating travel time using the video image data provided by traffic surveillance cameras. Each vehicle is characterized by its color, type, and length, which are extracted from the video record using image processing techniques. A data fusion rule is introduced to combine these features to generate a probabilistic measure for reidentification (matching) decision. The vehicle matching problem is then reformulated as a combinatorial problem and solved by a minimum-weight bipartite matching method. To reduce the computational time, the algorithm also utilizes the potential availability of the historical travel time data to define a potential time-window for the vehicle reidentification.

This probabilistic approach does not require vehicle sequential information and, hence, allows vehicle reidentification across multiple lanes. The algorithm is tested on a 3.6-km-long section of the freeway system in Bangkok, Thailand. The travel time estimation result is also compared with the manual observation data.

4.1 Introduction

Travel time is widely recognized as one of the best indicators of the quality of traffic facilities as it is easy for both the transportation engineers and the travelers to understand. However, travel time estimation is still a challenging issue. Traffic detectors can estimate

traffic information at discrete points, but the detectors can not provide information about the link between detectors, which means that the travel time cannot be measured directly. [Oh et al. \(2002\)](#) also pointed out that the estimates from point detection of average speeds are inaccurate when it comes to congested traffic conditions. Under this circumstance, vehicle reidentification method may be a promising way to infer travel time between two point detectors.

Generally speaking, vehicle reidentification is the process of matching vehicle signatures from one point detector to the next one in road network. Once a vehicle detected at one sensor is re-identified (i.e. matched) at another point, the travel time of the vehicle is simply the difference between its arrival times at two consecutive detectors. In this case, two key issues need to be considered during the development of an effective vehicle reidentification system: first, a suitable traffic detection system that allows the accurate and efficient extraction of traffic data is needed; second, a robust algorithm, which aims at improving the vehicle matching accuracy, must be developed.

With respect to traffic detection system, various technologies have been investigated such as image-based sensors, Bluetooth-based sensors, magnetic sensors, and inductive signature systems. Because of the worldwide deployment of inductive loop sensors, many studies focused on re-identifying vehicles using the measurements from loop detectors. [Coifman and Cassidy \(2002\)](#) explicitly compared vehicle lengths derived from loop detectors. The length measurement resolution, however, largely depends on the vehicle velocity and sampling rate of loop detector. Thus it would be impossible for single loop detectors to measure the lengths of most passenger vehicles accurately under free flow condition. To compensate for this, [Coifman and Krishnamurthy \(2007\)](#) tried to only reidentify those vehicles with distinct length measurements (i.e. the long vehicles). [Sun et al. \(1999\)](#) performed vehicle reidentification by utilizing the sensor waveforms from inductive loops. The waveforms are first transformed to be speed invariant based on the assumption that the vehicle speed is constant. Thus the measurement would be rather unreliable if a vehicle were accelerating or decelerating when it crossed the loop detectors. Some researchers also investigated the feasibility of a vehicle reidentification scheme using the data from magnetic wireless sensors. [Kwong et al. \(2009\)](#) extracted the vehicle signatures from the peak values of magnetic signal and the peak values are independent of vehicle speed. Although this approach is relatively reliable, it requires the deployment of a magnetic sensor at each lane, and hence monitoring a complete intersection is expensive. An automatic license plate number reader system that provides the unique license

number for each vehicle (Chang et al., 2004), could make the reidentification problem trivial. However, this technique may not be applicable in some cases because of privacy concerns and technical limitations in image processing. Quayle et al. (2010) estimated travel time by utilizing the emerging Bluetooth detection technology. Since the Bluetooth sensor would generate a unique 48 bit media access control (MAC) address for the vehicle containing a Bluetooth device, the vehicle reidentification can be easily performed by matching the MAC addresses. Although this technology appears promising for travel time estimation, it requires an efficient deployment of in-vehicle Bluetooth devices. An alternative detection system is intelligent video surveillance system (IVS¹). In this chapter, we aim to investigate the feasibility of utilizing IVS for the development VRI system.

A variety of well-studied vehicle reidentification algorithms exist that can be broadly divided into distance-based methods and probabilistic methods. Distance-based methods incorporate distance measures (e.g. Bhattacharyya distance² and L_1 distance) to represent the similarity between each pair of vehicle signatures, and then an upstream vehicle is matched to the most "similar" downstream vehicle (i.e. the vehicle with the minimum vehicle signature distance). These approaches, however, have several weaknesses. First and most significantly, the vehicle signature derived from the detector is not unique, and hence the distance measure can not really reflect the similarities between the vehicles. Second, it is unavoidable that traffic data contain potential noise, and thus uncertainty from the vehicle signatures must be considered. To overcome these limitations and improve the matching accuracy, some studies tried to reidentify a platoon of vehicles rather than an individual vehicle. Coifman (1998) compared the lengths of vehicle platoons at the consecutive detectors based on the assumption that platoons of five to ten vehicles do not change lanes. Sun et al. (2004) utilized the data fusion technique to combine the measurements from various traffic detectors and built one single similarity score to reidentify vehicle platoons. However, these last two methods would not be applicable in the presence of vehicles that change lanes frequently. In probabilistic approaches, the vehicle signature is treated as a random variable, and a probabilistic measure is incorporated for the reidentification decision. Kwong et al. (2009) proposed a probabilistic model to reidentify vehicles with a maximum *posterior* probability. Their approach, however, is limited to the case with only one lane arterial, and assumed no overtaking between vehicles.

This chapter presents a probabilistic vehicle matching approach to estimate the travel time

¹A detailed introduction of IVS can be found in Section 2.3.

²Equation (3.2)

4.2 Overall framework of the travel time estimation system

distribution from video image data (i.e. basic vision-based VRI system). The method extends the probabilistic framework for vehicle reidentification illustrated by Kwong et al. (2009) to a more general case in which overtaking between vehicles as well as the reidentification across multiple lanes are both allowed. Since various vehicle features such as color, shape and size could be derived from the video image data using image processing techniques, a probabilistic fusion technique of vehicle features is introduced to provide a probabilistic measure (i.e. *posterior* probability) for reidentification decision. The vehicle reidentification method illustrated in this chapter is performed in two stages. In the first stage, a probabilistic measure based on probabilistic data fusion technique is introduced to evaluate the likelihood of a vehicle being matched with the other vehicles given their feature distances. In the second stage, a bipartite matching method is adopted to solve the vehicle reidentification as an assignment problem. The study also evaluates the performance and accuracy of the probabilistic reidentification approach using the video record data of a section of the expressway system in Bangkok, Thailand.

The rest of the chapter is organized as follows. Section 4.2 presents the overall framework of basic VRI system using intelligent video surveillance technology. The description and analysis of the vehicle reidentification methodology are proposed in the following two sections (i.e. Section 4.3 and Section 4.4). Some test results regarding travel time estimation and reidentification accuracy are discussed in Section 4.5. Finally, we close this chapter with the conclusions (see Section 4.6).

4.2 Overall framework of the travel time estimation system

This section presents the overall framework of the vision-based basic VRI system. Since the travel time for each vehicle is simply the difference between arrival times at two consecutive sites, the success of our estimation system lies in the effectiveness of data collection (e.g. vehicle detection and feature extraction explained in Section 3.2) from intelligent video surveillance technology and the robustness of vehicle reidentification algorithm.

The test site of our system is a 3.6-km section of the closed three-lane expressway system in Bangkok, Thailand, as shown in Figure 4.1. At each station a gantry-mounted video camera using upstream viewing functions as a traffic detector and two hours of video

4.2 Overall framework of the travel time estimation system

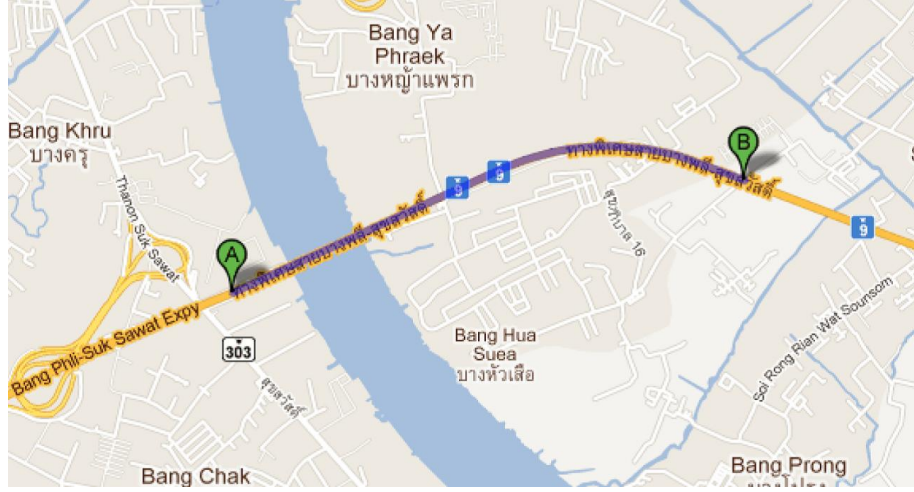


Figure 4.1: Test site in Bangkok, Thailand.

record data were collected between 10 a.m. and noon on March 15, 2011. The frame rate of the video record is 25 FPS, and the still image size is 563×764 .

Various traffic data such as vehicle color, type and length could be extracted from the video record data (i.e. single-camera analytics). Traffic data collection from video image data involves two main steps. First, the raw video record is digitized and stored in the computer (i.e. low-level image processing explained in Section 2.3.2). Background estimation technology is then utilized to detect the moving object (i.e. individual vehicle) from the video. The still image regarding the individual vehicle is stored for further application. Second, myriad image processing techniques such as equalization and template matching are performed on the vehicle images to extract the feature vectors. Upon completion of the traffic data collection, the length, color, and type feature vectors are obtained for each vehicle. The probabilistic formalization of the vehicle reidentification problem is described in detail below.

Consider a multi-lane link demonstrated in Figure 4.1. Let $U = \{1, 2, \dots, N\}$ denote the N vehicles crossing the upstream site during a time interval. $D = \{1, 2, \dots, M\}$ is a set of candidate downstream vehicles that are selected within a predefined time window (this action is discussed in Section 4.3.1). Let $X_i^U = \{C_i^U, S_i^U, L_i^U\}$ denote the signature for the i th upstream vehicle, where C_i^U and S_i^U are the normalized color feature vector and type (shape) feature vector, respectively. L_i^U denotes the normalized length of vehicle i . Accordingly, $X_j^D = \{C_j^D, S_j^D, L_j^D\}$ represents the signature for the j th downstream vehicle. For each pair of signatures (X_i^U, X_j^D) , distance measures are incorporated to represent the similarities between the feature vectors (see Section 3.3). Thereby the difference be-

4.2 Overall framework of the travel time estimation system

tween the two signature sets X^U and X^D could be represented in the form of three $N \times M$ distance matrixes, i.e. $\mathcal{D}_{\text{color}}$, $\mathcal{D}_{\text{type}}$ and $\mathcal{D}_{\text{length}}$.

In other words, the vehicle reidentification problem is to find the corresponding pairs between upstream vehicle set U and downstream set D . Herein we introduce the assignment function ψ between the sets of U and D using the definition

$$\psi : \begin{cases} \{1, 2, \dots, N\} \rightarrow \{1, 2, \dots, M\} \\ i \mapsto j, \quad i = 1, 2, \dots, N, \quad j = 1, 2, \dots, M \end{cases}$$

where $\psi(i) = j$ indicates that upstream vehicle i is the same as downstream vehicle j . In practice, it is necessary to deal with complex situations in which the upstream vehicle does not necessarily correspond to any downstream vehicle. Due to the detection error of the IVS system or some other reasons (e.g. the existence of on/off-ramps), the upstream vehicle i may not be detected at the downstream site. In this case, the assignment function ψ is modified as follows:

$$\psi : \begin{cases} \{1, 2, \dots, N\} \rightarrow \{1, 2, \dots, M, \tau\} \\ i \mapsto j, \quad i = 1, 2, \dots, N, \quad j = 1, 2, \dots, M, \tau \end{cases} \quad (4.1)$$

where $\psi(i) = \tau$ means that upstream vehicle i does not match any downstream vehicle. Therefore, the vehicle reidentification problem is equivalent to finding the assignment function ψ based on some decision rules.

In this research, the maximum *a posterior* probability (MAP) rule is used to estimate the assignment function. The optimal solution to the vehicle reidentification problem is then given by

$$\psi^* = \arg \max_{\psi} P(\psi | \mathcal{D}_{\text{color}}, \mathcal{D}_{\text{type}}, \mathcal{D}_{\text{length}}) \quad (4.2)$$

A two-stage method for problem (4.2) is adopted. First, a probabilistic data fusion rule is introduced to estimate the *posterior* probability of an assignment function ψ being the ground truth, i.e. $P(\psi | \mathcal{D}_{\text{color}}, \mathcal{D}_{\text{type}}, \mathcal{D}_{\text{length}})$. In the second stage, the reidentification problem is formulated and solved by the bipartite matching method.

Figure 4.2 depicts a block diagram for the implementation of the basic VRI system. Note that the traffic data acquisition component, which can also be referred to as the high-level intelligent video surveillance, has already been discussed in Chapter 3. In what follows, the vehicle signature matching method is explained in detail.

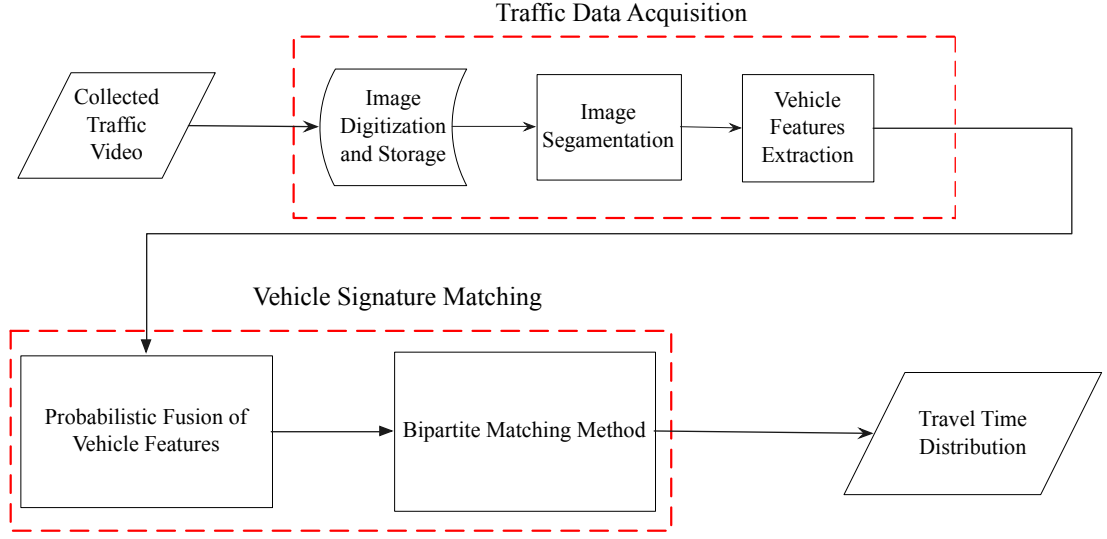


Figure 4.2: Overall framework of travel time estimation system.

4.3 Probabilistic fusion of vehicle features

This section presents a probabilistic fusion strategy to integrate information from multiple vehicle features (e.g. color, type and length). Three individual statistical models are constructed corresponding to the three feature distances. Bayesian rule is then employed to generate a *posterior* probability of the assignment function ψ from the feature distance matrix (i.e. $P(\psi | \mathcal{D}_{\text{color}}, \mathcal{D}_{\text{type}}, \mathcal{D}_{\text{length}})$). In the concluding step the three *posterior* probabilities are fused for the final vehicle reidentification (i.e. data fusion).

4.3.1 Time window constraint

Before proceeding to consider the vehicle features fusion strategy, it is necessary to explain the concept of time window constraint, which has been commonly utilized in the existing VRI systems. As demonstrated in Section 4.2, three feature vectors regarding the individual vehicle are extracted. To quantify the difference between each pair of upstream and downstream vehicle signatures, i.e. the difference between $X_i^U = \{C_i^U, S_i^U, L_i^U\}$ and $X_j^D = \{C_j^D, S_j^D, L_j^D\}$, several distance measures (e.g. Bhattacharyya distance and L_1 distance) are then incorporated and the associated vehicle feature distances (i.e. $d_{\text{color}}(i, j)$, $d_{\text{type}}(i, j)$ and $d_{\text{length}}(i, j)$) can be calculated on the basis of Equations (3.2), (3.3), and (3.4).

However, in practice, it is unnecessary to compute the distances between all pairs of upstream and downstream vehicle signatures. A time window constraint, which sets the upper and lower bounds of travel time, is introduced to rule out the unlikely candidate vehicles and improve the overall computational efficiency.

Given an upstream vehicle i , the available historical travel time is used to define a time-window for it. This time-window constraint is used to identify the potential matches for vehicle i and rule out the vehicles with unreasonable travel times at downstream site. Specifically, the set of potential matches at downstream site for vehicle i is defined as follows

$$D_i = \{j | t_i^U + t_{\min} \leq t_j^D \leq t_i^U + t_{\max}\} \quad (4.3)$$

where t_{\min} and t_{\max} are the minimum and maximum vehicle travel time based on the historical data; t_i^U and t_j^D denote the arrival time at upstream and downstream site, respectively. For a sequence of upstream vehicles $U = \{1, 2, \dots, N\}$, the set of the candidate downstream vehicles is given by

$$D = \{j | t_1^U + t_{\min} \leq t_j^D \leq t_N^U + t_{\max}\} \quad (4.4)$$

Having selected the downstream set $D = \{1, 2, \dots, M\}$, to each pair of signatures (X_i^U, X_j^D) the feature distance $\{d_{\text{color}}(i, j), d_{\text{type}}(i, j), d_{\text{length}}(i, j)\}$ can be assigned, obtaining three $N \times M$ distance matrices $\mathcal{D}_{\text{color}}$, $\mathcal{D}_{\text{type}}$ and $\mathcal{D}_{\text{length}}$. Since the scales and distributions of feature distances are unlikely to be the same, the three distance matrixes can not be combined directly using linear combination method (Sun et al., 2004). To overcome this problem, the authors propose a probabilistic data fusion approach to integrate information from multiple vehicle features.

4.3.2 Probabilistic modeling of feature distance

We start with the introduction of a statistical model which allows the probabilistic description of feature distance. Without loss of generality, we only describe the probabilistic modeling of color feature distance.

For each pair of color feature vectors (C_i^U, D_j^D) , the distance measure $d_{\text{color}}(i, j)$ is assumed to be a random variable. We also assume that conditional on knowing the ground

truth ψ , $\{d_{\text{color}}(i, j), i = 1, 2, \dots, N, j = 1, 2, \dots, M\}$ are independent of each other. The conditional probability of $d_{\text{color}}(i, j)$ is then given by

$$p(d_{\text{color}}(i, j)|\psi) = \begin{cases} p_1(d_{\text{color}}(i, j)) & \text{if } \psi(i) = j \\ p_2(d_{\text{color}}(i, j)) & \text{if } \psi(i) \neq j \text{ or } \psi(i) = \tau \end{cases} \quad (4.5)$$

where p_1 and p_2 are two probability density functions (pdf). p_1 denotes the pdf of obtaining distance $d_{\text{color}}(i, j)$ when color feature vectors C_i and D_j belong to the same vehicle, while p_2 is the pdf of obtaining distance $d_{\text{color}}(i, j)$ between different vehicles.

Based on the independency assumption, the likelihood of obtaining the feature distance matrix $\mathcal{D}_{\text{color}}$ allows the following factorization:

$$p(\mathcal{D}_{\text{color}}|\psi) = \prod_{i=1}^N \prod_{l=1}^M p(d_{\text{color}}(i, l)|\psi) = \prod_{i=1}^N \prod_{l=1}^M p(d_{\text{color}}(i, l)|\psi(i)) \quad (4.6)$$

From Equation (4.5), we have

$$\prod_{l=1}^M p(d_{\text{color}}(i, l)|\psi(i)) = \begin{cases} \frac{p_1(d_{\text{color}}(i, j))}{p_2(d_{\text{color}}(i, j))} \prod_{k=1}^M p_2(d_{\text{color}}(i, k)) & \text{if } \psi(i) = j, j = 1, 2, \dots, M \\ \prod_{k=1}^M p_2(d_{\text{color}}(i, k)) & \text{if } \psi(i) = \tau \end{cases}$$

Let $\lambda_{\text{color}}(i, j) = \frac{p_1(d_{\text{color}}(i, j))}{p_2(d_{\text{color}}(i, j))} \prod_{k=1}^M p_2(d_{\text{color}}(i, k))$ and $\lambda_{\text{color}}(i, \tau) = \prod_{k=1}^M p_2(d_{\text{color}}(i, k))$, then we may have

$$\prod_{l=1}^M p(d_{\text{color}}(i, l)|\psi(i)) = \begin{cases} \lambda_{\text{color}}(i, j) & \text{if } \psi(i) = j, j = 1, 2, \dots, M \\ \lambda_{\text{color}}(i, \tau) & \text{if } \psi(i) = \tau \end{cases} \quad (4.7)$$

By substituting Equation (4.7) into Equation (4.6), we may calculate the pdf of obtaining the color feature distance matrix. Similarly, we could also construct the probabilistic models for the type feature distance and length feature distance. Since the calculation of the likelihoods largely relies on pdfs p_1 and p_2 , the estimation of the pdfs statistical distribution is required.

4.3.3 Probability distribution estimation

Here we are mainly concerned with the estimation of pdf p_1 and p_2 for the color feature distance. Due to the complexity and flexibility of the probability distribution, we utilize finite gaussian mixture model (e.g. [Frühwirth-Schnatter, 2006](#)) to approximate p_1 and p_2 . In gaussian mixture modeling, the pdf p_2 can be written in the form

$$p_2(d_{\text{color}}) = \sum_{k=1}^2 \pi_k g_k(d_{\text{color}}; \theta_k, \sigma_k), \quad \sum_{k=1}^2 \pi_k = 1 \quad (4.8)$$

where $g_k(d_{\text{color}}; \theta_k, \sigma_k)$ is the k th component gaussian density function, θ_k and σ_k are the mean and standard variance, respectively. π_k denotes the weight associated with the k th component.

Collecting reliable training sample is a major challenge for estimating the unknown parameters $\{(\pi_k, \theta_k, \sigma_k), k = 1, 2\}$. In this study, the ground-truth matches (i.e. actual matching result) were verified by the human operators viewing the video record frame by frame, and a training dataset that contains a number of pairs of correctly matched vehicles is built up. From this dataset we could obtain the feature distances (e.g. d_{color}) between the correctly matched and mismatched vehicles, respectively. Then we apply the well-known Expectation Maximization (EM) algorithm (e.g. [McLachlan and Krishnan, 2008](#); [Huang and Russell, 1998](#)) to solve the parameter estimation problem.

As shown in Figure 4.3, pdfs p_1 and p_2 are estimated by fitting gaussian mixture model to a training dataset which contains 449 pairs of correctly matched vehicles.

4.3.4 Calculation of *posterior* probability

From the estimates of the likelihood, the *posterior* probability of the assignment function ψ being the ground truth, i.e. $P(\psi | \mathcal{D}_{\text{color}}, \mathcal{D}_{\text{type}}, \mathcal{D}_{\text{length}})$, could be calculated directly. By applying the Bayesian rule, we have

$$P(\psi | \mathcal{D}_{\text{color}}, \mathcal{D}_{\text{type}}, \mathcal{D}_{\text{length}}) = \frac{p(\mathcal{D}_{\text{color}}, \mathcal{D}_{\text{type}}, \mathcal{D}_{\text{length}} | \psi) P(\psi)}{p(\mathcal{D}_{\text{color}}, \mathcal{D}_{\text{type}}, \mathcal{D}_{\text{length}})} \quad (4.9)$$

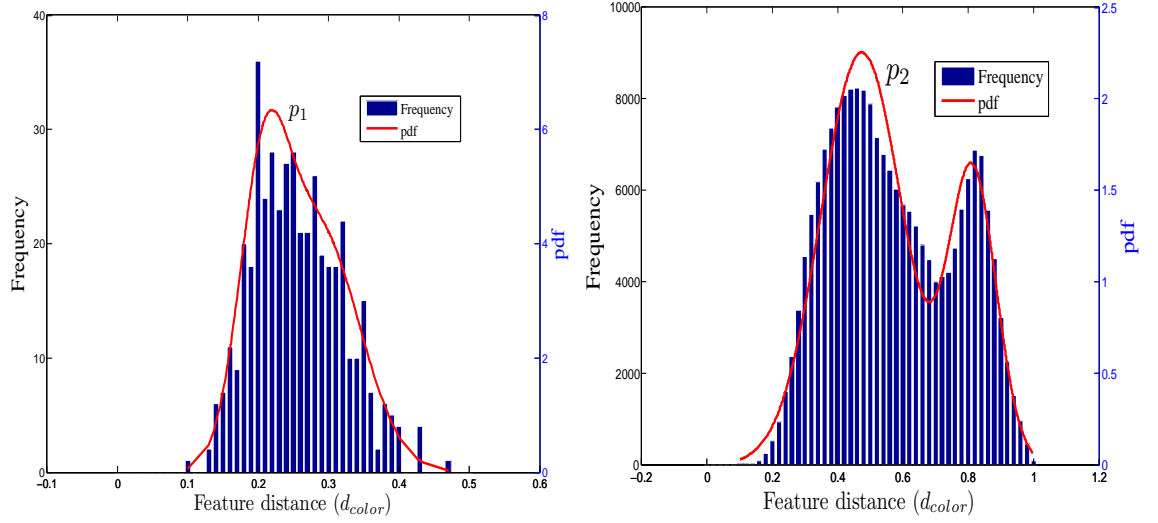


Figure 4.3: The pdfs p_1 and p_2 estimated by gaussian mixture model

where $p(\mathcal{D}_{\text{color}}, \mathcal{D}_{\text{type}}, \mathcal{D}_{\text{length}} | \psi)$ is the likelihood function; $P(\psi)$ is the *prior* knowledge about the assignment function without observing the detailed vehicle feature distances. Based on Equation (4.9), it is easily observed that the calculation of the posterior probability is dependent on the deduction of the likelihood function and the definition of *prior* probability (i.e. $P(\psi)$).

In the following we discuss the definition of the *prior* probability $P(\psi)$. With the independency assumption, we have

$$P(\psi) = \prod_{i=1}^N P(\psi(i)) \quad (4.10)$$

For each $i \in \{1, 2, \dots, N\}$, $P(\psi(i))$ is a discrete probability distribution and the random variable $\psi(i)$ can only take on the values $j = 1, 2, \dots, M$ and τ . $P(\psi(i) = j)$ denotes the probability that upstream vehicle i matches downstream vehicle j , whereas $P(\psi(i) = \tau)$ is the probability that vehicle i does not match any downstream vehicle. In this study, we use the continuous historical travel time distribution $f(\cdot)$ to approximate discrete prior probability $P(\psi(i))$. Given a pair of vehicles (i, j) and their arrival time difference $t(i, j)$, if the values of $f(t(i, j))$ is sufficiently large, then we are more willing to believe that vehicle i matches vehicle j (this is also referred to as the prior knowledge).

The remaining part is then to use $f(t(i, j))$ to approximate $P(\psi(i))$ such that it satisfied

the definition of discrete probability definition, i.e.

$$\begin{cases} \sum_{j=1}^M P(\psi(i) = j) + P(\psi(i) = \tau) = 1 \\ P(\psi(i) = \tau) = \kappa \end{cases} \quad (4.11)$$

where κ is the pre-defined probability that vehicle i does not match any candidate vehicles. As explained in last paragraph, we also believe

$$\frac{P(\psi(i) = j)}{P(\psi(i) = k)} = \frac{f(t(i, j))}{f(t(i, k))}, \quad \forall j, k \in \{1, 2, \dots, M\} \quad (4.12)$$

By simple mathematical manipulation, we may obtain the following equations regarding the *prior* probability.

$$P(\psi(i) = j) = \frac{(1 - \kappa)}{\eta} f(t(i, j)), \quad j = 1, 2, \dots, M; \quad \eta = \sum_{j=1}^M f(t(i, j)) \quad (4.13)$$

$$P(\psi(i) = \tau) = \kappa \quad (4.14)$$

It is noted that the definition of the prior probability varies with different strategies and application scenarios. After all, prior probability stands for the prior knowledge (or "opinion") on vehicle matching. Different people may have totally different "opinions" regarding the matching result.

4.3.5 Data fusion rule

Since the ultimate goal is to calculate the *posterior* probability $P(\psi | \mathcal{D}_{\text{color}}, \mathcal{D}_{\text{type}}, \mathcal{D}_{\text{length}})$ in Equation (4.9), a data fusion technique is then required to combine the multiple vehicle features such that the joint probability density function $p(\mathcal{D}_{\text{color}}, \mathcal{D}_{\text{type}}, \mathcal{D}_{\text{length}} | \psi)$ could be inferred. Assuming that the observed feature distance matrixes are conditionally statistically independent, we may have

$$p(\mathcal{D}_{\text{color}}, \mathcal{D}_{\text{type}}, \mathcal{D}_{\text{length}} | \psi) = p(\mathcal{D}_{\text{color}} | \psi) p(\mathcal{D}_{\text{type}} | \psi) p(\mathcal{D}_{\text{length}} | \psi) \quad (4.15)$$

where $p(\mathcal{D}_{\text{color}} | \psi)$, $p(\mathcal{D}_{\text{type}} | \psi)$, and $p(\mathcal{D}_{\text{length}} | \psi)$ are the likelihood functions of observing each feature distance matrix (see Section 4.3.2). Due to its theoretical simplicity, Equation (4.15), which is also referred to as the product rule (Kittler et al., 1998), has been

4.3 Probabilistic fusion of vehicle features

widely used in research of data fusion. To further indicate the degree of contribution of each probability measure, the logarithmic opinion pool (LOP) approach (e.g. [Benediktsson and Swain, 1992](#); [Smith et al., 2005](#)) is applied in this study. The LOP is evaluated as a weighted product of the probabilities and the fusion equation is given by

$$p(\mathcal{D}_{\text{color}}, \mathcal{D}_{\text{type}}, \mathcal{D}_{\text{length}}|\psi) = \frac{1}{Z_{\text{LOP}}} p(\mathcal{D}_{\text{color}}|\psi)^\alpha p(\mathcal{D}_{\text{type}}|\psi)^\beta p(\mathcal{D}_{\text{length}}|\psi)^\gamma, \quad \alpha + \beta + \gamma = 1 \quad (4.16)$$

where α , β and γ are the fusion weights of the feature distances, which can also be calibrated from the training dataset; Z_{LOP} is the normalizing constant. One important and desirable property of the LOP rule is that zeros in the logarithmic opinion pool are vetoes; i.e. if any likelihood function of the feature distance is close to zero (e.g. $p(\mathcal{D}_{\text{type}}|\psi) = 0$), then the overall likelihood is also zero (i.e. $p(\mathcal{D}_{\text{color}}, \mathcal{D}_{\text{type}}, \mathcal{D}_{\text{length}}|\psi) = 0$) regardless of the likelihoods of other two feature distances. To be more specific, a low matching likelihood of one vehicle feature will lower the overall matching probability, which could eventually come to a conclusion that vehicle i cannot be matched to vehicle j . This behavior of the data fusion approach is exactly what we are expecting.

By substituting Equations (4.13), (4.14) and (4.16) into Equation (4.9), we have

$$P(\psi|\mathcal{D}_{\text{color}}, \mathcal{D}_{\text{type}}, \mathcal{D}_{\text{length}}) = \frac{p(\mathcal{D}_{\text{color}}|\psi)^\alpha p(\mathcal{D}_{\text{type}}|\psi)^\beta p(\mathcal{D}_{\text{length}}|\psi)^\gamma P(\psi)}{Z_{\text{LOP}} p(\mathcal{D}_{\text{color}}, \mathcal{D}_{\text{type}}, \mathcal{D}_{\text{length}})} \quad (4.17)$$

Therefore the optimization problem (4.2) can be reformulated as follows:

$$\max_{\psi} p(\mathcal{D}_{\text{color}}|\psi)^\alpha p(\mathcal{D}_{\text{type}}|\psi)^\beta p(\mathcal{D}_{\text{length}}|\psi)^\gamma P(\psi) \quad (4.18)$$

In practice it is more convenient to work with the negative logarithm of the objective function in problem (4.18), i.e.

$$\min_{\psi} [-\alpha \ln(P(\mathcal{D}_{\text{color}}|\psi)) - \beta \ln(P(\mathcal{D}_{\text{type}}|\psi)) - \gamma \ln(P(\mathcal{D}_{\text{length}}|\psi)) - \ln P(\psi)] \quad (4.19)$$

On the basis of Equations (4.6) and (4.7), the term $\ln(P(\mathcal{D}_{\text{color}}|\psi))$ in Problem (4.19) can

be expressed as follows:

$$\begin{aligned} \ln(P(\mathcal{D}_{\text{color}}|\psi)) &= \sum_i \sum_j \ln(\lambda_{\text{color}}(i, j))\delta(\psi(i) = j) \\ &+ \sum_i \ln(\lambda_{\text{color}}(i, \tau))\delta(\psi(i) = \tau) \end{aligned} \quad (4.20)$$

where $\delta(\cdot)$ is the indicator function, and $\delta(\psi(i) = j) = 1$ if upstream vehicle i matches downstream vehicle j . Likewise, the terms $\ln(P(\mathcal{D}_{\text{type}}|\psi))$ and $\ln(P(\mathcal{D}_{\text{length}}|\psi))$ can also be obtained, and $\ln P(\psi)$ is given by

$$\ln(P(\psi)) = \sum_i \sum_j \ln\left(\frac{1-\kappa}{\eta} f(t(i, j))\right)\delta(\psi(i) = j) + \sum_i \ln(\kappa)\delta(\psi(i) = \tau) \quad (4.21)$$

By replacing the terms in Problem (4.19) with Equations (4.20) and (4.21), we obtain the following optimization problem:

$$\min_{\psi} \sum_i \sum_j \varpi(i, j)\delta(\psi(i) = j) + \sum_i \varpi(i, \tau)\delta(\psi(i) = \tau) \quad (4.22)$$

where $\varpi(i, j)$ and $\varpi(i, \tau)$ are the associated coefficients defined as follows:

$$\begin{aligned} \varpi(i, j) &= -\alpha \ln(\lambda_{\text{color}}(i, j)) - \beta \ln(\lambda_{\text{type}}(i, j)) - \gamma \ln(\lambda_{\text{length}}(i, j)) \\ &- \ln\left(\frac{1-\kappa}{\eta} f(t(i, j))\right) \end{aligned}$$

$$\varpi(i, \tau) = -\alpha \ln(\lambda_{\text{color}}(i, \tau)) - \beta \ln(\lambda_{\text{type}}(i, \tau)) - \gamma \ln(\lambda_{\text{length}}(i, \tau)) - \ln(\kappa)$$

Vehicle reidentification problem (4.22) is an unconstrained combinatorial optimization problem. The solution to Problem (4.22) might not be feasible in practice. For example, two different upstream vehicles may be matched to the same downstream one. In this case, some constraints should be introduced to guarantee a feasible solution, and a polynomial-time algorithm is required to solve the constrained optimization problem. The next section presents a bipartite matching method for Problem (4.22).

4.4 Bipartite matching method

In this section a weighted bipartite graph representation for the feasible solution set of the Problem (4.22) is proposed, and a well-known polynomial-time method based on minimum-weight bipartite matching is also discussed.

4.4.1 Reduction to a weighted bipartite graph

We now consider a bipartite graph $G = (U, D, E)$ (see Figure 4.4) whose vertices can be divided into two disjoint sets U and D such that every edge connects a vertex in U to one in D . Given the two sets of vehicles U and D , a weighted graph representation

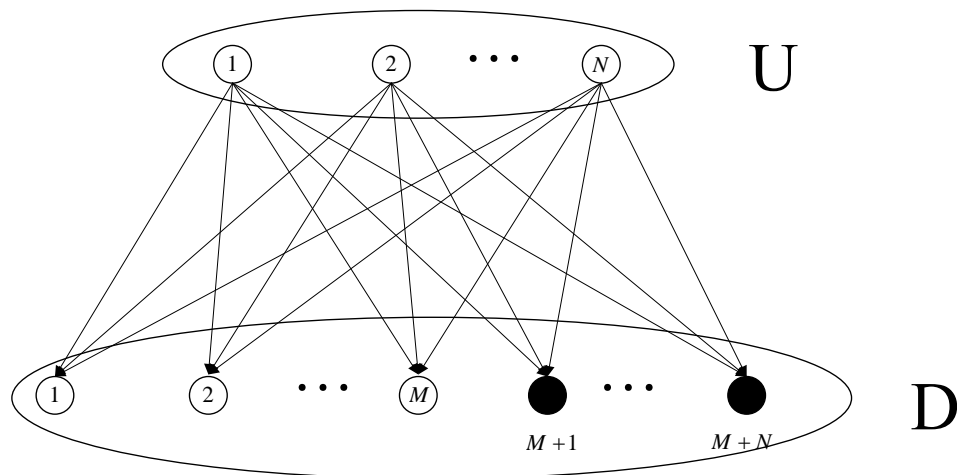


Figure 4.4: Bipartite graph representation

$G = (U, D, E)$ can be constructed as follows: the nodes in set U , indexed by $i = 1, 2, \dots, N$ denote the vehicles at the upstream site, whereas the first M nodes in set D denote the vehicles at the downstream site and the next N nodes are the "dummy" vehicles. Each edge $e(i, j)$, $i = 1, \dots, N$; $j = 1, \dots, M$, corresponds to a potential match between the upstream vehicle i and the downstream one j . The edge $e(i, j)$, $i = 1, \dots, N$; $j = M+1, \dots, M+N$,

indicates that upstream vehicle i does not match any downstream vehicle¹. The weight associated with each edge is defined as follows:

$$\omega(i, j) = \begin{cases} \varpi(i, j) & i = 1, 2 \dots, N; j = 1, 2 \dots, M \\ \varpi(i, \tau) & i = 1, 2 \dots, N; j = M + 1, \dots, M + N \end{cases} \quad (4.23)$$

Obviously, the graph structure arising in such a case is capable of representing the constraints on the vehicle matching problem (e.g. Sedgewick, 2002; Gao et al., 2011). In practice, the matching allows no duplicate, which means that each vehicle can only have, at most, one matched vehicle at downstream site. This bipartite graph matching is considerably simpler, and can be solved in polynomial time.

4.4.2 Formulation as a minimum-weight bipartite matching problem

By substituting Equation (4.23) into Problem (4.22), the optimization problem can be reformulated as follows:

$$\min_{\psi} \sum_{i=1}^N \sum_{j=1}^{M+N} \omega(i, j) \delta(\psi(i) = j) \quad (4.24)$$

$$\text{s.t. } \delta(\psi(i) = j) \in \{0, 1\}, \quad \forall i \in \{1, 2, \dots, N\}, j \in \{1, 2, \dots, M + N\} \quad (4.25)$$

$$\sum_{j=1}^{M+N} \delta(\psi(i) = j) = 1, \quad \forall i \in \{1, 2, \dots, N\} \quad (4.26)$$

$$\sum_{i=1}^N \delta(\psi(i) = j) \leq 1, \quad \forall j \in \{1, 2, \dots, M + N\} \quad (4.27)$$

Objective (4.24) is to minimize the overall weight in the bipartite matching graph. Constraint (4.25) ensures that the $\delta(\cdot)$ are indicator variables (i.e. binary integers). Constraint (4.26) requires that an upstream vehicle must be matched to a downstream vehicle or a dummy vehicle (see Figure 4.4), whereas Constraint (4.27) guarantees that an downstream vehicle, can have, at most, one matched upstream vehicle.

¹Note that this situation may arise when the freeway segment has on/off-ramps. The vehicles detected at upstream station may not necessarily arrive at downstream station. As there are no video cameras installed at on/off-ramps, we use $\psi(i) = \tau$ to represent this scenario (see Equation (4.1)). However, we show in Appendix 4.A that the bipartite graph representation can still be applied to this situation (i.e. freeway segment with on/off-ramps under the surveillance of video cameras).

The constrained optimization problem described above is equivalent to a minimum-weight bipartite matching problem: given the weighted bipartite graph G (see Figure 4.4), the problem is solved by computing the max cardinality minimum weight matching (see Figure 4.5). The minimum-weight bipartite matching problem has been widely studied in the

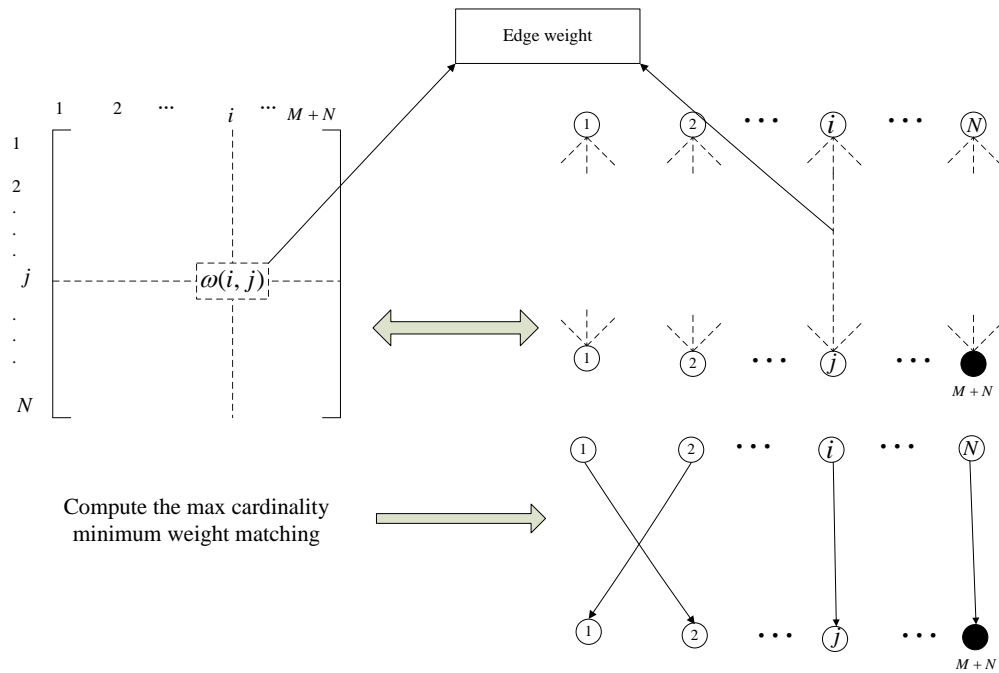


Figure 4.5: Bipartite matching procedure

field of computer science and a wealth of algorithms has been developed for it (e.g. Conte et al., 2003; Belongie and Malik, 2000; Hsieh et al., 1995). In this research, we adopt the successive shortest path algorithm which is an efficient method for solving the bipartite matching problem (Ahuja et al., 1993), and the computation complexity is $O(N^2M)$.

4.5 Test results

In this section, the performance and accuracy of the basic vision-based VRI system is presented. In order to validate the matching accuracy, the ground-truth matches were determined by a human operator viewing the video record frame by frame.

Our system starts with the probability parameter estimation from the historical data. Here we utilize a training dataset which contains 449 pairs of correctly matched vehicles to

estimate the probability parameter as well as the historical travel time distribution (see Figure 4.6(a)).

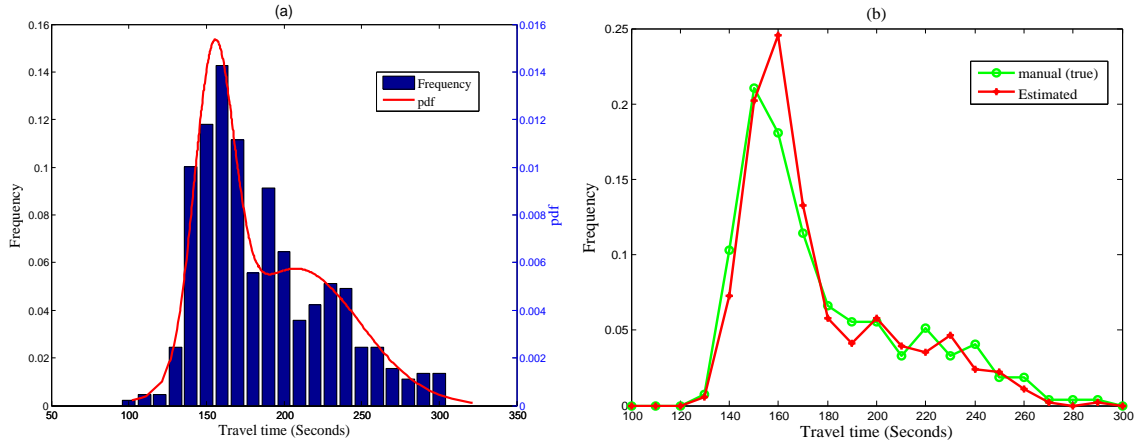


Figure 4.6: Travel time distribution: (a) the pdf of historical travel time distribution; (b) estimated and manual observed travel time distribution.

4.5.1 Travel time distribution

Upon completion of the vehicle detection, 574 vehicles are detected at upstream site in 10 minutes. By applying our vehicle reidentification method, 271 vehicles are correctly matched, while 79 vehicles does not correspond to any downstream vehicle. Thus the matching accuracy is $271/(574 - 79) = 54.75\%$. From the matched vehicles one could obtain the travel time distribution. As shown in Figure 4.6(b), the measured travel time histogram is computed directly from our system, while the manual observed distribution is obtained by calculating the time differences between the 271 pairs of correctly matched vehicles. To validate the reliability of our travel time estimation system, Root Mean Square (RMS) error is applied as performance index. The equation of RMS error is given by:

$$\text{RMS error} = \sqrt{\frac{1}{n} \sum_{i=1}^n \left| \frac{Y_i - Y_i^*}{Y_i^*} \right|^2} = 0.2387 \quad (4.28)$$

where n indicates the number of the bins of the histogram, Y_i is the estimated frequency of travel time and Y_i^* is the manual observed (true) frequency. The relative small RMS error suggests that these two travel time distributions are "statistically" similar. In addition to the RMS error, we could also obtain the differences between the two means and the two

stand deviations:

difference between the two mean travel times: $|175.2934 - 177.4331| = 2.1397$ secs

difference between the two standard deviations: $|30.7744 - 33.7277| = 2.9533$

Based on these performance indices, we can draw a conclusion that our travel time estimation system is reliable.

4.5.2 Performance of probabilistic feature fusion approach

Table (4.1) shows the performance of our vehicle reidentification algorithm for different features, namely, color, type and length individually, as well as for the probabilistic fusion cases. The first three rows indicate that the reidentification accuracy of color, type and length, when used individually, is 36.04%, 23.58% and 17.39%, respectively. From these results, we observe that the performance for color feature is much better than the other two features. This is reasonable due to several reasons. First, the color information regarding each vehicle is represented by a 360-dimensional vector. Thus our system is very sensitive to the difference between vehicle colors. Second, although the vehicle length measurement is accurate, it is not enough for us to distinguish the vehicle from others. Actually, we can only re-identify those "long vehicles" when only the length information is used. Third, due to the limitation of image processing techniques, the vehicle type recognition is not so successful, which results in the low reidentification accuracy.

The last two rows in Table (4.1) show that the reidentification accuracy after fusion increased to 48.57% and 54.75%, respectively. Therefore, we could observe that the probabilistic fusion approach clearly outperforms other three vehicle features.

Table 4.1: Performance of Vehicle Re-Identification Algorithm Regarding Different Fusion Weights

Color weight α	Type weight β	Length weight γ	Matching accuracy
1	0	0	36.04%
0	1	0	23.58%
0	0	1	17.39%
0.7143	0	0.2857	48.57%
0.4680	0.3062	0.2258	54.75%

4.5.3 Vehicle reidentification across multiple lanes

As was previously mentioned, our system does not require vehicle platoon information to perform reidentification. Therefore it can be applied across multiple lanes, which means that the vehicles changing lanes can also be re-identified (see Figure 4.7). Among the 271

Upstream vehicle	Corresponding downstream vehicle
	
Lane3	Lane 1; Travel time: 187.36s

Figure 4.7: Vehicle matching across multiple lanes

pairs of correctly matched vehicles, there are 63 pairs of vehicles changing lanes. From the test result we can conclude that the number of lane changes amounts for 25% of the traffic. Since the length of the test section of the expressway system is only 3.6 kilometers, it can be expected that lane changes will become more frequent on certain longer sections of the roadway. Thus, the development of an algorithm that allows reidentification across multiple lanes is of great importance.

4.6 Conclusion remarks

This chapter examines the fusion of vehicle features in a probabilistic framework for vehicle reidentification and travel time estimation. Three feature vectors are extracted from the video image data based on various image processing techniques. Since the vehicle reidentification algorithm does not require lane sequence information, it can be applied to re-identify vehicle across multiple lanes. The approach is tested on a 3.6-kilometer segment of the freeway system in Bangkok, Thailand. The overall reidentification accuracy is about 54.75%. For travel time estimation purpose, the result shows that the travel time distribution estimated by our system is reliable.

For the proposed basic VRI system, the following two comments should be taken into account.

- First, it is observed that the basic vision-based VRI heavily depends on the specification of the time window constraint (Section 4.3.1) and the *prior* probability, both of which are derived from the historical travel time data and remain unchanged during the vehicle matching process. The above-mentioned phenomenon also implies that the basic VRI system is specifically devised for a short time period in which the traffic condition is relatively stable. And the travel time estimator is expected to be reliable under static traffic condition, as the prior knowledge will not deviate dramatically from the ground-truth traffic information. For travel time estimation under dynamic traffic conditions, an improved self-adaptive VRI system is developed in Part III of the thesis.
- Second, the basic VRI focuses on improving the overall matching accuracy, which could be potentially beneficial to the efficient traffic incident management (see Chapter 5). As explained in this chapter, the performance of VRI system relies on the quality of the feature data and the robustness of the matching method. The high quality of feature data (e.g. high resolution of vehicle length) would greatly relieve the burden of the matching method. And accordingly, a simple distance-based method would satisfy the need for vehicle reidentification. However, the feature data obtained from various sensing technologies may be of poor qualities in practical implementation. In our experience, IVS technology is subject to the effects of inclement weather (e.g. rain, snow) and illumination changes. Under these circumstances, the quality of the video image will decrease dramatically and hence

undermine the effectiveness of vehicle data extraction. Therefore, this study utilizes the statistical matching method such that the uncertainties of the feature data are explicitly considered (see Section [4.3.2](#)).

Appendix

4.A Freeway segment with entry/exit ramps

Consider a freeway segment with entry/exit ramps along which the video cameras are installed (see Figure 4.8). It is observed that a vehicle could enter this freeway segment through the upstream station or the entry ramp. And accordingly, this very vehicle could appear at downstream station or leave the freeway through the exit ramp. Therefore, the associated VRI problem can be viewed as a network-wide matching of the vehicle signatures. In this part, we would demonstrate that the proposed bipartite matching method (Section 4.4) can still be applied to this network case.

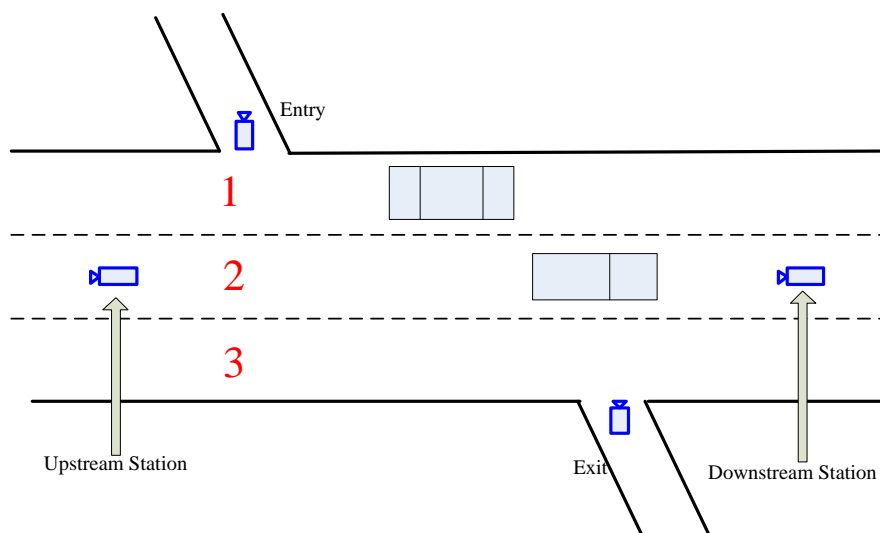


Figure 4.8: Conceptual test site

Specifically, all the nodes (i.e. the stations under the surveillance of video cameras) in the

4.A Freeway segment with entry/exit ramps

"network" can be divided into two parts, i.e. origins and destinations. In this particular case, the set of origins O consists of the upstream station and entry ramp, while the set of destinations D comprises of exit ramp and downstream station (see Figure 4.9). All the vehicles detected at origins (e.g. node 1 and node 2) will be indexed based on their arrival times and the origin vehicle set can still be defined as $O = \{1, 2, \dots\}$. Likewise, the candidate vehicle set D can be derived based on the time window constraint. The *posterior* probability between these two sets is then given by

$$P(\psi | \mathcal{D}_{\text{color}}, \mathcal{D}_{\text{type}}, \mathcal{D}_{\text{length}}) = \frac{p(\mathcal{D}_{\text{color}}, \mathcal{D}_{\text{type}}, \mathcal{D}_{\text{length}} | \psi) P(\psi)}{p(\mathcal{D}_{\text{color}}, \mathcal{D}_{\text{type}}, \mathcal{D}_{\text{length}})} \quad (4.29)$$

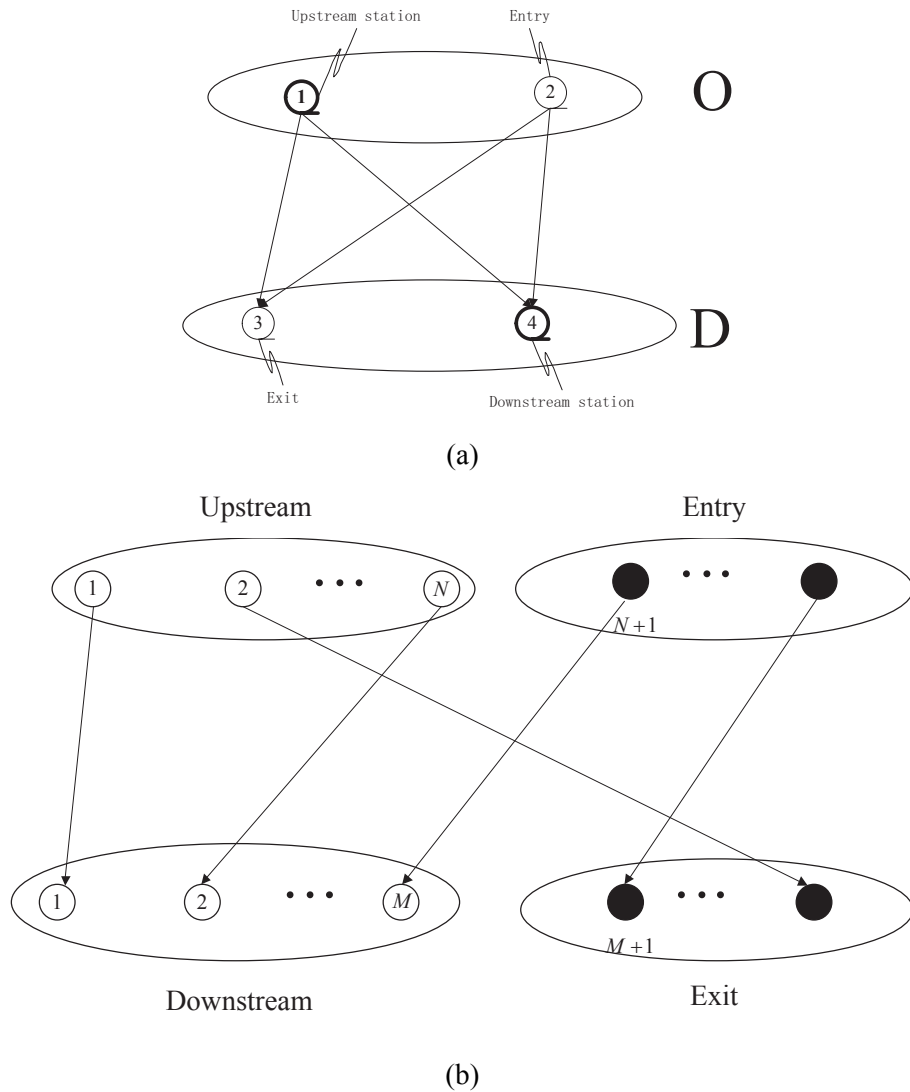


Figure 4.9: (a) Topological structure; (b) Bipartite graph representation

In this case, the definition of the *prior* knowledge is of great importance to the success of

network matching. Several additional factors should be considered for the formation of the *prior* knowledge $P(\psi)$:

- Time difference (i.e. historical travel time distribution): for each route (e.g. path from node 1 to node 3), the historical travel time distribution can be utilized for defining the *prior* probability (i.e. temporal reasoning), which can be found in Equations (4.13) and (4.14).
- Route choice model (e.g. historical origin-destination matrix): the presence of multiple origins/destinations would give rise to multiple routes. In such case, an appropriate route choice model (i.e. spatial reasoning mentioned in Section 3.3.2) would allow for the efficient prediction of the vehicle's destination. We suggest utilizing the historical origin-destination matrix to approximate the likelihood of traveling on specific route.

Theoretically speaking, the bipartite matching method proposed in basic VRI is equally applicable to the network case. However, it still suffers from two serious limitations.

- First, the computational time of vehicle matching would increase dramatically when it comes to the network case. The size of the candidate vehicles would increase due to the existence of multiple origins, and consequently lead to the massive computation in the process of bipartite matching.
- Second, the definition of the *prior* probability becomes much more difficult when it comes to large network. The estimated route choice may deviate dramatically from the actual route decision, which could eventually undermine the performance of the vehicle matching.

To sum up, the network-wide matching of vehicle signatures is still challenging in practical implementation and the matching accuracy would decrease significantly with respect to the increase in the size of the traffic network.

Chapter 5

VRI based incident detection under free flow condition

This chapter proposes a vehicle reidentification (VRI) based automatic incident algorithm (AID) for freeway system under free flow condition. An enhanced vehicle feature matching technique is adopted in the VRI component of the proposed system. In this study, arrival time interval, which is estimated based on the historical database, is introduced into the VRI component to improve the matching accuracy and reduce the incident detection time. Also, a screening method, which is based on the ratios of the matching probabilities and arrival time windows, is introduced to the VRI component to reduce false alarm rate. The proposed AID algorithm is tested on a 3.6-km segment of a closed freeway system in Bangkok, Thailand. The results show that in terms of incident detection time, the proposed AID algorithm outperforms the traditional vehicle count approach.

5.1 Introduction

Traffic incidents have been widely recognized as a serious problem for its negative effects on traffic congestion and safety. Under heavy traffic condition, one minor incident could result in gridlock and hence serious traffic congestion. In addition, traffic injuries are likely to be more severe if incidents occur at higher speeds (e.g. free flow condition). Statistics also suggest the high chance of a more severe secondary accident following the

initial incident on freeway (e.g. [Chou and Miller-Hooks, 2010](#); [Fries et al., 2007](#); [Vlahogianni et al., 2012](#)). An ability to detect incident in a timely and accurate manner would allow the traffic manager to efficiently remove the incident, to notify the follow-up traffic of the incident and the corresponding impacts, and to better manage the traffic for minimizing impact caused by the incident. Therefore, considerable research efforts have been dedicated to the development of automatic incident detection (AID) algorithms by utilizing the traditional detectors (i.e. inductive loops) over the past few decades (e.g. the California algorithm series ([Payne and Tignor, 1978](#)), McMaster algorithm ([Hall et al., 1993](#))). The underlying assumption of these algorithms is that the aggregated traffic parameters (e.g. travel time, traffic flow) would change dramatically when incidents occur under congested situation. By comparing the real-time traffic data with the incident-free data, one can determine the likelihood that an incident has happened. Based on the above-mentioned principle, various advanced data mining approaches (e.g. neural network, Bayesian network, Kalman filter) are adopted for detecting the abnormal traffic delay or abrupt change in traffic flow pattern ([Srinivasan et al., 2004](#); [Zhang and Taylor, 2006](#)). However, most of the existing incident detection algorithms are specifically designed for congested traffic conditions¹ and may not be applicable for free flow situations.

Detecting incidents under free flow condition is difficult as it faces the following two major challenges. First, the conventional traffic sensors (i.e. single inductive loops) are not able to provide traffic data with satisfactory quality under free flow condition. Due to the limitation of the sampling rate of single inductive loops, the passenger vehicle data (e.g. vehicle speed and vehicle length) cannot be collected accurately if a vehicle is traveling at high speed ([Coifman and Krishnamurthy, 2007](#)). Such inaccurate traffic data causes a serious problem for developing the aforementioned data mining based incident detection algorithm. Second, under the free flow condition, a drop in traffic capacity due to an incident (e.g. one lane blocking) may not cause any traffic delay or change in the traffic flow pattern. Therefore, it is not feasible to detect the incident through analyzing the macroscopic traffic parameters. To handle the aforementioned challenges, [Shehata et al. \(2008\)](#) conducted a study to detect the incident by identifying non-moving vehicle (i.e. caused by an incident) from vide records by using image processing techniques. Although this method appears to be theoretically sound, the deployment of such system requires the installations of camera at all key locations along the freeway, which is not practically feasible for monitoring a long distance freeway. In this case, the approaches that focus

¹A more detailed review regarding the incident detection algorithms for congested traffic conditions can be found in Section [2.4.2](#).

on the continuous tracking of individual vehicles across consecutive detectors provide a promising way for incident detection. The rationale behind this idea is straightforward. For a closed freeway system, if one can track all the vehicles along the designated points, a disappearance of any vehicle movement between consecutive points can be classified as a potential incident. Based on this principle, [Fambro and Ritch \(1980\)](#) designed a "vehicle count approach" to trace and identify the "missing" vehicle through the vehicle count data obtained from the loop detectors. Given the vehicle speed at upstream, the arrival time window at downstream could be estimated. By comparing the vehicle counts in this arrival time window with the corresponding vehicle counts in the upstream, one may be able to identify the missing vehicle (if any) for incident detection. However, the performance of this approach is largely dependent on the accuracy of the vehicle count data and the estimated arrival time window. Also, the overlapping of arrival time windows of different vehicles would lead to a significant increase in the detection time (this will be discussed in more detail in Section 5.3). To further reduce the incident detection time, much attention has been paid to track the vehicle by utilizing the emerging automatic vehicle identification (AVI) systems¹: automatic number plate recognition ([Chang et al., 2004](#)), or Bluetooth identification technology ([Quayle et al., 2010](#)). Although the AVI technologies enable a more efficient tracking of vehicles across multiple points by accurately matching their unique identity (e.g. plate number, media access control address), the success of these systems relies on the high level of market penetration of the AVI-equipped vehicles (in principle 100% of penetration rate is required). Also, the AVI technologies may raise privacy issues. In this case, the vehicle re-identification (VRI) scheme, which does not intrude driver's privacy, provides a tool to devise a more practical and effective incident detection algorithm under free flow condition.

Generally, vehicle re-identification is a process of matching vehicle signature (e.g. waveform, vehicle length, etc) from one detector to the next one in the traffic network. The non-uniqueness of the vehicle signature would allow the VRI system to track the vehicle anonymously ([Cetin et al., 2011](#)). During the past few years, extensive researches were carried out to develop VRI systems based on conventional loop detectors ([Coifman and Cassidy, 2002](#); [Coifman, 1998](#); [Sun et al., 1999](#)). As presented in Chapter 4, the basic VRI system based on the emerging video surveillance technology (see Chapter 3) is developed. Various detailed vehicle features (e.g. vehicle color, length and type) are extracted and a probabilistic data fusion rule was then introduced to combine these features to generate a

¹The AVI systems also contribute to the development of probe-vehicle-based methods introduced in Section 2.1.4.

matching probability for the re-identification purpose. To account for the large variance in travel time, basic VRI also introduces a fixed time window constraint to reduce the computational time of the vehicle matching problem. However, it is noteworthy that the aforementioned VRI systems are specifically designed for the purpose of traffic data collection (e.g. travel time). To our knowledge, very few studies were explicitly conducted to investigate the potential feasibility of utilizing VRI system for incident detection. Also, as the existing VRI system cannot guarantee an accurate matching due to the non-uniqueness of the vehicle signatures, the mismatches between the upstream and downstream vehicles may potentially lead to false alarms in the incident detection system.

To this end, this paper aims to propose a VRI-based automatic incident detection algorithm under free flow condition. The revised VRI system adopted in the proposed incident algorithm is based on basic VRI (see Chapter 4) with several major changes to cope with the purpose of incident detection (i.e. incident-detection-oriented VRI).

- Note that in basic VRI a unified and fixed time window constraint (i.e. $[t_{\min}, t_{\max}]$ in Section 4.3.1) is imposed on all the vehicles. However, the vehicle would maintain a relatively stable speed under free flow condition, which allows for the estimation of a flexible time window for each individual vehicle. Therefore, this incident-detection-oriented VRI would introduce a flexible time window to further improving the matching accuracy and reduce the incident detection time.
- Rather than finding the matching results between two sets of vehicles (i.e. bipartite matching method in Section 4.4), the incident-detection-oriented VRI attempts to make an instant matching decision for each individual vehicle such that the "missing" vehicle can be identified promptly. In other words, the matching probability for each pair of vehicle signatures is explicitly calculated.
- Last but not least, a screening method, which is based on the ratios of the matching probabilities, is introduced to screen out the mismatched vehicles for reducing the false alarm rate.

The rest of the chapter is organized as follows. Section 5.2 describes the traffic dataset collected for the algorithm development and evaluation. In Section 5.3, the overall framework of the proposed automatic incident detection system is introduced. The description and analysis of the incident-detection-oriented VRI system under free flow condition are

5.2 Dataset for algorithm development and evaluation

proposed in the following two sections (Section 5.4 and Section 5.5). In Section 5.6, simulated tests and real-world case studies are carried out to evaluate the performance of the proposed AID system against the traditional vehicle count approach. Finally, we close this chapter with the conclusion remarks.

5.2 Dataset for algorithm development and evaluation

The test site is a 3.6-km-long section of the closed three-lane freeway in Bangkok, Thailand (the green section in Figure 5.1). At each station (i.e. location 10B and 08B in Figure 5.1) a gantry-mounted video camera, which is viewed in the upstream direction, is installed and two hours of video record (10 a.m. and noon on March 15, 2011) was collected. The frame rate of the video record is 25 FPS and the still image size is 563×764 .

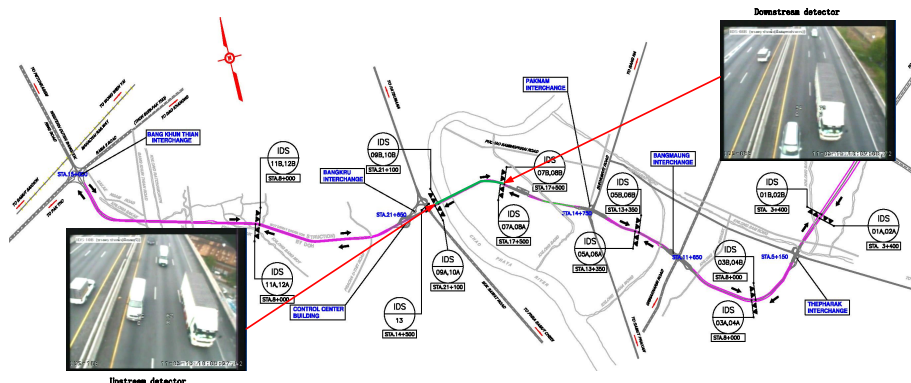


Figure 5.1: Test site in Bangkok, Thailand

As the detailed traffic data (especially the individual vehicle data) are not readily obtainable from the raw video record, the intelligent video surveillance (IVS) is then employed for extracting the required information (e.g. vehicle feature data and spot speed). Detailed implementation of the IVS for traffic data extraction can be found in Section 2.3 and Chapter 3. In the following, a formal description of the dataset obtained from IVS is presented.

5.2.1 Dataset description

IVS provides a large amount of traffic data to develop and validate the automatic incident detection algorithms proposed in this chapter. Let $U = \{1, 2, \dots, N\}$ denote the N vehicles detected at upstream station during the time interval. $D = \{1, 2, \dots, M\}$ is the set of downstream vehicles. In addition, t_i^U and v_i^U are the associated arrival time and the spot speed of the i th upstream vehicle, respectively. Accordingly, t_j^D and v_j^D are the corresponding arrival time and spot speed of the j th downstream vehicle. As discussed in Section 3.2, for each detected individual vehicle, the intrinsic feature data (e.g. color, size, length) are also obtained. Let $X_i^U = \{C_i^U, S_i^U, L_i^U\}$ denote the signature of the i th upstream vehicle, where C_i^U and S_i^U are the normalized color feature vector and type (shape) feature vector, respectively. L_i^U denotes the normalized the length of vehicle i . Similarly, $X_j^D = \{C_j^D, S_j^D, L_j^D\}$ is the signature of the j th downstream vehicle. To sum up, dataset from the IVS during a time interval consists of the upstream vehicle dataset $\{(t_i^U, v_i^U, X_i^U), i = 1, 2, \dots, N\}$ and the downstream vehicle set $\{(t_j^D, v_j^D, X_j^D), j = 1, 2, \dots, M\}$. In order to quantify the difference between each pair of upstream and downstream vehicle signatures, several distance measures are then incorporated. Specifically, for a pair of signatures (X_i^U, X_j^D) , the Bhattacharyya distance is utilized to calculate the degree of similarity between color features:

$$d_{\text{color}}(i, j) = \left[1 - \sum_{k=1}^{360} \sqrt{C_i^U(k) \cdot C_j^D(k)} \right]^{1/2} \quad (5.1)$$

where k denoted the k th component of the color feature vector. The L_1 distance measure is introduced to represent the difference between the type feature vectors:

$$d_{\text{type}}(i, j) = \sum_{k=1}^q |S_i^U(k) - S_j^D(k)| \quad (5.2)$$

where q is the number of vehicle type template and is taken as 6 in this study. The length difference is given by

$$d_{\text{length}}(i, j) = |L_i^U - L_j^D| \quad (5.3)$$

Based on the video record collected at the test site, 3,628 vehicles are detected at both stations (10B and 08B) during the two-hour video record. For the purpose of the algorithm development and evaluation, these 3,628 pairs of vehicles are manually matched (i.e. re-identified) by the human operators viewing the video record frame by frame. In

5.3 Overall framework of automatic incident detection system

other words, the ground-truth matching results of the 3,628 pairs of vehicles are obtained in advance. The mean travel time is 170.9 seconds. The first 800 pairs of vehicle data are used for the model training and calibration (which are discussed in the following sections), while the rest of the vehicle dataset are used for the simulation test of the proposed automatic incident detection algorithm.

5.3 Overall framework of automatic incident detection system

The basic idea of incident detection under free flow condition is to track the individual vehicle so as to identify the missing vehicle due to an incident. Owing to its computational and theoretical simplicity, the vehicle count approach (Fambro and Ritch, 1980) is the most well-known free-flow incident detection algorithm. Thus, it is necessary to revisit this method in detail.

5.3.1 Vehicle count approach

The basic operation of the vehicle count approach is illustrated in Figure 5.2. When a vehicle U_i arrives at upstream station at time t_i^U , the expected arrival time window $[t_i^U + Lb_i, t_i^U + Ub_i]$ of this vehicle at downstream station is estimated, where Lb_i and Ub_i respectively represent the lower and upper bounds of the vehicle's travel time. If another vehicle U_j is detected at upstream station, the corresponding arrival time window $[t_j^U + Lb_j, t_j^U + Ub_j]$ can also be obtained. Unsurprisingly, there may be overlap between these two time windows, and both of these two vehicles are likely to arrive at downstream during time interval $[t_j^U + Lb_j, t_i^U + Ub_i]$. The incident would then be detected by comparing the collected vehicle count data to the expected number of vehicles in the time interval. In the case that vehicle U_i is missing, if vehicle U_j arrives at downstream during time interval $[t_j^U + Lb_j, t_i^U + Ub_i]$, then the incident alarm will not be triggered until time $t_j^U + Ub_j$, which is clearly later than the upper bound of the arrival time of vehicle U_i (i.e. $t_i^U + Ub_i$). Because of the overlapping between the time windows, the vehicle count approach, which is solely based on comparing the vehicle counts data, cannot promptly detect the incident (i.e. delay in incident detection). In general, the incident detection time

5.3 Overall framework of automatic incident detection system

would significantly increase with respect to the increase in size of vehicle platoon at the upstream detector, which increases the number of overlapping in arrival time intervals at the downstream detector.

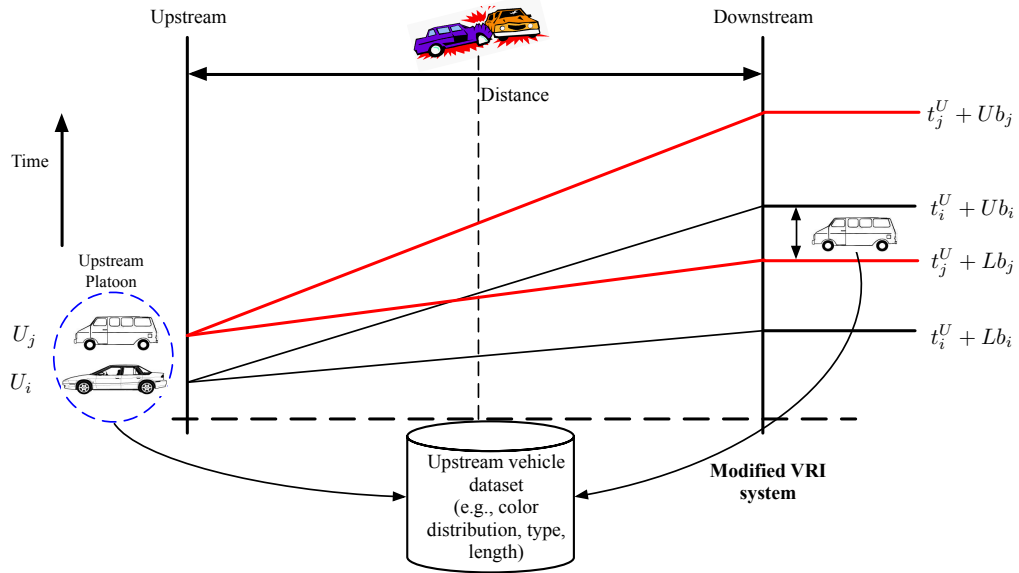


Figure 5.2: Illustrative example of vehicle count approach

To reduce the detection time, this research proposes a novel incident detection algorithm by incorporating the vision-based VRI system. As shown in Figure 5.2, vehicle U_i and U_j are detected and their detailed feature data (e.g. color, type and length) are also extracted. Once a vehicle is detected at downstream site, the proposed VRI system is performed to find a matched upstream vehicle based on the vehicle feature data. In the case that vehicle U_i is missing, if the downstream vehicle could be matched to the vehicle U_j based on the vehicle feature, an incident alarm would be triggered at time $t_i^U + Ub_i$, as vehicle U_i is not re-identified during time window $[t_i^U + Lb_i, t_i^U + Ub_i]$. As shown by this "toy" example, the additional VRI component could potentially reduce the incident detection time to some extent. However, it is also observed that the basic VRI proposed in Chapter 4 is not readily transferable to the field of incident detection and several modifications should be made regarding the vehicle matching process.

- First, instead of finding the matching result for upstream vehicle, the incident-detection-oriented VRI attempts to match the vehicles at downstream site such that proposed AID algorithm can be implemented in real-time.
- Second, once a vehicle passes the downstream station, the incident-detection-oriented

5.3 Overall framework of automatic incident detection system

VRI should be capable of making matching decision immediately such that the missing vehicle (i.e. the vehicle does not appear at downstream) could be promptly identified, which means that the bipartite matching method may not be applicable. Therefore, this study calculates the matching probability for each pair of vehicles on which the following screening method could be imposed to further reduce the false alarm rate.

The overall framework of the proposed algorithm is presented in the following subsection.

5.3.2 AID algorithm based on VRI system

The detailed implementation of the VRI-based incident detection system is summarized in the following flowchart (Figure 5.3). First, the system will initialize the timestamp, t , and check whether a vehicle is detected at the upstream and/or downstream station. If a vehicle is detected at upstream detector, the expected arrival time window of this vehicle at downstream station will be estimated based on the historical data. The record of the detected vehicle at upstream will be stored in the database as unmatched upstream vehicle. On the other hand, if a vehicle is captured at the downstream station, the system will perform the incident-detection-oriented VRI subsystem to check whether this detected vehicle match with any of the unmatched upstream vehicle. The time window constraint is utilized to identify the potential matches for this vehicle detected at downstream station. Once the match is found, the matched vehicle data will be removed from the list of the unmatched upstream vehicles.

After the previous two steps for handling the detected vehicles at upstream and downstream stations, the system will proceed to determine whether there is an incident occurs on the monitored segment. For incident detection, the system will screen through the list of unmatched vehicles. If the current time (t) is out of the expected arrival time window (i.e. greater than the upper bound of the arrival time interval) of the unmatched vehicle, an incident alarm will be issued. If not, t will be set to $t + 1$ and the system will move forward to the next time step. It could be easily observed that the performance of the incident detection system is heavily dependent on two critical components, i.e. flexible time window constraint and incident-detection-oriented VRI system.

For the aforementioned framework, the following three comments should be taken into account.

5.3 Overall framework of automatic incident detection system

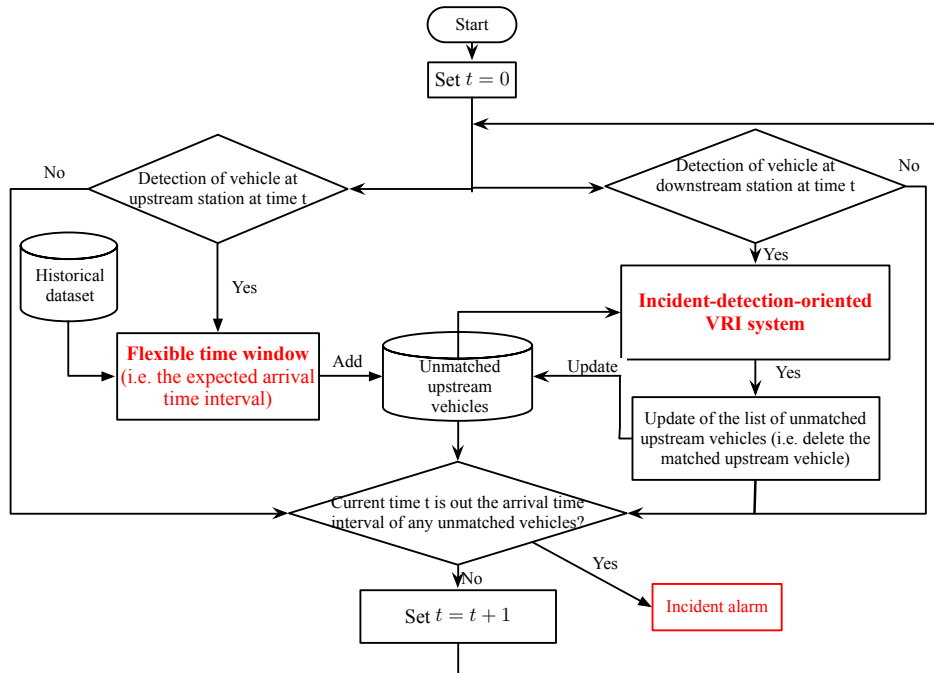


Figure 5.3: Overall framework of AID system

- First, the detection error is not considered in this study. In other words, it is assumed that all the vehicles cross the video cameras will be detected. This is achievable under free flow condition, as there is no occlusion between the vehicles and, consequently, IVS performs generally well and are able to detect most of the individual vehicles.
- Second, under free flow condition, the traveling behavior of the individual vehicle is more predictable. This phenomenon enables the estimation of the flexible arrival time window for each individual vehicle based on the current spot speed and the historical data. It is expected that the accurate estimation of the arrival time window could potentially lead to an improved matching accuracy of the VRI method, and hence reduce the incident detection time.
- Third, it should be noted that the proposed VRI cannot guarantee an accurate matching because of the non-uniqueness of the vehicle signatures. Instead, the proposed VRI scheme in this paper can only provide the matching probability between the downstream and upstream vehicles. Therefore, some of the mismatches resulted from the matching probability could potentially lead to false alarms. To handle this, a ration method is introduced to screen out those mismatches for reducing the false alarms.

5.4 Flexible time window estimation

Under free flow condition, each individual vehicle would maintain in a relatively stable speed (i.e. low variance in travel time). In this case, the arrival time of the vehicle at downstream station could be estimated based on the spot speed and historical data. Let U_i represent an upstream vehicle detected at time t_i^U , and the associated upstream spot speed is denoted as v_i^U . The expected arrival time Arr of vehicle U_i is given by

$$Arr = t_i^U + \frac{l}{0.5(v_i^U + v_i^D)} \quad (5.4)$$

where l is the distance between the upstream and downstream detectors; v_i^D is the estimated vehicle speed at downstream detector based on the historical speed database. To account for the error in estimating the downstream spot speed, the upper and lower bounds of v_i^D are provided by the following equations

$$v_{ub}^D = \sigma_{ub} \times V_{hist}^D(t') \times \frac{v_i^U}{V^U} \quad (5.5)$$

$$v_{lb}^D = \sigma_{lb} \times V_{hist}^D(t') \times \frac{v_i^U}{V^U} \quad (5.6)$$

where v_{ub}^D and v_{lb}^D are respectively the upper and lower bounds of the vehicle at downstream detector; V^U is the current average speed of the upstream detector; $\sigma_{ub} \geq 1$ and $\sigma_{lb} \leq 1$ are respectively the associated upper and lower bound factors; V_{hist}^D is the historical average speed of the downstream detector at time t' . The time t' is chosen such that it is matched with the arrival time, which is estimated by a linear speed profile of the modeled section, at the downstream detector. The estimation of downstream spot speeds can be viewed as a prediction-correction process. First, the historical average speed $V_{hist}^D(t')$ is adopted to predict the speed of this vehicle at downstream site. Then this prediction is corrected by the factor v_i^U/V^U for the better representation of the current traffic condition. Finally, the upper and lower bound factors (σ_{ub} and σ_{lb}) are applied for determining the upper of lower bounds of the downstream spot speed. With the estimated downstream speeds, the corresponding upper and lower bounds of the travel time of vehicle U_i can be calculated as follows:

$$Ub_i = \frac{l}{0.5(v_i^U + v_{ub}^D)} \quad (5.7)$$

$$Lb_i = \frac{l}{0.5(v_i^U + v_{lb}^D)} \quad (5.8)$$

However, it should be noted that the proposed incident detection system is not confined to the above method for estimating the time window. Any other estimation methods are equally applicable to the proposed AID algorithm. With the estimated time windows, vehicles on the monitored freeway section could be "partially" tracked and re-identified in a timely and accurate manner.

5.5 Incident-detection-oriented VRI

As explained previously, the proposed VRI system is devised based on the video image data provided by IVS technology. By applying myriad image processing techniques, the detailed vehicle feature data (e.g. color, type and length) could be obtained. The vehicle matching process is then performed by comparing these vehicle feature data. In this section, the methodologies involved in the incident-detection-oriented VRI system are presented.

5.5.1 Reidentification problem

For a vehicle D_k arrives at downstream station at time t_k^D , the vehicle signature, denoted as $X_k^D = \{C_k^D, S_k^D, L_k^D\}$, is then obtained from the IVS. A search space, $\mathcal{S}(k)$, which represents the potential matches at upstream station for vehicle D_k , is determined based on the calculated arrival time window. Specifically, $\mathcal{S}(k)$ is given by

$$\mathcal{S}(k) = \{U_i \in U \mid t_i^U + Lb_i \leq t_k^D \leq t_i^U + Ub_i\} \quad (5.9)$$

where U_i represents the vehicle detected at upstream station; $[Lb_i, Ub_i]$ is the associated travel time window. The vehicle reidentification problem is to find the corresponding upstream vehicle for D_k through the search space $\mathcal{S}(k)$. Herein we introduce the assignment function ψ to represent the matching result, i.e.

$$\psi(k) : \begin{cases} D_k \rightarrow \{U_i \in \mathcal{S}(k) \mid i = 1, 2, \dots, N\} \\ k \mapsto i, \quad i = 1, 2, \dots, N \end{cases} \quad (5.10)$$

where $\psi(k) = i$ indicates that vehicle D_k is the same as U_i . Recall that for each vehicle $U_i \in \mathcal{S}(k)$, one may assign to the pair of signatures (X_i^U, X_k^D) the distances $d_{\text{color}}(i, k)$,

$d_{\text{type}}(i, k)$ and $d_{\text{length}}(i, k)$ based on Equations (5.1), (5.2) and (5.3). In this case, one simple method (i.e. distance-based method) is to find the matched upstream vehicle with the minimum feature distance. However, it should be noted that the vehicle signatures derived from IVS contain noise and are not unique. Therefore the distance measure cannot really reflect the similarities between the vehicles. Instead of directly comparing the feature distances, this study utilizes the statistical matching method. Based on the calculated feature distances, i.e. $d_{\text{color}}(i, k)$, $d_{\text{type}}(i, k)$ and $d_{\text{length}}(i, k)$, a matching probability $P(\psi(k) = i | d_{\text{color}}, d_{\text{type}}, d_{\text{length}})$ between vehicles U_i and D_k is provided for the matching decision making.

5.5.2 Calculation of matching probability

The matching probability, also referred to as the *posterior* probability, plays a fundamental role in the proposed VRI system. By applying the Bayesian rule, we have

$$P(\psi(k) = i | d_{\text{color}}, d_{\text{type}}, d_{\text{length}}) = \frac{p(d_{\text{color}}, d_{\text{type}}, d_{\text{length}} | \psi(k) = i) P(\psi(k) = i)}{p(d_{\text{color}}, d_{\text{type}}, d_{\text{length}})} \quad (5.11)$$

where $p(d_{\text{color}}, d_{\text{type}}, d_{\text{length}} | \psi(k) = i)$ is the likelihood function; $P(\psi(k) = i)$ is the prior knowledge of the assignment function. To obtain the explicit matching probability, the denominator in Equation (5.11) can further be expressed as

$$p(d_{\text{color}}, d_{\text{type}}, d_{\text{length}}) = p(d_{\text{color}}, d_{\text{type}}, d_{\text{length}} | \psi(k) = i) P(\psi_k = i) + p(d_{\text{color}}, d_{\text{type}}, d_{\text{length}} | \psi(k) \neq i) P(\psi_k \neq i) \quad (5.12)$$

On the basis of Equations (5.11) and (5.12), it is easily observed that the calculation of the matching probability is dependent on the deduction of the likelihood function and the *prior* probability. In this particular case, the *prior* probability is defined as $P(\psi(k) = i) = 0.5$, which suggests that the matching is solely based on the comparison between the vehicle feature data. The calculation of the likelihood function is completed in two steps.

- First, individual statistical models for the three feature distances are constructed and the corresponding likelihood functions are also obtained (i.e. $p(d_{\text{color}} | \psi(k))$, $p(d_{\text{type}} | \psi(k))$ and $p(d_{\text{length}} | \psi(k))$).
- Second, a data fusion rule is employed to provide the overall likelihood functions

(i.e. $p(d_{\text{color}}, d_{\text{type}}, d_{\text{length}} | \psi(k))$) in Equations (5.11) and (5.12).

5.5.2.1 Statistical modeling of feature distance

Without loss of generality, only the probabilistic modeling of color feature distance is described. In the framework of statistical modeling, the distance measure is assumed to be a random variable. Thus, for a pair of color feature vectors (C_i^U, C_k^D) , the distance $d_{\text{color}}(i, k)$ follows a certain statistical distribution. The conditional probability (i.e. likelihood function) of $d_{\text{color}}(i, k)$ is then given by

$$p(d_{\text{color}}(i, k) | \psi(k)) = \begin{cases} p_1(d_{\text{color}}(i, k)) & \text{if } \psi(k) = i \\ p_2(d_{\text{color}}(i, k)) & \text{if } \psi(i) \neq i \end{cases} \quad (5.13)$$

where p_1 denotes the probability density function (pdf) of distance $d_{\text{color}}(i, k)$ when color feature vectors C_i^U and C_k^D belong to the same vehicle, while p_2 is the pdf of the distance $d_{\text{color}}(i, k)$ between different vehicles. A historical training dataset that contains a number of pairs of correctly matched vehicles is built up for estimating the pdfs p_1 and p_2 . Finite Gaussian mixture model is used to approximate the pdfs and the well-known Expectation Maximization (EM) algorithm is applied to solve the associated parameter estimation problem¹. Likewise, the likelihood functions for the type and length distances can also be obtained in a similar manner.

5.5.2.2 Data fusion rule

In this study, the logarithmic opinion pool (LOP) approach (see Section 4.3.5) is employed to fuse the individual likelihood functions. The LOP is evaluated as a weighted product of the probabilities and the equation is given by

$$p(d_{\text{color}}, d_{\text{type}}, d_{\text{length}} | \psi(k)) = \frac{1}{Z_{\text{LOP}}} p(d_{\text{color}} | \psi(k))^\alpha p(d_{\text{type}} | \psi(k))^\beta p(d_{\text{length}} | \psi(k))^\gamma, \quad \alpha + \beta + \gamma = 1 \quad (5.14)$$

where the fusion weights, α , β and γ are used to indicate the degree of contribution of each likelihood function. The weights can also be calibrated from the training dataset. By

¹A detailed explanation on Finite Gaussian mixture model can be found in Section 4.3.2.

substituting Equations (5.12), (5.13) and (5.14) into (5.11), the desired matching probability for each pair of vehicles (U_i, D_k) could be obtained. For the sake of simplicity, let P_{ik} denote the matching probability between the vehicle U_i and D_k . In this case, we may obtain a set of probabilistic measures $\{P_{ik}|i = 1, 2, \dots, N\}$ to represent the likelihood of a correct match between D_k and the vehicles in the search space $\mathcal{S}(k)$. The final matching decision-making based on these matching probabilities, becomes the major concern in the following subsection.

5.5.3 Ratio method for final matching decision

An intuitive decision-making process (i.e. the greedy method) is to sort the matches via the matching probability $\{P_{ik}|i = 1, 2, \dots, N\}$ and choose the vehicle U_i with the maximum matching likelihood, i.e.

$$\psi(k) = i, \text{ if } P_{jk} \leq P_{ik} \quad \forall j \in \{1, 2, \dots, N\} \quad (5.15)$$

However, it is noteworthy that the proposed VRI system is utilized for incident detection purpose, the final matching decision would produce significant impacts on the performance of the AID system. Based on the greedy method (5.15), the potential false alarms would be triggered. As shown in Figure 5.4, the downstream vehicle D_k arrives at time 10:39:39 a.m. U_j and U_i are respectively the two candidate vehicles with the largest and second largest matching probabilities with the downstream vehicle D_k (i.e. $P_{jk} = 0.9295$ and $P_{ik} = 0.8392$). Although vehicle D_k actually matches with vehicle U_i (based on the manual matching), the greedy method yields the matching result $\psi(k) = j$, which could lead to a false alarm at time $t_i^U + Ub_i$.

To reduce the false alarms mentioned above, a ratio method is then introduced for the final matching decision-making. Let $\{P_i|i = 1, 2, \dots, N\}$ denote the set of matching probabilities in descending order. The ratio method proposed in this study involves two major steps. First, by imposing a threshold τ on the value of the ratio between the neighboring probabilities in the ordered set $\{P_i|i = 1, 2, \dots, N\}$, one may be able to screen through the search space and rule out those unlikely matches. The screening process is described

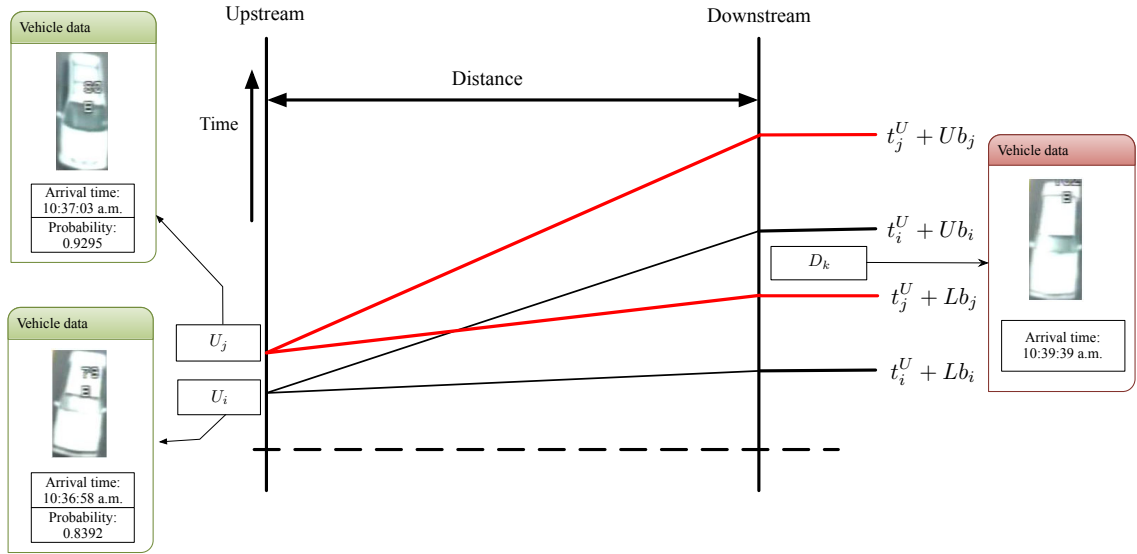


Figure 5.4: Illustrative example of a false alarm

as follows.

Procedure 5.1: Screening process

Input: A finite set $\{P_i | i = 1, 2, \dots, N\}$ of matching probabilities in descending order

Output: The set of unlikely matches for downstream vehicle D_k

- 1 $i \leftarrow 1$;
 - 2 **while** $i \leq N - 1 \wedge P_i/P_{i+1} \leq \tau$ **do**
 - 3 $i \leftarrow i + 1$;
 - 4 **return** $\{i + 1, i + 2, \dots, N\}$;
-

The underlying implication of Procedure 5.1 is that if the ratio (i.e. P_i/P_{i+1}) is sufficiently large, then it could come to a conclusion that vehicles $\{i + 1, i + 2, \dots, N\}$ are the unlikely matches due to their relatively smaller matching probabilities. Otherwise, if the ratio $P_i/P_{i+1} \leq \tau$, then we may declare that vehicle i and $i + 1$ are not distinctive from each other and a matching decision cannot be made at current stage.

Upon the completion of the above screening process, unlikely matches could be ruled out and the search space is further reduced. The second step is then to make a matching decision based on the remaining search space $\mathcal{S}_R(k)$. Let $\mathcal{S}_R(k) = \{U_m | m = 1, 2, \dots, i\}$

(clearly $i \leq N$), the matching result is then given by

$$\psi(k) = m^*, \quad \text{if } t_l^U + Ub_l \geq t_{m^*}^U + Ub_{m^*}, \quad \forall l \in \{1, 2, \dots, i\} \quad (5.16)$$

It is obvious that vehicle D_k is matched to the vehicle in $\mathcal{S}_R(k)$ with the smallest upper bound in the predicted arrival time window. The rationale behind this approach is that a matching decision could not be made based on the matching probabilities (as the matching probabilities for vehicles in $\mathcal{S}_R(k)$ are not significantly different from each other). In this case, the vehicle D_k is matched to upstream vehicle with smallest upper bound in the predicted arrival time window to avoid the potential false alarms. As a matter of fact, the second step could be viewed as a standard vehicle count approach in which only the counts data is utilized.

To sum up, the matching decision-making process of the incident-detection-oriented VRI is a hybrid of the vehicle feature comparison and the classic vehicle count approach. The overall procedure for the matching decision-making is given by

Procedure 5.2: Final matching decision-making

Input: A set $\{P_i | i = 1, 2, \dots, N\}$ of matching probabilities and the set $\{t_i^U + Ub_i | i = 1, 2, \dots, N\}$ of upper bounds in arrival time interval

Output: The final matching decision for vehicle D_k

<pre> 1 $i \leftarrow 1$; 2 while $i \leq N - 1 \wedge P_i/P_{i+1} \leq \tau$ do 3 $i \leftarrow i + 1$; 4 $\mathcal{S}_R(k) \leftarrow \{1, 2, \dots, i\}$; 5 $m^* \leftarrow \arg \min_l \{t_l^U + Ub_l l \in \mathcal{S}_R(k)\}$; 6 return $\psi(k) = m^*$; </pre>	<div style="display: flex; align-items: center;"> <div style="font-size: 3em; margin-right: 10px;">}</div> <div style="text-align: left;"> <p style="color: blue; margin: 0;">Screening Method</p> <p style="color: red; margin: 0;">Vehicle Count Approach</p> </div> </div>
--	---

5.6 Test results

In this section, the performance of the proposed AID algorithm is evaluated against the classical vehicle count approach in terms of mean time-to-detect and false alarm rate (i.e.

false alarms per hour). As the performance of the proposed AID system relies on its two critical components (i.e. flexible time window estimation and incident-detection-oriented VRI), different sizes of time window and thresholds for final matching decision are tested in this section. The dataset described in Section 5.2 are used to perform the simulated tests for the algorithm evaluation. Also, the real-world case studies are carried out in this section.

5.6.1 Simulated tests

For calibrating and testing the proposed AID system, the 3,682 pairs of vehicle matching results from the collected dataset are divided into two parts. First, a dataset of 800 pairs of correctly matched vehicles are used for model calibration and training. The upper and lower bound factors for time window estimation (i.e. σ_{ub} and σ_{lb}) are calibrated by the using the travel time data of the 800 vehicles and the historical averaging speed on Thursday, which is the same as the test day (i.e. 16/2/2012, 23/2/2012, 1/3/2012 and 8/3/2012). In addition, the parameters of the statistical model (i.e. p_1 and p_2) are estimated by utilizing the feature data extracted from the captured images of these 800 pairs of vehicles. Second, the remaining 2,828 pairs of vehicles detected at both upstream and downstream detectors are fed into the calibrated AID system for model evaluation. In order to mimic an incident between the upstream and downstream detectors, the record of vehicle at downstream site is intentionally removed to simulate the situation that the vehicle has passed the upstream detector but not the downstream one. In the testing of the proposed AID system, the AID algorithm is run for 2,828 times, which for each run the record of one of the 2,828 vehicles at downstream detector is removed, for determining the mean detection time. Specifically, the incident detection time is defined as

$$T_D = t_{\text{incident}} - t^U \quad (5.17)$$

Since we do not know the exact time when the incident happened, the incident detection time is then defined as the difference between the time when an alarm is issued (i.e. t_{incident}) and the arrival time of incident vehicle at upstream station (i.e. t^U).

By setting the threshold value equals to 2 (i.e. $\tau = 2$), the mean detection time of the proposed AID algorithm is 203.2 seconds, whereas the mean detection time of the classical vehicle count approach is 644.1 seconds. As it is expected, the mean detection time

is reduced substantially by incorporating the modified VRI system. Figure 5.5 shows the performance of the VRI-based incident detection algorithm for different threshold values adopted in final matching decision. It could be observed that the false alarm rate reduces as the threshold value increases. When the threshold value equals to one, the VRI system will always match the downstream vehicle to the upstream one with the largest matching probability. Therefore, it would lead to a large number of false alarms (see Section 5.5.3). With the increase in threshold value, the modified VRI system is more relied on the traditional vehicle count approach, and results in a decrease in the false alarm rate. On the other hand, as the proposed VRI system is more relied on the traditional vehicle count approach (e.g. $\tau \rightarrow \infty$), the mean detection time also increases (see Section 5.3.1). To sum up, for the proposed VRI system, the lowering of the false alarm rates is at the expense of incident detection time. Thus, a balance should be struck between the rapid incident detection and low false alarm rate.

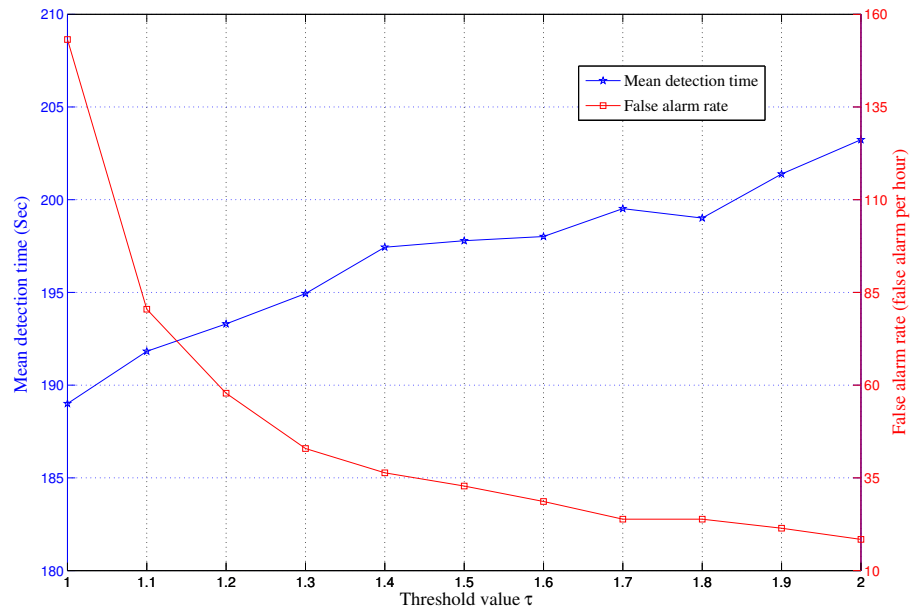


Figure 5.5: Mean detection time and false alarm rate

The estimation of arrival time window also has a significant impact on the performance of the proposed AID algorithm. It is not difficult to understand that a small time window size would result in faster incident detection. To test the performance of the proposed AID algorithm under different time window sizes, a time window with fixed size is assigned for each individual vehicle. Figure 5.6 shows the mean detection of the algorithm for different time window sizes. The mean detection time of the vehicle count approach increases dramatically as the size of the time window grows. It is also observed that the vehicle

count approach is not capable of detecting the missing vehicle as the size of time window is larger than 50 seconds. To sum up, for the simulation that a large arrival time window is applied, the proposed AID algorithm clearly outperforms the vehicle count approach.

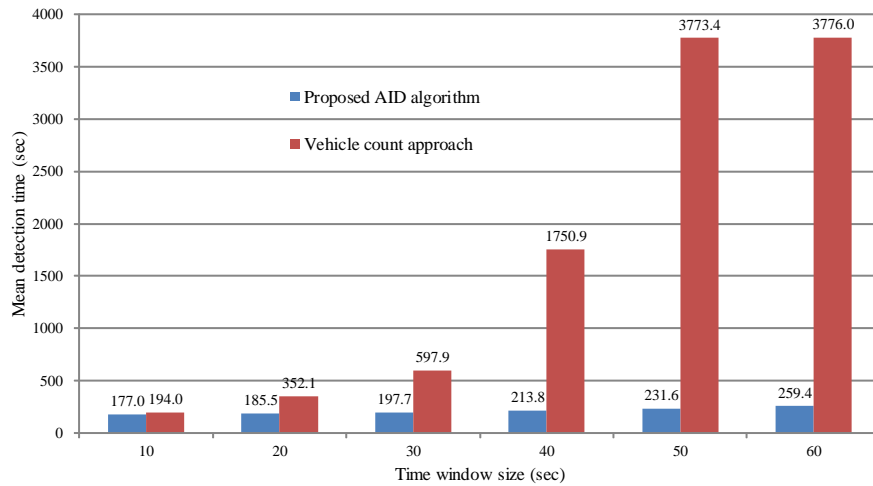


Figure 5.6: Comparison between the proposed AID algorithm and vehicle count approach

5.6.2 Real-world case study

Apart from the above-mentioned simulation tests, two real-world case studies are also carried out. Based on the record from the freeway authority, the first incident is reported on 13-Jun-2012 at 16:03. The reported incident location is at 20+600 westbound, which is in the section between camera 7A/8A and 9A/10A (see Figure 5.1). Based on this information, the research team has screened through the captured videos for identifying the incident vehicle. It is found out that on 13-Jun-2012, the incident vehicle has passed the upstream detector (7A/8A) at 15:55 (Figure 5.7(a)) and has an incident before it reaches the downstream detector (9A/10A). Four minutes later, a tow-truck, which is probably called by the driver of the incident vehicle, has passed the upstream detector (Figure 5.7(b)) and towed the incident vehicle to pass the downstream detector at 16:09 (Figure 5.7(c)).

According to the above information of the incident vehicle, a 35-minutes video record data (from 15:33 to 16:08 on 13-Jun-2012) of locations 8A and 10A are extracted and input into the proposed AID system for free flow condition. In this case, apart from the incident vehicle, 739 vehicles are detected at both stations during the 35-minute video record. By setting the threshold value of the ratio of matching probabilities equals to **8.5**, the time of



Figure 5.7: Real-world case study #1: (a) Incident vehicle passes the upstream detector; (b) Tow truck passes the upstream detector; (c) Incident vehicle and truck passes through the downstream detector

incident detection and the false alarm rate for this case study are found to be **15:58:22**, and **3.42** false alarms per hour, respectively. Compared with the classic vehicle count approach, which would trigger an incident alarm at **16:01:28**, the proposed AID system performs better in terms of the incident detection time.

The incident vehicle of the second real-world case study is shown in Figure 5.8. This

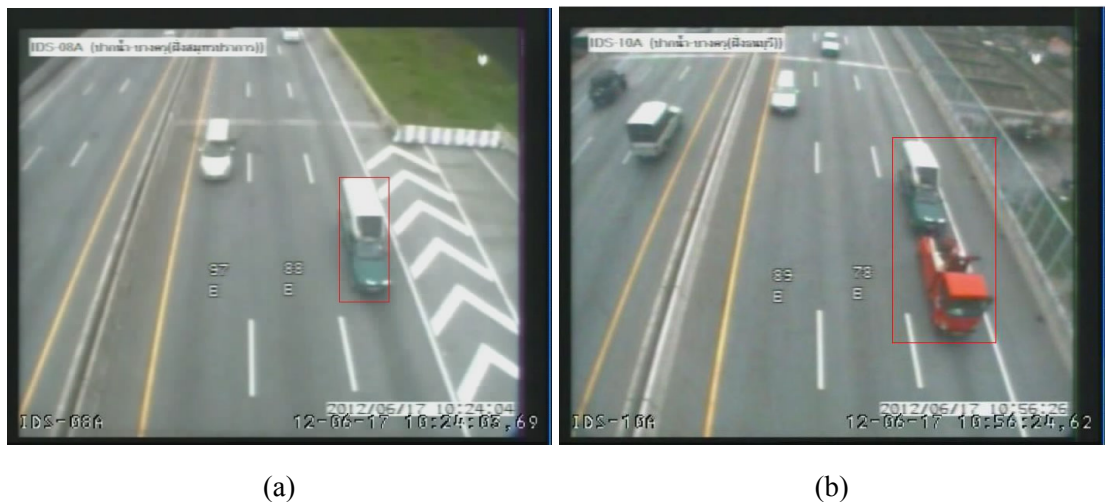


Figure 5.8: Real-world case study #2: (a) Incident vehicle passes the upstream detector; (b) Incident vehicle and truck passes through the downstream detector

incident is reported on 17-Jun-2012 at **10:31** a.m. and its detailed location is at 19+300A westbound (between 7A/8A and 9A/10A). By setting the threshold value of the ratio of matching probabilities equals to **8.5**, the time of incident detection and the false alarm rate for this case study are found to be **10:28:22**, and **2** false alarms per hour, respectively. Compared with the classic vehicle count approach, which would trigger an incident alarm

at **10:33:50**, the proposed AID system still performs better in terms of the incident detection time.

On the basis of these two real-world studies, we may observe that the time of incident detection of the proposed AID algorithm is largely dependent on the actual information associated with the incident vehicle (e.g. distinctiveness of the incident vehicle feature and the size of the vehicle platoon). In real-world case study #2, the incident vehicle has "distinctive" vehicle color distribution (see Figure 5.8(a)), and consequently, the disappearance of this very vehicle can be identified earlier than the classical vehicle count approach. The size of vehicle platoon may also have significant impact on the performance of the AID algorithm. The larger the platoon size is, the more likely it is that the arrival arrival time windows of these vehicles may overlap each other at the downstream site and, hence, leads to the significant increase in incident detection time.

5.7 Conclusion remarks

This chapter investigates the feasibility of utilizing the vehicle reidentification system for incident detection on a closed freeway section under the free flow condition. A modified vision-based VRI system is proposed to partially track the individual vehicle for identifying the "missing" vehicle due to an incident. A flexible arrival time window is estimated for each of the individual vehicle at upstream station to improve the matching accuracy. To reduce the potential false alarms, a screening method, which is based on the ratios of the matching probabilities and arrival time windows, is introduced to rule out the potential mismatches.

The proposed AID algorithm is tested on a 3.6-km segment of a closed freeway in Bangkok, Thailand. Based on the test results, it is found out that the detection time of the proposed AID algorithm is substantially shorter than the traditional vehicle count approach. Also, there is a tradeoff between the false alarms rate and detection time for the proposed AID algorithm. Therefore, a balance should be struck between the rapid incident detection and low false alarm rate by adjusting the thresholding value τ . As demonstrated in Procedure 5.2, the proposed AID algorithm is a hybrid of the vehicle feature comparison method and the classical vehicle count approach, and the threshold value τ can be viewed as a switch between these two methods. Therefore, the selection of τ may be of great

importance to the proposed AID algorithm. In this study, we adjust the threshold value manually based on the reliability of VRI system (the performance of the VRI system in different time period may be slightly different due to the changes in outdoor environment, and the threshold value τ should be adjusted accordingly). Some other automatic thresholding processes (e.g. [Otsu, 1979](#)) will be investigated in our future works.

Note that the proposed AID algorithm is specifically devised to detection incident on closed freeway system under free-flow conditions. As a natural and necessary extension, the ability of detecting incidents on freeway segment with entry/exit ramps is required for the further development of incident detection system. We would show in [Appendix 5.A](#) that the AID algorithm proposed in this chapter is equally applicable to the case where the freeway has entry/exit ramps.

Appendix

5.A Incident detection on freeway segment with entry/exit ramps

As demonstrated in Appendix 4.A, the basic VRI system (i.e. probabilistic vehicle feature fusion and bipartite matching method) could be readily extended to the "small" network case where the freeway segment may have entry/exit ramps (see Figure 5.9). In this part, we would illustrate that the incident-detection-oriented VRI proposed in Chapter 5 can also be applied to this particular case for incident detection purpose.

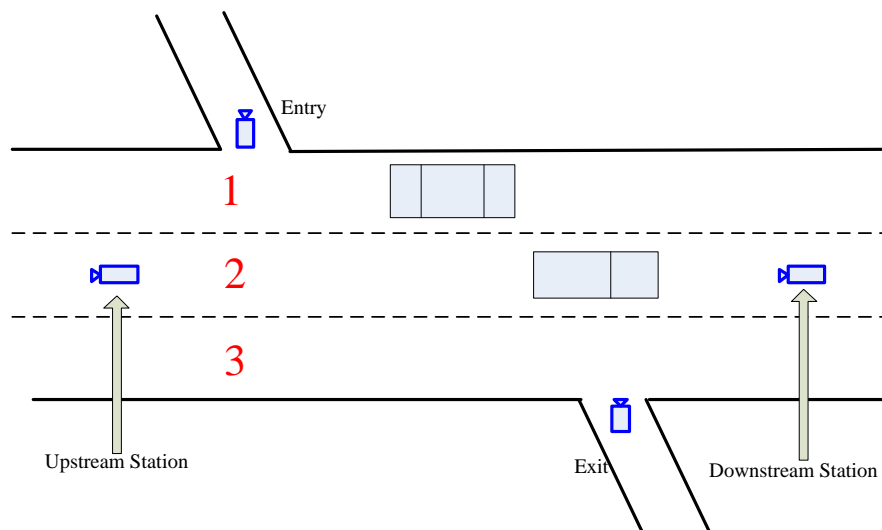


Figure 5.9: Conceptual test site

Assume that the freeway segment in Figure 5.9 can be represented by a link-node formu-

5.A Incident detection on freeway segment with entry/exit ramps

lation, as depicted in Figure 5.10. Denote the upstream station as node 1, and the entry as node 2. Likewise, node 3 and node 4, respectively, represent the exit and downstream station. The basic principle of incident detection is then to "partially" track and identify the "missing" vehicle across this camera "network". Unlike the incident-detection-oriented VRI proposed in Chapter 5, the vehicle feature comparison should be performed simultaneously across the network. In other words, all the vehicles detected at the source nodes (i.e. node 1 and node 2) will be labeled as the upstream vehicle, whereas the vehicles detected at the destination nodes (i.e. node 3 and node 4) will be categorized as the downstream vehicles. In this case, the matching probability for each pair of vehicle signatures can be obtained based on the method proposed in Section 5.5.2, and the final matching decision-making can follow the same procedure as described in Procedure 5.2. The conceptual framework for incident detection on freeway segment with entry/exit ramps is illustrated as follows.

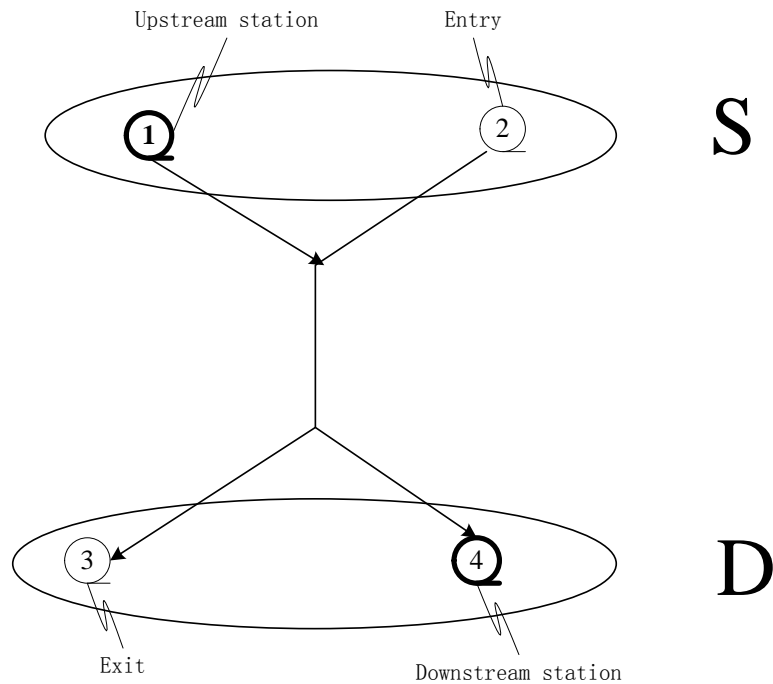


Figure 5.10: Topological structure

First, the system will initialize the timestamp, t , to check whether a vehicle is detected at the sources (node 1 and node 2, etc) and/or destinations (node 3 and node 4, etc). If a vehicle i is detected at source detectors, the expected arrival time window of this vehicle at the destinations will be estimated based on the historical data and current spot speed.

5.A Incident detection on freeway segment with entry/exit ramps

Let $[Lb_i^{N(3)}, Ub_i^{N(3)}]$ and $[Lb_i^{N(4)}, Ub_i^{N(4)}]$ respectively denote the arrival time at node 3 and node 4. The record of vehicle i (e.g. color, type and length) will then be stored in the database as unmatched upstream vehicle. On the other hand, if a vehicle k is captured at the destinations (node 3 and/or node 4), the system will perform the Vision-based VRI subsystem to check whether this detected vehicle match with any of the unmatched upstream vehicle. Once the decision is made, the matched vehicle data will be removed from the list of the unmatched upstream vehicles. In particular, a search space, $\mathcal{S}(k)$, which represents the potential matches, is determined based on the time window. The matching probability, $P(\psi(k) = i | d_{\text{color}}, d_{\text{type}}, d_{\text{length}})$, which indicates the likelihood of vehicle $i \in \mathcal{S}(k)$ matching with vehicle k , is obtained from the VRI system. The associated ratio method is performed to reach a final matching decision. After performing the vehicle feature comparison, the system will screen through the list of unmatched vehicles. If current time (t) is out of the expected arrival time window of the unmatched vehicle i (i.e. $\max\{Ub_i^{N(3)}, Ub_i^{N(4)}\} < t$), an incident alarm will be issued. For the aforementioned framework, two comments should be taken into account.

- First, it is expected that the incident detection time should be longer than that for closed corridor case. Give a vehicle i detected at the source nodes (e.g. node 1 or node 2), the arrival time of this vehicle at the possible destinations can be denoted as $[Lb_i^{N(3)}, Ub_i^{N(3)}]$ and $[Lb_i^{N(4)}, Ub_i^{N(4)}]$, respectively. In the case the vehicle i is missing, the incident alarm will not be issued until time $\max\{Ub_i^{N(3)}, Ub_i^{N(4)}\}$.
- Second, the false alarm rate would also increase accordingly due to the complex topological structure of the traffic network. Since we do not know the actual route choice for each vehicle, the size the search space $\mathcal{S}(k)$ would be much larger than that for closed corridor case and, consequently, leads to a large number of mismatches.

Chapter 6

Hierarchical Bayesian model for VRI on freeway with multiple detectors

This chapter proposes a hierarchical Bayesian model for vehicle reidentification on freeway with multiple detectors. To take full advantage of the traffic information (e.g. vehicle color, length, and type) obtained at multiple detectors, a hierarchical matching model is proposed such that vehicle matching over multiple detectors is treated as an integrated process. To further improve the vehicle matching accuracy, a hierarchical Bayesian model is introduced to describe the spatial dependencies between feature distances. The *posterior* probability in the hierarchical structure is then calculated for the final matching decision-making. The proposed method is tested on a 9.7-km segment of a freeway system in Bangkok, Thailand. The results show that hierarchical Bayesian matching method could further improve the matching accuracy on the freeway segment with multiple detectors.

6.1 Introduction

The continuous tracking of individual vehicles is potentially beneficial to the development of intelligent transportation systems (Sivaraman and Trivedi, 2013). The extrinsic vehicle data such as vehicle speed and its arrival time at different locations are considered essential in advanced traveller information system (ATIS) for providing the updated traffic information (e.g. traffic flow, speed and travel time). Moreover, the additional intrinsic vehicle

data (e.g. vehicle color, type and length) would contribute to the development of efficient traffic incident detection algorithms (see Chapter 5), which is recognized one of the critical components of advanced traffic management systems (ATMS). In light of this, the basic vision-based VRI (Chapter 4) is devised to re-identify the individual vehicles across two consecutive detectors (i.e. video camera stations). Despite the encouraging results and its ease of implementation, the basic VRI still suffers from two serious problems.

First, the performance (i.e. matching accuracy) of basic VRI is heavily dependent on the quality of vehicle feature data extracted from the IVS technology. Although the statistical approach has been adopted to explicitly consider the uncertainties of vehicle feature data, the matching accuracy still may not be satisfactory when the outdoor environment (e.g. weather condition and illumination conditions) changes significantly. Second, the complex topological structure may also impose a great challenge on the performance of the basic VRI. As explained in Appendix 4.A, the vehicle matching accuracy may decrease on a freeway segment with on/off-ramps due to vehicles' unobservable route choices and the potentially large set of candidate vehicles. The above-mentioned two problems may get worse when the distance between the two consecutive detectors becomes extremely long.

For a long-distance freeway segment, the outdoor environment (i.e. illumination conditions) at two detectors may be different from each other, which may result in high variance in the feature distance¹ (Song and Roy-Chowdhury, 2008) and, consequently, undermine the performance (i.e. decrease the matching accuracy) of the VRI system. Also, a much larger time window is imposed to cope with the purpose of vehicle matching on long-distance freeway and, accordingly, the size of the candidate vehicle set would increase dramatically, which eventually leads to the significant decrease in matching accuracy (e.g. Ndoye et al., 2011; Lin and Tong, 2011). To deal with truck reidentification over long distances, Cetin et al. (2011) introduced an additional screening/thresholding process to match the trucks with distinctive features (e.g. axle weight and axle spacing) without considering the other vehicles. Although this approach may be applicable for some specific purposes (e.g. estimation of truck travel time over long distance), it still can not solve the basic problems arising from the vehicle matching over long distance (i.e. large variance in feature distances and large size of candidate vehicle set). In this case, an alternative approach to the long-distance VRI would be to install additional video cameras at the

¹The variance in the feature distance indicates the degree of uncertainty associated with the feature data (see Figure 4.3).

intermediate locations along the freeway segment (e.g. camera station B in Figure 6.1), which eventually gives rise to the problem of vehicle reidentification (VRI) on freeway corridor with multiple detectors. A natural and straightforward response to this problem is to apply the basic VRI to each individual detector pair (i.e. pair-wise vehicle matching process). For the freeway segment demonstrated in Figure 6.1, there are three detector pairs, i.e. A-to-B, B-to-C, and A-to-C. As we explained before, the direct vehicle matching on pair A-to-C is not practically applicable due to the long distance from A to C. Therefore, by performing the basic VRI method independently to detector pairs A-to-B and B-to-C¹, we may still "efficiently" track/reidentify the individual vehicle on the freeway segment. Although the aforementioned detector-pair-wise matching process appears promising for

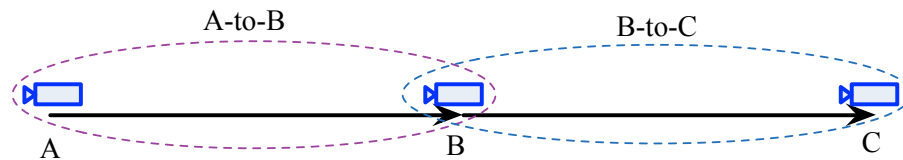


Figure 6.1: Freeway segment with multiple detectors

reidentification over long distance, it tends to suffer from two inherent problems.

- First, the pair-wise matching process is highly sensitive to the mismatches generated by each basic VRI component². Once a vehicle is mismatched over a detector pair, the final matching result regarding this vehicle would not be correct even if this vehicle is correctly matched over the other detector pairs. As the basic VRI for each detector pair is performed independently, the matching results of the same vehicle over different detector pairs may be totally irrelevant and, hence, results in the decrease in matching accuracy on the freeway segment. In view of this, an additional hierarchical matching model is proposed in this study to simultaneously match the vehicle across the multiple detectors.
- Second, the pair-wise VRI method fails to consider the interdependence of the feature distances between different detector pairs (i.e. interdependence of feature distance over space). As shown in Figure 6.1, the detector pairs A-to-B and B-to-C share a common camera station (i.e. station B), at which the vehicle feature data are extracted and utilized for both basic VRI systems (i.e. VRI on A-to-B and B-to-C).

¹These two detector pairs have relatively shorter distance, and accordingly the matching accuracy on these two pairs would be relatively higher.

²This will be further discussed and illustrated in Section 6.2.

Therefore, the associated feature distances on these two detector pairs should be correlated with each other. Mathematically speaking, a statistical model considering the interdependence of feature distances over space (i.e. consecutive segments) is required.

To sum up, this study attempts to deal with the aforementioned problems arising from the pair-wise VRI matching process. To be more specific, we furnish the pair-wise VRI with additional hierarchical Bayesian matching model in the hope of refining and improving the matching results. Rather than performing basic VRI independently, the proposed method considers the vehicle matching over multiple detectors as an integrated process in which a more suitable statistical model is introduced to describe the spatial dependencies between the vehicle feature distances.

The remainder of this chapter is organized as follows. Section 6.2 presents the overall framework of the pair-wise VRI process. The problems arising from this process are further illustrated. The formal description and analysis regarding the hierarchical matching model are then proposed in Section 6.3. Section 6.4 explains the underlying hierarchical Bayesian model of feature distances. Some preliminary test results regarding the vehicle matching accuracy are discussed in Section 6.5. Finally, we close this chapter with conclusion remarks.

6.2 Pair-wise VRI process

As the name suggests, pair-wise VRI aims to apply basic VRI independently to each detector pair. In this sense, the task would be considered "trivial" due to basic VRI's ease of implementation. However, it is noteworthy that pair-wise VRI provides preliminary insight into the tracking/reidentification of vehicles across the multiple detectors, which may be beneficial for the following hierarchical matching model. Therefore, it is necessary to present a formal description of pair-wise VRI model. To facilitate the presentation of the essential ideas without loss of generality, we consider the case where the freeway segment has three detectors (i.e. two consecutive detector pairs).

6.2.1 Basic VRI subsystem

Consider a freeway corridor with three traffic detectors (i.e. video cameras) demonstrated in Figure 6.2. The associated pair-wise VRI model is comprised of two independently operated basic VRI subsystems, i.e. basic VRI on A-to-B and B-to-C. Each basic VRI subsystem is performed such that the vehicles at the downstream stations (i.e. station C of pair B-to-C and station B of pair A-to-B) are reidentified at the corresponding upstream stations. Without loss of generality, only the basic VRI subsystem for detector pair of B-to-C is described.

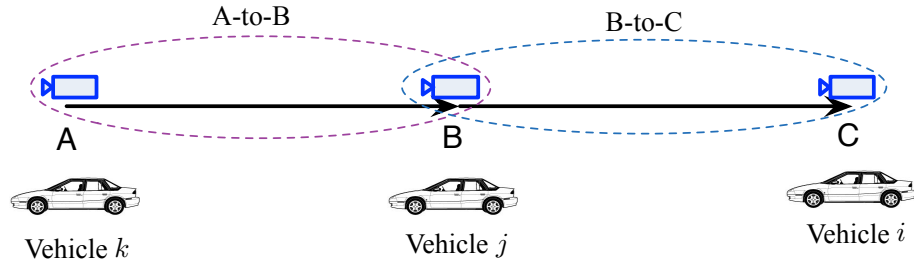


Figure 6.2: Conceptual freeway corridor

For a vehicle i arrives at downstream station (i.e. station C) at time t_i^D (Figure 6.2), the vehicle signature, denoted as $X_i^D = \{C_i^D, S_i^D, L_i^D\}$, is then obtained from IVS¹. A search space, $\mathcal{S}(i)$, which represents the potential matches at upstream station (i.e. station B) for vehicle i , is determined based on the pre-defined time window. Given a candidate vehicle $j \in \mathcal{S}(i)$, we may compute the associated feature distance vector, which can be denoted as $(d_{\text{color}}(j, i), d_{\text{type}}(j, i), d_{\text{length}}(j, i))$. Also, we introduce an indicator variable to represent the matching result between each pair of vehicle signatures, i.e.

$$x_{ji} = \begin{cases} 1, & \text{downstream vehicle } i \text{ matches upstream vehicle } j \in \mathcal{S}(i) \\ 0, & \text{otherwise} \end{cases} \quad (6.1)$$

The matching probability, also referred to as the *posterior* probability, is then calculated to represent the possibility of each pair of vehicles being the same one given their feature

¹The detailed explanation on the extraction of vehicle signature data (C_i^D and S_i^D are the normalized color feature vector and type feature vector, respectively; L_i^D denotes the vehicle length) can be found in Section 3.2.

distances. By applying the Bayesian rule, we may have

$$P(x_{ji} = 1 | d_{\text{color}}, d_{\text{type}}, d_{\text{length}}) = \frac{p(d_{\text{color}}, d_{\text{type}}, d_{\text{length}} | x_{ji} = 1)P(x_{ji} = 1)}{p(d_{\text{color}}, d_{\text{type}}, d_{\text{length}})} \quad (6.2)$$

To obtain the explicit matching probability, the denominator in Equation (6.2) can be further expressed as

$$p(d_{\text{color}}, d_{\text{type}}, d_{\text{length}}) = p(d_{\text{color}}, d_{\text{type}}, d_{\text{length}} | x_{ji} = 1)P(x_{ji} = 1) + p(d_{\text{color}}, d_{\text{type}}, d_{\text{length}} | x_{ji} = 0)P(x_{ji} = 0) \quad (6.3)$$

The *prior* probability, i.e. $P(x_{ji})$, is approximated by the historical travel time distribution

$$P(x_{ji} = 1) = \frac{f(t(j, i))}{\eta} \times 0.5 \quad (6.4)$$

$$P(x_{ji} = 0) = 1 - \frac{f(t(j, i))}{\eta} \times 0.5 \quad (6.5)$$

where $f(\cdot)$ denotes the historical travel time distribution, $t(j, i)$ is the time difference between upstream vehicle i and downstream vehicle j , and η is the normalizing factor. Note that the deducing of the matching probability in this chapter is slightly different from that in Chapter 4. In this chapter, we attempt to "explicitly" calculate the matching probability based on the observation of the feature distances of only one pair of vehicle signatures, which may be more suitable for the following processing (e.g. bipartite matching and thresholding).

The calculation of the likelihood function, i.e. $p(d_{\text{color}}, d_{\text{type}}, d_{\text{length}} | x_{ji} = 1)$, generally follows the same procedure described in Chapter 4. First the statistical model for each feature distance over the detector pair is built up. For example, the conditional probability of $d_{\text{color}}(j, i)$ is given by

$$p(d_{\text{color}}(j, i) | x_{ji}) = \begin{cases} p_1(d_{\text{color}}(j, i)), & \text{if } x_{ji} = 1 \\ p_2(d_{\text{color}}(j, i)), & \text{if } x_{ji} = 0 \end{cases} \quad (6.6)$$

where p_1 denotes the probability density function (pdf) of distance $d_{\text{color}}(j, i)$ when the color feature vectors belong to the same vehicle, whereas p_2 is the pdf of the distance between different vehicles. Second, the logarithmic opinion pool (LOP) is employed to fuse the individual likelihood functions in Equation (6.6), and the fusion equation is given

by

$$p(d_{\text{color}}, d_{\text{type}}, d_{\text{length}} | x_{ji}) = \frac{1}{Z_{\text{LOP}}} p(d_{\text{color}} | x_{ji})^\alpha p(d_{\text{type}} | x_{ji})^\beta p(d_{\text{length}} | x_{ji})^\gamma, \quad \alpha + \beta + \gamma = 1 \quad (6.7)$$

where the fusion weights α , β and γ are used to indicate the degree of contribution of each likelihood function, and Z_{LOP} is the normalizing constant. By substituting Equations (6.7) and (6.3) into Equation (6.2), the desired matching probability can be obtained. In common with the basic VRI, the bipartite matching method (see Section 4.4) is introduced to find the matching result (i.e. x_{ji}) such that the overall matching probability between the downstream and upstream vehicles is maximized.

6.2.2 A discussion on pair-wise VRI

Basically, pair-wise VRI is simply the combination of multiple basic VRI systems. Each basic VRI subsystem would generate its own matching result, e.g. $x_{ji}^{(\text{BC})} = 1$ and $x_{kj}^{(\text{AB})} = 1$, which respectively indicate that vehicle j matches vehicle i over B-to-C, and vehicle i matches k over A-to-B as shown in Figure 6.2. The connection between these two basic VRI subsystems can be built up by screening through the vehicle records detected at the common station (i.e. camera station B) and the final vehicle matching result across the multiple detectors can be obtained (i.e. $x_{ki}^{(\text{AC})} \triangleq x_{kj}^{(\text{AB})} x_{ji}^{(\text{BC})} = 1$). The detailed screening procedure is given as follows

Procedure 6.1: Screening process

Input: Index i and k ; matching results $\mathbf{x}^{(\text{AB})}$ and $\mathbf{x}^{(\text{BC})}$ from basic VRI

Output: Matching result $x_{ki}^{(\text{AC})}$

```

1  $\mathcal{S}(i) \leftarrow \{1, 2, \dots, M\}$  /* Search space at station B */;
2  $j \leftarrow 1$ ;
3 while  $j \leq M \wedge x_{kj}^{(\text{AB})} x_{ji}^{(\text{BC})} == 0$  do
4    $j \leftarrow j + 1$ ;
5 return  $x_{ki}^{(\text{AC})} \triangleq x_{kj}^{(\text{AB})} x_{ji}^{(\text{BC})}$ ;
```

For the aforementioned pair-wise VRI, the following two comments should be taken into account.

- As the basic VRI subsystem (e.g. basic VRI over A-to-B and B-to-C) is performed independently, the associated matching results (e.g. $\mathbf{x}^{(AB)}$ and $\mathbf{x}^{(BC)}$) may be inconsistent. Given the vehicle feature vector $\mathbf{F}_i = \{C_i, S_i, L_i\}$ of vehicle i detected at station C, basic VRI over B-to-C may match it to vehicle j (with feature vector $\mathbf{F}_j = \{C_j, S_j, L_j\}$) at station B (i.e. $x_{ji}^{(BC)} = 1$), whereas basic VRI over A-to-B may wrongly match vehicle j to vehicle k (with feature vector $\mathbf{F}_k = \{C_k, S_k, L_k\}$) at station A (i.e. $x_{kj}^{(AB)} = 1$). According to the screening process described in Procedure 6.1, we may come to the wrong conclusion that vehicle i matches vehicle k , i.e. $x_{ki}^{(AC)} \triangleq x_{kj}^{(AB)} x_{ji}^{(BC)} = 1$. This inconsistency arising from the pair-wise VRI process may frequently exist when the matching accuracy of basic VRI over some detector pairs decreases significantly. In other words, the pair-wise VRI is highly sensitive to the mismatches generated by each basic VRI subsystem. To this end, we propose an additional hierarchical matching model in which the VRI processes over multiple detector pairs are considered simultaneously and the matching result of basic VRI is further adjusted/refined to improve the overall matching accuracy along the freeway segment.
- The pair-wise VRI method also fails to consider the interdependence of the feature distances between different detector pairs. It is noticed that the consecutive freeway segments (e.g. A-to-B and B-to-C) may share a common camera station, at which the extracted vehicle feature data are utilized by both basic VRI subsystems. Let \mathbf{F}_i , \mathbf{F}_j and \mathbf{F}_k , respectively, denote the feature vectors extracted at the stations A, B, and C. The corresponding feature distance vectors, e.g. $\mathbf{d}(i, j)$ and $\mathbf{d}(j, k)$, are expected to be correlated with other. Within the framework of hierarchical matching model, we may gain additional benefits (i.e. improving the matching accuracy) by further considering the spatial correlation of feature distances.

To sum up, this chapter aims to propose an additional hierarchical Bayesian matching model to further refine the preliminary matching results generated by basic VRI subsystem. Also, a novel statistical model considering the interdependence of feature distances over space is built up for further improving the matching accuracy. In what follows, the detailed introduction regarding hierarchical matching model will be presented.

6.3 Hierarchical matching model

In order to analyze all the detector pairs simultaneously, an integrated framework (i.e. hierarchical matching model) is developed such that each individual vehicle can be re-identified across multiple detectors. As a matter of fact, the idea of hierarchical matching has already been evaluated with several other applications in the field of computer vision (e.g. [Borgefors, 1988](#); [Stenger et al., 2006](#)). In this section, the presentation of the hierarchical matching model is completed in three steps. First, a new hierarchical structure for representing the vehicle matching result is built up (Section 6.3.1). Second, the detailed methodologies for constructing the vehicle tree structure is introduced (Section 6.3.2). Last but not least, the unified statistical framework is proposed to calculate the overall *posterior* probability based on the observation of a sequence of feature distances along the freeway segment (Section 6.3.3).

6.3.1 Hierarchical structure for vehicle matching

It is easy to understand that the matching results of VRI over multiple detectors can be represented by a hierarchical tree structure demonstrated in Figure 6.3. Given a vehicle i detected at station C, the associated vehicle record (i.e. $\mathbf{F}_i = \{C_i, S_i, L_i\}$) is then represented as a root node in the tree (Figure 6.3). By imposing the time window constraint based on the arrival time of vehicle i , its corresponding search space $\mathcal{S}(i)$ at the intermediate station B can be obtained and, accordingly, all the vehicle records in search space $\mathcal{S}(i)$ are classified as the children nodes (i.e. level 1 nodes) of the root in the tree structure. For a vehicle $j \in \mathcal{S}(i)$ at station B, several distance measures can be incorporated to calculate the difference between feature data \mathbf{F}_j and its father node's feature \mathbf{F}_i . Let $\mathbf{d}_1 = \{d_{\text{color}}(j, i), d_{\text{type}}(j, i), d_{\text{length}}(j, i)\}$ denote the feature distance vector at level 1 of the tree structure. Likewise, the level 2 of the tree structure in Figure 6.3 can also be established. This process will continue until it reaches the first camera station (i.e. station A/level 2 in Figure 6.3).

In such a case, the problem of VRI over multiple detectors is equivalent to finding a path from the root (i.e. vehicle i) to the leaf level node (i.e. the node at level 2) in the tree structure (Figure 6.3). In other words, each path in the tree structure corresponds to a potential matching result for vehicle i , and different path searching strategies may result

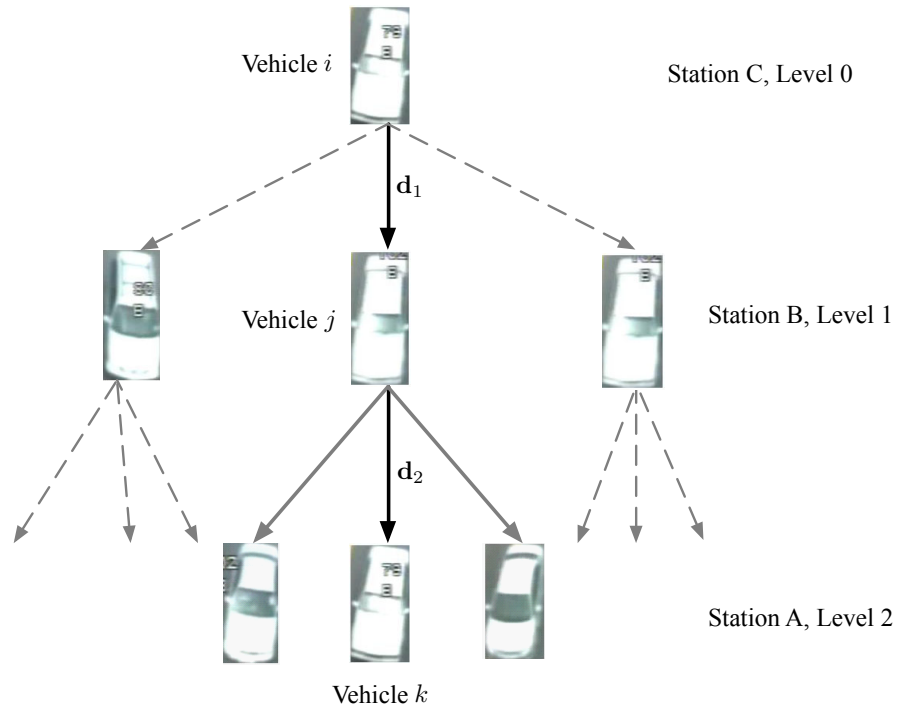


Figure 6.3: A hierarchical structure of vehicle matching across multiple detectors

in different VRI methods. The pair-wise VRI method proposed in Section 6.2 attempts to find the path level by level from top to bottom in the tree structure. Rather than making a matching decision instantly and independently on each level, this study proposes a new path searching algorithm based on the hierarchical structure such that the observations of a sequence of feature distances (e.g. \mathbf{d}_1 and \mathbf{d}_2) are considered simultaneously.

6.3.2 Construction of vehicle tree structure: Preliminary clustering

Before proceeding to introduce the detailed path searching algorithm, it is essential to refine the vehicle tree structure in Figure 6.3 so that the overall computational and searching efficiency of hierarchical vehicle matching can be improved. Note that the number of the nodes in the tree structure would increase dramatically with respect to the increase in the number of detectors (i.e. the number of levels in the tree), which may undermine the efficiency of the searching algorithm. Therefore, this study incorporates a preliminary clustering/thresholding approach based on the pair-wise VRI to further refine the vehicle tree.

As the name suggests, the refinement of vehicle tree is completed by reducing the size of the candidate vehicle size (i.e. the size of the associated search space \mathcal{S}). In this sense, a preliminary clustering/thresholding method based on the matching probabilities obtained from pair-wise VRI is then introduced to eliminate those unlikely matches. Given a vehicle i and its search space $\mathcal{S}(i) = \{1, 2, \dots, N\}$, the associated matching probabilities are calculated on the basis of Equations (6.2), (6.3) and (6.7)¹. Let $\{P_j | j = 1, 2, \dots, N\}$ denote the set of matching probabilities in descending order. By imposing a threshold τ on the value of the ratio between the neighboring probabilities in the ordered set $\{P_j | j = 1, 2, \dots, N\}$, one may be able to screen through the search space and rule out those unlikely matches. The screening process is described as follows.

Procedure 6.2: Preliminary clustering based on pair-wise VRI

Input: A finite set $\{P_j | j = 1, 2, \dots, N\}$ of matching probabilities in descending order

Output: The set of remaining matches for vehicle i , i.e. $\mathcal{S}_R(i)$

```

1  $j \leftarrow 1$ ;
2 while  $j \leq N - 1 \wedge P_j/P_{j+1} \leq \tau$  do
3    $j \leftarrow j + 1$ ;
4 return  $\mathcal{S}_R(i) \triangleq \{1, 2, \dots, j\}$ ;
```

Figure 6.4 shows the overall framework for the construction of the vehicle tree structure, which is of great importance to the following development of hierarchical matching method. On one hand, the proposed hierarchical matching method serves as a correction step on the matching results generated by pair-wise VRI. On the other hand, the pair-wise VRI provides preliminary insight (e.g. refined candidate vehicle set) into the task of VRI over multiple detectors.

6.3.3 Statistical framework for hierarchical matching

As previously explained, the task of VRI over multiple detectors is equivalent to find the "optimal" path from root node to the leaf level node. One natural approach would be to find the path with the minimum feature distance, which can also be referred to as distance-based method. Consider a vehicle tree structure (see Figure 6.4), where the root node represents

¹The readers can refer to Section 6.2.1 for a more detailed explanation on the calculation of the matching probabilities.

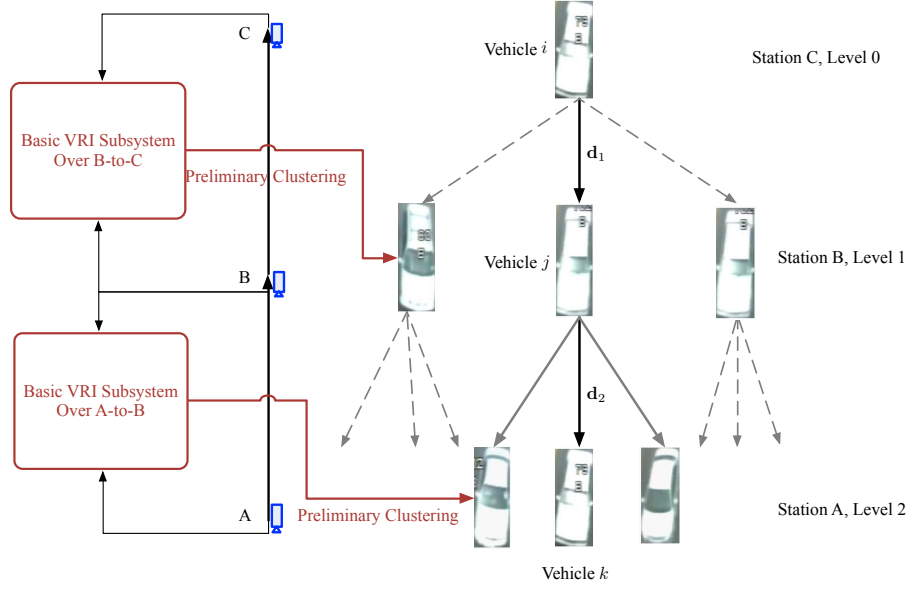


Figure 6.4: Illustrative example of the construction of vehicle tree

the record of vehicle i , and the set of leaf nodes is denoted as $\mathcal{L} = \{1, 2, \dots, M\}$, which implies that there are M paths from top level to bottom level. In addition, we may also obtain a sequence of feature distances $(\mathbf{d}_1^{(k)}, \mathbf{d}_2^{(k)}, \dots)$ for each vehicle $k \in \mathcal{L}$. Within the framework of distance-based method, the final matching result for vehicle i is then given by

$$\arg \min_{k \in \mathcal{L}} \sum_l \mathbf{d}_l^{(k)} \quad (6.8)$$

where k denotes the index of the vehicle in the leaf level and $\mathbf{d}_l^{(k)}$ is the associated feature distance observed at l th level. Despite its computational efficiency and ease of implementation, distance based method fails to consider the uncertainty of the feature distance and the interdependence of feature distances over space (i.e. different levels in the vehicle tree). In view of this, this study proposes a Bayesian framework for hierarchical matching decision-making.

For each node (vehicle j at level l) in the tree structure, a binary state random variable $x_l^{(j)} \in \{1, 0\}$ is introduced to represent the matching results:

$$x_l^{(j)} = \begin{cases} 1, & \text{the vehicle matches the root vehicle } i \\ 0, & \text{otherwise} \end{cases} \quad (6.9)$$

Given a specific vehicle j at level l , the corresponding path from root node (i.e. vehicle

6.4 Hierarchical Bayesian modeling on feature distances

i) to this node is also obtained. For simplicity, let $\mathbf{d}_{1:l}^{(j)} \triangleq \{\mathbf{d}_\omega^{(j)}\}_{\omega=1}^l$ denote the associated measurements of feature distances from top level to level l along this particular path. By building up appropriate statistical models for feature distances over space, we may be able to calculate the *posterior* probability (i.e. $P(x_l^{(j)} = 1 | \mathbf{d}_{1:l}^{(j)})$) of vehicle j being matched to the root node (i.e. vehicle i) given the observations of a sequence of feature distances $\mathbf{d}_{1:l}^{(j)}$. Likewise the *posterior* probability for other nodes can also be obtained. Within the framework of statistical matching method, the matching result is then given by

$$\arg \max_{k \in \mathcal{L}} P(x_l^{(k)} = 1 | \mathbf{d}_{1:l}^{(k)}) \quad (6.10)$$

In other words, the hierarchical matching problem is solved by finding the "optimal" path from the root to the leaf level node, such that the a *posterior* probability of a correct match (i.e. $x_l^{(k)} = 1$) at particular leaf node, given the feature distances along the path, is maximized. In the remainder of this study, a hierarchical Bayesian framework is introduced for calculating the *posterior* probability in Equation (6.10).

6.4 Hierarchical Bayesian modeling on feature distances

For the sake of simplicity, let $\mathbf{d}_{1:l} = \{\mathbf{d}_\omega\}_{\omega=1}^l$ denote a sequence of feature distance measurements along a particular path (i.e. the path from the root node to the node of interest at level l) in the tree structure. Also, the matching result of the node of interest at level l is denoted as x_l . By applying Bayes rule on Equation (6.10), we may have

$$P(x_l = 1 | \mathbf{d}_{1:l}) = \frac{P(x_l = 1)p(\mathbf{d}_{1:l} | x_l = 1)}{p(\mathbf{d}_{1:l})} \quad (6.11)$$

where $x_l = 1$ indicates that the node of interest at level l matches the root node (i.e. vehicle i). To obtain the explicit *posterior* probability, the denominator in Equation (6.11) can further be expressed as

$$p(\mathbf{d}_{1:l}) = P(x_l = 1)p(\mathbf{d}_{1:l} | x_l = 1) + P(x_l = 0)p(\mathbf{d}_{1:l} | x_l = 0) \quad (6.12)$$

6.4 Hierarchical Bayesian modeling on feature distances

By substituting Equation (6.12) into Equation (6.11), we may obtain

$$\begin{aligned}
 P(x_l = 1 | \mathbf{d}_{1:l}) &= \frac{P(x_l = 1)p(\mathbf{d}_{1:l} | x_l = 1)}{P(x_l = 1)p(\mathbf{d}_{1:l} | x_l = 1) + P(x_l = 0)p(\mathbf{d}_{1:l} | x_l = 0)} \\
 &= \frac{1}{1 + \frac{P(x_l = 0)p(\mathbf{d}_{1:l} | x_l = 0)}{P(x_l = 1)p(\mathbf{d}_{1:l} | x_l = 1)}}
 \end{aligned} \tag{6.13}$$

As illustrated in Equation (6.13), the calculation of the *posterior* probability is dependent on the deducing of the likelihood function (i.e. $p(\mathbf{d}_{1:l} | x_l)$) and the *prior* probability (i.e. $P(x_l)$). In what follows, the calculation of the likelihood function would become the major concern.

6.4.1 Hierarchical model of a sequence of feature distances

Within the framework of hierarchical modeling, the joint distribution of observing a sequence of feature distances $\mathbf{d}_{1:l}$ can be represented as products of conditionals, i.e.

$$p(\mathbf{d}_{1:l} | x_l) = \prod_{\omega} p(d_{\omega} | \mathbf{d}_{1:\omega-1}, x_l) \tag{6.14}$$

where d_{ω} is the observed feature distance at level ω . The implication of Equation (6.14) is that the feature distances observed at different levels are correlated with each other (i.e. spatial dependencies exist), and it is mathematically tractable to express full joint probability (i.e. left-hand side of Equation (6.14)) with the hierarchical model.

To further simplify the hierarchical model mentioned above, an assumption of Markov property of the feature distances along the path from the root to the node of interest is imposed. Specifically, the observation of a sequence of feature distances $\mathbf{d}_{1:l}$ is considered as a first order homogeneous Markov process (Riños Insua et al., 2012), and it has the following property

$$p(d_{\omega} | \mathbf{d}_{1:\omega-1}) = p(d_{\omega} | d_{\omega-1}) \quad \forall \omega \in \{1, 2, \dots, l\} \tag{6.15}$$

which means that the observation of the feature distance d_{ω} at level ω is only dependent on the distance $d_{\omega-1}$ at level $\omega - 1$. The physical interpretation of Equation (6.15) is that only the feature distances observed at two consecutive segments are considered correlated

6.4 Hierarchical Bayesian modeling on feature distances

with other¹.

According to the law of total probability, we may obtain

$$\begin{aligned} p(\mathbf{d}_{1:l}|x_l = 1) &= p(\mathbf{d}_{1:l}|x_l = 1, x_{l-1} = 1)P(x_{l-1} = 1|x_l = 1) \\ &\quad + p(\mathbf{d}_{1:l}|x_l = 1, x_{l-1} = 0)P(x_{l-1} = 0|x_l = 1) \end{aligned} \quad (6.16)$$

Also, we have $P(x_{l-1} = 1|x_l = 1) = 1$, which suggests that if a child node at level l is a correct match to the root node (i.e. $x_l = 1$), then its parent node at level $l - 1$ should also match the root node (i.e. $x_{l-1} = 1$). Therefore, Equation (6.16) can be reformulated as

$$\begin{aligned} p(\mathbf{d}_{1:l}|x_l = 1) &= p(\mathbf{d}_{1:l}|x_l = 1, x_{l-1} = 1) \\ &= p(d_l|\mathbf{d}_{1:l-1}, x_l = 1, x_{l-1} = 1)p(\mathbf{d}_{1:l-1}|x_{l-1} = 1) \end{aligned} \quad (6.17)$$

Based on the above-mentioned Markov assumptions (Equation (6.15)), we may have

$$p(\mathbf{d}_{1:l}|x_l = 1) = p(d_l|d_{l-1}, x_l = 1, x_{l-1} = 1)p(\mathbf{d}_{1:l-1}|x_{l-1} = 1) \quad (6.18)$$

By applying Bayes rule, we may further obtain

$$\begin{aligned} p(\mathbf{d}_{1:l}|x_l = 1) &= p(d_l|d_{l-1}, x_l = 1, x_{l-1} = 1) \frac{P(x_{l-1} = 1|\mathbf{d}_{1:l-1})p(\mathbf{d}_{1:l-1})}{P(x_{l-1} = 1)} \\ &= \frac{p(d_l|d_{l-1}, x_l = 1, x_{l-1} = 1)p(\mathbf{d}_{1:l-1})}{P(x_{l-1} = 1)} P(x_{l-1} = 1|\mathbf{d}_{1:l-1}) \end{aligned} \quad (6.19)$$

where $P(x_{l-1} = 1|\mathbf{d}_{1:l-1})$ is a *posterior* probability of the its parent node at level $l - 1$ being matched to the root node, given a sequence of feature distance measurements $\mathbf{d}_{1:l-1}$; $p(d_l|d_{l-1}, x_l = 1, x_{l-1} = 1)$ is the conditional probability, which is introduced for characterizing the spatial dependencies of the feature distances. Given $P(x_{l-1} = 1|x_l = 1) = 1$, we get

$$P(x_{l-1} = 1) = \frac{P(x_{l-1} = 1|x_l = 1)P(x_l = 1)}{P(x_l = 1|x_{l-1} = 1)} = \frac{P(x_l = 1)}{P(x_l = 1|x_{l-1} = 1)} \quad (6.20)$$

On the basis of Equations (6.19) and (6.20), the term $P(x_l = 1)p(\mathbf{d}_{1:l}|x_l = 1)$ in Equa-

¹The two consecutive segments may share the common camera station (detailed explanation can be found in Section 6.2.2.)

6.4 Hierarchical Bayesian modeling on feature distances

tion (6.13) can be expressed as

$$P(x_l = 1)p(\mathbf{d}_{1:l}|x_l = 1) = p(d_l|d_{l-1}, x_l = 1, x_{l-1} = 1)p(\mathbf{d}_{1:l-1})P(x_l = 1|x_{l-1} = 1)P(x_{l-1} = 1|\mathbf{d}_{1:l-1}) \quad (6.21)$$

Likewise, $p(\mathbf{d}_{1:l}|x_l = 0)$ can also be calculated as follows:

$$\begin{aligned} p(\mathbf{d}_{1:l}|x_l = 0) &= p(\mathbf{d}_{1:l}|x_l = 0, x_{l-1} = 1)P(x_{l-1} = 1|x_l = 0) \\ &\quad + p(\mathbf{d}_{1:l}|x_l = 0, x_{l-1} = 0)P(x_{l-1} = 0|x_l = 0) \\ &= p(d_l|d_{l-1}, x_l = 0, x_{l-1} = 1)p(\mathbf{d}_{1:l-1}|x_{l-1} = 1)P(x_{l-1} = 1|x_l = 0) \\ &\quad + p(d_l|d_{l-1}, x_l = 0, x_{l-1} = 0)p(\mathbf{d}_{1:l-1}|x_{l-1} = 0)P(x_{l-1} = 0|x_l = 0) \end{aligned}$$

By applying Bayes rule, we may obtain

$$\begin{aligned} p(\mathbf{d}_{1:l}|x_l = 0) &= \frac{p(d_l|d_{l-1}, x_l = 0, x_{l-1} = 1)p(\mathbf{d}_{1:l-1})}{P(x_{l-1} = 1)}P(x_{l-1} = 1|x_l = 0) \\ &\quad + \frac{p(d_l|d_{l-1}, x_l = 0, x_{l-1} = 0)p(\mathbf{d}_{1:l-1})}{P(x_{l-1} = 0)}P(x_{l-1} = 0|x_l = 0) \quad (6.22) \end{aligned}$$

Then, the term $P(x_l = 0)p(\mathbf{d}_{1:l}|x_l = 0)$ in Equation (6.13) can be reformulated as

$$\begin{aligned} P(x_l = 0)p(\mathbf{d}_{1:l}|x_l = 0) &= p(d_l|d_{l-1}, x_l = 0, x_{l-1} = 1)p(\mathbf{d}_{1:l-1}) \\ &\quad P(x_l = 0|x_{l-1} = 1)P(x_{l-1} = 1|\mathbf{d}_{1:l-1}) \\ &\quad + p(d_l|d_{l-1}, x_l = 0, x_{l-1} = 0)p(\mathbf{d}_{1:l-1}) \\ &\quad P(x_{l-1} = 0|\mathbf{d}_{1:l-1}) \end{aligned} \quad (6.23)$$

Therefore, by substituting Equations (6.21) and (6.23) into Equation (6.13), we may get

$$P(x_l = 1|\mathbf{d}_{1:l}) = \frac{1}{1 + \xi_l} \quad (6.24)$$

where ξ_l is defined as

$$\begin{aligned} \xi_l &\triangleq \frac{p(d_l|d_{l-1}, x_l = 0, x_{l-1} = 1)P(x_l = 0|x_{l-1} = 1)}{p(d_l|d_{l-1}, x_l = 1, x_{l-1} = 1)P(x_l = 1|x_{l-1} = 1)} \\ &\quad + \frac{p(d_l|d_{l-1}, x_l = 0, x_{l-1} = 0)P(x_{l-1} = 0|\mathbf{d}_{1:l-1})}{p(d_l|d_{l-1}, x_l = 1, x_{l-1} = 1)P(x_l = 1|x_{l-1} = 1)P(x_{l-1} = 1|\mathbf{d}_{1:l-1})} \end{aligned} \quad (6.25)$$

6.4 Hierarchical Bayesian modeling on feature distances

It is easily observed that ξ_l is the function of $P(x_{l-1} = 1 | \mathbf{d}_{1:l-1})$ and the associated conditional probability density function $p(d_l | d_{l-1}, x_l, x_{l-1})$. Therefore, the *posterior* probability along a particular path (i.e. the path from the root node at top level to the node of interest at level l) can be recursively calculated using the recursion Equations (6.24) and (6.25). For the aforementioned recursion equations, the following four comments should be taken into account.

- The term $P(x_l | x_{l-1})$ in Equation (6.25) can be viewed as the prior knowledge for conducting hierarchical vehicle matching. In this study, the *prior* probability is defined as $P(x_l | x_{l-1}) = 0.5$, which suggests that the hierarchical matching is solely based on the comparison between the vehicle feature data. Since the set of candidate vehicles has already been refined by performing pair-wise VRI (Section 6.3.2), the additional prior knowledge may not be beneficial for the hierarchical matching process.
- The term $P(x_{l-1} | \mathbf{d}_{1:l-1})$ in Equation (6.25) indicates that the matching probability at current level l is dependent on the probability at previous level in the vehicle tree, which also implies that the vehicle matching across multiple detectors is considered simultaneously.
- Although the recursion equations are derived based on the assumption of first order Markov property of the feature distances (see Equation (6.15)), a higher order Markov model is equally applicable to the hierarchical matching process.
- The conditional probability density function $p(d_l | d_{l-1}, x_l, x_{l-1})$ is another critical component in the hierarchical Bayesian modeling. By considering the spatial dependencies between feature distances, the proposed hierarchical model is expected to outperform the pair-wise VRI method in terms of the matching accuracy. In what follows, a statistical model, which allows the probabilistic description of feature distances over space, is introduced.

6.4.2 Probabilistic modeling of feature distances over space

By applying Bayes rule, the conditional probability $p(d_l | d_{l-1}, x_l, x_{l-1})$ can be expressed as

$$p(d_l | d_{l-1}, x_l, x_{l-1}) = \frac{p(d_l, d_{l-1} | x_l, x_{l-1})}{p(d_{l-1} | x_l, x_{l-1})} = \frac{p(d_l, d_{l-1} | x_l, x_{l-1})}{p(d_{l-1} | x_{l-1})} \quad (6.26)$$

6.4 Hierarchical Bayesian modeling on feature distances

For the denominator (i.e. $p(d_{l-1}|x_{l-1})$) in the right-hand side of Equation (6.26), we utilize the same statistical model (see Equation (6.6)) that proposed in Section 6.2.1. The readers can also refer to Section 4.3.3 for a more detailed explanation on the calibration of this statistical model (e.g. finite Gaussian mixture model and estimation of the model parameters). In this case, the estimation of the joint probability density function $p(d_l, d_{l-1}|x_l, x_{l-1})$ would become the major concern.

As the feature distance d_l consists of multiple vehicle feature distances (e.g. color, length, type), the logarithmic opinion pool (same as Equation (6.7)) is then employed to fuse the information and, accordingly, the joint probability can be reformulated as

$$p(d_l, d_{l-1}|x_l, x_{l-1}) = \frac{1}{Z_{\text{LOP}}} p(d_{\text{color}}^{(l)}, d_{\text{color}}^{(l-1)}|x_l, x_{l-1})^\alpha p(d_{\text{type}}^{(l)}, d_{\text{type}}^{(l-1)}|x_l, x_{l-1})^\beta p(d_{\text{length}}^{(l)}, d_{\text{length}}^{(l-1)}|x_l, x_{l-1})^\gamma, \alpha + \beta + \gamma = 1 \quad (6.27)$$

where $d_{\text{color}}^{(l)}$ and $d_{\text{color}}^{(l-1)}$ denote the observed color feature distance at level l and level $l-1$, respectively; the fusion weights α , β and γ are used to indicate the degree of contribution of each joint probability function, and Z_{LOP} is the normalizing constant. To facilitate the presentation of the essential ideas without loss of generality, we only consider the estimation of joint probability for color feature distance. For the sake of simplicity, denote d_l as the color feature distance $d_{\text{color}}^{(l)}$.

First, let us consider the definition of the joint probability $p(d_l, d_{l-1}|x_l = 1, x_{l-1} = 1)$ by revisiting the framework of hierarchical matching (Figure 6.4). Assume that vehicles i , j and k are the same vehicle appearing at three stations. Therefore the associated distance measures d_1 and d_2 can be obtained and the multivariate statistical model (i.e. multivariate normal distribution) can be calibrated from these training data. To be more specific, a training database containing sequential records of 600 vehicles is built up. Figure 6.5 shows the calibration result of the joint probability density function (pdf of multivariate normal distribution) of d_1 and d_2 . Mathematically speaking, the formula can be expressed as follows:

$$f(\mathbf{d}, \boldsymbol{\mu}, \boldsymbol{\Sigma}) = \frac{1}{\sqrt{2\pi|\boldsymbol{\Sigma}|}} e^{-\frac{1}{2}(\mathbf{d}-\boldsymbol{\mu})^T \boldsymbol{\Sigma}^{-1}(\mathbf{d}-\boldsymbol{\mu})} \quad (6.28)$$

where $\mathbf{d} = (d_1, d_2)^T$ is the random color feature vector and $\boldsymbol{\mu} = (\mu_1, \mu_2)^T$ is the associated

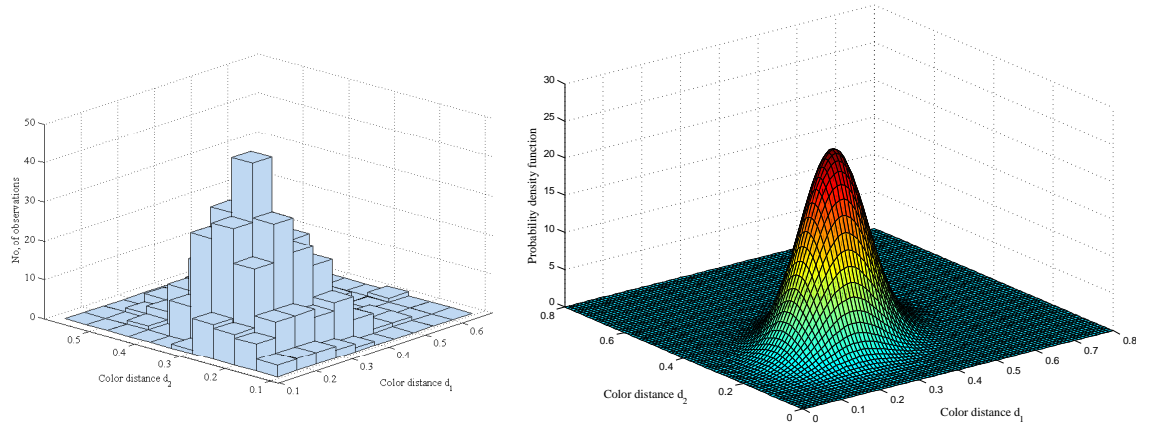


Figure 6.5: Multivariate histogram and the fitted normal distribution

the mean value. By applying the maximum likelihood estimation method, we may have:

$$\mu = \begin{pmatrix} 0.3032 \\ 0.2925 \end{pmatrix} \quad \text{and} \quad \Sigma = \begin{pmatrix} 0.0074 & 0.0020 \\ 0.0020 & 0.0056 \end{pmatrix} \quad (6.29)$$

The correlation coefficient ρ_{12} is then given by:

$$\rho_{12} = \frac{cov(d_1, d_2)}{\sigma_1 \sigma_2} = \frac{0.0020}{\sqrt{0.0074 \times 0.0056}} = 0.3107 \quad (6.30)$$

where σ_1 and σ_2 are the standard deviations of d_1 and d_2 , respectively. The fact that $\rho_{12} \neq 0$ indicates that the color feature distances d_1 and d_2 are actually correlated with each other. Similarly, the other joint probabilities, such as $p(d_l, d_{l-1} | x_l = 0, x_{l-1} = 1)$ and $p(d_l, d_{l-1} | x_l = 0, x_{l-1} = 0)$ in Equation (6.25), can also be estimated. On the basis of the calibrated statistical model of feature distances over space, the *posterior* probability at each node along a particular path in the vehicle tree could be calculated. The final solution for the hierarchical matching can then be obtained by solving the optimization Problem (6.10). In the next section, we will present the preliminary test results regarding the performance of the hierarchical Bayesian matching model.

6.5 Test results

In this research, the performance of the proposed hierarchical Bayesian matching model is evaluated against the pair-wise VRI method in terms of the matching accuracy over

multiple camera detectors.

6.5.1 Dataset for algorithm evaluation

Before presenting the experimental results, a brief introduction of the dataset that are utilized for algorithm evaluation is presented. The test site is a 34.9-kilometer-long three-lane freeway segment in Bangkok, Thailand (see Figure 6.6). At each station a gantry-mounted video camera, which is viewed in the upstream direction, is installed, and two hours of video record were collected between 10 a.m. and noon on June 20, 2012. The frame rate of the video record is 25 FPS, and the still image size is 563×764 . Two consecutive segments (i.e. the green section in Figure 6.6) are chosen for algorithm evaluation: 1) a 4.2-kilometer-long segment (i.e. between 02A and 04A); 2) a 5.5-kilometer-long segment (i.e. between 04A and 06A). As the detailed vehicle feature data are not readily obtainable from the raw video record, the intelligent video surveillance (IVS) is then employed for extracting the required information¹. Based on the video record collected at the test site,

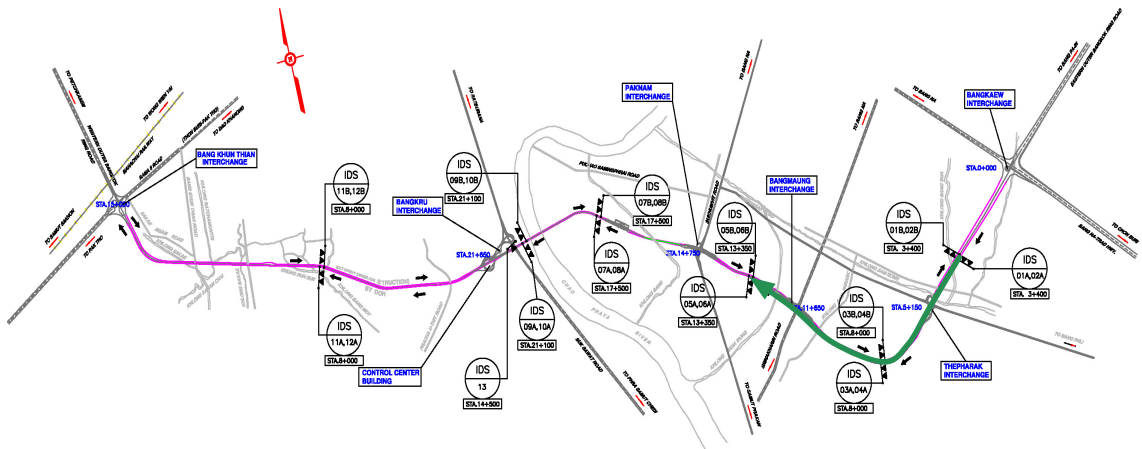


Figure 6.6: Test site in Bangkok, Thailand

1406 vehicles are detected at there camera stations (i.e. 02A, 04A and 06A) during the two-hour video record. For the purpose of model calibration and algorithm evaluation, these 1406 vehicles are manually matched/reidentified by the human operators viewing the video record frame by frame. In other words, the ground-truth matching results of the 1406 vehicles are obtained in advance. Sequential records of the first 600 vehicles are used for model training and calibration (see Section 6.4.2), while the rest of vehicle

¹Detailed implementation of the IVS for traffic data extraction can be found in Section 2.3 and Chapter 3.

dataset are utilized for the test of the proposed hierarchical Bayesian matching model.

6.5.2 Comparison between pair-wise VRI and the improved method

As discussed in Section 6.2, the fundamental component of the pair-wise VRI is the basic VRI subsystem. In this particular case, two basic VRI subsystems are applied independently such that the matching result on each segment can be obtained and, consequently, the matching accuracy of pair-wise VRI over three detectors can be easily calculated. Meanwhile, the construction of vehicle tree structure (threshold value $\tau = 3$) can be completed based on the results of basic VRI subsystem (see Section 6.3.2). By performing the hierarchical matching method on the vehicle tree structure (see Equations (6.24) and (6.25)), the improved matching results are then obtained.

Table 6.1: Comparison between pair-wise VRI and the improved method

Matching method \ Detector pair	Detector pair			
	06A-04A ^a	04A-02A	06A-02A ^b	06A-04A-02A
Basic VRI	44.91% ^c	62.28%	28.98%	---
Pair-wise VRI	---	---	---	34%
Improved method^d	---	---	---	41.19%

^a Match vehicle from 06A to 04A.

^b Match vehicle from 06A to 02A regardless of the information obtained at intermediate point (i.e. 04A).

^c Matching accuracy of the proposed method.

^d Hierarchical Bayesian matching method.

Table 6.1 compares the performances (i.e. matching accuracies) of different vehicle matching methods. The first row of Table 6.1 indicates that the performance of basic VRI subsystem would gradually decrease with respect to the increase in the length of freeway segment (which has already been explained in Section 6.1). The primary reason for low matching accuracy (i.e. 28.98%) of basic VRI over 06A-to-02A is that we did not take full advantage of the vehicle feature data observed at the intermediate station (i.e. station 04A). By applying pair-wise VRI, the connection between two basic VRI subsystems (e.g. VRI over 06A-04A and 04A-02A) can be built up (see Procedure 6.1) and, hence, a higher matching accuracy over multiple detectors can be expected (i.e. 34% in the second row of Table 6.1). The proposed hierarchical Bayesian matching method further considers the vehicle matching over multiple detectors as an integrated process, and proposes a suitable statistical model to describe the spatial dependencies between the feature distances.

Therefore, the matching accuracy is further improved to 41.19%.

Figure 6.7 shows the matching results for a vehicle at station 06A by respectively applying the pair-wise VRI and hierarchical matching method. Note that basic VRI subsystem over

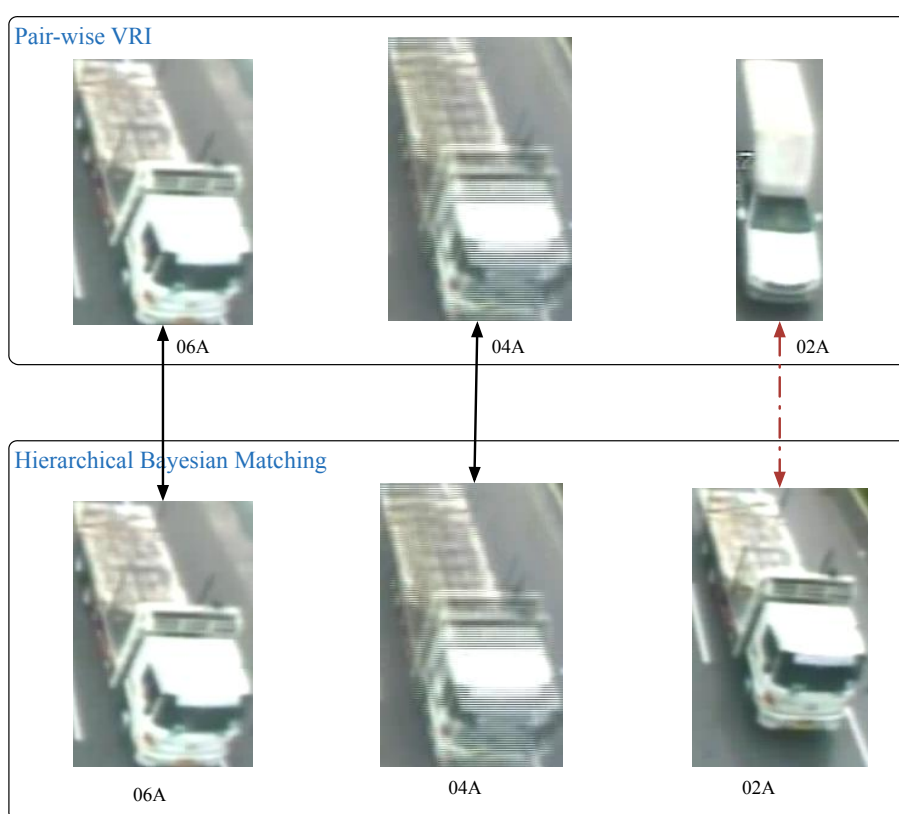


Figure 6.7: Illustrative matching example

04A-02A produces a mismatch¹. As pair-wise VRI performs basic VRI independently, the mismatches of a single subsystem could fail the whole system. On the other hand, the proposed hierarchical Bayesian matching method could correct/refine the matching results by considering the spatial correlations between the feature distances.

¹The reason for generating this mismatch is still unknown. The most likely explanation is that the vehicle image at 04A becomes extremely blurry and, hence, the calculated feature distance is less reliable, which eventually leads to the mismatch.

6.6 Conclusion remarks

This chapter aims to develop an additional hierarchical Bayesian model for vehicle re-identification on freeway segment with multiple detectors. A hierarchical matching component is introduced so that vehicle matching over multiple segments is treated as an integrated process. By utilizing the preliminary information (i.e. refined candidate vehicle set) obtained from basic VRI, the hierarchical tree structure is built up. A statistical model considering the spatial dependencies between feature distances is also incorporated to further improve the matching accuracy. The hierarchical matching problem is then solved by finding the optimal path in the hierarchical tree structure, such that the *posterior* probability of a correct match given a sequence of feature distances along this path, is maximized. This novel method is further evaluated against the pair-wise VRI in terms of matching accuracy over multiple detectors.

Part III

Self-adaptive VRI system under dynamic traffic conditions

Chapter 7

Iterative VRI system with temporal adaptive time window

This chapter proposes an iterative vehicle reidentification (VRI) system with temporal adaptive time window to estimate the mean travel time for each time period on the freeway under traffic demand and supply uncertainty. To capture the traffic dynamics in real-time application, inter-period adjusting based on the exponential smoothing technique is introduced to define an appropriate time window constraint for each time period (i.e. temporal adaptive time window). In addition, an intra-period adjusting technique (i.e. iterative VRI) is also employed to handle the non-predictable traffic congestions. To further reduce the negative effect caused by the mismatches, a post-processing technique including the thresholding and stratified sampling, is performed on the travel time data derived from the VRI system. Several representative tests are carried out to evaluate the performance of the proposed VRI against the potential changes in traffic conditions, e.g. recurrent traffic congestion, freeway bottlenecks and traffic incidents. The results show that this method can perform well under traffic demand and supply uncertainty.

7.1 Introduction

As one of the best indicators for evaluation of the performance of traffic system, accurate travel time data are crucial for efficient traffic management and transport planning.

Therefore, it is of great importance to estimate the mean travel time in a robust and accurate manner. Because of the worldwide deployment of inductive loops, a large number of studies focused on utilizing the traffic data (e.g. spot speed, traffic flow) obtained from the traditional sensors to indirectly measure the mean travel time¹ (e.g. [Soriguera and Robuste, 2011](#); [Celikoglu, 2013](#)). Despite their computational efficiency and analytical simplicity, these indirect methods based on traditional sensors would result in large errors when it comes to serious traffic congestion ([Li et al., 2006](#)). To overcome this difficulty, considerable attention has been paid to use the emerging sensing technologies to directly track the individual probe vehicle and hence collect the associated travel time (which could be termed as probe-vehicle-based method²). Various advanced technologies, such as Bluetooth ([Quayle et al., 2010](#)), Global Positioning System technologies ([Hofleitner et al., 2012](#)), license plate recognition technique ([Chang et al., 2004](#)) and cellular phones ([Rose, 2006](#)) have been incorporated to assign a unique identity (e.g. plate number, media access control address and radio frequency identification tag) to the probe vehicle. By the accurate matching of the vehicle identities, the travel time of probe vehicle can be measured directly. Although these probe-vehicle-based approaches appear promising for travel time estimation, their successes rely on a high penetration rate of probe vehicles. Also, vehicle tracking based on the unique identity could raise privacy concerns. In this case, the vehicle reidentification (VRI) scheme, which does not intrude driver's privacy, provides an alternative way to measure the travel time.

As explained in Chapter 4, VRI is a process of matching vehicle signatures (e.g. waveform ([Sun and Ritchie, 1999](#)), vehicle length ([Coifman, 2002](#)), vehicle color ([Kamijo et al., 2005](#)), and partial plate number ([Watling and Maher, 1992](#))) from one detector to the next one in the traffic network. On one hand, the non-uniqueness of the vehicle signature would allow the VRI system to track the vehicle anonymously. Also, the penetration rate is 100% in principle as no in-vehicle equipment is required. On the other hand, this property of very non-uniqueness imposes a great challenge on the development of the vehicle signature matching method. To improve the matching accuracy, [Coifman \(1998\)](#) compared the lengths of vehicle platoons (i.e. vehicle platoon matching method). To further consider the noise as well as the non-uniqueness of vehicle signature, [Kwong et al. \(2010\)](#) proposed a statistical matching method in which the vehicle signature is treated as random variable and a probabilistic measure is introduced for matching decision-making. The aforementioned approaches, however, are limited to the case with only one lane arterial,

¹The readers can refer to Section 2.1.2 and 2.1.3 for a more comprehensive review of indirect travel time estimation methods.

²A detailed introduction regarding this method can be found in Section 2.1.4

and have a set of stringent assumptions on vehicle traveling behaviors (e.g. no overtaking, no lane-changing). The basic vision-based VRI proposed in Chapter 4 extends the statistical signature matching method to a more practical case in which overtaking between vehicles as well as the vehicle matching across multiple lanes are both allowed. A probabilistic data fusion rule is then introduced to combine these features derived from IVS systems to generate a matching probability (*posterior* probability) for matching decision-making. Basic VRI system also introduces a *prior* (fixed) time window, which sets the upper and lower bounds of the travel time in the hope of ruling out the unlikely candidate vehicles and, hence, improving the matching accuracy, which, in turn, would yield a more reliable travel time estimator. However, it is noteworthy that this basic VRI was specifically designed for a short time period in which the traffic condition is relatively stable (i.e. steady-state condition) and may not be applicable for "real-time" application under dynamic traffic conditions (see Section 4.6).

The development of VRI system for "real-time" implementation under dynamic traffic conditions is still difficult as it faces the following two major challenges. First, due to the traffic demand and supply uncertainty (e.g. fluctuation in travel demand, bottleneck effect and traffic incidents), the traffic conditions may substantially change from period to period (i.e. free flow to congested). Under these circumstances, the fixed time-window constraint may compromise the performance of the basic VRI system. Thus, instead of explicitly incorporating the time window, [Lin and Tong \(2011\)](#) utilized the travel time information estimated from the spot speed data and proposed a combined estimation model to reidentify the vehicles. As previously discussed that the travel time estimated from spot speed data is not reliable, this approach may not perform well under demand and supply uncertainty. Second, vehicle mismatches, which are caused by the non-uniqueness of vehicle signatures and the complex topological structure of the traffic network, are to be expected. This situation could get worse when a traffic incident happens. Therefore, a robust post-processing technique regarding the individual travel time obtained from VRI system is required. [Ndoye et al. \(2011\)](#) suggested a data clustering method to filter out the erroneous individual travel time caused by the mismatches. For practical implementation, however, it may still be difficult to distinguish between the correct and erroneous travel time under "abnormal" traffic conditions (e.g. the occurrence of an incident or the bottleneck effect).

To this end, the objective of this chapter is to propose an improved self-adaptive VRI system to cope with the purpose of real-time travel time estimation under dynamic traffic

conditions. Specifically, this study aims to estimate the mean travel time for each time period (e.g. 5-min period) on the freeway under traffic demand and supply uncertainty. The proposed VRI system is based on basic vision-based VRI with two major improvements as follows.

- First, to filter out the erroneous travel time caused by the mismatches, a thresholding process based on the matching probability¹ is performed. A stratified sampling technique based on vehicle type is then introduced to reduce the bias in the mean travel time estimates.
- Second, a self-adaptive time window component (i.e. inter-period and intra-period adjusting) is introduced into the basic VRI system to improve its robustness against potential changes in traffic conditions. Inter-period adjusting of time window (i.e. temporal adaptive time window) based on exponential smoothing technique is adopted to capture the traffic dynamics from period to period (Lo and Sumalee, 2013), whereas the intra-period adjusting (i.e. iterative VRI) is employed to handle the non-predictable traffic congestion (e.g. caused by traffic incidents or the bottleneck effect).

After the theoretical development, various numerical tests are conducted to demonstrate the application of the improved VRI system. The first simulation test investigates the feasibility of utilizing the improved VRI system to estimate the mean travel time for a closed freeway segment containing recurrent congestions due to exceeding traffic demand. In the second simulations, the method is evaluated on a freeway corridor with on- and off-ramps. A freeway bottleneck then arises due to the high merging demand and lane drops. The simulation results show that the proposed method performs well under bottleneck effect. The third simulation test is then conducted to test the performance of the algorithm under non-recurrent congestions (caused by traffic incidents).

The rest of the chapter is organized as follows. Section 7.2 presents a brief review on the simplified version of basic VRI system. In Section 7.3, the post-processing technique (e.g. thresholding and stratified sampling) regarding the individual travel time obtained from the VRI system is introduced. The detailed description and analysis of the self-adaptive time window component is proposed in the following section. In Section 7.5, simulated

¹The matching probability in this chapter is explicitly calculated for each pair of vehicle signatures (see Section 7.2.2), which is slightly different from that in Chapter 4.

tests are carried out to evaluate the performance of the proposed system. Finally, we close this chapter with the conclusions and future works.

7.2 Simplified version of basic VRI

The basic vision-based VRI with fixed time window is devised to estimate the mean travel time under static traffic conditions (e.g. a steady-state of free flow/congestion). In line with the other traditional VRI schemes, the basic vision-based VRI also involves two major steps: 1) vehicle feature extraction; 2) vehicle signature matching method. As the detailed traffic data (especially the vehicle feature data) are not readily obtainable from the raw video record, the intelligent video surveillance (IVS) system is then employed for extracting the required information (e.g. various vehicle feature data). Detailed implementation of the IVS for traffic data extraction can be found in Section 2.3 and Chapter 3. In what follows, a formal description of vehicle feature data obtained from IVS is presented.

7.2.1 Vehicle feature data

IVS provides a large amount of vehicle feature data (e.g. vehicle color, length, and type) for system development and evaluation. The intrinsic vehicle signature, $X = \{C, S, L\}$, is generated for each detected vehicle, where C and S are the normalized color feature vector and type (shape) feature vector, respectively; L denotes the vehicle length. To be more specific, the color feature (i.e. frequencies of different colors across the vehicle image) is represented by a 360-dimensional vector C , the type/shape feature S is a 6-dimensional vector that consists of the similarity score for each template, and vehicle length L is simply represented by the height of vehicle image. Also, the extrinsic vehicle data, such as the vehicle's arrival time t and spot speed v , are obtained during the detection process. Therefore, the individual vehicle record can then be represented as (t, v, X) .

For practical implementation, the vehicle records detected at upstream station will be stored in the upstream database. Let $U_i = (t_i^U, v_i^U, X_i^U)$ denote the record of the i th upstream vehicle, where $X_i^U = \{C_i^U, S_i^U, L_i^U\}$ represents the associated vehicle signatures (i.e. color, type, and length). In this case, the upstream database is denoted as

$U = \{U_i | i = 1, 2, \dots\}$, which could be updated with time propagation. Let $D = \{D_j | D_j = (t_j^D, v_j^D, X_j^D), j = 1, 2, \dots, M\}$ denote the M vehicle records generated at downstream station during a specific time period (e.g. 5-min period). The VRI is to find the corresponding upstream vehicles for these M downstream vehicles based on the generated vehicle signatures.

In order to quantify the difference between each pair of upstream and downstream vehicle signatures, several distance measures are then incorporated. Specifically, for a pair of signatures (X_i^U, X_j^D) , the Bhattacharyya distance is utilized to calculate the degree of similarity between color features, i.e.

$$d_{\text{color}}(i, j) = \left[1 - \sum_{k=1}^{360} \sqrt{C_i^U(k) \cdot C_j^D(k)} \right]^{1/2} \quad (7.1)$$

where k denotes the k th component of the color feature vector. The L_1 distance measure is introduced to represent the difference between the type feature vectors, i.e.

$$d_{\text{type}}(i, j) = \sum_{k=1}^6 |S_i^U(k) - S_j^D(k)| \quad (7.2)$$

The length difference is given by

$$d_{\text{length}}(i, j) = |L_i^U - L_j^D| \quad (7.3)$$

However, in practice it is unnecessary to compute the distances between all pairs of upstream and downstream vehicle signatures. To rule out the unlikely candidate vehicles at upstream database and improve the overall computational efficiency, a time window constraint is then introduced for vehicle signature matching.

7.2.2 Vehicle signature matching method

7.2.2.1 Time window constraint

A time window, which sets the upper and lower bounds of travel time, is introduced to define the search space (i.e. set of potential upstream matches) for the downstream vehicle.

Given a downstream vehicle $j \in \{1, 2, \dots, M\}$, its search space, $\mathcal{S}(j)$, is given by:

$$\mathcal{S}(j) = \{i | t_j^D - t_{max} \leq t_i^U \leq t_j^D - t_{min}\} \quad (7.4)$$

where t_{max} and t_{min} are, respectively, the upper and lower bounds of the time window. For a sequence of downstream vehicles $\{1, 2, \dots, M\}$, the set of the candidate upstream vehicles, i.e. \mathcal{S} is defined as

$$\mathcal{S} = \bigcup_{j=1}^M \mathcal{S}(j) \quad (7.5)$$

Under static traffic condition, the time window $[t_{min}, t_{max}]$ can be calibrated from the available historical travel time data.

With the associated search space \mathcal{S} , the vehicle signature matching method is equivalent to finding the correspondence between $\{1, 2, \dots, M\}$ and \mathcal{S} . Herein we introduce an indicator variable to represent the matching result, i.e.

$$x_{ij} = \begin{cases} 1, & \text{downstream vehicle } j \text{ matches upstream vehicle } i \in \mathcal{S} \\ 0, & \text{otherwise} \end{cases} \quad (7.6)$$

Recall that for each pair of vehicle signatures, (X_i^U, X_j^D) , $i \in \mathcal{S}, j \in \{1, 2, \dots, M\}$, one may compute the distance $(d_{color}(i, j), d_{type}(i, j), d_{length}(i, j))$ based on Equations (7.1), (7.2) and (7.3). A simple solution (i.e. distance-based method) is then to find the matching result x_{ij} with the minimum feature distance. However, it should be noted that the vehicle signatures contain potential noise and are not unique. Therefore the distance measure cannot really reflect the similarities between the vehicles. Instead of directly comparing the feature distances, this study utilizes the statistical matching method. Based on the calculated feature distance $(d_{color}(i, j), d_{type}(i, j), d_{length}(i, j))$, a matching probability $P(x_{ij} = 1 | d_{color}, d_{type}, d_{length})$ is provided for the matching decision-making.

7.2.2.2 Calculation of matching probability

The matching probability, also referred to as the *posterior* probability, plays a fundamental role in the proposed VRI system. By applying the Bayesian rule, one may have

$$P(x_{ij} = 1 | d_{color}, d_{type}, d_{length}) = \frac{p(d_{color}, d_{type}, d_{length} | x_{ij} = 1)P(x_{ij} = 1)}{p(d_{color}, d_{type}, d_{length})} \quad (7.7)$$

where $p(d_{\text{color}}, d_{\text{type}}, d_{\text{length}} | x_{ij} = 1)$ is the likelihood function; $P(x_{ij} = 1)$ is the prior knowledge about the matching result without observing the detailed vehicle feature data. In addition, one may also have

$$\begin{aligned} p(d_{\text{color}}, d_{\text{type}}, d_{\text{length}}) &= p(d_{\text{color}}, d_{\text{type}}, d_{\text{length}} | x_{ij} = 1)P(x_{ij} = 1) \\ &+ p(d_{\text{color}}, d_{\text{type}}, d_{\text{length}} | x_{ij} = 0)P(x_{ij} = 0) \end{aligned} \quad (7.8)$$

On the basis of Equations (7.7) and (7.8), it is observed that the calculation of the matching probability is dependent on the deduction of the likelihood function and the prior probability. In this particular case, the prior probability is approximated by the historical travel time distribution

$$P(x_{ij} = 1) = \frac{f(t(i, j))}{\eta} \times 0.5 \quad (7.9)$$

$$P(x_{ij} = 0) = 1 - \frac{f(t(i, j))}{\eta} \times 0.5 \quad (7.10)$$

where $f(\cdot)$ denotes the historical travel time distribution, $t(i, j)$ is the time difference between upstream vehicle i and downstream vehicle j , and η is the normalizing factor.

The calculation of the likelihood function is completed in two steps. First, individual statistical models for the three feature distances are constructed and the corresponding likelihood functions are also obtained (i.e. $p(d_{\text{color}} | x_{ij} = 1)$, $p(d_{\text{type}} | x_{ij} = 1)$, and $p(d_{\text{length}} | x_{ij} = 1)$). Then a data fusion rule is employed to provide an overall likelihood function used in the *posterior* probability (7.7).

7.2.2.3 Statistical modeling of feature distance

Without loss of generality, only the probabilistic modeling of color feature distance is described. In the framework of statistical modeling, the distance measure is assumed to be a random variable. Thus, for a pair of color feature vectors (C_i^U, C_j^D) , the distance $d_{\text{color}}(i, j)$ follows a certain statistical distribution. The conditional probability (i.e. likelihood function) of $d_{\text{color}}(i, j)$ is then given by

$$p(d_{\text{color}}(i, j) | x_{ij}) = \begin{cases} p_1(d_{\text{color}}(i, j)), & \text{if } x_{ij} = 1 \\ p_2(d_{\text{color}}(i, j)), & \text{if } x_{ij} = 0 \end{cases} \quad (7.11)$$

where p_1 denotes the probability density function (pdf) of distance $d_{\text{color}}(i, j)$ when color feature vectors C_i^U and C_j^D belong to the same vehicle, whereas p_2 is the pdf of the distance $d_{\text{color}}(i, j)$ between different vehicles. A historical training dataset that contains a number of pairs of correctly matched vehicles are utilized for estimating the pdfs p_1 and p_2 . Likewise, the likelihood functions for the type and length distances can also be obtained in a similar manner.

7.2.2.4 Data fusion rule

In this study the logarithmic opinion pool (LOP) approach is employed to fuse the individual likelihood functions. The LOP is evaluated as a weighted product of the probabilities and the equation is given by

$$p(d_{\text{color}}, d_{\text{type}}, d_{\text{length}} | x_{ij}) = \frac{1}{Z_{\text{LOP}}} p(d_{\text{color}} | x_{ij})^\alpha p(d_{\text{type}} | x_{ij})^\beta p(d_{\text{length}} | x_{ij})^\gamma, \quad \alpha + \beta + \gamma = 1 \quad (7.12)$$

where the fusion weights α , β and γ are used to indicate the degree of contribution of each likelihood function, and Z_{LOP} is the normalizing constant. The weights can also be calibrated from the training dataset. By substituting Equations (7.8), (7.9) and (7.12) into (7.7), the desired matching probability can be obtained. For the sake of simplicity, let P_{ij} denote the matching probability between upstream vehicle $i \in \mathcal{S}$ and downstream vehicle j .

Note that the aforementioned matching probability in Equation (7.7) is slightly different from that (see Equation (4.9)) in chapter 4. In this chapter, we attempt to "explicitly" calculate the *posterior* probability based on the observation of the feature distances of only one pair of vehicle signatures, whereas the basic VRI is trying to calculate an overall *posterior* probability based on the observations of feature distances between two sets of vehicles (i.e. upstream set and downstream set). Therefore, the simplified equation (Equation (7.7)) could provide an explicit matching probability for each individual pair of vehicles, which may be more suitable for the following processing (i.e. post-processing in Section 7.3).

7.2.2.5 Bipartite matching method

Recall that the basic VRI system is to find the matching result x_{ij} between the downstream vehicle set $\{1, 2, \dots, M\}$ and its search space \mathcal{S} (assume that there are N candidate vehicles) simultaneously based on matching probability $\{P_{ij} | i = 1, 2, \dots, N; j = 1, 2, \dots, M\}$. The signature matching problem is then formulated as

$$\min_{\mathbf{x}} \sum_{i=1}^N \sum_{j=1}^M -P_{ij} x_{ij} \quad (7.13)$$

$$\text{s.t. } x_{ij} \in \{0, 1\}, \quad \forall i \in \mathcal{S}, j \in \{1, 2, \dots, M\} \quad (7.14)$$

$$\sum_{i=1}^N x_{ij} = 1, \quad \forall j \in \{1, 2, \dots, M\} \quad (7.15)$$

$$\sum_{j=1}^M x_{ij} \leq 1, \quad \forall i \in \mathcal{S} \quad (7.16)$$

Objective (7.13) is to maximize the overall matching probabilities between the two sets. Constraint (7.14) ensures that the decision variables are binary integers. Constraint (7.15) requires that a downstream vehicle can have one matched vehicle at upstream station, whereas constraint (7.16) guarantees that an upstream vehicle can have, at most, one matched vehicle at downstream (normally $N > M$). This combinatorial optimization problem is equivalent to a minimum-weight bipartite matching problem, which has already been widely studied and can be efficiently solved by the successive shortest path algorithm with computational complexity of $O(M^2N)$. This optimization problem is also different from the original one (Equation (4.22)) in Chapter 4. The formulation of the original optimization problem is strictly based on the MAP (i.e. maximum a *posterior* probability) rule, whereas the simplified problem just intuitively maximize the overall matching probability. Although the basic VRI is simplified to some extent, it provides essentially the same results (i.e. matching accuracy) as our original work in Chapter 4. The potential benefits for the simplification is presented in Section 7.3.

7.2.2.6 A discussion on the application of the basic VRI system

The detailed implementation of the basic VRI for mean travel time estimation (e.g. from 10:00 a.m. to 10:05 a.m.) is summarized in the following flowchart (Figure 7.1). First, the

system will initialize the time stamp t and check whether a vehicle is detected at the upstream and/or downstream stations. The generated upstream vehicle records are stored in upstream vehicle database. Once a vehicle is detected at downstream station, the candidate vehicle set will be selected based on the time window constraint. Meanwhile, the matching probability for each pair of vehicles is calculated. When the current time t reaches 10:05 a.m., the bipartite matching process based on matching probability will begin and the travel time data can be obtained. Detailed implementation of this system can be found in Chapter 4. For the aforementioned framework, the following four comments should be

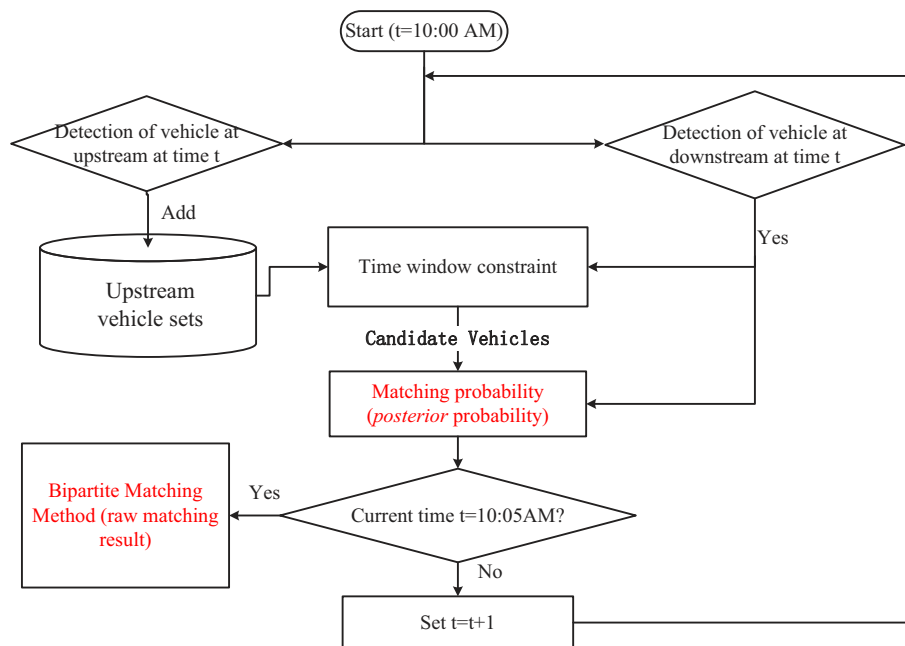


Figure 7.1: Illustrative example of the basic VRI system for real-time implementation

taken into account.

- First, it is noteworthy that the calculation of matching probability can be simultaneously performed along with the vehicle detection process at downstream site (i.e. during the 5-min time period). In addition, the bipartite matching process can be carried out efficiently as explained before. Thus, the basic VRI can be implemented in real time (which will be explained in detail in Section 7.5.1).
- Second, it is observed that the basic VRI heavily depends on the specification of the time window. When a large time window is applied, search space \mathcal{S} would include too many candidate vehicles, which could lead to a significant increase in computational time. On the other hand, a relatively smaller time window may enable

the algorithm to find the corresponding vehicle more efficiently, but it may also wrongly exclude the correct match from search space \mathcal{S} .

- Third, by using the historical travel time distribution to approximate the prior knowledge ($P(x_{ij} = 1)$), one may obtain a more reliable matching probability. In a word, the basic VRI accepts the predefined time window and the historical travel time distribution as exogenous inputs and then perform the vehicle matching method. Both of these two inputs can be derived from the mean travel time data (which will be explained in Section 7.4).
- Fourth, the basic VRI cannot work well under traffic demand and supply uncertainty, as the time window and prior knowledge may not be well-defined. From the perspective of mean travel time estimation, two novel components (i.e. post-processing and self-adaptive time window) can be incorporated to improve the overall performance.

7.3 Post-processing technique

Upon completion of the basic VRI system, the raw travel time for the j th, $j \in \{1, 2, \dots, M\}$ downstream vehicle during the evaluation period can be obtained and denoted as t_j^r . Thus the mean travel time without post-processing is given by

$$\mu^r = \frac{1}{M} \sum_{j=1}^M t_j^r \quad (7.17)$$

As the mismatches due to the non-uniqueness of vehicle signature are inevitable, the raw travel time may include erroneous information. Hence, accordingly, the estimator μ^r may not be reliable in practice.

7.3.1 Stratified sampling technique

One natural method is to perform thresholding on the raw travel time data based on the explicit matching probability (which is provided by the simplified basic VRI) in an attempt to rule out the mismatches. However, another problem (i.e. biased estimation) may

arise along with this thresholding process. It is commonly believed that the travel time of vehicles of different types (e.g. small cars, long trucks) are significantly different. Figure 7.2 shows the travel time of different vehicle types fitted by a normal distribution, where vehicle type 1 denotes the smaller cars and vehicle type 2 represents the long trucks. These ground truth travel time data are collected from a freeway segment in Bangkok, Thailand. The authors also conducted various hypothesis tests (i.e. t-tests) to validate this assumption:

$$H_0 : \mu_{\text{type1}} = \mu_{\text{type2}} \quad \text{vs.} \quad H_a : \mu_{\text{type1}} \neq \mu_{\text{type2}}$$

where μ_{type1} and μ_{type2} are respectively the mean travel time of small cars and long trucks. The results show that the null hypothesis should be rejected, which means that the travel times of different types of vehicles are "statistically" different. In view of this, to further

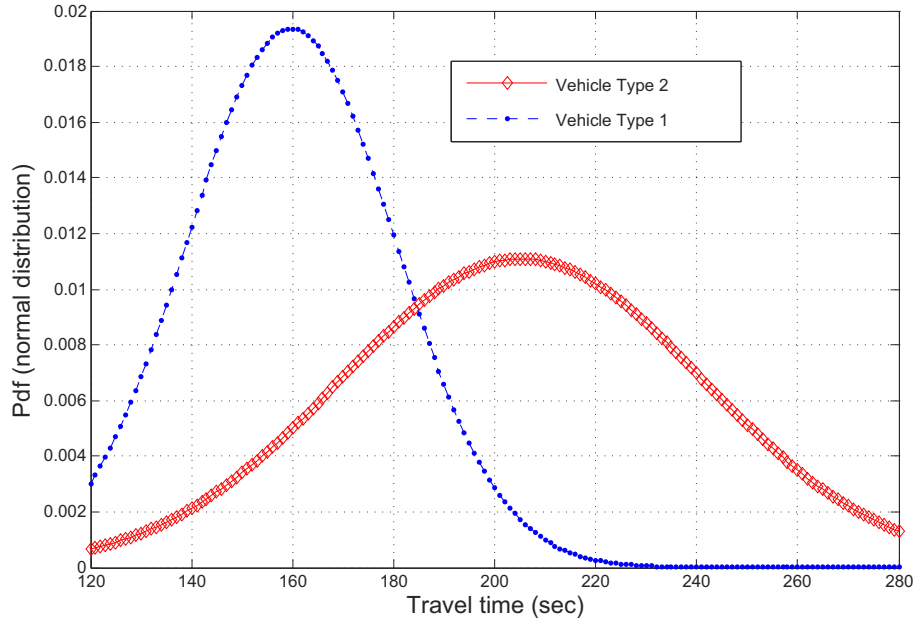


Figure 7.2: Travel time for different vehicle types.

reduce the bias in mean travel time estimation, the stratified sampling technique (Hellings and Fu, 2002) based on vehicle type is proposed. Specifically, the raw travel time data $\{t'_j | j = 1, 2, \dots, M\}$ are divided into two strata (i.e. small car stratum and long truck stratum). The thresholding processes are performed independently on these two strata. The final mean travel time μ is then computed as the weighted average of the mean travel time over all vehicle type strata. The equation is then given as

$$\mu = \sum_{k=1}^2 \frac{M_k}{M} \left(\frac{1}{n_k} \sum_{j=1}^{n_k} t_{jk} \right) \quad (7.18)$$

where M_k is the number of vehicles of type k ; n_k denotes the sample size of vehicles of type k after the thresholding process; t_{jk} is the travel time of the j th vehicle of type k after thresholding process. The design of thresholding process becomes the major concern in the following section.

7.3.2 Thresholding process

For each individual vehicle stratum, the thresholding process is performed independently. As explained before, one of the outputs of basic VRI is the matching result x_{ij} , whereas the other output is the associated matching probability P_{ij} . The overall idea of the thresholding is to apply a certain rule to these outputs (i.e. x_{ij} and P_{ij}) in order to identify the associated erroneous travel time. For a downstream vehicle j in vehicle stratum k , the matched upstream vehicle $i^* = \{i \in \mathcal{S} | x_{ij} = 1\}$ and the associated matching probability is P_{i^*j} . One naive approach to rule out those mismatches would be to impose a threshold value on the matching probability. If P_{i^*j} is greater than the threshold value, then the travel time data regarding this vehicle j would be retained for the following stratified sampling (see Equation (7.18)). However, in practical implementation, we find that the single matching probability cannot really reflect the correctness of the matching. It is quite possible that the other matching probability $P_{lj} \approx P_{i^*j}, l \in \mathcal{S}; l \neq i^*$, which means that the VRI system cannot distinguish between the candidate vehicles. To account for this problem, this study proposes a new measure to represent the distinctiveness of the vehicle. For this specific vehicle j , the distinctiveness value is defined as follows

$$\frac{P_{i^*j}}{P_j^{(2)}}, P_j^{(2)} \text{ is the second largest matching probability of } \{P_{ij} | \forall i \in \mathcal{S}\} \quad (7.19)$$

Recall that the proposed bipartite matching method finds the matching result with the overall maximum probability (see Equation (7.13)). In this case, for certain downstream vehicle, it may not be matched to the upstream vehicle with the maximum likelihood. Therefore by calculating the distinctiveness value, one may get more information about the matching result, i.e.

$$\frac{P_{i^*j}}{P_j^{(2)}} = \begin{cases} \geq 1, & \text{vehicle } j \text{ matches upstream vehicle with maximum probability} \\ = 1, & \text{vehicle } j \text{ matches upstream vehicle with the second largest probability} \\ < 1, & \text{vehicle } j \text{ matches the other ones} \end{cases}$$

If vehicle j and upstream vehicle i^* are true matches, then the ratio between P_{i^*j} and $P_j^{(2)}$ are expected to be relatively larger. Based on this basic idea, a predefined threshold value $\tau > 1$ is then imposed on this distinctiveness value, i.e.

$$\begin{cases} P_{i^*j}/P_j^{(2)} > \tau, & \text{travel time } t_{jk} \text{ is retained for stratified sampling} \\ \text{Otherwise,} & \text{travel time } t_{jk} \text{ is discarded} \end{cases} \quad (7.20)$$

By applying the rule (7.20), the erroneous individual travel time data are expected to be identified and ruled out.

7.4 Self-adaptive time window constraint

Although the basic VRI is improved to some extent by imposing the post-processing technique on the raw travel time data (see Section 7.3), it still cannot perform well under traffic demand and supply uncertainty (some preliminary results are presented in Section 7.5). As mentioned in Section 7.2, the basic VRI heavily depends on the specification of two exogenous inputs, i.e. time window and prior knowledge. Therefore, to further improve the robustness of VRI system against the potential changes in traffic conditions, these two inputs should be adjusted accordingly (i.e. self-adaptive).

Intuitively, the time window can be derived from the travel time data (i.e. travel time distribution). Given the mean value μ_t and the variance σ_t^2 of the travel time distribution during time period t , a suitable time window $[Lb_t, Ub_t]$ could be easily obtained. Assume that the travel time follows normal distribution $N(\mu_t, \sigma_t)$, then the tolerance interval with 95% confidence level can be utilized to define the time window, i.e.

$$[Lb_t, Ub_t] = [\mu_t - 1.96\sigma_t, \mu_t + 1.96\sigma_t] \quad (7.21)$$

Given the coefficient of variation (CV) ϕ , the time window constraint can be rewritten as

$$[Lb_t, Ub_t] = [(1 - 1.96\phi)\mu_t, (1 + 1.96\phi)\mu_t] \quad (7.22)$$

Moreover, the prior knowledge can be approximated by the normal distribution $N(\mu_t, \phi\mu_t)$. Therefore, both of these two critical inputs of basic VRI can be derived from the prediction of the mean travel time in time period t . In other words, the self-adjusting of the time window as well as the prior knowledge can be completed by iteratively predicting

the mean travel time for each time period. In this research, the self-adjusting of the time window for real-time application involves two major steps as follows.

- Inter-period adjusting: Based on current traffic information (e.g. average spot speed) and the mean travel time value in previous time period (i.e. obtained from VRI system), one may predict the mean travel time value for the next time period (i.e. inter-period adjusting), from which the time window is derived. The exponential forecasting technique integrated with the average spot speed information is adopted during the inter-period adjusting process (i.e. temporal adaptive time window).
- Intra-period adjusting: Since the non-recurrent traffic congestion (e.g. caused by incident) is not predictable, the additional intra-period adjustment (i.e. iterative process) is required for providing an appropriate time window under these extreme circumstances. An iterative bipartite matching method is proposed for adjusting the time window, in which the basic VRI is iteratively solved (i.e. iterative VRI).

Note that the purpose of predicting the mean travel time is to derive an appropriate time window, and the accuracy of the prediction is not our major concern. As a matter of fact, the estimated mean travel time is obtained from the VRI system with post-processing technique.

7.4.1 Inter-period adjusting: Temporal adaptive time window

We introduce time series theory for short-term travel time prediction. As a classical statistical approach, time series forecasting has already been evaluated with several other applications in transportation, such as short-term traffic flow prediction (Tan et al., 2009) and traffic speed forecasting (Ye et al., 2012).

In this chapter, the underlying model equation for the mean travel time data is assumed as:

$$\mu_t = \mu_t^* + \varepsilon_t \quad (7.23)$$

where μ_t is the mean travel time calculated from the VRI system, μ_t^* represents the ground truth data and ε_t is the white noise error term. Our goal is to roughly forecast the mean travel time in period $t + 1$ (i.e. short-term prediction). Therefore, the exponential smooth-

ing technique integrated with spot speed information is employed for this particular purpose.

7.4.1.1 Exponential smoothing technique

The smoothing (forecasting) equation is given as follows:

$$\tilde{\mu}_{t+1} = \tilde{\mu}_t + \varphi(\mu_t - \tilde{\mu}_t) \quad (7.24)$$

$$\tilde{\mu}_{t+1} = \frac{V_t^U + V_t^D}{V_{t+1}^U + V_{t+1}^D} \tilde{\mu}_{t+1} \quad (7.25)$$

where $\tilde{\mu}_{t+1}$ and $\tilde{\mu}_t$ denote the forecasters of the mean travel time in time period $t + 1$ and period t , respectively; φ represents the smoothing parameter that is calibrated from the historical data; V_t^U and V_t^D are the average speed at upstream and downstream stations, respectively, during time period t ; and likewise, V_{t+1}^U and V_{t+1}^D are the average speed at upstream and downstream stations, respectively, during time period $t + 1$. Equation (7.24) serves as a simple exponential estimation based on the estimates from previous steps, whereas Equation (7.25) is a correction step by utilizing the average spot speed. The rationale behind (7.25) is as follows. If the average spot speeds at both stations (i.e. upstream and downstream) decrease from period t to period $t + 1$, the mean travel time during time period $t + 1$ is expected to be larger. Following the prediction of $\tilde{\mu}_{t+1}$, the time window for period $t + 1$ is given by:

$$[Lb_{t+1}, Ub_{t+1}] = [(1 - 1.96\phi)\tilde{\mu}_{t+1}, (1 + 1.96\phi)\tilde{\mu}_{t+1}] \quad (7.26)$$

Based on these recursive formulas, one may be able to predict the mean travel time as well as the time window from period to period (i.e. inter-period/temporal adjusting). However, it should be noted that a "bad" prediction could potentially lead to low matching accuracy of VRI system and, hence, unreliable travel time estimates. Thus, the additional intra-period adjusting method (i.e. iterative process) should be developed.

7.4.2 Intra-period adjusting: Iterative VRI

From time period $t + 1$, the predicted time window $[Lb_{t+1}, Ub_{t+1}]$ and $\tilde{\mu}_{t+1}$ are derived during the inter-period adjusting process and then fed into the basic VRI system, from

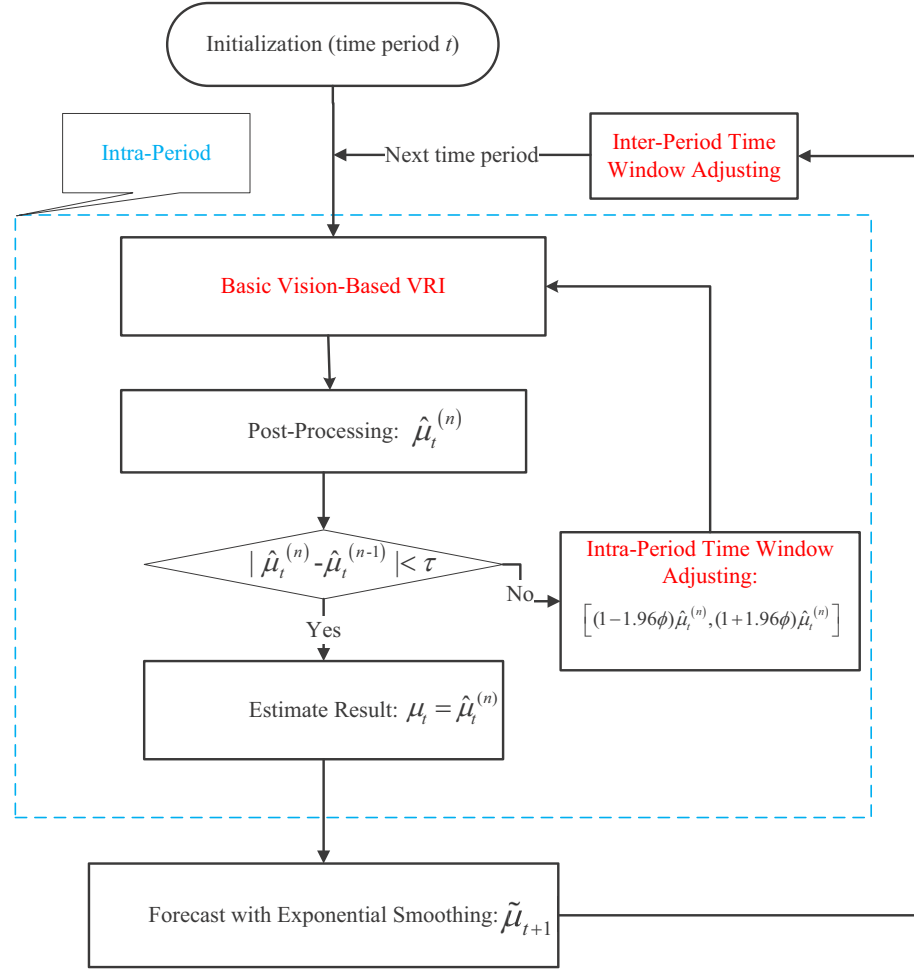


Figure 7.3: Detailed implementation of the improved VRI system.

which the raw travel time data can be obtained. By performing the post-processing technique (e.g. thresholding and stratified sampling), an improved mean travel time estimator, i.e. $\hat{\mu}_{t+1}^{(1)}$, is then calculated. In practice, the initial prediction of time window may not be reliable (especially when incident happens), which could significantly decrease the performance of the VRI system. Thus it is expected that $\hat{\mu}_{t+1}^{(1)}$ would not be accurate. In light of this, an iterative process is devised to solve the basic VRI problems iteratively with different exogenous inputs (i.e. time window and prior probability). To be more specific, a new time window, $[(1 - 1.96\phi)\hat{\mu}_{t+1}^{(1)}, (1 + 1.96\phi)\hat{\mu}_{t+1}^{(1)}]$, is calculated based on the estimated mean travel time $\hat{\mu}_{t+1}^{(1)}$. Then the basic VRI and the associated post-processing technique are performed again using this new time window. This iterative process will continue until the relative change of the estimated mean travel time is sufficiently small. In this research, the error for stopping tolerance of the convergence is given by:

$$|\hat{\mu}_{t+1}^{(n)} - \hat{\mu}_{t+1}^{(n-1)}| \leq \tau \quad (7.27)$$

where the superscript n represents the iteration number and τ is the stopping tolerance (See Figure 7.3).

To sum up, the inter-period/temporal adjusting is designed to capture the traffic dynamics from period to period, whereas the intra-period adjusting (i.e. iterative process) is introduced to handle the non-predictable traffic conditions (e.g. traffic incidents and bottleneck effect).

7.5 Experimental results

To verify the effectiveness and feasibility of the proposed improved VRI system, various simulation-based experiments are conducted. In this research, a VISSIM-based simulation model is devised to simulate freeway system operations under traffic demand and supply uncertainty (e.g. free flow, congestion, bottleneck effect and traffic incident)

7.5.1 Simulation model configuration and calibration

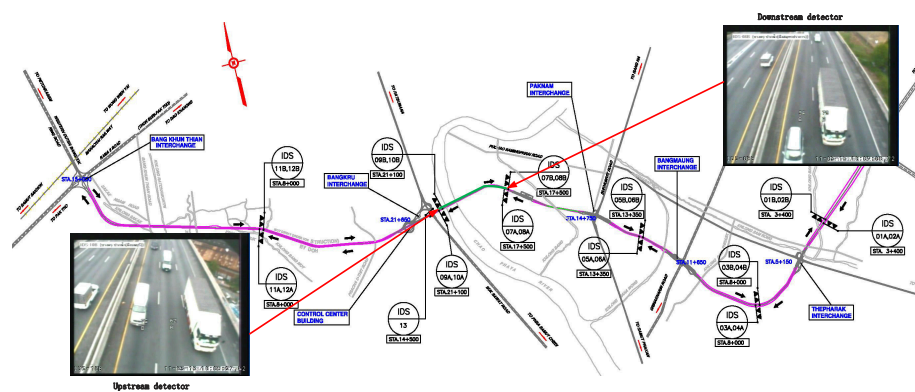


Figure 7.4: Test site in Bangkok, Thailand.

Before presenting the experimental results, the detailed procedures for simulation model development and calibration are introduced. The test site for this research is 34.9-kilometer-long three lane freeway system in Bangkok, Thailand (see Figure 7.4). At each station a gantry-mounted video camera, which is viewed in the upstream direction, is installed, and the associated video record are collected. Two segments are chosen for simulation model development: 1) 3.6-kilometer-long closed segment (i.e. between 08A and 10A, the green

section in Figure 7.4); 2) a 4.2-kilometer-long corridor with on-/off-ramps (i.e. between 02A and 04A). The simulation model is then configured based on the exact roadway geometric feature, including the length of the segment, location of on-/off-ramps, and the number of lanes.

To guarantee realistic representations of the simulated experiments, model calibration is required. With the video record collected at the test site, the individual vehicle can be detected and manually reidentified across multiple stations. Accordingly, the ground truth data, such as vehicle counts, traffic demand and travel time data can be obtained for model calibration. The correctly matched pairs of vehicle images are stored in the image database for further application.

Upon completion of the simulation model configuration and calibration, the travel behavior and characteristic of each individual vehicle (e.g. speed, vehicle type, and arrival time at each station) can be collected. As the very heart of the proposed method is the vision-based VRI, a vehicle image, which is randomly selected from the image database, is assigned to the vehicle record generated from the simulation model. These newly created vehicle records are then fed into the improved VRI system.

To sum up, we simulate all traffic conditions (recurrent and non-recurrent traffic congestion) using VISSIM and implement the proposed method in MATLAB. To be more specific, the experiments are performed under Windows 7 Home Premium and MATLAB v7.14 (R2012a) running on a Dell desktop with an Intel(R) Core(TM) i3 CPU at 3.20GHz and with 4.00 GB of memory. It is easily observed that the computational time of the proposed method largely depends on the number of intra-period iteration steps and the CPU time of the basic VRI system (see Figure 7.3). Some preliminary experiments also show that the average CPU time used by bipartite matching method in basic VRI under free flow condition is 0.0896 seconds, whereas the average CPU time under congested situation is about 0.3294 seconds. Therefore, it is reasonable to believe that the improved VRI system can be implemented for real time application.

7.5.2 Preliminary comparison between basic VRI and improved VRI

To conduct the comparison of the basic VRI and the improved VRI system, a Vissim-based simulation model is designed for the closed segment between 08A and 10A (Westbound).

During the 4-h simulation time period, approximately 16,000 pairs of vehicle records are generated. These vehicles can roughly be categorized into two types (see Section 7.3): 70% of small cars and 30% of long vehicles. For this specific segment, the associated image database, which includes 6,280 pairs of vehicle images, is built up. Therefore, a complete record for vehicle i can be denoted as (ID_i, t_i, v_i, X_i) , where ID_i is the unique identity derived from the simulation model; t_i and v_i are, respectively, the arrival time and spot speed of vehicle i ; and X_i represents vehicle feature data extracted from the vehicle image. Based on these simulation data, the proposed VRI system is performed and evaluated in terms of the matching accuracy and the effectiveness of mean travel time estimation.

For the closed freeway segment, each vehicle can be detected at both stations. Therefore, it is expected that the matching accuracy should be relatively higher, especially for a static time period (i.e. 5-min interval). However, for real-time application, the potential changes in traffic condition would lead to dramatic decrease/increase in matching accuracy. Figure 7.5 shows the effectiveness of the basic VRI by employing the temporal-adaptive time window. As the traffic volume increases significantly during the second hour of the simulation experiment, the corresponding traffic condition changes from free-flow to congested case. It is quite obvious that the fixed time window cannot handle this complicated situation (i.e. significant drop in matching accuracy from period 12 to 26), whereas the VRI system with temporal-adaptive time window can maintain a relatively stable matching accuracy (around 60% of matching accuracy).

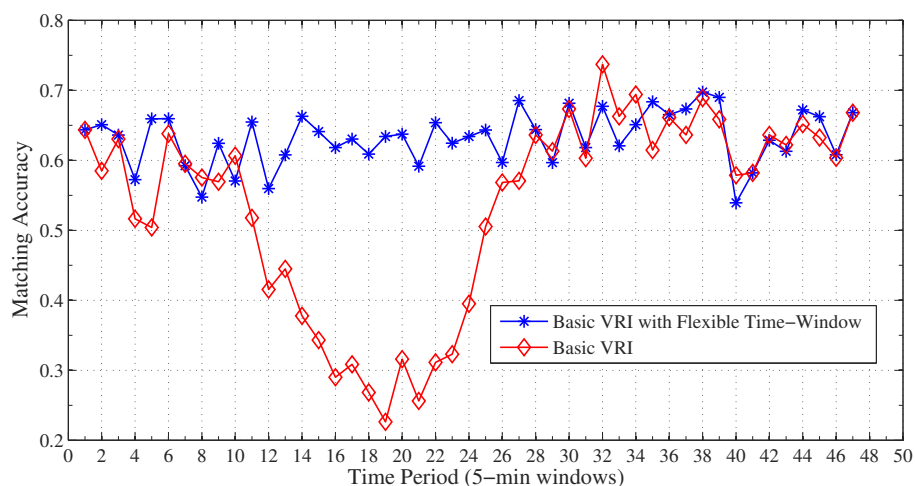


Figure 7.5: Effectiveness of temporal-adaptive time window.

On the other hand, given the fixed time window, a proper post-processing technique (i.e. thresholding and stratified sampling) can still improve the model performance from the

travel time estimation purpose. As shown in Figure 7.6, the performance of the basic VRI decays significantly under congested case due to the decrease in matching accuracy. However, it is worthwhile to notice that the accuracy in mean travel time estimation improves a lot by imposing the post-processing technique.

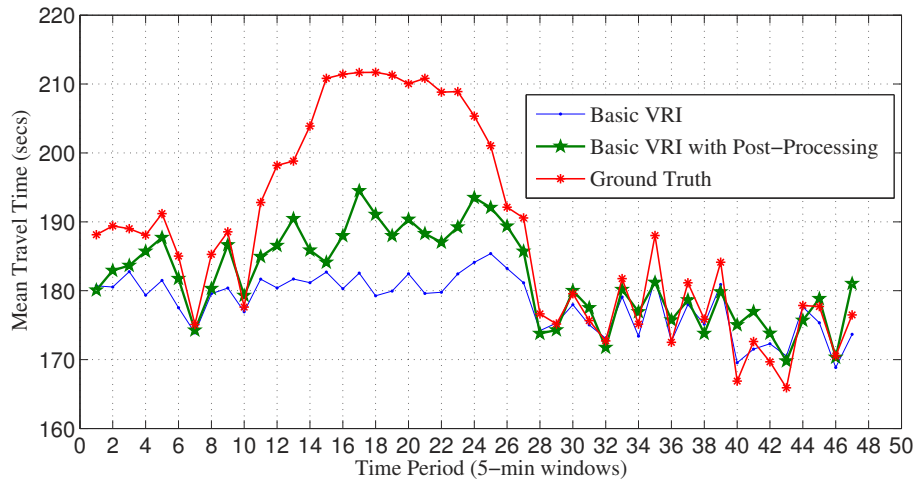


Figure 7.6: Effectiveness of post-processing technique under fixed time window.

7.5.3 Performance evaluation under recurrent traffic congestion

To further evaluate the performance of the improved VRI system (i.e. with post-processing and self-adaptive time window) under recurrent traffic congestion (due to exceeding traffic demand), the three-lane closed segment (between 08A and 10A) is chosen for test site. The stochastic vehicle inputs of the VISSIM-based simulation model are defined as

$$Q = \begin{cases} 4000 \text{ veh/h,} & 0 \leq t \leq 60 \text{ min;} \\ 7000 \text{ veh/h,} & 60 \leq t \leq 120 \text{ min;} \\ 8000 \text{ veh/h,} & 120 \leq t \leq 180 \text{ min;} \\ 4000 \text{ veh/h,} & 180 \leq t \leq 240 \text{ min;} \end{cases} \quad (7.28)$$

The vehicle inputs are chosen such that all the traffic states ranging from free-flow to congested can be activated. The freeway segment operates under free-flow condition in the first stage (i.e. first hour). Congestion may be observed when the vehicle inputs switch to the second stage. Then the traffic tends to a steady-state of congestion during the following two hours. In the fourth stage, congestion dissolve will be observed and the traffic will gradually be cleared from the freeway system. Table 7.1 shows descriptive statistics for

the outputs from the vissim-based simulation model. To validate the overall performance

Table 7.1: Descriptive statistics from simulation outputs

Time: (0 min - 240 min)	Simulation outputs				
	Vehicle Inputs (veh/h)	No. of small vehicles	No. of long vehicles	Upstream mean speed (km/h)	Downstream mean speed (km/h)
First hour	3982	2786	1196	82.7	73.3
Second hour	5964	4203	1761	68.0	69.1
Third hour	6214	4390	1824	47.3	65.1
Fourth hour	3934	2746	1188	80.7	72.7

of the improved VRI system, we run the method 50 times based on the simulation outputs. For each run, the vehicle image is randomly selected from the database and assigned to the vehicle record generated from the simulation model. The root mean square error (RMSE) and the mean absolute percentage error (MAPE) are applied as performance indices. The equation of RMSE is given by

$$RMSE = \sqrt{\frac{1}{50} \sum_{s=1}^{50} \sum_{i=1}^I \frac{(\mu_{i(s)} - \mu_i^*)^2}{I}} \quad (7.29)$$

where $\mu_{i(s)}$ is the estimate for the i th time period and the s th run; I indicates the total number of time periods; μ_i^* represents the i th ground truth data. The MAPE is calculated as follows:

$$MAPE = \frac{1}{50 \times I} \sum_{s=1}^{50} \sum_{i=1}^I \left[\left| \frac{\mu_{i(s)} - \mu_i^*}{\mu_i^*} \right| \times 100 \right] \quad (7.30)$$

By simple calculation, the RMSE and MAPE of the improved VRI system for 5-min aggregation interval are 3.28 seconds and 1.0%, respectively, while the RMSE of the basic VRI is 14.61 seconds. It is observed that the improved VRI clearly outperforms the basic VRI. Figure 7.7 shows the mean travel time estimates from one experiment. By integrating the average spot speed information (see Table 7.1), the inter-period/temporal adjusting can capture the traffic dynamics well, which could contribute to the following intra-period adjusting (i.e. less intra-period iteration steps).

7.5.4 Performance evaluation under bottleneck effect

As one of the major causes for freeway traffic congestion, the freeway bottleneck can arise from many conditions, such as high merging and diverging demand at on-/off-ramps and

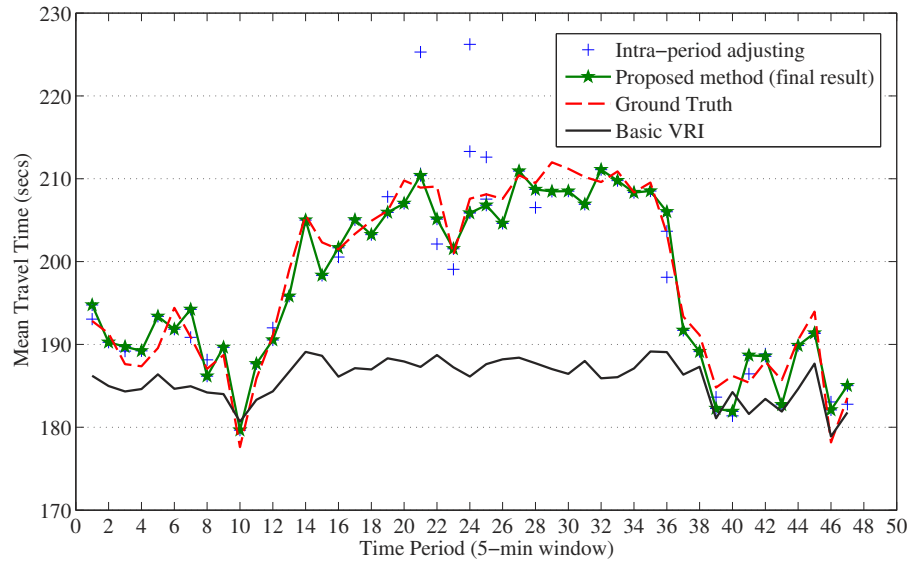


Figure 7.7: Performance of the proposed method with exceeding traffic demand

lane drops. In this part, we will evaluate the performance of the proposed method under bottleneck effect. A 4.6-kilometer-long three-lane freeway segment between 02A and 04A (see Figure 7.4) is chosen as the test site. As shown in Figure 7.8, one two-lane on-ramp (2 kilometers away from upstream station) and one two-lane off-ramp are distributed along this segment. We will ignore the off-ramp at this location since it does not affect the bottleneck area. The vehicle inputs at upstream station are the same as Equation (7.28) and we assume the following distribution of vehicle flows

- 02A to 04A: 100%.
- Off-ramp: 15% of the vehicle flow will exit from the two-lane off-ramp.
- On-ramp to the freeway segment: 25% of the vehicle flow will enter the freeway system through on-ramp (different flow distribution will be tested in the experiment).

With respect to the above simulation outputs, we run the proposed method 50 times. Figure 7.9 shows the estimation results from one experiment. Compared with the basic VRI, the proposed method provides more reliable estimates of the mean travel time. In general, the bottleneck effect cannot be detected through the average speed at upstream and downstream stations, which means that the inter-period/temporal adjusting cannot capture the traffic dynamics (congestion) well. Therefore the number of iteration steps of iterative VRI would increase accordingly (see Figure 7.9).



Figure 7.8: Merge and Diverge along the freeway segment

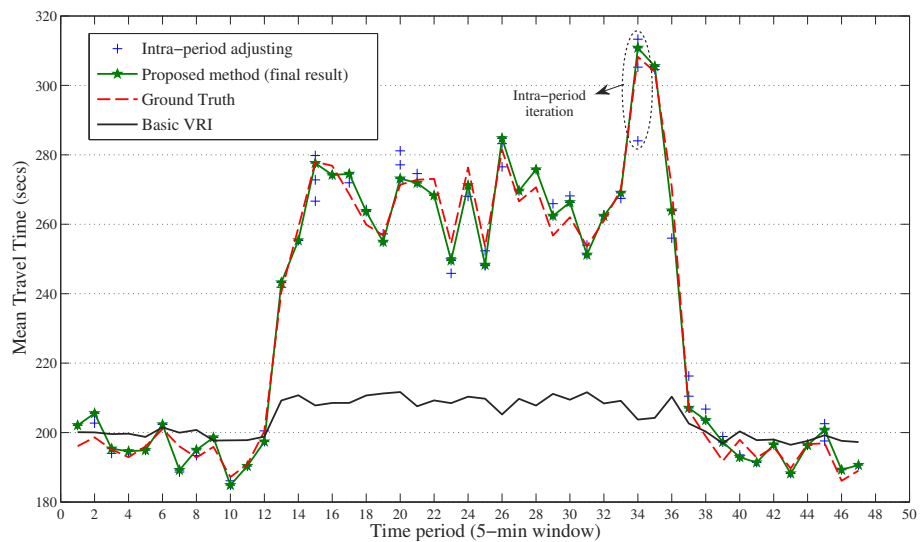


Figure 7.9: Performance of the proposed method (on-ramp vehicle flow distribution: 25%)

Table 7.2 also shows the performance of the improved VRI system under different vehicle flow distributions (i.e. on-ramp vehicle flow distribution). Since the test site is a freeway

corridor with on-/off-ramps, the vehicle arrives at upstream station may not necessarily appear at downstream. Also, some vehicles may enter this corridor through the on-ramp. Thus, it is expected that the matching accuracy of the proposed method is relatively lower. With the increase in the vehicle flow from on-ramp, the performance would gradually decay. However, it should be noted that the proposed method can still perform well against the bottleneck effect.

Table 7.2: Performance of the proposed method with different vehicle flow distributions

On-ramp vehicle flow distribution (%)	Performance indices	
	RMSE (secs)	MAPE (%)
15%	3.62	1.3%
25%	5.50	1.9%
35%	5.54	1.8%
50%	9.42	2.8%

7.5.5 Performance evaluation under non-recurrent traffic congestion

As the non-recurrent congestion is largely produced by traffic incidents, this research will investigate the performance of the proposed method under traffic incidents. The test site is also a three-lane closed segment (between 08A and 10A) and with the same vehicle inputs as Equation (7.28). To mimic the situation of incident happening, a parking lot locating at lane 1 (2 kilometers away from the upstream station) is utilized to simulate the incident vehicle (see Figure 7.10). When incident happens (i.e. incident starts from 90 minutes), a vehicle would stop in the parking lot and the partial route is activated to simulate the driving behavior under incident condition.

The proposed algorithm is further tested with different incident durations (e.g. 10 min, 15 min, 20 min and 30 min). Due to the unpredictability of the traffic incidents, the inter-period adjusting cannot generate a suitable time window. Therefore, it is expected that the steps of intra-period/temporal iteration would increase significantly, especially when traffic incident occurs. Figure 7.11 shows the mean travel time estimates from one experiment when incident duration is 10 minutes. It is observed that the mean travel time increases sharply during time period 20 (i.e. from 100 min to 105 min). And accordingly, the number of iteration steps of iterative VRI during this time period increases significantly. Figure 7.12 also illustrates the adjustment of the time window constraint for each iteration step. On the other hand, the basic VRI system cannot adapt well to the sudden

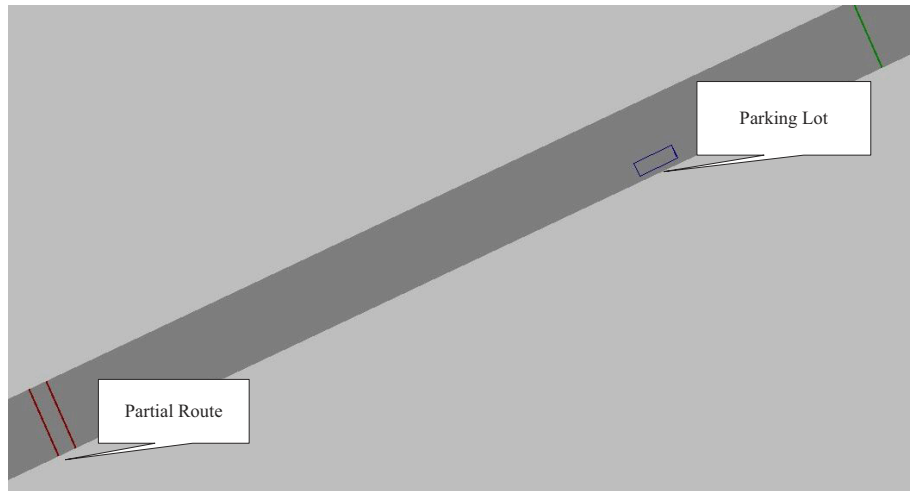


Figure 7.10: Incident simulation

changes in traffic condition when incident happens (See Figure 7.11). Due to the fixed time window constraint, the matching accuracy of basic VRI drops to 0% during time period 20, which eventually leads to a totally unreliable estimate of the mean travel time.

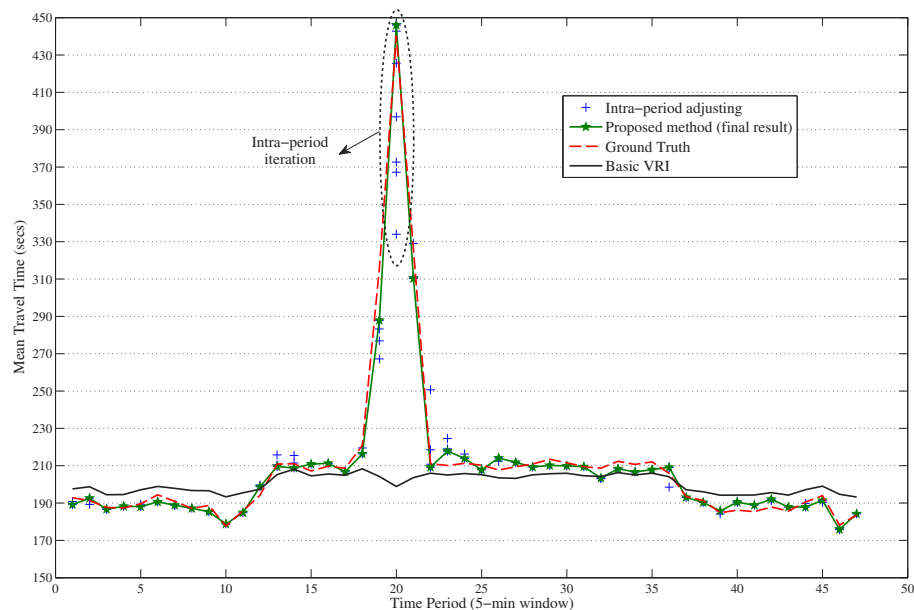


Figure 7.11: Performance of the proposed method (incident duration: 10 min; starts from 90 min)

Parallel to the previous experiments, we also run the method 50 times based on the simulation outputs for different incident durations (e.g. 10 min, 20 min and 30 min). The detailed estimation results are shown in Table 7.3. With the increase in incident durations,

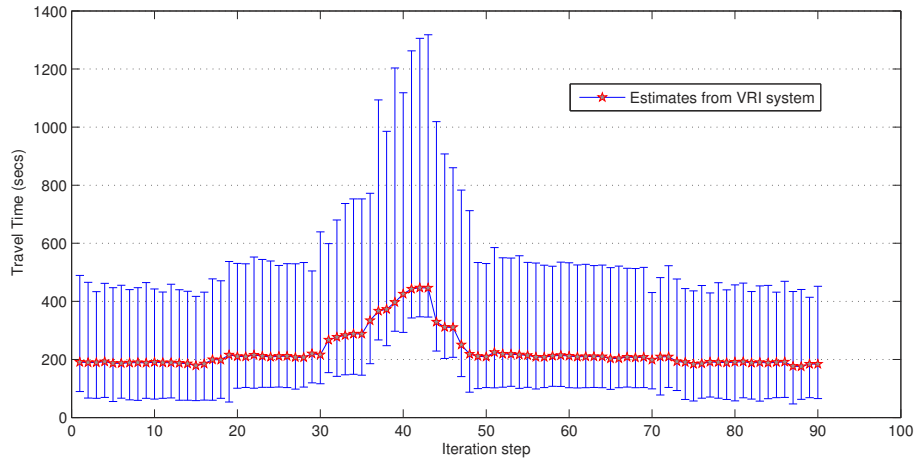


Figure 7.12: Adjustment of time window constraint

the RMSE and MAPE increase as well. With the time propagation, it is also observed that the variance of travel time increases dramatically (period 21 and 22). The "abnormal" vehicle (seriously delayed by the incident at lane 1) and those normal vehicles may arrive at downstream during the same time period. In this case, it renders a heavy burden on the processing of the improved VRI system (e.g. larger time window, more candidate vehicles and of course low matching accuracy). Therefore the results shown in Table 7.3 are reasonable.

Table 7.3: Performance of the proposed method with different incident durations

Incident durations (min) (%)	Performance indices	
	RMSE (secs)	MAPE (%)
10 min	5.61	1.5%
20 min	22.41	2.3%
30 min	25.63	2.8%

7.6 Conclusion remarks

This chapter aims to develop an improved VRI system based on the basic VRI to estimate the real-time travel time under traffic demand and supply uncertainty. A self-adaptive time window component (e.g. temporal adaptive time window and iterative VRI) is introduced into the basic VRI system to improve its adaptability against the potential significant changes in traffic conditions. Also, the associated post-processing technique (i.e. thresholding based on matching probability and stratified sampling based on vehicle type) is

employed to identify and rule out the erroneous travel time data. The proposed method is evaluated by conducting various representative simulation tests. Some performance indices such as RMSE and MAPE are also introduced to quantify the performance of this method.

Further research will be focused on the real-world application of this proposed method. It is undeniable that the video image processing (VIP) systems are subject to the effects of inclement weather (e.g. rain, snow) and illumination changes. Under these circumstances, the quality of the video image will decrease dramatically and hence compromise the effectiveness of vehicle feature extraction. During evening hours, the vehicle may still be partially identified by detecting the vehicle headlight and taillight. But the color information and vehicle type may not be obtained from the image. In this case, improving the external lighting condition at each station may be a promising way for vehicle feature extraction.

As validated by the simulated tests, the proposed VRI system for travel time estimation performs well under different scenarios (e.g. recurrent traffic congestions, freeway bottlenecks and minor traffic accidents). However, it is noteworthy that the proposed method may not work well under extremely abnormal traffic conditions (e.g. severe traffic accident with longer incident duration). As explained in Section 7.5.5, the longer incident duration would inevitably lead to a larger time window, low matching accuracy of the proposed VRI system, and hence unreliable travel time estimator. Therefore, future efforts should be dedicated to overcome these drawbacks. As the lane blocking caused by incidents would produce significant impact on the travel time experienced by the vehicles at different lanes, one possible way is then to perform stratified sampling based on vehicle lane position.

Chapter 8

Iterative VRI system with spatial-temporal adaptive time window

This chapter aims to propose an improved iterative VRI system with spatial-temporal adaptive time window to estimate the dynamic travel time for each time period on the freeway with multiple segments. By fully utilizing the spatial and temporal traffic information along the freeway system, the time window for each segment could be adjusted in a more efficient and timely manner. In addition to exploring the temporal changes in traffic information, the shrinkage-thresholding method is employed to further integrate the spatial traffic information from other freeway segments (e.g. sudden changes in travel time estimators on other freeway segments). The proposed iterative VRI system with spatial-temporal adaptive time window is tested on a freeway with two consecutive segments in Bangkok, Thailand. The preliminary results justify the potential advantages of the proposed VRI system over the original one proposed in Chapter 7 for capturing serious non-recurrent traffic congestions.

8.1 Introduction

Due to the stochastic and dynamic nature of traffic network (Fu and Rilett, 1998), travel time may exhibit stochastic and time-variant (dynamic) behavior (see Section 2.1.1), which imposes a great challenge on the development of a robust VRI system for dynamic travel

time estimation. Since travel time is by nature stochastic, the mean value of travel time during a time period (e.g. 5-min period) would be the desired information for the development of advanced traveller information systems (ATIS) and advanced traffic management systems (ATMS). In this sense, the high matching accuracy of VRI would not be the major concern. A suitable post-processing (e.g. thresholding and sampling) technique would allow us to select those vehicles with "distinctive" features, from which a reliable mean travel time estimator could be obtained. To handle the time-variant travel time arising from the dynamic traffic conditions (e.g. recurrent and non-recurrent congestion), the flexible time window constraint is required for improving the self-adaptivity of basic VRI system. Based on the above-mentioned principles, an iterative VRI system with temporal adaptive time window constraint is proposed in Chapter 7. Despite its encouraging experimental results (see Section 7.5), the proposed VRI system still suffers from two limitations.

First, the proposed VRI system is specifically designed for a single freeway segment with two consecutive detectors. And accordingly, the time window adjustment is completed by exploring the temporal changes of traffic information (e.g. average traffic speed) observed on the single segment (i.e. temporal adaptive time window). For a freeway with multiple detectors (i.e. multiple segments), the strategy of time window adjustment may not be suitable as it fails to consider the additional spatial traffic information (e.g. traffic information on other freeway segments). Second, the proposed VRI system in Chapter 7 still cannot perform well for serious non-recurrent traffic congestions (i.e. caused by serious traffic incident with long duration). Although the iterative process (i.e. intra-period adjusting) of VRI is designed to capture the sudden changes in traffic conditions, the extremely long incident duration would disrupt the normal traffic flow and, hence, lead to an unreliable travel time estimator (see Section 7.5.5). The primary reason for this failure is that the temporal adjustment of time window cannot provide a suitable prediction of the mean travel time when serious traffic congestion occurs. Therefore, the strategy of time window constraint should be redesigned so that the derived VRI system can be practically applicable to the freeway with multiple detectors.

For a freeway with multiple detectors demonstrated in Figure 8.1, there are two consecutive detector pairs (two freeway segments), i.e. A-to-B and B-to-C. Naturally, the dynamic travel time on these two segments (i.e. segment AB and BC) can be obtained by performing the VRI system proposed in Chapter 7 independently to the associated detector pairs (e.g. detector pairs A-to-B and B-to-C). In this case, the adjustments of time window of VRI system for each detector pair are also independent. Although this approach appears

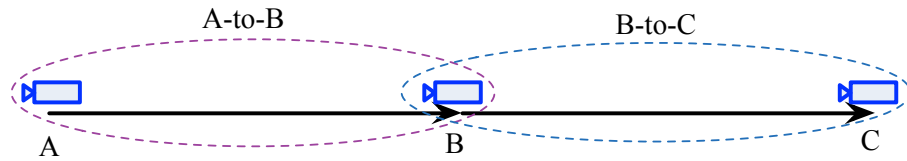


Figure 8.1: Freeway with multiple detectors

to be simple and straightforward, it fails to consider the temporal and spatial dynamics of travel time (Pan, 2012; Min and Wynter, 2011), which may provide potential advantages for time window adjustment. Due to the spatial-temporal evolution of traffic flow (e.g. freely flowing to congested conditions), travel time may be correlated (i.e. interdependent) in both space and time domains. A serious traffic congestion on segment BC in Figure 8.1 would incur a backward propagating congestion wave (Laval and Leclercq, 2010; Gentile et al., 2007; Zhang and Gao, 2012), which may eventually lead to the increase in travel time on segment AB in the future time period. In this case, the traffic information (e.g. sudden change in travel time) derived from VRI system on detector pair B-to-C may be potentially useful for the VRI system on detector pair A-to-B. A better mean travel time prediction may be achieved by considering the additional spatial information, which would yield a more reliable time window constraint and prior knowledge¹, and eventually improve the performance (i.e. the accuracy of mean travel time estimation) of the proposed VRI system under serious non-recurrent traffic congestions.

To sum up, this chapter aims to propose an enhanced self-adaptive VRI system for estimating dynamic travel time on freeway with multiple detectors. To be more specific, a spatial-temporal adaptive time window component is introduced to take full advantage of both temporal and spatial traffic information (e.g. vehicle spot speed and travel time estimators from spatially distributed VRI system). By exploring the temporal changes in vehicle's average speed, a preliminary prediction regarding the mean travel time for each time period is obtained. By integrating spatial information from other VRI system (e.g. sudden changes in travel time estimators), the time window constraint is further adjusted based on the shrinkage-thresholding method. The proposed iterative VRI system with spatial-temporal adaptive time window is then evaluated against the VRI system presented in Chapter 7 under serious non-recurrent traffic congestions.

The rest of the chapter is organized as follows. Section 8.2 briefly review the strategy of

¹The time window constraint and the prior knowledge can be derived from the prediction of mean travel time for each time period (see Section 7.4).

temporal adjustment of time window, which serves as the building blocks for this research. Section 8.3 presents the improved spatial-temporal adaptive time window component in which the detailed methodology, i.e. shrinkage-thresholding method, is described. In Section 8.4, simulated testes are carried out to evaluate the performance of the proposed system. Finally, we conclude this chapter in Section 8.5.

8.2 Basic temporal adaptive time window

Before proceeding to discuss the detailed spatial-temporal adaptive time window component, it is necessary to briefly review the strategy of temporal adjustment of time window. Mathematically speaking, a freeway with multiple detectors can be divided into $i = 1, 2, \dots, I$ sections, where I is the most downstream section, and $\mu_i(t)$ is the desired mean travel time of freeway section i for time period t . A natural response to this problem is to apply the original VRI system presented in Chapter 7 independently to each freeway section i and, accordingly, the mean travel time estimator $\mu_i(t)$ can be obtained. The original VRI is comprised of two critical components, i.e. iterative process of basic VRI and the temporal adaptive time window constraint (see Figure 8.2). Given the mean value $\mu_i(t)$ and the variance $\sigma_i(t)^2$ of the travel time distribution on freeway section i during time period t , a suitable travel time window $[Lb_i(t), Ub_i(t)]$ could be easily obtained. Assume that the travel time follows normal distribution $N(\mu_i(t), \sigma_i(t))$, then the tolerance interval with 95% confidence level can be utilized to define the time window, i.e.

$$[Lb_i(t), Ub_i(t)] \triangleq [\mu_i(t) - 1.96\sigma_i(t), \mu_i(t) + 1.96\sigma_i(t)] \quad (8.1)$$

By feeding the above-mentioned travel time window into the iterative VRI component (i.e. the block of intra-period time window adjusting in Figure 8.2), the basic VRI is performed iteratively in the hope of capturing the non-recurrent traffic congestions. Also, it is noteworthy that the success of iterative VRI is highly dependent on the initialization of time window (i.e. the block of temporal time window adjusting in Figure 8.2) for each time period. In this case, the temporal adaptive time window component is introduced as

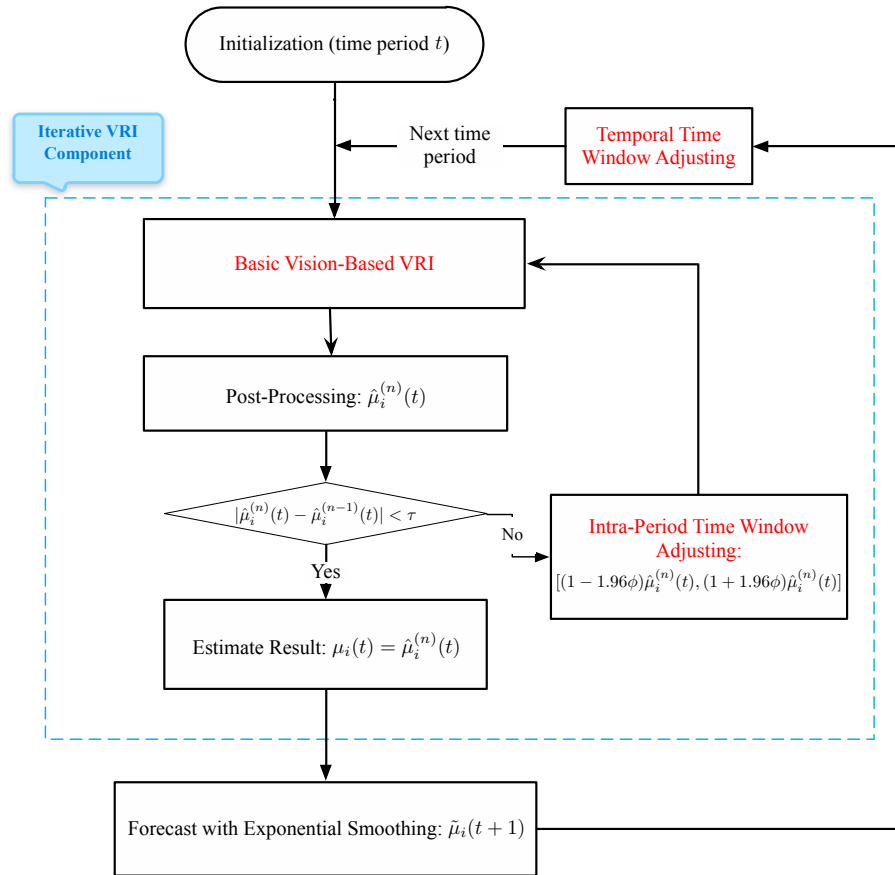


Figure 8.2: Temporal adjustment of time window

follows¹

$$\tilde{\mu}_i(t+1) = \tilde{\mu}_i(t) + \varphi(\mu_i(t) - \tilde{\mu}_i(t)) \quad (8.2)$$

$$\tilde{\mu}_i(t+1) = \frac{V_i^U(t) + V_i^D(t)}{V_i^U(t+1) + V_i^D(t+1)} \tilde{\mu}_i(t+1) \quad (8.3)$$

where $\tilde{\mu}_i(t+1)$ and $\tilde{\mu}_i(t)$ denote the forecasters of the mean travel time in time period $t+1$ and period t , respectively; φ represents the smoothing parameter which is calibrated from the historical data; $V_i^U(t)$ and $V_i^D(t)$ are respectively the average spot speed at upstream and downstream stations on freeway section i during time period t ; likewise, $V_i^U(t+1)$ and $V_i^D(t+1)$ are respectively the average spot speed at upstream and downstream stations during time period $t+1$. Equation (8.2) serves as a simple exponential prediction based on the estimates from previous steps, whereas Equation (8.3) is a correction step by exploring

¹The readers can refer to Section 7.4 for a more detailed explanation regarding the temporal adaptive time window constraint.

the temporal changes in the average spot speed.

This adjustment strategy based on the temporal information is proven to be effective for capturing recurrent traffic congestions due to exceeding traffic demand. For those unpredictable traffic scenarios (e.g. serious traffic incident), the time window may not be able to adjust in an efficient and timely manner (see Section 8.1). The primary reason is that the original VRI is performed independently (i.e. the system is isolated) for each freeway section without considering/utilizing the spatial traffic information on its neighboring freeway sections. In what follows, a novel spatial-temporal adaptive time window component is introduced such that the isolated VRI system on each freeway section can be connected and, hence, the performance of the proposed VRI system could be further improved.

8.3 Spatial-temporal adaptive time window

In this section, we first recall some basic facts on exploring the spatial and temporal correlations in travel time, which serves as the motivation for this research direction. Then we propose a shrinkage-thresholding method to integrate the spatial information such that a spatial-temporal adaptive time window constraint is generated. Finally, we present the overall framework of the improved iterative VRI system with spatial-temporal adaptive time window.

8.3.1 Spatial and temporal correlation in travel time

Over the last decades, a rich variety of traffic flow theories, such as car following model (Chandler et al., 1958), kinematic wave theory (Lighthill and Whitham, 1955), cell transmission model (Daganzo, 1994) and stochastic cell transmission model (Sumalee et al., 2011), have been developed towards modeling the propagation of traffic flow on a transport network, which eventually governs the network performance in terms of travel time (Szeto and Lo, 2006). In this sense, the spatial-temporal dependency of traffic flow (Yue, 2006) may give rise to the spatio-temporally correlated travel time. Based on the above-mentioned principle, several studies were also conducted to predict link travel time by utilizing the spatial-temporal correlation (e.g. Lam et al., 2005; Pan et al., 2013). As ex-

8.3 Spatial-temporal adaptive time window

plained in Section 8.2, the adjustment of time window is completed by roughly predicting the mean travel time for each time period. Therefore, a "better" prediction of travel time could be obtained by exploring the spatial-temporal correlation.

However, it should be noted that this research does not attempt to propose any traffic flow model to accurately predict the travel time. Instead we just revisit some basic facts on the propagation of traffic flow (i.e. especially the propagation of congestion wave), which may potentially contribute to our development of spatial-temporal adaptive time window:

- Backward propagation of congestion waves: In a traffic network, it is observed that traffic congestion (e.g. recurrent and non-recurrent) on freeway segment i may propagate backward to its upstream segment $i - 1$. Due to traffic queue build-up, the traffic flow may propagate backward with a certain speed (i.e. backward speed), which means that the travel time on segment $i - 1$ may increase in the near future. Figure 8.3 shows that ground truth travel time on two consecutive segments when incident occurs on segment 2. It is observed that the peak value of mean travel time on segment 2 occurs during time period 19, whereas the peak value on segment 1 appears after time period 20. In such a case, the time window on segment 1 can be adjusted in a more efficient and timely manner based on the traffic information (e.g. occurrence of congestion) on segment 2.

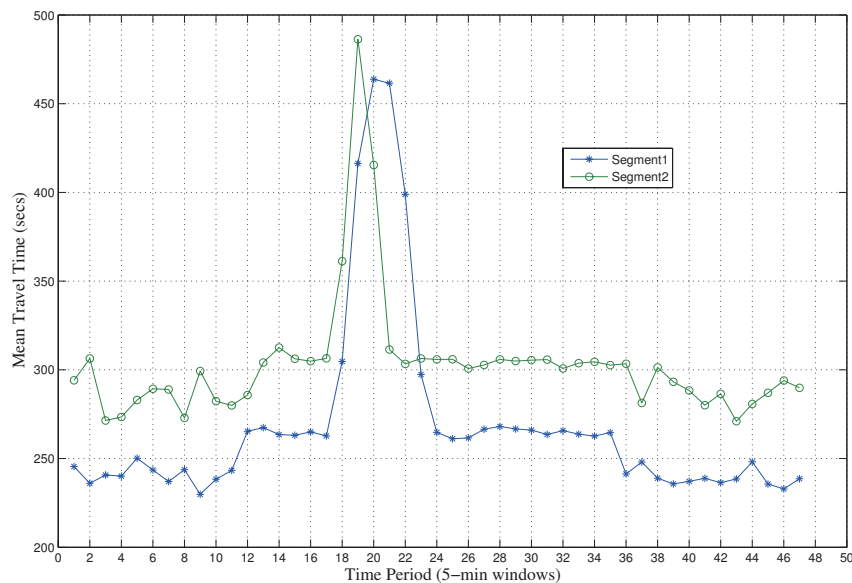


Figure 8.3: Ground truth travel time on two consecutive segments with incident happening on segment 2 (incident duration: 10 minutes)

- Dissipation of traffic congestion: Roughly speaking, traffic congestion dissolve will be observed through the decrease in the travel time. As shown in Figure 8.3, the traffic congestion on freeway segment 2 is gradually cleared from time period 20, whereas the traffic congestion on segment 1 is cleared from period 22. Therefore, this addition spatial information on segment 2 (e.g. clearance of congestion) can also be utilized for adjusting the time window on segment 1.
- Forward propagation of traffic flow with free-flow speed: Since the existing VRI system can perform well under free flow condition, we may not benefit from this information. Therefore, we will not consider the forward wave in the development of time window adjustment.

On the basis of the facts mentioned above, a heuristic approach (i.e. shrinkage-thresholding method) is then introduced to integrate the spatial information for generating a spatial-temporal adaptive time window constraint.

8.3.2 Shrinkage-thresholding method

The shrinkage/soft-thresholding method has already been widely studied and used in the field of image processing (e.g. Chambolle et al., 1998; Daubechies et al., 2004; Figueiredo and Nowak, 2003). In this chapter, the shrinkage-thresholding operator is employed for integrating the spatial information (i.e. spatial adaptive time window).

For each freeway segment i , the mean travel time $\mu_i(t + 1)$ during time period $t + 1$ is affected by the past traffic conditions on its neighboring segments (correlated in spatial domain), i.e. the traffic conditions on segment $i + 1$ during time period t (see Section 8.3.1). In addition, mean travel time $\mu_i(t + 1)$ is also dependent on its previous state (correlated in temporal domain). Therefore, the associated spatial and temporal adjusting factors, i.e. \mathcal{F}_{sp} and \mathcal{F}_{tm} , are introduced into the spatial-temporal adaptive time window component.

First, the equations (i.e. Equations (8.2) and (8.3)) for temporal adaptive time window are reformulated as follows

$$\tilde{\mu}_i(t + 1) = \tilde{\mu}_i(t) + \varphi(\mu_i(t) - \tilde{\mu}_i(t)) \quad (8.4)$$

$$\tilde{\mu}_i(t + 1) = \mathcal{F}_{tm} \tilde{\mu}_i(t + 1) \quad (8.5)$$

8.3 Spatial-temporal adaptive time window

where $\mathcal{F}_{\text{tm}} = \frac{V_i^U(t)+V_i^D(t)}{V_i^U(t+1)+V_i^D(t+1)}$ is the temporal adjusting factor. Second, the additional spatial factor \mathcal{F}_{sp} is then introduced based on a shrinkage-thresholding operator:

$$\mathcal{F}_{\text{sp}} = 1 + \Phi_{\kappa} \left(\frac{\mu_{i+1}(t)}{\mu_{i+1}(t-1)} - 1 \right) \quad (8.6)$$

where κ is the appropriate shrinkage value, and $\Phi_{\kappa} : \mathbb{R} \rightarrow \mathbb{R}$ is the shrinkage operator defined by

$$\Phi_{\kappa}(x) = \text{sgn}(x) \max(|x| - \kappa, 0) \quad (8.7)$$

where $\text{sgn}(x)$ is the sign function defined as follows:

$$\text{sgn}(x) = \begin{cases} -1 & \text{if } x < 0 \\ 0 & \text{if } x = 0 \\ 1 & \text{if } x > 0 \end{cases} \quad (8.8)$$

The rationale behind Equation (8.6) is as follows. If the mean travel time on segment $i + 1$ in current time period t is larger than that during the previous time period $t - 1$ (i.e. $\mu_{i+1}(t)/\mu_{i+1}(t-1) > 1$), then traffic congestion may potentially be generated and, consequently, be propagated backward, which also suggests that travel time on segment i will increase in near future, i.e. time period $t + 1$. In such a case, the shrinkage and thresholding process is performed (i.e. $\max(|x| - \kappa, 0)$ in Equation (8.7)). Since the congestion wave may have a relatively slower backward speed, the shrinkage step mentioned above is necessary. On the other hand, if the mean travel time on segment $i + 1$ in current time period t is smaller than that during the previous time period $t - 1$ (i.e. $\mu_{i+1}(t)/\mu_{i+1}(t-1) < 1$), the dissipation of traffic congestion on segment $i + 1$ may be observed and, accordingly, the travel time on segment $\mu_i(t + 1)$ will decrease.

To sum up, the spatial-temporal adaptive time window for segment i is expressed by the following equations:

$$\tilde{\mu}_i(t + 1) = \tilde{\mu}_i(t) + \varphi(\mu_i(t) - \tilde{\mu}_i(t)) \quad (8.9)$$

$$\tilde{\mu}_i(t + 1) = \mathcal{F}_{\text{sp}} \mathcal{F}_{\text{tm}} \tilde{\mu}_i(t + 1) \quad (8.10)$$

The overall framework for the proposed iterative VRI system with spatial-temporal adaptive time window constraint on freeway segment i is illustrated in Figure 8.4. First, the system will initialize a time period t , the associated travel time window constraint $[Lb_i(t), Ub_i(t)]$, and the corresponding *prior* probability. Then the iterative VRI com-

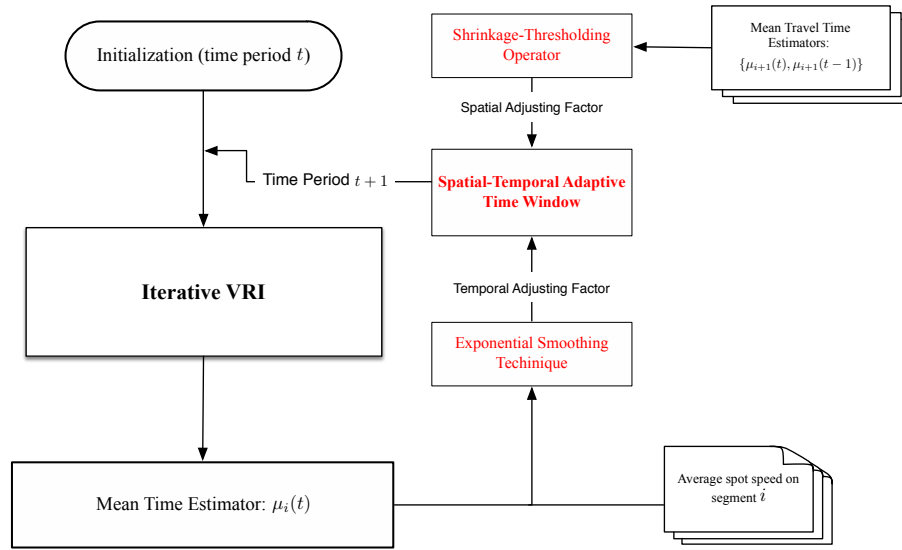


Figure 8.4: Overall framework of the proposed VRI system

ponent in Figure 8.4 will accept these initialized exogenous inputs and perform vehicle matching method repeatedly until the satisfactory travel time estimator $\mu_i(t)$ for time period t is obtained. By applying the proposed spatial-temporal adaptive time component, a new prediction regarding the mean travel time for time period $t + 1$ is obtained and, accordingly, the iterative VRI component will be activated again such that the mean travel time estimator $\mu_i(t + 1)$ will be produced.

8.4 Preliminary Results

To verify the effectiveness and feasibility of the proposed spatial spatial-temporal adaptive time window component, various simulation-based experiments are conducted. In this research VISSIM-based simulation model is devised to simulate freeway system (i.e. with two consecutive segments) operations under serious non-recurrent traffic congestions.

8.4.1 Simulation model configuration and calibration

Before presenting the experiments, the detailed procedures for simulation model development and calibration are introduced. The test site for this research is 34.9-kilometer-long

three lane freeway system in Bangkok, Thailand (see Figure 8.5). At each station a gantry-mounted video camera, which is viewed in the upstream direction, is installed, and two hours of video record were collected between 10 a.m. and noon on June 20, 2012. The frame rate of the video record is 25 FPS, and the still image size is 563×764. Two consecutive segments (i.e. the green section in Figure 8.5) are chosen for simulation model development: i) a 4.2-kilometer-long corridor with on-/off-ramps (i.e. between 02A to 04A), which is referred to as segment 1; ii) a 5.5-kilometer-long corridor with on-/off-ramps (i.e. between 04A to 06A), which is referred to as segment 2. The simulation model is then configured based on the exact roadway geometric feature, including the length of the segment, location of on/off-ramps, and the number of lanes. To guarantee realistic repre-

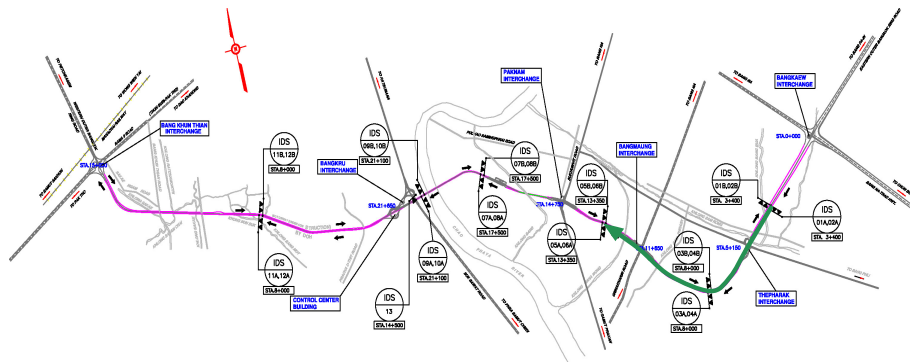


Figure 8.5: Test site in Bangkok, Thailand

sentation of the simulated experiments, the model calibration is required. As the detailed vehicle feature data are not readily obtainable from the raw video record, the intelligent video surveillance (IVS) is then employed for extracting the required information. Based on the video record collected at the test site, 1406 vehicles are detected at three camera stations (i.e. 02A, 04A and 06A) during the two-hour video record. These 1406 vehicles are then manually matched/reidentified by the human operators viewing the video record frame by frame. In other words, the sequential records of 1406 correctly matched vehicles are obtained and stored in the image database for further application.

8.4.2 Performance evaluation under serious non-recurrent traffic congestion

As this study is specifically designed to capture the non-recurrent traffic congestions caused by serious traffic incidents on freeway with multiple detectors (i.e. multiple seg-

ments), we will investigate the performance of the proposed method under traffic incidents with long incident durations. To mimic the situation of incident happening and the backward propagation of the congestion wave, a parking lot locating at lane 1 of Segment 2 (2 kilometers away from station 04A) is utilized to simulate the incident vehicle¹. When incident happens (i.e. incident starts from 90 minutes), a vehicle would stop in the parking lot and the partial route is activated to simulate the driving behavior under incident condition. The stochastic vehicle inputs of VISSIM-based simulation model are defined as follows:

$$Q = \begin{cases} 4000 \text{ veh/h,} & 0 \leq t \leq 60 \text{ min;} \\ 7000 \text{ veh/h,} & 60 \leq t \leq 120 \text{ min;} \\ 8000 \text{ veh/h,} & 120 \leq t \leq 180 \text{ min} \\ 4000 \text{ veh/h,} & 180 \leq t \leq 240 \text{ min;} \end{cases} \quad (8.11)$$

The vehicle inputs are chosen such that all the traffic rates ranging from free-flow to congested can be activated. The proposed method is further tested with different incident durations (e.g. 10 min, 20 min, 30 min).

As demonstrated in Section 7.5.5, the performance of the original method (i.e. temporal adaptive time window) would gradually decrease with the increase in incident durations (see Table 7.3). By incorporating the improved spatial-temporal adaptive time window component, it is expected that the proposed VRI may produce a more accurate travel time estimator. Figure 8.6 shows the mean travel time estimates of segment 1 from one experiment when incident duration is 20 minutes. It is evident that the original method (see Chapter 7), which is solely based on the temporal adjustment of time window, cannot adapt well against the dramatic change of traffic conditions, whereas the proposed method with spatial-temporal adaptive time window can still perform well. The additional spatial information of its downstream segment (i.e. segment 2) enable us to obtain a "better" prediction of the mean travel time for segment 1, which eventually lead to a more accurate travel time estimator. The similar results can also be found when the incident duration is 10 minutes (see Figure 8.7). Note that the primary advantage of the proposed VRI in this chapter over the original one in Chapter 7 is that it can capture the serious non-recurrent traffic congestion during the congestion period (e.g. time period 22 in Figure 8.6, and time period 21 in Figure 8.7). For the other time periods in which the traffic conditions remain stable, the performances of the methods proposed in Part III of this thesis are "equally" good. Therefore, the potential advantages of the proposed VRI system in this chapter can-

¹The readers can refer to Section 7.5.5 for a more detailed introduction regarding the simulation model for traffic incident.

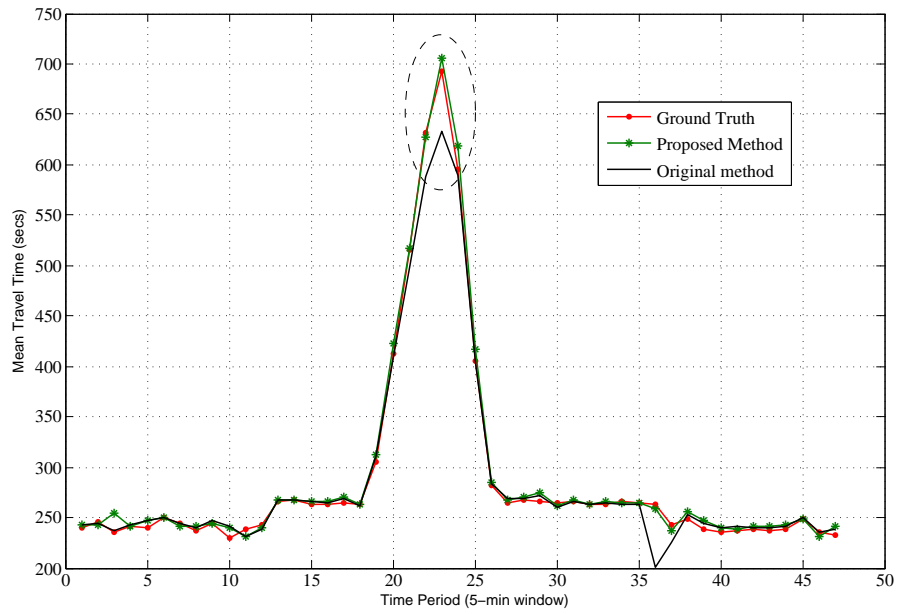


Figure 8.6: Performance of spatial-temporal adaptive time window (incident duration: 20 minutes; Segment 1)

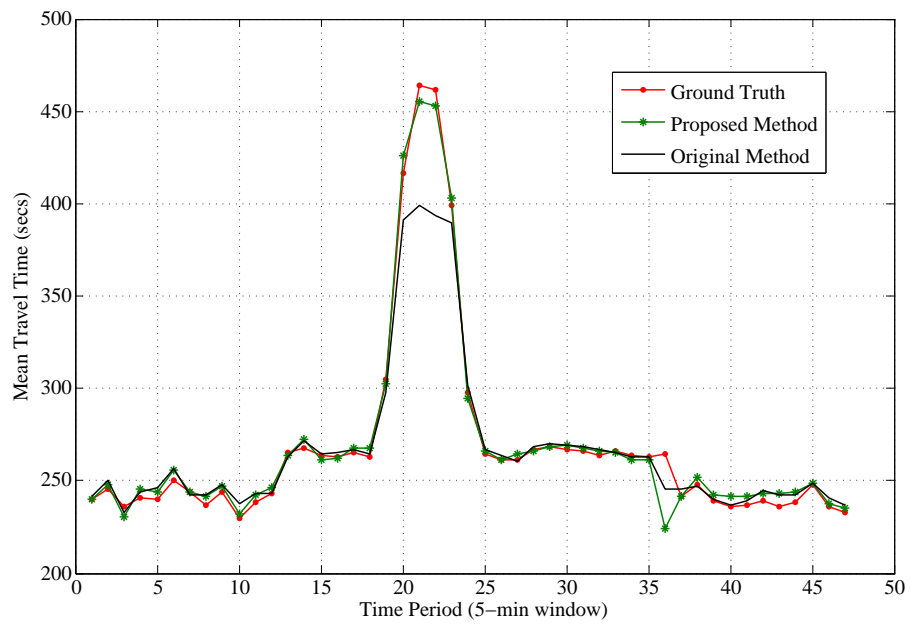


Figure 8.7: Performance of spatial-temporal adaptive time window (incident duration: 10 minutes; Segment 1)

not not reflected in the root mean square error (RMSE) and the mean absolute percentage

error (MAPE)¹.

In contrast to segment 1, segment 2 does not have its own downstream segment, which means that there is no available spatial information that can be utilized. In this case, the spatial-temporal adaptive time window component is equivalent to the original one proposed in Chapter 7 and may not work well for segment 2 (see Figure 8.8).

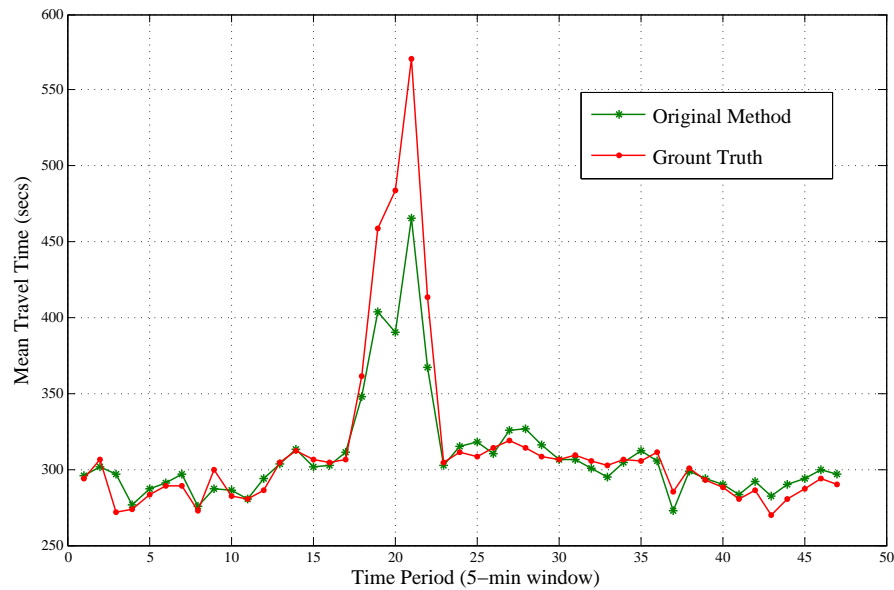


Figure 8.8: Performance of spatial-temporal adaptive time window (incident duration: 20 minutes; Segment 2)

8.5 Conclusion remarks

This chapter extends the self-adaptive VRI system proposed in Chapter 7 to a more general case where multiple detectors exist. An improved spatial-temporal adaptive time window component is introduced to take full advantage of both temporal and spatial traffic information such that the time window can be adjusted in a more efficient and timely manner. In addition to exploring the temporal changes in traffic information, the shrinkage-thresholding method is employed to further integrate the spatial traffic information from other freeway segments (e.g. sudden changes in travel time estimators on other freeway

¹The detailed definition of RMSE and MAPE can be found in Section 7.5.3.

segments). The proposed iterative VRI system with spatial-temporal adaptive time window is tested on a 9.7-kilometer-long freeway with two consecutive segments in Bangkok, Thailand. The preliminary results justify the potential advantages of the proposed method for capturing serious non-recurrent traffic congestions.

Part IV

Conclusions and future works

Chapter 9

Summary of the thesis and future research topics

9.1 Summary of the thesis

The main objective of this study were to develop a self-adaptive vision-based vehicle reidentification system for dynamic freeway travel time estimation. A brief summary of this thesis is given as follows.

Chapter 2 described the basic problem statements (e.g. travel time estimation problem, vehicle reidentification and automatic incident detection) and reviewed the relevant literatures on these problems.

As this study focused on utilizing the emerging video surveillance system, a comprehensive review on this sensing technology was presented in Chapter 3. Various image processing techniques involved in intelligent video surveillance (IVS) for vehicle feature extraction (e.g. vehicle color, length and type) were also discussed. Two research directions (e.g. improving the matching accuracy, and introducing self-adaptive time window component) were pointed out, which eventually lead to the work presented in Part II and Part III.

Within the second part of this thesis, a basic vision-based VRI system was developed under

static traffic condition. Chapter 4 provided a comprehensive framework regarding the basic VRI system. The main contributions of this chapter were as follows. First, IVS was investigated for the purpose of extracting a rich body of disaggregate data such as vehicle color, type, and size. Second, a probabilistic fusion strategy was devised to integrate the obtained vehicle feature data. Specifically, the logarithmic opinion pool (LOP) approach was utilized for generating an overall *posterior* probability for vehicle matching decision-making. Third, the vehicle signature matching was then formulated as a combinatorial optimization problem and solved by the minimum-weight bipartite matching method. As a by-product of the basic VRI system, various traffic data including vehicle counts, speed, and travel time, could be derived. The approach was tested on a 3.6-kilometer segment of the freeway system in Bangkok, Thailand. The overall reidentification accuracy was about 54.75%. For travel time estimation purpose, the result shows that the travel time distribution estimated by our system is reliable under static traffic conditions.

Due to its potential for efficient vehicle tracking in the freeway system, the basic VRI system was further designed and improved for automatic incident detection purpose. A VRI based incident detection algorithm under free flow condition was presented in Chapter 5. The main contributions of this chapter were as follows. First, an enhanced vehicle feature matching technique was adopted in the VRI component for explicitly calculating the matching probability for each pair of vehicles. Second, A screening method based on ratio of the matching probabilities was introduced for vehicle matching decision-making such that the incident vehicle could be identified in a timely and accurate manner. The performance of the proposed algorithm was evaluated against the classical vehicle count approach in terms of mean time-to-detect and false alarm rate. Also, the real-world case studies were carried out to demonstrate the potential advantages of the proposed algorithm for reducing the incident detection time.

To handle the task of vehicle reidentification over multiple detectors, an additional hierarchical Bayesian matching model was proposed such that the vehicle matching accuracy could be further improved (see Chapter 6). The main contributions of this chapter were as follows. First, a hierarchical matching model was proposed such that vehicle matching over multiple detectors could be treated as an integrated process. A hierarchical tree structure was also employed for representing the matching result over multiple detectors. Second, the associated hierarchical Bayesian model was introduced to describe the spatial dependencies between vehicle feature distances, which would yield a more reliable probabilistic measure for matching decision-making. The proposed method was then tested on

a 9.7-km freeway segment with three detectors. The results suggested that the hierarchical matching method outperforms the pair-wise VRI matching method.

For the dynamic traffic conditions (i.e. the third part of this thesis), an iterative VRI system with temporal adaptive time window constraint was proposed to improve its self-adaptivity in response to the substantial changes in traffic conditions (see Chapter 7). The main contributions of this chapter were as follows. First, a temporal adaptive time window component was introduced into the basic VRI system. Also, the post-processing technique was performed on the raw results produced by basic VRI to rule out the erroneous travel time and, hence, obtain a more reliable mean travel time estimator. Second, an appropriate iterative process was developed to perform basic VRI iteratively with different exogenous (e.g. time window constraint and prior knowledge) such that the non-recurrent traffic congestions can be captured. Various numerical tests were conducted to demonstrate the application of the proposed VRI system under dynamic traffic conditions. The first simulation test investigated the feasibility of utilizing the proposed VRI to estimate the mean travel time for a closed freeway segment containing recurrent traffic congestions. In the second simulation was evaluated on a freeway corridor with on- and off-ramps. The experimental results suggested that the proposed method performs well under bottleneck effect. The third simulation test was then conducted to test the performance of the algorithm under non-recurrent congestions.

In Chapter 8, a further improved self-adaptive VRI system with spatial-temporal adaptive time window constraint was proposed to handle the serious non-recurrent traffic congestions (e.g. occurrence of a traffic accident with extremely long incident duration) on a freeway system with multiple segments. By fully utilizing the spatial and temporal traffic information along the freeway system, the time window for each segment could be adjusted in a more efficient and timely manner. In addition to exploring the temporal changes in traffic information, the shrinkage-thresholding method was employed to further integrate the spatial traffic information from other freeway segments (e.g. sudden changes in travel time estimators on other freeway segments). The proposed iterative VRI system with spatial-temporal adaptive time window was tested on a freeway with two consecutive segments in Bangkok, Thailand. The preliminary results justified the potential advantages of the proposed VRI system for capturing serious non-recurrent traffic congestions.

9.2 Future works

The future works will concentrate on the following aspects with special attention paid to the network-wide travel time estimation using partial VRI data.

9.2.1 Extension of the VRI system to a network case

As explained in Chapter 4 and Appendix 4.A, the complexity of the vehicle matching problem would increase dramatically when it comes to the network case where multiple video cameras exist. Although the typical bipartite matching method still can be applied to reidentify the vehicles simultaneously across the whole network, the extremely long computational time would render it impractical for application in large-scale network.

In view of the above mentioned problems, we will propose a priority-based searching scheme for solving the VRI problem in a network with multiple cameras. Unlike the corridor case, each upstream camera has a number of corresponding downstream cameras (one-to-many) in the network. The priority-based searching scheme serves as a strategy to perform VRI iteratively across each pair of cameras. For the one-to-many (downstream) camera network, we will assign a priority value to each downstream camera based on the historical travel time (camera-to-camera) data and covariance information (e.g. path-flow information). In general, the camera with a shorter travel time will be assigned a relatively higher priority value. To be specific, once a group of vehicles are detected at upstream camera, the proposed search method will be utilized to find the downstream camera with the highest priority value. The basic VRI system (see Chapter 4) will be performed on this pair of detectors. The matching result together with the matching accuracy will be generated. By comparing the matching accuracy with the predefined threshold value (i.e. typical threshold accepting mechanism), we will be able to determine whether vehicles are re-identified at the downstream site. After eliminating the matched vehicles and the respective downstream camera, the priority value of the remaining downstream cameras will be updated according to the matching result.

By performing the proposed searching method iteratively, we would be able to handle the network case with multiple detectors more efficiently.

9.2.2 Network-wide travel time estimation using partial VRI data

It is noteworthy that the proposed self-adaptive VRI systems in this thesis were developed to estimate detector-to-detector journey time. As a natural and necessary extension, the network-wide/link travel time estimation is required for the further development of Intelligent Transportation Systems (ITS). However, the task of network-wide travel time estimation is far from straightforward. The primary reason is that the network-wide travel time estimation is a highly under-specified problem, where the number of traffic detectors (e.g. AVI detector, image-based sensors) is typically much less than the number of unknown parameters of interest (Castillo et al., 2013). Due to the complex topological structure of the traffic network and the limitation of resources in practice, it is not possible for us to install the detectors at all key locations. Therefore, in order to resolve this identifiability problem, an equilibrium assignment component is included and the link travel time estimation is formulated as a bi-level optimization problem (e.g. Lam et al., 2005; Lam et al., 2010). In these models, the upper level model is generally a least square problem for fitting the model outputs with the observed journey times on partial links/paths, whereas the lower level models are various kinds of equilibrium assignments. Tam and Lam (2008) estimated the network-wide travel times with AVI data on partial links by exploring the variance-covariance relationships between the link travel times. It should be noted that the success of the above mentioned algorithms relies on knowing the exact travel times on partial links and/or paths. However, in practice, there could be multiple paths between two detectors and thus the specific path travel time cannot be deduced directly from the AVI system.

In view of this, we attempt to address these issues using the maximum likelihood based approach to estimate the static link travel time from the VRI data (i.e. detector-to-detector journey time data). The proposed algorithm does not require the additional traffic information on specific links/paths (i.e. partial link/path travel time) and, hence, is expected to be more suitable for real-world application. As a classical statistical approach, maximum likelihood estimation (MLE) has also been evaluated with several other applications, such as the OD estimation in transport networks (e.g. Hazelton, 2000; Parry and Hazelton, 2012) and communication network tomography (e.g. Castro et al., 2004; Vardi, 1996). The basic principle of MLE is quite straightforward. Given a set of detector-to-detector travel times (obtained from VRI data), a statistical model is proposed to describe the uncertainty of these observed data. The MLE problem is then formulated as to find the underlying parameter values (i.e. mean/variance of the link travel time) which would be most likely

(i.e. maximum likelihood) to give rise to the detector-to-detector travel times. Although the theoretic basis is simple, a number of detailed issues need to be carefully considered during the development of MLE method.

Principal amongst them is that we should propose an appropriate and flexible statistical model to represent the detector-to-detector travel times. As a matter of fact, different topological structures of the network requires different statistical models. For the most simple corridor case, an univariate normal distribution would be able to represent the random journey times. However in practice multiple routes may exist between the two detectors (i.e. two-detectors-parallel-routes situation), and the route travel time cannot be observed directly without knowing the detailed routing information. To this end, an indicator ("missing data") variable will be introduced to represent the actual route choice of each vehicle, and the joint distribution of the missing data and observed journey time data will be derived.

Following the model formulation, we should also consider the identifiability problem when it comes to the network case. As one of the most simple network, i.e. two-detector-with-common-link, the link travel times are unidentifiable (i.e. non-unique) by solely using the detector-to-detector travel time. This lack of identifiability is partially due to the rank deficiency of the incidence matrix, and there is no unique mapping of the route travel time to the link travel time. The other reason is that we haven't fully exploited the available VRI data (i.e. vehicle arrival time). As part of the VRI data, the arrival time of each vehicle provides an opportunity to collect more informative statistics, and to some extent it could resolve the problem of identifiability.

9.2.2.1 Notation and model assumption

To facilitate the representation of the basic idea, the notations are listed as follows unless otherwise specified:

$\mathbf{G} = (\mathcal{N}, \mathcal{A})$	A traffic road network in which \mathcal{N} is the node sets and \mathcal{A} the link (arc) set.
N	Total number of DD journey times that could be observed during a predefined observational time window.
$y_i, \quad i = 1, 2, \dots, N$	The observed detector-to-detector travel times of vehicle i .
$t_i, \quad i = 1, 2, \dots, N$	The observed arrival time of vehicle i at the upstream detector.
$\boldsymbol{\mu} = \{\mu_1, \mu_2, \dots, \mu_R\}$	The vector of mean travel time on each route between two detectors.
$\boldsymbol{\xi} = \{\xi_1, \xi_2, \dots, \xi_A\}$	The mean travel time on each link in a road network.
β	The parameter of the logit route choice model.

In general, we make the following assumptions:

- A1. The link travel time estimation problem is considered in a static framework. In other words, the common length of the observed time period is sufficient long so that we may ignore the possibility of journeys that is only partially completed during the observational time window.
- A2. Vehicles travelling from Detector A to Detector B choose independently of one another which of the R available routes to follow. Given the N vehicles observed at detector A, the probability of any randomly selected vehicle choosing to travel on route r is given by a discrete choice model based on the so-called route choice parameter β . To simplify the model formulation, we specifically assume that this probability of a given vehicle choosing route r between two detectors is given by a logit model solely based on the mean route travel times $\boldsymbol{\mu} = \{\mu_1, \mu_2, \dots, \mu_R\}$:

$$p_r(\boldsymbol{\mu}; \beta) = \frac{\exp(-\beta\mu_r)}{\sum_{s=1}^R \exp(-\beta\mu_s)} \quad (\beta > 0; r = 1, 2, \dots, R) \quad (9.1)$$

- A3. The detector-to-detector journey times for vehicles using route r follows a normal distribution (independent between routes), which is independent of the arrival time at the Detector A. By introducing an additional assumption on mean-variance relationship: $\sigma_r^2 = \theta\mu_r$, we may obtain this probability density function:

$$f(y_i; \mu_r) = \frac{1}{\sqrt{2\pi\theta\mu_r}} \exp\left(-\frac{1}{2} \frac{(y_i - \mu_r)^2}{\theta\mu_r}\right) \quad (9.2)$$

9.2.2.2 Two-detector-parallel-route situation

Consider a two-detector-parallel-route network (as shown in Figure 9.1), in which two camera detectors are mounted at location A and B, respectively. R is denoted as the number of parallel routes that exist between the two detectors. Let $\mathbf{y} = (y_1, y_2, \dots, y_N)$ represent the random vector of observed detector-to-detector journey times. Without knowing the exact routing information of each vehicle, it is difficult for us to propose a statistical model to describe the stochastic behavior of random vector \mathbf{y} . In view of this, we introduce

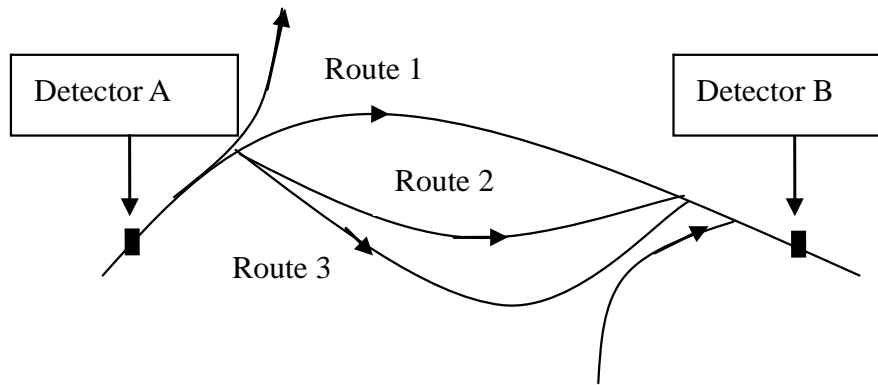


Figure 9.1: Conceptual network

the following unknown indicator variables to represent the actual route choice:

$$z_{ir} = \begin{cases} 1 & \text{if } i^{\text{th}} \text{ vehicle used route } r \\ 0 & \text{if this vehicle used a route other than } r \end{cases} \quad (9.3)$$

where $i \in \{1, 2, \dots, N\}$, and $r \in \{1, 2, \dots, R\}$. Therefore we can think of there being two kinds of random variables, i.e., the random vector $\mathbf{z}_i = (z_{ir}, r = 1, 2, \dots, R)$ that tells us which route vehicle i travels on, and the y_i variable which tells us the journey time experienced by vehicle i between detectors. The joint knowledge of all the (y_i, \mathbf{z}_i) variables provides an opportunity to track all the vehicles along the routes. Let (y_i, \mathbf{z}_i) denote the "complete information" of each vehicle. Therefore, the joint probability density/mass function (pdf) of the "complete information" (y_i, \mathbf{z}_i) , given the model parameters which we collect together in vector form as $(\beta, \theta, \boldsymbol{\mu})$, is given by:

$$q(y_i, \mathbf{z}_i; \beta, \theta, \boldsymbol{\mu}) = \prod_{r=1}^R \left\{ p_r(\boldsymbol{\mu}; \beta) \frac{1}{\sqrt{2\pi\theta\mu_r}} \exp\left(-\frac{1}{2} \frac{(y_i - \mu_r)^2}{\theta\mu_r}\right) \right\}^{z_{ir}} \quad (9.4)$$

It should be noted that the indicator variable z_{ir} is not observable in practice. By summing this probability distribution over all possible combinations \mathbf{z}_i would yield the probability

density function of observing the "incomplete data" y_i :

$$P(y_i; \beta, \theta, \boldsymbol{\mu}) = \sum_{\mathbf{z}_i} q(y_i, \mathbf{z}_i; \beta, \theta, \boldsymbol{\mu}) \quad (9.5)$$

In this parallel-route situation, we assume that the observation of each individual detector-to-detector journey time $\{y_i, i = 1, 2, \dots, n\}$ is mutually independent. Thus the incomplete-data likelihood of observing the random sample $\{y_i, i = 1, 2, \dots, n\}$ is given by:

$$L(\beta, \theta, \boldsymbol{\mu}; \mathbf{y}) = \prod_{i=1}^N P(y_i; \beta, \theta, \boldsymbol{\mu}) \quad (9.6)$$

Within the framework of maximum likelihood estimation, this estimation problem is equivalent to finding the parameter values which maximize the likelihood function (9.6), i.e.

$$\max_{(\beta, \theta, \boldsymbol{\mu})} L(\beta, \theta, \boldsymbol{\mu}; \mathbf{y}) = \prod_{i=1}^N P(y_i; \beta, \theta, \boldsymbol{\mu}) \quad (9.7)$$

Obviously, the direct maximization of (9.6) would yield the estimator $(\beta, \theta, \boldsymbol{\mu})$. To improve the computational efficiency, the well-known expectation and maximization (E&M) algorithm will be utilized to solve this MLE problem.

Since our ultimate goal is to estimate the link travel time in a network, we need to generalize the model formulation so as to apply to a link-based specification as opposed to a route-based one. A natural first step would be to assume that the travel time on link a follows a Normal distribution $N(\xi_a, \theta\xi_a)$, for $a = 1, 2, \dots, A$ (mutually independent between links). If the 0/1 indicator δ_{ar} takes the value 1 if link a is part of route r , and 0 otherwise, then this amounts to assuming that the travel time on any route r is also a normal distribution, with

$$\text{mean value } \mu_r = \sum_{a=1}^A \delta_{ar} \xi_a, \quad \text{variance } \sigma_r = \sum_{a=1}^A \theta \delta_{ar} \xi_a. \quad (9.8)$$

By substituting (9.8) into the incomplete-data likelihood function, we may also obtain a likelihood function of new parameters, as $L(\beta, \theta, \boldsymbol{\xi}; \mathbf{y})$. Accordingly, the link travel time estimator can be obtained by maximizing this new likelihood function.

Although this simple extension appears to be sound at first glance, the problem of identifiability (i.e. non-uniqueness) of the parameter estimates arises under this statistical model.

For the parallel route situation mentioned above, this problem is trivial since there is a unique mapping of the route travel time to link travel time. However, for a more complicated network case (see Figure 9.2), there will be an infinity of solutions for the maximum likelihood estimation. Note that we can still treat it as a parallel-route situation and hence estimate the associated route travel time. Unfortunately, this model is incapable of estimating the link travel time due to the rank deficiency of incidence matrix. As shown in Figure 9.2, link 1 is a common link between the two routes. It is quite reasonable for us to assume that the travel times on these two routes are correlated with each other because of the common link. Nevertheless, the statistical model mentioned above fails to take into account the correlation factor between the routes. To overcome this difficulty and fully exploit the collected VRI data, the additional platoon information (i.e. arrival time data) will be utilized for the purpose of link travel time estimation.

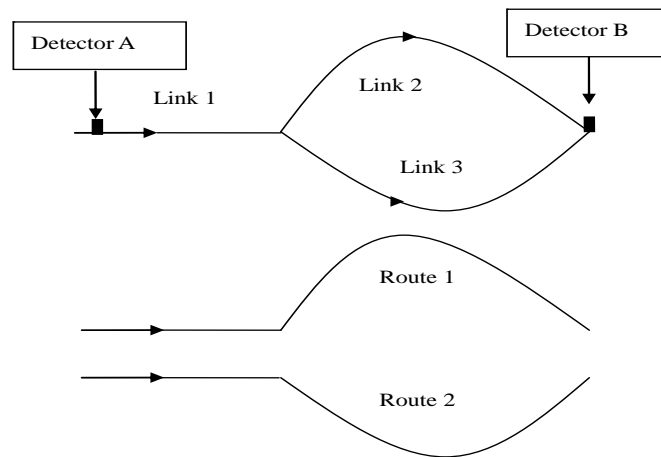


Figure 9.2: Two-detectors-with-common-links network

9.2.2.3 Two-detector-with-common-link situation

In this part, we are going to estimate the link travel time by explicitly considering the correlation (i.e. covariance) factor between the route travel times. Recall that the VRI data consists of two parts: a set of journey times $\{y_i : i = 1, 2, \dots, n\}$ and their associated arrival time $\{t_i : i = 1, 2, \dots, n\}$. As a matter of fact, the arrival time data also provide an opportunity to collect more informative statistics. By our observation, a number of vehicles tend to travel in a platoon. Accordingly, it is expected that the vehicles in the same platoon would experience the same travel time on the common link (where covariance arises).

To be more specific, for a given interval of time, detector A in Figure 9.2 captures a number of vehicles at certain time $\{t_i : i = 1, 2, \dots, n\}$ (see e.g. Figure 9.3). Based on their arrival time, we may calculate the time-headway between the vehicles and hence define the associated vehicle platoons. In this case, the measured VRI data will be divided into two groups: the individual observation (e.g. y_i, y_j) and the platoon observation (e.g. (y_k, y_m)).

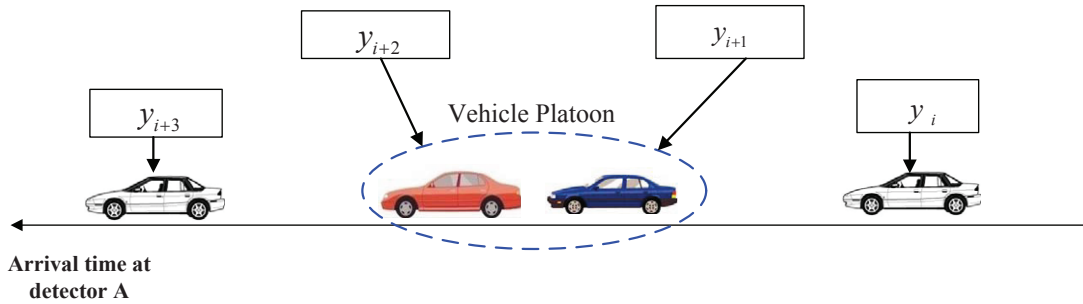


Figure 9.3: Vehicle platoon information

For the **individual observation**, the independency assumption is still reasonable because of the sufficiently large time-headway between the vehicles. And we can still utilize the statistical model proposed in Section 9.2.2.2. Therefore, the joint probability density function (pdf) of (y_i, \mathbf{z}_i) is given by:

$$q_1(y_i, \mathbf{z}_i; \beta, \theta, \xi) = \prod_{r=1}^R \left\{ p_r(\mu; \beta) \frac{1}{\sqrt{2\pi\theta\mu_r}} \exp\left(-\frac{1}{2} \frac{(y_i - \mu_r)^2}{\theta\mu_r}\right) \right\}^{z_{ir}} \quad (9.9)$$

where $\mu_r = \sum_{a=1}^A \delta_{ar} \xi_a$. By summing this probability distribution over all possible combinations \mathbf{z}_i would yield the probability density function of observing the "incomplete data" y_i :

$$P_1(y_i; \beta, \theta, \xi) = \sum_{\mathbf{z}_i} q(y_i, \mathbf{z}_i; \beta, \theta, \xi) \quad (9.10)$$

And accordingly, the likelihood function of the individual observation is given as follows:

$$L_1(\beta, \theta, \xi; \mathbf{y}) = \prod_{i=1}^{N_1} P_1(y_i; \beta, \theta, \xi) \quad (9.11)$$

in which N_1 represents the number of the individual observations.

With respect to the **vehicle platoon observation** (y_k, y_m) , as explained above they are not independent but following a multivariate normal distribution (MVN). In our particular case shown in Figure 9.2, knowing the routing information $(\mathbf{z}_k, \mathbf{z}_m)$, the platoon observation

$$(y_k, y_m) \sim MVN(\boldsymbol{\mu}, \boldsymbol{\Sigma}) \quad (9.12)$$

For example, assuming that vehicle k and m are traveling on route 1 and route 2, respectively, then we may have:

$$(y_k, y_m) \sim MVN \left((\xi_1 + \xi_2, \xi_1 + \xi_3), \begin{pmatrix} \theta\xi_1 + \theta\xi_2 & \theta\xi_1 \\ \theta\xi_1 & \theta\xi_1 + \theta\xi_3 \end{pmatrix} \right)$$

In this case, the joint probability density function (pdf) of $(y_k, \mathbf{z}_k; y_m, \mathbf{z}_m)$ is given by:

$$q_2(y_k, \mathbf{z}_k, y_m, \mathbf{z}_m; \boldsymbol{\beta}, \theta, \boldsymbol{\xi}) = \prod_{r_k=1}^R \prod_{r_m=1}^R \left\{ p_{r_k}(\boldsymbol{\mu}; \boldsymbol{\beta}) p_{r_m}(\boldsymbol{\mu}; \boldsymbol{\beta}) MVN(\boldsymbol{\mu}, \boldsymbol{\Sigma}) \right\}^{z_{kr_k} z_{mr_m}} \quad (9.13)$$

By summing this probability distribution over all possible combinations \mathbf{z}_k and \mathbf{z}_m would yield the probability density function of observing the "incomplete data" (y_k, y_m) :

$$P_2(y_k, y_m; \boldsymbol{\beta}, \theta, \boldsymbol{\xi}) = \sum_{\mathbf{z}_k} \sum_{\mathbf{z}_m} q_2(y_k, \mathbf{z}_k, y_m, \mathbf{z}_m; \boldsymbol{\beta}, \theta, \boldsymbol{\xi}) \quad (9.14)$$

Again, we may obtain the likelihood function of the platoon information, $L_2(\boldsymbol{\beta}, \theta, \boldsymbol{\xi}; \mathbf{y})$. The overall likelihood function is then given by:

$$L(\boldsymbol{\beta}, \theta, \boldsymbol{\xi}; \mathbf{y}) = L_1(\boldsymbol{\beta}, \theta, \boldsymbol{\xi}; \mathbf{y}) * L_2(\boldsymbol{\beta}, \theta, \boldsymbol{\xi}; \mathbf{y}) \quad (9.15)$$

Upon completion of the statistical model formulation, the upcoming task is estimate the link travel times by maximizing the likelihood function (9.6) and/or (9.15). As discussed earlier, the direct optimization method may not be mathematical tractable because of the potentially massive computational load. In the following part, we would apply the expectation and maximization (E&M) algorithm to solve the MLE problem.

9.2.2.4 Preliminary numerical results

To demonstrate the properties of the model formulation, we perform a series of simulation tests using the conceptual network in Figure 9.1 and Figure 9.2.

The test network shown in Figure 9.1 consists of three parallel routes and two VRI detectors. In this case, our goal is to estimate the unknown parameters $(\mu_1, \mu_2, \mu_3, \beta, \theta)$ through the observed the VRI data. In this research, we utilize Monte Carlo simulation approach to generate the VRI data using the statistical model described in Section 9.2.2.2. In our simulation test, the actual mean route travel time is $\mu = (30, 32, 34)$. The actual route choice parameter $\beta = 0.5$, whereas the mean-variance parameter $\theta = 0.1$. As mentioned before, the performance of proposed EM algorithm is highly dependent on the initial parameter. Therefore, we utilize the random initialization technique to generate a number of initial points.

Table 9.1: Performance of random initialization technique

Initial parameters					Estimated parameters					log-likelihood
μ_1	μ_2	μ_3	β	θ	μ_1	μ_2	μ_3	β	θ	
29.46	32.07	34.31	0	0.07	29.93	31.35	33.84	0.39	0.10	-2190.6
29.87	33.09	35.36	0.11	0.06	29.93	31.36	33.84	0.39	0.10	-2190.6
29.82	32.82	35.03	0.41	0.07	30.11	32.20	34.29	0.56	0.10	-2190.5
29.51	32.55	36.38	0.31	0.08	30.03	31.96	34.19	0.50	0.10	-2190.4

As shown in Table 9.1, the EM algorithm starting at different initial points would give rise to different solutions. The major reason for this phenomena is that the objective function is non-concave. In this case, the global maxima may not be guaranteed. By applying the proposed random initialization technique, we may achieve a "sub-optimal" estimate. The last row in Table 9.1 shows that a more reasonable estimate with relatively larger incomplete-data log-likelihood is obtained. We also calculate the scaled root mean squared error to indicate the accuracy the estimation. To be more specific, we first generate 50 sets of VRI data (the sample size of each set of data is 1000) using Monte Carlo simulation approach. Then the scaled root mean squared error is given by:

$$\text{SRMSE} = \frac{1}{\|\mu\|_1} \sqrt{\frac{1}{50} \sum_{i=1}^{50} \sum_{j=1}^3 (\hat{\mu}_j^{(i)} - \mu_j)^2} = 0.0125 \quad (9.16)$$

where $\hat{\mu}_j^{(i)}$ denotes the estimate for the j th route based on the i th data set.

To verify the asymptotic properties of the estimators, we apply this statistical estimation approach to a number of VRI data sets with different sample sizes. Assume that all the EM procedures start at the same initial point $(\mu_1^{(0)}, \mu_2^{(0)}, \mu_3^{(0)}, \beta^{(0)}, \theta^{(0)})$, then we may obtain the following results:

Table 9.2: Asymptotic properties of the estimators

Estimated parameters					Sample size
μ_1	μ_2	μ_3	β	θ	
29.4720	31.7402	34.3533	0.3484	0.0549	100
30.1222	32.3078	35.2306	0.5451	0.1107	200
30.0192	31.4881	33.5846	0.4541	0.0982	500
30.0310	31.9604	34.1854	0.5005	0.1003	1000

As shown in Table 9.2, the estimates become more and more accurate with the increasing of the sample size of the observed VRI data. This phenomena is quite reasonable as the maximum likelihood estimator is asymptotically unbiased and efficient.

Another test network shown in Figure 9.2 consists of 3 links and two routes. link 1 is the common link between the two routes. In our experiment, the actual mean link travel time is $\xi = (20, 10, 14)$. The actual route choice parameter $\beta = 0.5$, whereas the mean-variance parameter $\theta = 0.1$. By adopting the statistical model proposed in Section 9.2.2.3, we may generate the observed data through Monte Carlo simulation. Recall that by solely utilizing the individual observation, we may not achieve an unique solution. Therefore, two sources of data are explored: individual information and platoon information. In this test, the sample size of individual information is denoted by N_1 while the platoon information (i.e. number of pairs of vehicles) is N_2 .

Table 9.3: Performance of the link travel time estimation

Estimated parameters					N_1	N_2
ξ_1	ξ_2	ξ_3	β	θ		
18.9620	11.4027	16.0387	0.4084	0.0849	900	100
19.2482	9.3078	15.6732	0.5687	0.0845	800	200
19.8702	10.6504	14.2408	0.5402	0.1003	500	500
20.0271	9.98464	14.1002	0.4995	0.0981	200	800

Table 9.3 demonstrates the performance of our estimation approach by utilizing two sources of VRI data. It is evident that the unique solution can be obtained by incorporating the platoon information. With respect to the increase of N_2 , the estimates are becoming more and more accurate. This result is expectable, since the platoon information provide us more informative statistics. One interpretation for this result is that the individual information enable us to estimate the statistically independent route travel times, whereas the supplementary platoon information describe the covariance between different routes (here we assume the covariance results from the overlapping between routes). The combined usage of these two sources of data provide us a chance to resolve the identifiability problem. However, it should also be noted that incorporation of the platoon information would inevitably increase the complexity of the objective function (see Equation (9.13)) and hence the computational time. In other words, there is a trade-off between the estimation accuracy and computational efficiency.

9.2.2.5 A discussion on the proposed method

Several comments should be made on the proposed method. First, due to the non-concavity of the incomplete likelihood function (Equation (9.6)), we may not be able to obtain an "optimal" estimate. In this case, we suggest starting the E&M algorithms at a number of random initial points to avoid being "trapped" at the local maxima. Second, when it comes to a network case with multiple detectors, the growing complexity of the complete-data likelihood function and the large number of parameters to be estimated will be the major computational consideration. Third, in practice we may not achieve perfect matching through the VRI system. Thus, we should also consider the possible random error of the Detector-to-Detector journey time produced by this VRI system. Recall that the VRI system would also provide us a probability measure to represent the matching accuracy (see Chapter 4). In such case, we suggest that the joint likelihood function proposed earlier should also be modified by multiplying this additional factor (i.e. matching accuracy) to represent the reliability of the observed travel time data.

References

- Abhari, K., Marsousi, M., Babyn, P., Alirezaie, J., 2012. Medical image denoising using low pass filtering in sparse domain. In: Proceedings of Annual International Conference of the IEEE Engineering in Medicine and Biology Society, 114–117 (cit. on p. 26).
- Acharya, T., Ray, A.K., 2005. Image Processing: Principles and Applications. Hoboken, N.J.: John Wiley (cit. on p. 26).
- Aghdasi, H.S., Abbaspour, M., Moghadam, M.E., Samei, Y., 2008. An energy-efficient and high-quality video transmission architecture in wireless video-based sensor networks. *Sensors* 8 (8), 4529–4559 (cit. on p. 24).
- Ahuja, R.K., Magnanti, T.L., Orlin, J.B., 1993. Network Flows: Theory, Algorithms, and Applications. Prentice Hall (cit. on p. 64).
- Baek, N., Park, S.M., Kim, K.J., Park, S.B., 2007. Vehicle Color Classification Based on the Support Vector Machine Method. In: Advanced Intelligent Computing Theories and Applications. With Aspects of Contemporary Intelligent Computing Techniques. Ed. by D.-S. Huang, L. Heutte, M. Loog. Vol. 2. Communications in Computer and Information Science. Springer Berlin Heidelberg, 1133–1139 (cit. on p. 36).
- Balke, K.N., Chaudhary, N., Chu, C.L., Kunchangi, S., Nelson, P., Songhitruksa, P., Sunkari, S., Swaroop, D., Tyagi, V., 2005. Dynamic traffic flow modeling for incident detection and short-term congestion prediction. Tech. rep. (cit. on p. 30).
- Beckmann, M.J., 2013. Traffic congestion and what to do about it. *Transportmetrica B: Transport Dynamics* 1 (1), 103–109 (cit. on p. 1).

- Belongie, S., Malik, J., 2000. Matching with shape contexts. In: Proceedings of IEEE Workshop on Content-based Access of Image and Video Libraries, 20–26 (cit. on p. 64).
- Benediktsson, J., Swain, P., 1992. Consensus theoretic classification methods. *IEEE Transactions on Systems, Man and Cybernetics* 22 (4), 688–704 (cit. on p. 60).
- Beymer, D., McLauchlan, P., Coifman, B., Malik, J., 1997. A real-time computer vision system for measuring traffic parameters. In: Proceedings of IEEE Computer Society Conference on Computer Vision and Pattern Recognition, 495–501 (cit. on p. 21).
- Bhattacharyya, A., 1943. On a measure of divergence between two statistical populations defined by their probability distributions. *Bulletin of the Calcutta Mathematical Society* 35, 99–109 (cit. on p. 40).
- Bird, N.D., Masoud, O., Papanikolopoulos, N.P., Isaacs, A., 2005. Detection of loitering individuals in public transportation areas. *IEEE Transactions on Intelligent Transportation System* 6 (2), 167–177 (cit. on p. 41).
- Borgefors, G., 1988. Hierarchical chamfer matching: A parametric edge matching algorithm. *IEEE Transactions on Pattern Analysis and Machine Intelligence* 10 (6), 849–865 (cit. on p. 107).
- Castillo, E., Menéndez, J.M., Jiménez, P., 2008. Trip matrix and path flow reconstruction and estimation based on plate scanning and link observations. *Transportation Research Part B: Methodological* 42 (5), 455–481 (cit. on p. 16).
- Castillo, E., Nogal, M., Rivas, A., Sánchez-Cambronero, S., 2013. Observability of traffic networks. Optimal location of counting and scanning devices. *Transportmetrica B: Transport Dynamics* 1 (1), 68–102 (cit. on p. 172).
- Castro, R., Coates, M., Liang, G., Nowak, R., Yu, B., 2004. Network tomography: recent developments. *Statistical Science* 19 (3), 499–517 (cit. on p. 172).
- Celikoglu, H.B., 2013. Flow-based freeway travel-time estimation: A comparative evaluation within dynamic path loading. *IEEE Transactions on Intelligent Transportation Systems* 14 (2), 772–781 (cit. on p. 124).
- Cetin, M., Monsere, C.M., Nichols, A.P., 2011. Bayesian models for reidentification of trucks over long distances on the basis of axle measurement data. *Journal of Intelli-*

- gent Transportation Systems: Technology, Planning, and Operations 15, 1–12 (cit. on pp. 17, 19, 20, 75, 100).
- Chambolle, A., De Vore, R., Lee, N.Y., Lucier, B., 1998. Nonlinear wavelet image processing: Variational problems, compression, and noise removal through wavelet shrinkage. *IEEE Transactions on Image Processing* 7 (3), 319–335 (cit. on p. 159).
- Chandler, R.E., Herman, R., Montroll, E.W., 1958. Traffic dynamics: Studies in car following. *Operations research* 6 (2), 165–184 (cit. on p. 157).
- Chang, G.L., Su, C.C., 1995. Predicting intersection queue with neural network models. *Transportation Research Part C: Emerging Technologies* 3 (3), 175–191 (cit. on p. 27).
- Chang, S.L., Chen, L.S., Chung, Y.C., Chen, S.W., 2004. Automatic license plate recognition. *IEEE Transactions on Intelligent Transportation Systems* 5, 42–53 (cit. on pp. 16, 50, 75, 124).
- Chen, A., Yang, H., Lo, H.K., Tang, W.H., 2002. Capacity reliability of a road network: an assessment methodology and numerical results. *Transportation Research Part B: Methodological* 36 (3), 225–252 (cit. on p. 12).
- Chen, A., Zhou, Z., Chootinan, P., Ryu, S., Yang, C., Wong, S.C., 2011. Transport network design problem under uncertainty: a review and new developments. *Transport Reviews* 31 (6), 743–768 (cit. on p. 12).
- Choi, E., Lee, C., 2003. Feature extraction based on the Bhattacharyya distance. *Pattern Recognition* 36 (8), 1703–1709 (cit. on p. 40).
- Chou, C.S., Miller-Hooks, E., 2010. Simulation-based secondary incident filtering method. *Journal of Transportation Engineering* 136 (8), 746–754 (cit. on p. 74).
- Chowdhury, M.A., Sadek, A.W., 2003. *Fundamentals of Intelligent Transportation Systems Planning*. Boston, MA: Artech House (cit. on p. 1).
- Clark, S., Watling, D., 2005. Modelling network travel time reliability under stochastic demand. *Transportation Research Part B: Methodological* 39 (2), 119–140 (cit. on p. 12).
- Coifman, B., 2002. Estimating travel times and vehicle trajectories on freeways using dual loop detectors. *Transportation Research Part A: Policy and Practice* 36 (4), 351–364 (cit. on pp. 15, 124).

- Coifman, B., 1998. Vehicle re-identification and travel time measurement in real-time on freeways using existing loop detector infrastructure. *Transportation Research Record* 1643, 181–191 (cit. on pp. 19, 20, 50, 75, 124).
- Coifman, B., Cassidy, M., 2002. Vehicle reidentification and travel time measurement on congested freeways. *Transportation Research Part A: Policy and Practice* 36 (10), 899–917 (cit. on pp. 17, 20, 49, 75).
- Coifman, B., Krishnamurthy, S., 2007. Vehicle reidentification and travel time measurement across freeway junctions using the existing detector infrastructure. *Transportation Research Part C: Emerging Technologies* 15 (3), 135–153 (cit. on pp. 17, 20, 49, 74).
- Conte, D., Foggia, P., Sansone, C., Vento, M., 2003. Graph matching applications in pattern recognition and image processing. In: *Proceedings of International Conference on Image Processing* (cit. on p. 64).
- Cordeiro, P.J., Assuncao, P., 2012. Distributed coding/decoding complexity in video sensor networks. *Sensors* 12 (3), 2693–2709 (cit. on p. 24).
- Cortés, C.E., Lavanya, R., Oh, J.-S., Jayakrishnan, R., 2002. General-purpose methodology for estimating link travel time with multiple-point detection of traffic. *Transportation Research Record* 1802 (1), 181–189 (cit. on p. 14).
- Dadashi, N., Stedmon, A., Pridmore, T., 2009. Automatic components of integrated CCTV surveillance systems: functionality, accuracy and confidence. In: *Proceedings of Sixth IEEE International Conference on Advanced Video and Signal Based Surveillance*, 376–381 (cit. on p. 24).
- Daganzo, C.F., 1994. The cell transmission model: A dynamic representation of highway traffic consistent with the hydrodynamic theory. *Transportation Research Part B: Methodological* 28 (4), 269–287 (cit. on p. 157).
- Daubechies, I., Defrise, M., De Mol, C., 2004. An iterative thresholding algorithm for linear inverse problems with a sparsity constraint. *Communications on Pure and Applied Mathematics* 57 (11), 1413–1457 (cit. on p. 159).
- Dharia, A., Adeli, H., 2003. Neural network model for rapid forecasting of freeway link travel time. *Engineering Applications of Artificial Intelligence* 16 (7-8), 607–613 (cit. on p. 12).

- Dion, F., Rakha, H., 2006. Estimating dynamic roadway travel times using automatic vehicle identification data for low sampling rates. *Transportation Research Part B: Methodological* 40 (9), 745–766 (cit. on p. 16).
- Dong, W.S., Zhang, L., Shi, G.M., Wu, X.L., 2011. Image Deblurring and Super-Resolution by Adaptive Sparse Domain Selection and Adaptive Regularization. *IEEE Transactions on Image Processing* 20 (7), 1838–1857 (cit. on p. 26).
- Dufour, J.Y., 2013. *Intelligent Video Surveillance Systems*. London: ISTE (cit. on p. 22).
- Fambro, D.B., Ritch, G.P., 1979. Automatic detection of freeway incidents during low volume conditions. Tech. rep. FHWA/TX-79/23-210-1 (cit. on p. 31).
- Fambro, D.B., Ritch, G.P., 1980. Evaluation of an algorithm for detecting urban freeway incidents during low-volume conditions. *Transportation Research Record* 773, 31–39 (cit. on pp. 75, 79).
- Farenzena, M., Bazzani, L., Perina, A., Murino, V., Cristani, M., 2010. Person re-identification by symmetry-driven accumulation of local features. In: *Proceedings of IEEE Conference on Computer Vision and Pattern Recognition (CVPR)*, 2360–2367 (cit. on pp. 33, 41).
- Figueiredo, M.A.T., Nowak, R., 2003. An EM algorithm for wavelet-based image restoration. *IEEE Transactions on Image Processing* 12 (8), 906–916 (cit. on p. 159).
- Fries, R., Chowdhury, M., Ma, Y., 2007. Accelerated incident detection and verification: A benefit to cost analysis of traffic cameras. *Journal of Intelligent Transportation Systems: Technology, Planning, and Operations* 11 (4), 191–203 (cit. on p. 74).
- Frühwirth-Schnatter, S., 2006. *Finite Mixture and Markov Switching Models*. 1st ed. Springer (cit. on p. 57).
- Fu, L., Rilett, L.R., 1998. Expected shortest paths in dynamic and stochastic traffic networks. *Transportation Research Part B: Methodological* 32 (7), 499–516 (cit. on pp. 12, 152).
- Gao, Y., Dai, Q., Wang, M., Zhang, N., 2011. 3D model retrieval using weighted bipartite graph matching. *Signal Processing: Image Communication* 26 (1), 39–47 (cit. on p. 63).

- Gentile, G., Meschini, L., Papola, N., 2007. Spillback congestion in dynamic traffic assignment: A macroscopic flow model with time-varying bottlenecks. *Transportation Research Part B: Methodological* 41 (10), 1114–1138 (cit. on p. 154).
- Gheissari, N., Sebastian, T.B., Hartley, R., 2006. Person reidentification using spatiotemporal appearance. In: *Proceedings of IEEE Computer Society Conference on Computer Vision and Pattern Recognition (CVPR)*. Vol. 2, 1528–1535 (cit. on p. 41).
- Ghosh, S.K., 2013. *Digital Image Processing*. Oxford: Alpha Science International Ltd (cit. on p. 25).
- Goudail, F., Réfrégier, P., Delyon, G., 2004. Bhattacharyya distance as a contrast parameter for statistical processing of noisy optical images. *Journal of the Optical Society of America A* 21 (7), 1231–1240 (cit. on p. 40).
- Guner, A.R., Murat, A., Chinnam, R.B., 2012. Dynamic routing under recurrent and non-recurrent congestion using real-time ITS information. *Computers & Operations Research* 39 (2), 358–373 (cit. on p. 1).
- Haghani, A., Hamed, M., Sadabadi, K.F., Young, S., Tarnoff, P., 2010. Data collection of freeway travel time ground truth with bluetooth sensors. *Transportation Research Record* 2160, 60–68 (cit. on p. 16).
- Hall, F.L., Shi, Y., Atala, G., 1993. On-line testing of the McMaster incident detection algorithm under recurrent congestion. *Transportation Research Record* 1394, 1–7 (cit. on p. 74).
- Hazelton, M.L., 2000. Estimation of origin-destination matrices from link flows on uncongested networks. *Transportation Research Part B: Methodological* 34 (7), 549–566 (cit. on p. 172).
- Hellinga, B.R., Fu, L., 2002. Reducing bias in probe-based arterial link travel time estimates. *Transportation Research Part C: Emerging Technologies* 10 (4), 257–273 (cit. on p. 135).
- Hofleitner, A., Herring, R., Abbeel, P., Bayen, A., 2012. Learning the dynamics of arterial traffic from probe data using a dynamic Bayesian network. *IEEE Transactions on Intelligent Transportation Systems* 13 (4), 1679–1693 (cit. on pp. 16, 124).
- Hoh, B., Iwuchukwu, T., Jacobson, Q., Work, D., Bayen, A.M., Herring, R., Herrera, J.C., Gruteser, M., Annavaram, M., Ban, J., 2012. Enhancing privacy and accuracy in probe

- vehicle-based traffic monitoring via virtual trip lines. *IEEE Transactions on Mobile Computing* 11 (5), 849–864 (cit. on p. 16).
- Holt, R.B., Smith, B.L., Park, B., 2003. An Investigation of travel time estimation based on point sensors. Tech. rep. Smart Travel Laboratory (cit. on p. 2).
- Hsieh, A.J., Fan, K.C., Fan, T.I., 1995. Bipartite weighted matching for on-line handwritten Chinese character recognition. *Pattern Recognition* 28 (2), 143–151 (cit. on p. 64).
- Huang, T., Russell, S., 1998. Object identification: a Bayesian analysis with application to traffic surveillance. *Artificial Intelligence* 103 (1-2), 77–93 (cit. on pp. 19, 57).
- Jähne, B., 2005. *Digital Image Processing*. Berlin: Springer (cit. on p. 25).
- Javed, O., Rasheed, Z., Shafique, K., Shah, M., 2003. Tracking across multiple cameras with disjoint views. In: *Proceedings of Ninth IEEE International Conference on Computer Vision*, 952–957 (cit. on p. 42).
- Javed, O., Shafique, K., Shah, M., 2005. Appearance modeling for tracking in multiple non-overlapping cameras. In: *Proceedings of 2005 IEEE Computer Society Conference on Computer Vision and Pattern Recognition*. Vol. 2, 26–33 (cit. on pp. 33, 41).
- Jeng, S.T., 2007. Real-time vehicle reidentification system for freeway performance measurements. PhD Thesis. University of California, Irvine (cit. on p. 17).
- Jeng, S.-T., Tok, Y., Ritchie, S., 2010. Freeway corridor performance measurement based on vehicle reidentification. *IEEE Transactions on Intelligent Transportation Systems* 11 (3), 639–646 (cit. on p. 18).
- Kamijo, S., Kawahara, T., Sakauchi, M., 2005. Vehicle sequence image matching for travel time measurement between intersections. In: *Proceedings of IEEE International Conference on Systems, Man and Cybernetics*. Vol. 2, 1359–1364 (cit. on pp. 17, 19, 20, 124).
- Kittler, J., Hatef, M., Duin, R.P.W., Matas, J., 1998. On combining classifiers. *IEEE Transactions on Pattern Analysis and Machine Intelligence* 20 (3), 226–239 (cit. on p. 59).
- Klein, L.A., Mills, M.K., Gibson, D.R.P., 2006. *Traffic detector handbook*. English. 3rd ed. Washington, DC, USA: Federal Highway Administration (cit. on p. 21).

- Kwong, K., Kavalier, R., Rajagopal, R., Varaiya, P., 2010. Real-time measurement of link vehicle count and travel time in a road network. *IEEE Transactions on Intelligent Transportation Systems* 11 (4), 814–825 (cit. on p. 124).
- Kwong, K., Kavalier, R., Rajagopal, R., Varaiya, P., 2009. Arterial travel time estimation based on vehicle re-identification using wireless magnetic sensors. *Transportation Research Part C: Emerging Technologies* 17 (6), 586–606 (cit. on pp. 12, 17, 19, 20, 49–51).
- Ladson, J.A., 2005. The reproduction of colour. *Color Research & Application* 30 (6), 466–467 (cit. on p. 25).
- Lam, W., Chan, K., Tam, M., Shi, J., 2005. Short-term travel time forecasts for transport information system in Hong Kong. *Journal of Advanced Transportation* 39 (3), 289–306 (cit. on pp. 157, 172).
- Lam, W.H.K., Shao, H., Chen, A., 2010. Journey time estimator for assessment of road network performance under demand uncertainty. In: *Proceedings of 4th International Symposium on Transportation Network Reliability*. University of Minnesota (cit. on p. 172).
- Laval, J.A., Leclercq, L., 2010. A mechanism to describe the formation and propagation of stop-and-go waves in congested freeway traffic. *Physical and Engineering Sciences* 368 (1928), 4519–4541 (cit. on p. 154).
- Lee, J., Taylor, W., 1999. Application of a dynamic model for arterial street incident detection. *Journal of Intelligent Transportation Systems: Technology, Planning, and Operations* 5 (1), 53–70 (cit. on p. 30).
- Levin, M., Krause, G.M., 1978. Incident detection: a Bayesian approach. *Transportation Research Record* 682, 52–58 (cit. on p. 29).
- Li, R., Rose, G., Sarvi, M., 2006. Evaluation of speed-based travel time estimation models RID A-2397-2009. *Journal of Transportation Engineering* 132 (7), 540–547 (cit. on pp. 15, 124).
- Lighthill, M.J., Whitham, G.B., 1955. On kinematic waves. II. A theory of traffic flow on long crowded roads. In: *Proceedings of the Royal Society of London. Series A, Mathematical and Physical Sciences*. Vol. 229. 1178, 317–345 (cit. on p. 157).

- Lin, W.H., Tong, D., 2011. Vehicle re-identification with dynamic time windows for vehicle passage time estimation. *IEEE Transactions on Intelligent Transportation Systems* 12 (4), 1057–1063 (cit. on pp. [20](#), [100](#), [125](#)).
- Lindveld, C.D., Thijs, R., Bovy, P., Zijpp Van, der, 2000. Evaluation of online travel time estimators and predictors. *Transportation Research Record* 1719 (1), 45–53 (cit. on pp. [14](#), [15](#)).
- Lint, J.W.C. van, 2004. Reliable travel time prediction for freeways. PhD Thesis. Delft University of Technology, Delft, The Netherlands. (cit. on p. [13](#)).
- Lint, J., Zijpp, N., 2003. Improving a travel time estimation algorithm by using dual loop detectors. *Transportation Research Record* 1855, 41 (cit. on p. [14](#)).
- Lo, H.K., Luo, X.W., Siu, B., 2006. Degradable transport network: Travel time budget of travelers with heterogeneous risk aversion. *Transportation Research Part B: Methodological* 40 (9), 792–806 (cit. on p. [12](#)).
- Lo, H.K., Sumalee, A., 2013. Transport dynamics: its time has come! *Transportmetrica B: Transport Dynamics* 1 (1), 1–2 (cit. on p. [126](#)).
- Luathep, P., 2011. Stochastic transport network model and optimization for reliability and vulnerability analysis. PhD Thesis. The Hong Kong Polytechnic University. (cit. on p. [12](#)).
- Matei, B.C., Sawhney, H.S., Samarasekera, S., 2011. Vehicle tracking across nonoverlapping cameras using joint kinematic and appearance features. In: *Proceedings of IEEE Computer Society Conference on Computer Vision and Pattern Recognition (CVPR)*, 3465–3472 (cit. on p. [42](#)).
- Mazzon, R., Cavallaro, A., 2012. Multi-camera tracking using a multi-goal social force model. *Neurocomputing* 100, 41–50 (cit. on pp. [33](#), [42](#)).
- McLachlan, G., Krishnan, T., 2008. *The EM Algorithm and Extensions*. Wiley series in probability and statistics. Wiley-Interscience (cit. on p. [57](#)).
- Michalopoulos, P.G., 1991. Vehicle detection video through image-processing - the Autoscope system. *IEEE Transactions on Vehicular Technology* 40 (1), 21–29 (cit. on p. [24](#)).

- Min, W., Wynter, L., 2011. Real-time road traffic prediction with spatio-temporal correlations. *Transportation Research Part C: Emerging Technologies* 19 (4), 606–616 (cit. on p. 154).
- Nakajima, C., Pontil, M., Heisele, B., Poggio, T., 2003. Full-body person recognition system. *Pattern Recognition* 36 (9), 1997–2006 (cit. on p. 41).
- Nam, D.H., Drew, D.R., 1999. Automatic measurement of traffic variables for intelligent transportation systems applications. *Transportation Research Part B: Methodological* 33 (6), 437–457 (cit. on p. 15).
- Nam, D.H., Drew, D.R., 1996. Traffic dynamics: method for estimating freeway travel times in real time from flow measurements. *Journal of Transportation Engineering* 122 (3), 185–197 (cit. on p. 15).
- Nasri, M., Saryazdi, S., Nezamabadi-pour, H., 2013. A Fast Adaptive Salt and Pepper Noise Reduction Method in Images. *Circuits, Systems, and Signal Processing* 32 (4), 1839–1857 (cit. on p. 26).
- Ndoye, M., Totten, V.F., Krogmeier, J.V., Bullock, D.M., 2011. Sensing and signal processing for vehicle reidentification and travel time estimation. *IEEE Transactions on Intelligent Transportation Systems* 12 (1), 119–131 (cit. on pp. 100, 125).
- Ni, D., Wang, H., 2008. Trajectory reconstruction for travel time estimation. *Journal of Intelligent Transportation Systems: Technology, Planning, and Operations* 12 (3), 113–125 (cit. on p. 14).
- Oh, C., Ritchie, S.G., Jeng, S.T., 2007. Anonymous vehicle reidentification using heterogeneous detection systems. *IEEE Transactions on Intelligent Transportation Systems* 8 (3), 460–469 (cit. on p. 20).
- Oh, J.S., Jayakrishnan, R., Recker, W., 2002. Section travel time estimation from point detection data. Tech. rep. California PATH Research Report: UCI-ITS-WP-02-11 (cit. on p. 49).
- Ohkubo, M., Suzuki, K., Kinoshita, S., 2005. RFID privacy issues and technical challenges. *Communications of the ACM* 48 (9), 66–71 (cit. on p. 16).
- Oleari, C., Fermi, F., UAakar, A., 2013. Digital image-color conversion between different illuminants by color-constancy actuation in a color-vision model based on the OSA-UCS system. *Color Research & Application* 38 (6), 412–422 (cit. on p. 36).

- Otsu, N., 1979. A threshold selection method from gray-level histograms. *IEEE Transactions on Systems, Man and Cybernetics* 9 (1), 62–66 (cit. on pp. 34, 95).
- Ozbay, K., Kachroo, P., 1999. *Incident Management in Intelligent Transportation Systems*. Boston Mass.: Artech House (cit. on p. 27).
- Pan, T., 2012. The stochastic dynamic journey time reliability analysis by considering the spatial and temporal correlation. M.Phil. Thesis. The Hong Kong Polytechnic University. (cit. on p. 154).
- Pan, T., Sumalee, A., Zhong, R., Indra-Payoong, N., 2013. Short-term traffic state prediction based on temporal-spatial correlation. *IEEE Transactions on Intelligent Transportation Systems* 14 (3), 1242–1254 (cit. on p. 157).
- Parkany, E., Xie, C., 2005. A Complete review of incident detection algorithms and their deployment: What works and what doesn't. Tech. rep. University of Massachusetts Transportation Center (cit. on p. 2).
- Parry, K., Hazelton, M.L., 2012. Estimation of origin-destination matrices from link counts and sporadic routing data. *Transportation Research Part B: Methodological* 46 (1), 175–188 (cit. on p. 172).
- Patel, H.A., Thakore, D.G., 2013. Moving object tracking using Kalman filter. *International Journal of Computer Science and Mobile Computing* 2 (4), 326–332 (cit. on p. 34).
- Payne, H.J., Thompson, S.M., 1997. Development and testing of operational incident detection algorithms. Tech. rep. BSEO Report No. R-009-97. (cit. on p. 28).
- Payne, H.J., Tignor, S.C., 1978. Freeway incident detection algorithms based on decision tree with states. *Transportation Research Record* 682, 30–37 (cit. on pp. 28, 29, 74).
- Petty, K.F., Bickel, P., Ostland, M., Rice, J., Schoenberg, F., Jiang, J., Ritov, Y., 1998. Accurate estimation of travel times from single-loop detectors. *Transportation Research Part A: Policy and Practice* 32 (1), 1–17 (cit. on p. 15).
- Quayle, S.M., Koonce, P., DePencier, D., Bullock, D.M., 2010. Arterial performance measures with media access control readers, Portland, Oregon, pilot study. *Transportation Research Record* 2192, 185–193 (cit. on pp. 16, 50, 75, 124).

- Quiroga, C., Bullock, D., 1998. Travel time studies with global positioning and geographic information systems: an integrated methodology. *Transportation Research Part C: Emerging Technologies* 6 (1-2), 101–127 (cit. on p. 12).
- Riños Insua, D., Ruggeri, F., Wiper, M.P., 2012. *Bayesian Analysis of Stochastic Process Models*. Wiley (cit. on p. 112).
- Rose, G., 2006. Mobile phones as traffic probes: Practices, prospects and issues. *Transport Reviews* 26 (3), 275–291 (cit. on pp. 16, 124).
- Saha, S., Basu, S., Nasipuri, M., Basu, D.K., 2010. A novel scheme for binarization of vehicle images using hierarchical histogram equalization technique (cit. on p. 26).
- Schrank, D., Lomax, T., Eisele, B., 2012. The 2012 urban mobility report. Tech. rep. Texas Transportation Institute (cit. on p. 1).
- Sedgewick, R., 2002. *Algorithms in C++, part 5: Graph Algorithms*. Boston, MA, USA: Addison-Wesley Longman Publishing Co., Inc (cit. on p. 63).
- Shao, H., Lam, W.H.K., Sumalee, A., Chen, A., 2013. Journey time estimator for assessment of road network performance under demand uncertainty. *Transportation Research Part C: Emerging Technologies* 35, 244–262 (cit. on p. 11).
- Shapiro, L.G., Stockman, G.C., 2001. *Computer Vision*. Upper Saddle River, N.J.: Prentice Hall, 580 (cit. on pp. 40, 41).
- Shehata, M.S., Cai, J., Badawy, W.M., Burr, T.W., Pervez, M.S., Johannesson, R.J., Radmanesh, A., 2008. Video-based automatic incident detection for smart roads: the outdoor environmental challenges regarding false alarms. *IEEE Transactions on Intelligent Transportation Systems* 9 (2), 349–360 (cit. on pp. 30, 74).
- Sheu, J.B., Chou, Y.H., Shen, L.J., 2001. A stochastic estimation approach to real-time prediction of incident effects on freeway traffic congestion. *Transportation Research Part B: Methodological* 35 (6), 575–592 (cit. on p. 1).
- Sisiopiku, V.P., Roupail, N.M., 1994. Toward the Use of Detector Output for Arterial Link Travel Time Estimation: A Literature Review. *Transportation Research Record* 1457, 158–165 (cit. on p. 15).

- Sivaraman, S., Trivedi, M.M., 2013. Looking at vehicles on the road: A survey of vision-based vehicle detection, tracking, and behavior analysis. *IEEE Transactions on Intelligent Transportation Systems* 14 (4), 1773–1795 (cit. on p. 99).
- Smith, A., Cohn, T., Osborne, M., 2005. Logarithmic opinion pools for conditional random fields. In: *Proceedings of the 43rd Annual Meeting on Association for Computational Linguistics. ACL '05*. Ann Arbor, Michigan: Association for Computational Linguistics, 18–25 (cit. on p. 60).
- Song, B., Roy-Chowdhury, A., 2008. Robust tracking in a camera network: A multi-objective optimization framework. *IEEE Journal of Selected Topics in Signal Processing* 2 (4), 582–596 (cit. on p. 100).
- Soriguera, F., Robuste, F., 2011. Requiem for freeway travel time estimation methods based on blind speed interpolations between point measurements. *IEEE Transactions on Intelligent Transportation Systems* 12 (1), 291–297 (cit. on p. 124).
- Soro, S., Heinzelman, W.B., 2005. On the coverage problem in video-based wireless sensor networks. In: *Proceedings of 2nd International Conference on Broadband Networks*, 932–939 (cit. on p. 24).
- Spivak, A., Belenky, A., Fish, A., Yadid-Pecht, O., 2011. A Wide-dynamic-range CMOS image sensor with gating for night vision systems. *IEEE Transactions on Vehicular Technology* 58 (2), 85–89 (cit. on p. 24).
- Srinivasan, D., Jin, X., Cheu, R., 2004. Evaluation of adaptive neural network models for freeway incident detection. *IEEE Transactions on Intelligent Transportation Systems* 5 (1), 1–11 (cit. on p. 74).
- Stenger, B., Thayananthan, A., Torr, P.H.S., Cipolla, R., 2006. Model-based hand tracking using a hierarchical Bayesian filter. *IEEE Transactions on Pattern Analysis and Machine Intelligence* 28 (9), 1372–1384 (cit. on p. 107).
- Stephanedes, Y.J., Chassiakos, A.P., 1993a. Application of filtering techniques for incident detection. *Journal of Transportation Engineering* 119 (1), 13–26 (cit. on p. 30).
- Stephanedes, Y.J., Chassiakos, A.P., 1993b. Freeway incident detection through filtering. *Transportation Research Part C: Emerging Technologies* 1 (3), 219–233 (cit. on p. 30).
- Sumalee, A., Zhong, R.X., Pan, T.L., Szeto, W.Y., 2011. Stochastic cell transmission model (SCTM): A stochastic dynamic traffic model for traffic state surveillance and

- assignment. *Transportation Research Part B: Methodological* 45 (3), 507–533 (cit. on p. 157).
- Sun, C.C., Arr, G.S., Ramachandran, R.P., Ritchie, S.G., 2004. Vehicle reidentification using multidetector fusion. *IEEE Transactions on Intelligent Transportation Systems* 5 (3), 155–164 (cit. on pp. 17, 19, 20, 50, 55).
- Sun, C., Ritchie, S.G., 1999. Individual vehicle speed estimation using single loop inductive waveforms. *Journal of Transportation Engineering* 125 (6), 531–538 (cit. on pp. 15, 124).
- Sun, C., Ritchie, S.G., Tsai, W., Jayakrishnan, R., 1999. Use of vehicle signature analysis and lexicographic optimization for vehicle reidentification on freeways. *Transportation Research Part C: Emerging Technologies* 7, 167–185 (cit. on pp. 17, 20, 49, 75).
- Sun, L., Yang, J., Mahmassani, H., 2008. Travel time estimation based on piecewise truncated quadratic speed trajectory. *Transportation Research Part A: Policy and Practice* 42 (1), 173–186 (cit. on p. 14).
- Szeto, W.Y., Lo, H.K., 2006. Dynamic traffic assignment: Properties and extensions. *Transportmetrica* 2 (1), 31–52 (cit. on p. 157).
- Tam, M.L., Lam, W., 2008. Using automatic vehicle identification data for travel time estimation in Hong Kong. *Transportmetrica* 4 (3), 179–194 (cit. on pp. 12, 172).
- Tan, M.C., Wong, S.C., Xu, J.M., Guan, Z.R., Zhang, P., 2009. An aggregation approach to short-term traffic flow prediction. *IEEE Transactions on Intelligent Transportation Systems* 10 (1), 60–69 (cit. on p. 138).
- Tawfik, A.Y., Peng, A., Tabib, S.M., Abdulhai, B., 2002. Learning spatio-temporal context for vehicle reidentification. In: *Proceedings of 2nd IEEE International Symposium on Signal Processing and Information Technology*. Marrakesh, Morocco (cit. on p. 17).
- Taylor, M.A., 2013. Travel through time: the story of research on travel time reliability. *Transportmetrica B: Transport Dynamics* 1 (3), 174–194 (cit. on p. 12).
- Thiang, A.T.G., Lim, R., 2001. Type of vehicle recognition using template matching method. In: *Proceedings of International Conference on Electrical, Electronics, Communication and Information*. Jakarta, Indonesia (cit. on p. 37).

- Toledo, T., Beinhaker, R., 2006. Evaluation of the potential benefits of advanced traveler information systems. *Journal of Intelligent Transportation Systems: Technology, Planning, and Operations* 10 (4), 173–183 (cit. on p. 2).
- Tseng, B.L., Lin, C.Y., Smith, J.R., 2002. Real-time video surveillance for traffic monitoring using virtual line analysis. In: *Proceedings of IEEE International Conference on Multimedia and Expo*. Vol. 2, 541–544 (cit. on p. 21).
- Turner, S.M., Eisele, W.L., Benz, R.J., Holdener, D.J., 1998. Travel time data collection handbook. Tech. rep. FHWA-PL-98-035 (cit. on p. 14).
- Valera, M., Velastin, S.A., 2005. Intelligent distributed surveillance systems: a review. *IEEE Proceedings-Vision Image and Signal Processing* 152 (2), 192–204 (cit. on p. 23).
- Vanajakshi, L.D., Williams, B.M., Rilett, L.R., 2009. Improved flow-based travel time estimation method from point detector data for freeways. *Journal of Transportation Engineering* 135 (1), 26–36 (cit. on p. 15).
- Vardi, Y., 1996. Network tomography: estimating source-destination traffic intensities from link data. *Journal of the American Statistical Association* 91 (433), 365–377 (cit. on p. 172).
- Vlahogianni, E.I., Karlaftis, M.G., Orfanou, F.P., 2012. Modeling the effects of weather and traffic on the risk of secondary incidents. *Journal of Intelligent Transportation Systems: Technology, Planning, and Operations* 16 (3), 109–117 (cit. on p. 74).
- Wang, K., Zhenjiang, Yao, Q., Huang, W., Wang, F.-Y., 2007. An automated vehicle counting system for traffic surveillance. In: *Proceedings of IEEE International Conference on Vehicular Electronics and Safety*, 1–6 (cit. on p. 21).
- Wang, S.S., Xia, Y., Liu, Q.G., Luo, J.H., Zhu, Y.M., Feng, D.D., 2012. Gabor feature based nonlocal means filter for textured image denoising. *Journal of Visual Communication and Image Representation* 23 (7), 1008–1018 (cit. on p. 26).
- Wang, X., 2013. Intelligent multi-camera video surveillance: A review. *Pattern Recognition Letters* 34 (1), 3–19 (cit. on pp. 23, 39).
- Wang, Y., Nihan, N., 2000. Freeway traffic speed estimation with single-loop outputs. *Transportation Research Record* 1727 (1), 120–126 (cit. on p. 15).

- Wasson, J.S., Sturdevant, J.R., Bullock, D.M., 2008. Real-time travel time estimates using media access control address matching. *Journal of Transportation Engineers* 78 (6), 20–23 (cit. on p. 16).
- Watling, D.P., 1994. Maximum likelihood estimation of an origin-destination matrix from a partial registration plate survey. *Transportation Research Part B: Methodological* 28 (4), 289–314 (cit. on p. 17).
- Watling, D.P., Cantarella, G.E., 2013. Modelling sources of variation in transportation systems: theoretical foundations of day-to-day dynamic models. *Transportmetrica B: Transport Dynamics* 1 (1), 3–32 (cit. on p. 3).
- Watling, D.P., Maher, M.J., 1992. A statistical procedure for estimating a mean origin-destination matrix from a partial registration plate survey. *Transportation Research Part B: Methodological* 26 (3), 171–193 (cit. on pp. 17, 124).
- Willsky, A., Chow, E., Gershwin, S., Greene, C., Houpt, P., Kurkjian, A., 1980. Dynamic model-based techniques for the detection of incidents on freeways. *IEEE Transactions on Automatic Control* 25 (3), 347–360 (cit. on p. 30).
- Wu, B.F., Kao, C.C., Liu, C.C., Fan, C.J., Chen, C.J., 2008. The vision-based vehicle detection and incident detection system in Hsueh-Shan tunnel. In: *Proceedings of IEEE International Symposium on Industrial Electronics*, 1394–1399 (cit. on p. 30).
- Ye, Q., Szeto, W.Y., Wong, S.C., 2012. Short-term traffic speed forecasting based on data recorded at irregular intervals. *IEEE Transactions on Intelligent Transportation Systems* 13 (4), 1727–1737 (cit. on p. 138).
- Yilmaz, A., Javed, O., Shah, M., 2006. Object tracking: A survey. *ACM Computing Surveys* 38 (4), 13 (cit. on p. 33).
- Yuan, L., Sun, J., Quan, L., Shum, H.Y., 2007. Image deblurring with blurred/noisy image pairs. *ACM Transactions on Graphics* 26 (3) (cit. on p. 26).
- Yue, Y., 2006. Spatial-temporal dependency of traffic flow and its implications for short-term traffic forecasting. PhD Thesis. The University of Hong Kong. (cit. on p. 157).
- Zhang, A., Gao, Z., 2012. Effect of ATIS information under incident-based congestion propagation. *Procedia - Social and Behavioral Sciences* 43, 628–637 (cit. on p. 154).

- Zhang, K., Taylor, M.A.P., 2006. Effective arterial road incident detection: A Bayesian network based algorithm. *Transportation Research Part C: Emerging Technologies* 14 (6), 403–417 (cit. on p. 74).
- Zhang, X., Feng, X., Wang, W., Zhang, S., Dong, Q., 2012. Gradient-based Wiener filter for image denoising. *Computers and Electrical Engineering* 39 (3), 934–944 (cit. on p. 26).
- Zhou, J., Gao, D., Zhang, D., 2007. Moving vehicle detection for automatic traffic monitoring. *IEEE Transactions on Vehicular Technology* 56 (1), 51–59 (cit. on p. 34).
- Zhou, X., Mahmassani, H., 2006. Dynamic origin-destination demand estimation using automatic vehicle identification data. *IEEE Transactions on Intelligent Transportation Systems* 7 (1), 105–114 (cit. on p. 16).